



Modélisation des efflorescences de l'algue toxique(*Alexandrium minutum*) en compétition interspécifique en Rade de Brest, France

Samuelson Nzeneri

► To cite this version:

Samuelson Nzeneri. Modélisation des efflorescences de l'algue toxique(*Alexandrium minutum*) en compétition interspécifique en Rade de Brest, France. Ecosystèmes. Université de Bretagne occidentale - Brest, 2019. Français. NNT : 2019BRES0113 . tel-02534994

HAL Id: tel-02534994

<https://theses.hal.science/tel-02534994>

Submitted on 7 Apr 2020

HAL is a multi-disciplinary open access archive for the deposit and dissemination of scientific research documents, whether they are published or not. The documents may come from teaching and research institutions in France or abroad, or from public or private research centers.

L'archive ouverte pluridisciplinaire **HAL**, est destinée au dépôt et à la diffusion de documents scientifiques de niveau recherche, publiés ou non, émanant des établissements d'enseignement et de recherche français ou étrangers, des laboratoires publics ou privés.

THESE DE DOCTORAT DE

L'UNIVERSITE
DE BRETAGNE OCCIDENTALE

ECOLE DOCTORALE N° 598
Sciences de la Mer et du littoral
Spécialité: Ecologie Marine

Par

Samuelson NZENERI

Titre de la thèse:

Modélisation des efflorescences de l'algue toxique
(*Alexandrium minutum*)
en compétition interspécifique en Rade de Brest, France

Thèse présentée et soutenue à Brest, le 6 décembre 2019
Unité de recherche: IFREMER/DYNECO/PELAGOS

Rapporteurs avant soutenance:

Sébastien LEFEBVRE
Professeur des universités, Université de Lille 1

Laure GUILLOU
Directrice de Recherche, CNRS Roscoff

Composition du Jury:

Laure GUILLOU Directrice de Recherche, CNRS Roscoff
(Président du Jury)

Sébastien LEFEBVRE Professeur des universités, Université de Lille 1

Philippe PONDAVEN Maître de conférences, UBO, Plouzané

Directeur de thèse
Annie CHAPELLE Directrice de Recherche, IFREMER Centre de Bretagne

Invité(s)
Marc SOURISSEAU Chercheur, IFREMER Centre de Bretagne

Martin PLUS Chercheur, IFREMER Centre de Bretagne

Résumé

Alexandrium minutum est un dinoflagellé toxique ayant la capacité, lors d'épisodes de prolifération (en anglais HABs: Harmful Algal Blooms), de générer des crises aux niveaux sanitaire et économique (aquaculture, pêche, tourisme). En France, cette espèce est observée depuis 1988 dans la région Bretagne où elle continue à proliférer depuis lors. De hauts niveaux de toxicité PSP (toxines paralysantes mesurées dans les coquillages, en anglais Paralytic Shellfish Poisoning) ont déjà été détectés dans les estuaires de Morlaix, de la Penzé, de la Rance, dans les Abers et, plus récemment, dans la Rade de Brest. Cette étude tente de caractériser et de hiérarchiser les paramètres contrôlant le succès d'*A. minutum* au sein de la communauté phytoplanctonique. Deux approches ont été privilégiées. La première a consisté en un suivi temporel (abondance des espèces, température et concentration en nutriments) réalisé en Rade de Brest sur le site de l'estuaire de Daoulas, entre 2009 et 2018. La seconde approche repose sur l'utilisation d'un modèle numérique 0D développé pour simuler les impacts potentiels des interactions entre des processus connus et paramétrisés, physiques et biologiques, dans l'écosystème. Ce modèle est basé sur des traits physiologiques (température et irradiance optimales, taille des cellules, présence/absence de frustule siliceuse), utilisés pour estimer la capacité qu'ont les différentes espèces à pouvoir se développer dans un milieu à température, lumière et concentrations en nutriments (PO_4 , NH_4 , NO_3 et Si(OH)_4) variables, alors même qu'elles se trouvent en situation de compétition entre elles. Dans ce modèle *A. minutum* a été placé en compétition avec 72 autres espèces dont les caractéristiques physiologiques ont été choisies pour couvrir de manière uniforme l'espace des traits sélectionnés. Les résultats montrent une variabilité à la fois saisonnière et inter-annuelle de la phénologie des efflorescences. Cette dernière est marquée entre les mois d'avril et d'octobre par une succession voyant le micro précéder le nano puis le picophytoplancton. Les efflorescences phytoplanctoniques sont contrôlées dans notre zone d'étude par la température et la lumière durant l'hiver et par les nutriments, d'abord le phosphore puis l'azote, durant l'été. Les blooms d'*A. minutum* apparaissent entre juin et août, période marquée par des concentrations en nutriments basses entraînant une compétition accrue pour les ressources. Les résultats de la modélisation, corroborés par les données observées, ont aussi montré un retard des dates de début d'efflorescence lorsque le printemps est froid (2013) et au contraire une efflorescence précoce lorsque le printemps est chaud (2014). En outre, c'est durant l'année 2012, caractérisée par de forts débits de rivière

durant l'été, et donc d'apports en nutriments très élevés, que les abondances maximales ont été observées, alors que l'année 2011, la plus sèche sur la période considérée, a montré des abondances beaucoup plus réduites. En 2012, *A. minutum* était aussi l'espèce dominante dans la communauté microphytoplanctonique, à la fois dans le modèle et dans les données observées. Le modèle a permis aussi de tester l'impact de scénarios de réduction d'apports en azote et, ou phosphore. Seule une réduction de phosphore entraîne une diminution de l'abondance d'*A. minutum*. Ceci s'explique par le fait que c'est le phosphore qui est le nutriment limitant pour *A. minutum* au cours de son développement, les rapports N/P des nutriments en rivière étant largement supérieurs au rapport N/P de Redfield. En revanche la réduction d'apport de l'azote entraîne une diminution de l'abondance du picoplancton en été, celui-ci étant alors limité par ce nutriment. Cependant, les facteurs environnementaux n'expliquent qu'une part de la variabilité observée dans l'intensité et la durée des blooms d'*A. minutum* au sein de la communauté phytoplanctonique. En dépit de simulations reproduisant la variabilité saisonnière et inter-annuelle d'*A. minutum* certaines années, le modèle n'est pas consistant sur toute la période d'étude. Cette étude met donc en lumière l'importance d'autres facteurs biotiques (diversité intraspécifique, prédation, parasitisme, reproduction sexuelle, autres traits) dans la régulation des efflorescences sur une échelle décennale. La prise en compte de ces facteurs pourrait améliorer les modèles dans leurs capacités à prévoir de manière opérationnelle la présence/absence d'*A. minutum*. Bien que ce modèle ait été validé (localement) en utilisant des données *in situ*, l'objectif reste le développement d'un modèle plus général pouvant être appliqué et validé sur l'ensemble de la Rade de Brest.

Abstract

Alexandrium minutum is one of the toxic species that have the ability to produce Harmful Algal Blooms (HABs), threaten public health, aquaculture and tourism. In France, it was observed in 1988 in the region Bretagne and has continued to proliferate ever since. High levels of Paralytic Shellfish Poisoning (PSP) toxicity have been detected in the estuaries of Morlaix, Penzé, Rance, Abers and more recently, in the Bay of Brest. This work tries to define and place in order of hierarchy, the parameters driving *A. minutum* success in the phytoplankton community. Two approaches were adopted in this study. The first was a temporal survey (abundance of species, temperature and concentration of nutrients) at the study site (Daoulas estuary) since 2009-2018. The second approach was the use of a 0D numerical model to simulate the potential impact of known and parameterized interactions between the physical and biological processes in the ecosystem. This model is based on physiological traits (optimal temperature, optimal irradiance, cell size, siliceous/non siliceous) which can be used to evaluate the ability of a species to grow with respect to environmental factors such as light, temperature and nutrients (PO_4 , NH_4 , NO_3 and Si), while competing with other species. *A. minutum* was placed in competition with 72 species which were uniformly selected. Results showed both seasonal and interannual variability of bloom phenology. It was marked by micro, followed by nano and then pico phytoplankton from April to October. Phytoplankton bloom in the area is limited by temperature and light during the winter but limited by nutrients in the summer – first by P and then N. *A. minutum* bloom occurred between June and August, a period marked by low nutrient concentrations and high resource competition. Results also showed a delayed bloom start of *A. minutum* in a cold spring (2013) but early bloom start in a warm spring (2014) in both field and model. In addition, the year 2012 with the highest summer rainfall which implies increased nutrient input; showed higher abundances than the year 2011 with the lowest summer rainfall. In 2012, *A. minutum* was also the dominant species over the microphytoplankton diversity both in observed data and in the model. Nutrient reductions have been performed showing that only phosphorus reduction reduces *A. minutum* bloom. This may be explained by the fact that P is the limiting factor for *A. minutum*, river N/P ratio being largely over the N/P Redfield ratio. On the contrary, N reduction limits the picophytoplankton bloom in summer. However, environmental factors and competition explain only a part of the interannual variability in *A. minutum* bloom duration and intensity within the phytoplankton community. Though the model was able to reproduce the seasonal and

interannual variability of *A. minutum*, simulation was not consistent over the study period. The model highlights the increasing relevance of other biological processes (the intraspecific diversity, the predators and sexual reproduction) in bloom regulation at decade scale. It might improve some models which are able to correctly predict real-world instances of *A. minutum* presence or absence. Though the model was validated (locally) using field data, the perspective is to have a general model which can be applied and validated for the entire Bay of Brest.

Communications

International Conference on Harmful Algae (ICHA), October 2018

Oral presentation

Journées de l'Ecole Doctorale, February 2019

Poster presentation

Publication

Modeling Seasonal and Interannual Variability of *Alexandrium minutum* in the Bay of Brest, France

Nzeneri et al. (submitted in Harmful Algae)

Funding

This PhD. Thesis was jointly funded by IFREMER (50%) and the region Bretagne (50%)

Appreciation

Annie CHAPELLE, Marc SOURISSEAU, Martin PLUS and all staff of DYNECO/PELAGOS

Table of Contents

Résumé	2
Abstract	4
Communications	6
Publication	6
Funding	6
Appreciation	6
Table of contents	7
List of figures	11
List of tables	15
Chapter 1: General Introduction.....	17
1.1. Phytoplankton	18
1.2. Harmful Algal Blooms (HABs)	19
1.3. <i>Alexandrium</i>	20
1.4. Study site - Bay of Brest	22
1.5. Modeling	23
1.6. Aims of the study	24
Chapter 2: <i>In Situ</i> Data Survey.....	25
2.1. Data Acquisition Strategy	26
2.1.1. Sampling Protocol (<i>Alex-Breizh</i>)	27
2.1.2. Laboratory Protocol	29
2.1.3. Available Data	31
2.1.4. Data Analysis	33
2.2. Results of the Survey	35
2.2.1. Environmental variables	35
2.2.1.1. Daily temperature and light	36
2.2.1.2. Daily river flow and salinity	37
2.2.1.3. Tidal coefficient and dilution	38
2.2.1.4. Nutrients	39
2.2.1.5. Chlorophyll a	41
2.2.2. <i>Alexandrium minutum</i>	42
2.2.3. Phytoplankton	45
2.2.4. Phytoplankton diversity	49
2.3. Discussion	57
2.3.1. <i>Alexandrium minutum</i> and environmental variables	57
2.3.2. <i>Alexandrium minutum</i> and phytoplankton	58

Chapter 3: Simulations 0D.....	59
3.1. Simulated Area.....	60
3.2. Model Equations.....	62
3.2.1. Abundance of species.....	62
3.2.2. Growth of species.....	63
3.2.3. Concentration of nutrients.....	64
3.2.4. Absorption of nutrients.....	67
3.2.5. Cell quota.....	68
3.2.6. Allometric relationship.....	68
3.2.7. Limitations.....	69
3.3. Phenotypic Variability.....	71
3.3.1. Number of species.....	71
3.3.2. Characteristics of species.....	72
3.4. Simulation Analysis.....	75
3.5. Results of the Simulations.....	76
3.5.1. Seasonal variability.....	76
3.5.1.1. Environmental variables.....	76
3.5.1.2. Phytoplankton community.....	79
3.5.1.3. <i>Alexandrium minutum</i>	81
3.5.2. Interannual variability.....	84
3.5.2.1. <i>Alexandrium minutum</i>	84
3.5.2.2. Phytoplankton community.....	85
3.5.2.3. Environmental variables.....	89
3.6. Discussion.....	93
3.6.1. Methodological challenges.....	93
3.6.2. <i>Alexandrium minutum</i> and environmental variables.....	95
3.6.3. Phytoplankton community and environmental variables.....	98
 Chapter 4: Scenarios of Nutrient Reduction.....	 99
4.1. Context.....	100
4.2. Method.....	100
4.3. Results.....	101
4.4. Discussion.....	106

Chapter 5: Summary.....	109
5.1. First year.....	110
5.2. Second year.....	112
5.3. Third year.....	115
5.4. Conclusion.....	118
5.5. Perspective.....	118
Bibliographic References.....	119

Annexes

A1: Nutrients in the Bay of Brest.....	134
Pointe du Château and river Daoulas.....	135
Lanveoc and Portzic.....	140
A2: Summer conditions.....	142
Context.....	143
Warm and cold.....	143
Wet and dry.....	144
A3: Photoinhibition on phytoplankton.....	145
Context.....	146
Jassby and Platt (1976).....	149
Steele (1962).....	150
Lacroix (2002).....	152
A4: Simulated phenology of phytoplankton (2009-2016).....	153
Phenology and limitations by category.....	154
Phenology by cell size.....	160
<i>Alexandrium minutum</i> and sp29.....	166
Nutrient limitations.....	169
General limitations.....	181
By optimal temperature.....	181
By optimal irradiance.....	184
Weibull analysis.....	187
A5: Code 0D.....	199
Biotic data.....	200
Name-list.....	200
Creating species.....	201
Example of species data.....	205
Abiotic data.....	207
Creating forcings.....	207
Example of forcings data.....	213
Simulation (Biotic + Abiotic).....	225
A6: Formation Doctorale.....	233
A7: Abstract ICHA.....	234
A8: Article (Submitted).....	235

List of Figures

Figure 1.1: Microscopic view of marine phytoplankton.....	18
Figure 1.2: Life cycle of <i>Alexandrium</i>	19
Figure 1.3.A: Vegetative cell of <i>A. minutum</i>	20
Figure 1.3.B: Chemical structure of PSP.....	20
Figure 1.4: Spatial distribution and occurrence of <i>A. minutum</i>	21
Figure 1.5: Bay of Brest showing study site, rivers and measurement stations.....	22
Figure 1.6: Monod and Droop approaches to phytoplankton physiology.....	23
Figure 2.1: Maximum abundances of <i>A. minutum</i>	26
Figure 2.1b: Guallar et al. (2017) bloom analysis using Weibull.....	34
Figure 2.2: Interannual variability of environmental variables.....	35
Figure 2.3: Daily temperature and light distribution over the study period.....	36
Figure 2.4: Daily river flow and salinity.....	37
Figure 2.5: Tidal coefficient and dilution.....	38
Figure 2.6: Concentration of inorganic nutrients.....	39
Figure 2.7: Concentration of Chlorophyll a from 2012 to 2018.....	41
Figure 2.8: Abundances of <i>Alexandrium minutum</i>	43
Figure 2.9: Weibull presentation of <i>Alexandrium minutum</i> abundances.....	44
Figure 2.10: Abundance of phytoplankton by category.....	46
Figure 2.11: Heatmap diagram (field survey).....	47
Figure 2.12: Most dominant taxons.....	49
Figure 2.13: Interannual MA of phytoplankton category C.....	53
Figure 2.14: Interannual DMA of phytoplankton category C.....	55
Figure 2.15: Average MA (2009-2018) of phytoplankton category C.....	54
Figure 3.1: The Bay of Brest showing simulated area.....	60
Figure 3.2: Concept of the model describing the simulated area.....	61
Figure 3.3: Maximum growth rate (Eppley, 1972).....	63

Figure 3.4: Distribution of 73 Species.....	74
Figure 3.5: Seasonal variability of environmental variables.....	77
Figure 3.5b: Simulated ratio (in blue) of Nitrogen to Phosphorus, 2016.....	78
Figure 3.6: Field and model seasonal variability of phytoplankton abundance in 2016.....	79
Figure 3.7: Seasonal and interannual variability in the abundances of <i>A. minutum</i>	82
Figure 3.8: Maximum limitations on the growth of <i>A. minutum</i>	82
Figure 3.9: Heatmap diagram (field and model).....	84
Figure 3.10: Taylor diagrams.....	85
Figure 3.11: Field and model interannual variability of phytoplankton abundances.....	86
Figure 3.12: Simulated abundances of phytoplankton phenotypes of 18µm.....	87
Figure 3.13: NH ₄ concentrations in field (points) and model (line).....	90
Figure 3.14: PO ₄ concentrations in field (points) and model (line).....	90
Figure 3.15: NO ₃ concentrations in field (points) and model (line).....	91
Figure 3.16: Si(OH) ₄ concentrations in field (points) and model (line).....	91
Figure 3.17: Interannual variability in simulated N/P ratio.....	92
Figure 3.18: N/P ratio on the DMA of <i>A. minutum</i>	97
 Figure 4.1: N and P reduction by 50 per cent.....	 102
Figure 4.2: Changes in the MA of <i>A. minutum</i> following a reduction in nutrients.....	103
Figure 4.3: Percentage reduction in the MA of <i>A. minutum</i>	103
Figure 4.4: Percentage reduction in the cumulative abundance of phytoplankton.....	105
Figure 4.5: Minimum concentrations of N and P before and after reduction.....	106
Figure 4.6: Phytoplankton responses to N and P limitations.....	108

Figure A1.1: Nutrients-salinity relationship.....	135
Figure A1.2: Daoulas estuary.....	136
Figure A1.3: Nutrient variation in River Daoulas and Pointe du Château.....	136
Figure A1.4: Dilution of nutrients with respect to salinity.....	138
Figure A1.5: Interpolated nutrient data in Pointe du Château.....	139
Figure A1.6: Nutrient concentrations in Lanveoc and Portzic stations.....	141
Figure A2.1: Warm and cold summer.....	143
Figure A2.2: Wet and dry summer.....	144
Figure A3.1: Light intensity and Photosynthetically Available Radiation (PAR).....	148
Figure A3.2: Relationship between cell size and I_{opt}	148
Figure A3.3: Light limitation by Jassby and Platt (1976).....	149
Figure A3.4: Abundance of species using Jassby and Platt equation.....	150
Figure A3.5: Light limitation by Steele (1962).....	151
Figure A3.6: Abundance of species using Steele's equation.....	151
Figure A3.7: Light limitation by Lacroix (2002).....	152
Figure A3.8: Abundance of species using Lacroix's equation.....	152
Figure A4.1: Phenology of phytoplankton.....	154
Figure A4.2: Nitrogen limitation on phytoplankton.....	155
Figure A4.3: Phosphorus limitation on phytoplankton.....	156
Figure A4.4: Silica limitation on phytoplankton.....	157
Figure A4.5: Temperature limitation on phytoplankton.....	158
Figure A4.6: Light limitation on phytoplankton.....	159
Figure A4.7: Species of 1 μ m.....	160
Figure A4.8: Species of 2 μ m.....	161
Figure A4.9: Species of 5 μ m.....	162
Figure A4.10: Species of 18 μ m.....	163
Figure A4.11: Species of 28 μ m.....	164
Figure A4.12: Species of 64 μ m.....	165
Figure A4.13: <i>A. minutum</i> and sp29.....	166

Figure A4.14: Temperature and light limitations on <i>A. minutum</i> and sp29.....	167
Figure A4.15: N and P limitations on <i>A. minutum</i> and species 29.....	168
Figure A4.16: Nitrogen limitation on species of 1µm.....	169
Figure A4.17: Phosphorus limitation on species of 1µm.....	170
Figure A4.18: Nitrogen limitation on species of 2µm.....	171
Figure A4.19: Phosphorus limitation on species of 2µm.....	172
Figure A4.20: Nitrogen limitation on species of 5µm.....	173
Figure A4.21: Phosphorus limitation on species of 5µm.....	174
Figure A4.22: Nitrogen limitation on species of 18µm.....	175
Figure A4.23: Phosphorus limitation on species of 18µm.....	176
Figure A4.24: Nitrogen limitation on species of 28µm.....	177
Figure A4.25: Phosphorus limitation on species of 28µm.....	178
Figure A4.26: Nitrogen limitation on species of 64µm.....	179
Figure A4.27: Phosphorus limitation on species of 64µm.....	180
Figure A4.28: Temperature limitation by T_{opt}	181
Figure A4.29: Temperature limitation by species.....	183
Figure A4.30: Light limitation by I_{opt}	184
Figure A4.31: Light limitation by species.....	186
Figure A4.32: Weibull analysis on species of 1µm.....	187
Figure A4.33: Weibull analysis on species of 2µm.....	189
Figure A4.34: Weibull analysis on species of 5µm.....	191
Figure A4.35: Weibull analysis on species of 18µm.....	193
Figure A4.36: Weibull analysis on species of 28µm.....	195
Figure A4.37: Weibull analysis on species of 64µm.....	197

List of Tables

Table 2.1: List of <i>Alex-Breizh</i> field sampling materials.....	27
Table 2.2: Availability and frequency of <i>in situ</i> data.....	31
Table 2.3: Supplementary <i>in situ</i> data.....	32
Table 2.4: Minimum concentrations of inorganic.....	40
Table 2.5: Maximum concentration of chlorophyll a.....	41
Table 2.6: Bloom phenology of <i>Alexandrium minutum</i>	42
Table 2.7: Maximum abundance of phytoplankton.....	45
Table 2.8: Phytoplankton diversity and MA over ten year period.....	50
Table 2.9: Diatoms and dinoflagellates whose MA>10000cells.L ⁻¹	51
Table 2.10: Interannual MA of phytoplankton category C.....	52
Table 2.11: Interannual DMA of phytoplankton category C.....	54
Table 2.12: Interannual variability in temperature dates at 15°C.....	57
Table 3.1: Table of symbols.....	66
Table 3.2: Coefficient of Allometry.....	69
Table 3.3: Simulated abundance of <i>A. minutum</i> as a function of NS.....	71
Table 3.4: Characteristics of Species.....	73
Table 3.5: Interannual variability in the bloom characteristics of phytoplankton.....	83
Table 3.6: Interannual variability in the MA of each dinoflagellate phenotype.....	88
Table 3.7: Highest N and P limitations on <i>A. minutum</i>	96
Table 4.1: % change in the annual cumulative concentration of nutrients.....	101
Table 4.2: DMA of <i>A. minutum</i> with N and P reductions.....	104
Table 4.3: Cumulative abundance of <i>A. minutum</i> and phytoplankton.....	104
Table 4.4: Seasonal and interannual conditions of river flow in Daoulas estuary.....	106

Table A3.1: Identified optimal irradiance of species.....	147
Table A3.2: Cell size and I_{opt}	148
Table A4.1: Weibull of species $1\mu m$	188
Table A4.2: Weibull of species $2\mu m$	190
Table A4.3: Weibull of species $5\mu m$	192
Table A4.4: Weibull of species $18\mu m$	194
Table A4.5: Weibull of species $28\mu m$	196
Table A4.6: Weibull of species $64\mu m$	198

Chapter 1

General Introduction

1.1. Phytoplankton

The word phytoplankton comes from two Greek words – ‘phyto’ (vegetal, for autotrophic capacity) and ‘plankton’ (vagabond, as without any significant swimming). These photosynthetic organisms are found in marine and freshwater environments all around the world. Their nutritional strategies are diverse, including the ability to utilize a range of organic and inorganic nutrient sources and feeding by ingestion of other organisms (Anderson et al., 2012). Species of phytoplankton are also very diverse in size, morphology and physiology. There are currently more than 20,000 species (Chapelle, 2016) and the discovery of new species is in constant evolution. Phytoplankton absorb mineral compounds (nitrogen, phosphorus, silicon) from different biogeochemical cycles and play a key role in the cycles by being responsible for the production of about 45 per cent of oxygen in the atmosphere (Burkholder et al, 2008; Field et al., 1998). In environments where resources (nutrients) are limited, all phytoplankton species compete for them in order to survive and multiply. This process is assumed to be one of the key drivers of structural and functional diversity. It is particularly true in coastal areas where a high production of biomass has been linked to nutrient enrichment through agricultural practices and river inputs (Menesguen et al., 2003). In addition, a phytoplankton community, identified as toxic algae, has also caused disorders such as Harmful Algal Blooms (HABs) in several ecosystems.

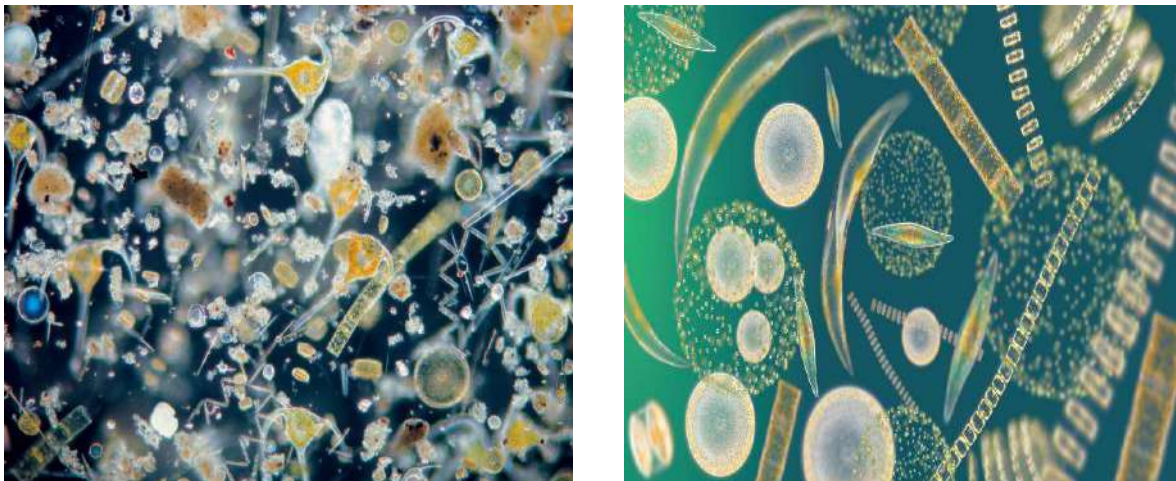


Figure 1.1: Microscopic view of marine phytoplankton
Source: GEOMAR

1.2. Harmful Algal Blooms (HABs)

Research on HABs (the production of phytotoxins that are poisonous to humans) has been intense in years because the frequency of observed events has rapidly increased in global coastal waters (Hallegraeff, 1993, 2010). Human health is usually affected through the consumption of contaminated sea food, skin contact and possible inhalation. Some of these toxins are powerful and deadly (Anderson et al., 2002) and thus, cause a problem at global scale. For these reasons, the proliferation of HABs has become a subject of study with strong societal demands. They pose numerous scientific questions such as - why some species are toxic and others are not; why/when some species become dominant in the phytoplankton community; is the occurrence/frequency of toxic events related to human activity etc. Harmful algae, by their regular monitoring, are therefore ideal models to study ecological niches and to contribute to more global research challenges (Sourisseau et al., 2017). HAB events in France date back to the late 1980s (Belin, 1993; Erard-Le Denn, 1997; Probert, 1999) and one of the causative species is *Alexandrium*.

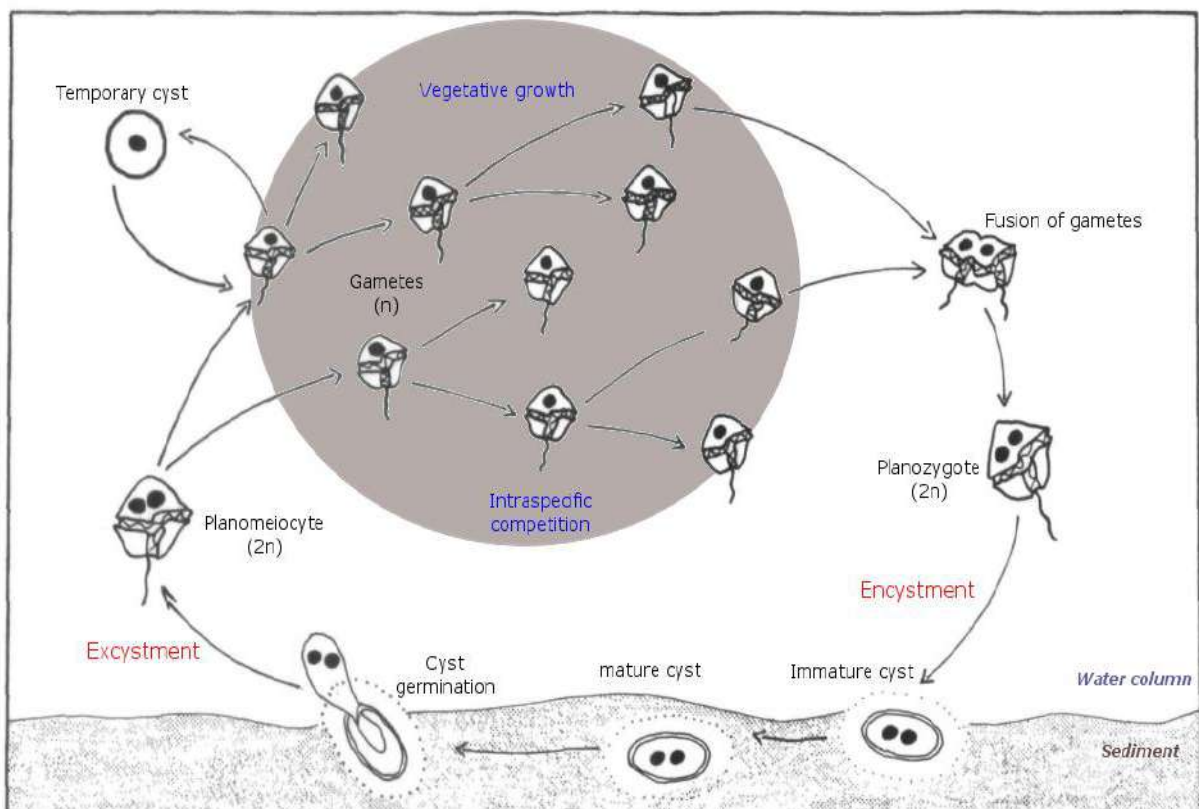


Figure 1.2: Life cycle of *Alexandrium*
(Wyatt and Jenkinson, 1997)

1.3. *Alexandrium*

Halim (1960) formally established the description of the genus *Alexandrium*, a small-sized dinoflagellate that produced a ‘red tide’ in the harbor of Alexandria in Egypt. This genus is believed to include more than 30 species, many of which have been described under a different species name. It has been described as an opportunistic genus relative to nutrition and has the ability to grow from nutrient-rich (Townsend et al., 2005; Spatharis et al., 2007) to pristine waters (Anderson et al., 2002) including waters where nutrient abatement has been carried out (Collos et al., 2009). At the scale of species, *Alexandrium minutum* has been identified as a very coastal species, able to grow over a large range of salinity and to store phosphate in high quantities (Yamamoto and Tarutani, 1999) thereby, making it appear more like a ‘storage specialist’ that uptakes PO_4 pulses for luxury consumption (storage) and then, later utilizes the stored PO_4 for cell growth (Labry et al. 2008).

In coastal waters, the principle nutrient source is the river but the sediment, containing high concentrations of organic matter, is a secondary nutrient source based on the remineralization that releases nutrients such as phosphorus and nitrogen with a high spatial and temporal variability (Andrieux-Loyer et al., 2008). This additional nutrients input from sediment enhances the growth of species like *A. minutum*.

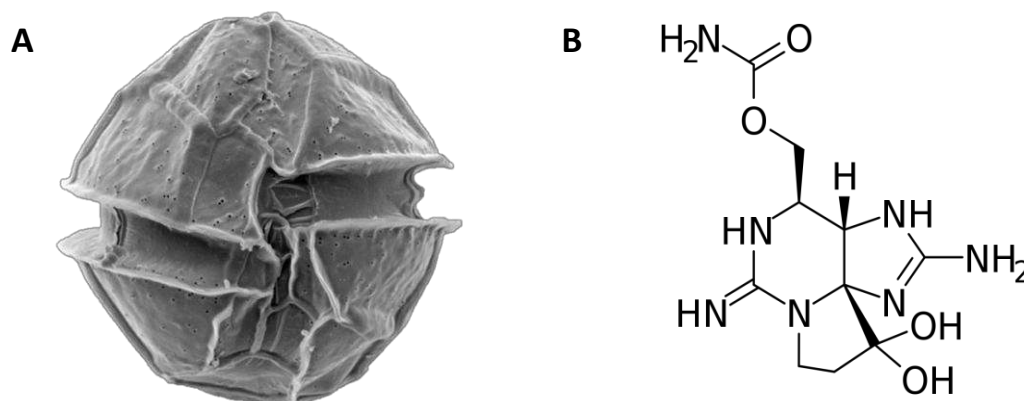


Figure 1.3.A: Vegetative cell of *A. minutum*, B: Chemical structure of PSP
Sources: Ifremer (A), Wikipedia (B)

A. minutum produces the Paralytic Shellfish Poison (PSP) toxin (Anderson et al., 2012). It is common along the Atlantic and English Channel coasts and mostly found in rich-nutrient confined ecosystems, mostly estuaries, from mid-May to August when nutrients, water temperature and irradiance support sufficient growth to compensate mortality rates and dilution rates (Chapelle et al. 2015; Raine, 2014; Cosgrove et al. 2014). High abundances of the species have thus been detected in northern Brittany in the estuaries of Morlaix, Penzé, Rance, Abers and recently, in the Bay of Brest (Maguer et al. 2004; Chambouvet et al. 2008; Chapelle, 2016). The period of bloom toxicities (in shellfish) correspond with the period of maximum cell abundance and maximum cellular concentration or production of toxins which is enhanced by high temperatures (Lim et al. 2006).



Figure 1.4: Spatial distribution and occurrence of *A. minutum* (>10 000 cells.L⁻¹) in Bretagne and rest of France, showing the number of occurrences ≥ 5 times (squares) and ≤ 2 times (circles) between 1987 and 2014. Source: Ifremer envlit

1.4. Study Site – Bay of Brest

Situated in North/West of France, the Bay of Brest (Fig 1.5) has an oceanic temperate climate and is characterized by a vast basin of 180km² (Le Pape and Menesguen, 1997). Its largest dimensions are 27km in the East/West direction and 11km in the North/South (Monbet and Bassoullet, 1989). This ecosystem has two principal continental river flows (the Elorn and Aulne rivers), a central zone and narrow estuaries such as Daoulas.

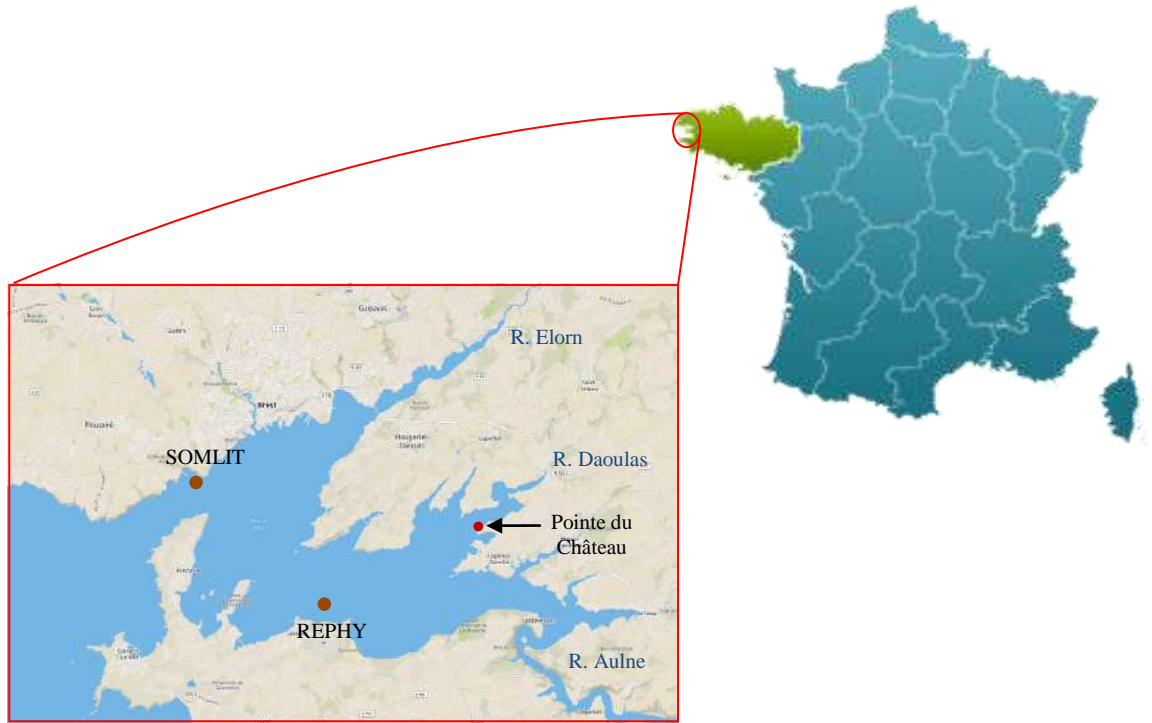


Figure 1.5: Bay of Brest showing study site, rivers and measurement stations

Intensive agricultural activities have made the Bay of Brest an ecosystem which is quite rich in nutrients (Chapelle et al 2015). These nutrients notably nitrogen and phosphorus have contributed to eutrophication in the region (Le Pape and Ménesguen, 1997) and some studies (Guallar et al., 2017; Sourisseau et al., 2017; Chapelle, 2016) have also been conducted as a result of *A. minutum* bloom in the summer of 2012 within the bay particularly at Pointe du Château. The maximum abundance of *A. minutum* has always been observed in this part of the bay (Daoulas estuary) compared to other locations and therefore, was assumed to be the location with population growth. Studies on its physical parameters (tide, residence time, nutrient exchanges and water temperature etc.) have been done with a hydrodynamic model (Le Pape and Ménesguen, 1997).

1.5. Modeling

Several mechanistic models for *Alexandrium* have been developed to explore interactions, population dynamics and water circulation and to identify the effect of physical processes on bloom development and transport across estuary (Fauchot et al., 2008; McGillicuddy et al. 2005). They can consistently reproduce past observations (He et al., 2008; Stock et al., 2005; Li et al., 2009) and are thus, proposed for weekly nowcasts and forecasts (looking forward 3 or 4 days) and even seasonal or annual forecasts (McGillicuddy et al., 2011). It is a useful tool or technique to unravel the growth rate and spread of *Alexandrium* blooms and takes into account the biotic and abiotic parameters which sustain and promote the development of species.

Various models have been developed to describe and investigate the physiology and bloom dynamics of phytoplankton (Flynn, 2005). Droop and Monod are two of such common models (Fig. 1.6). Although both models share the same interest, the Monod (1942) model linking growth directly to ‘extra-cellular’ nutrient concentrations is one of the simplest but it is poorly adapted to simulate growth dynamics with nutrient pulses. Although the idealizations and limitations of this approach have been criticized (e.g. Flynn 2003, Droop 2003), computational economy has been a significant motivation to use it extensively at global and regional scales (Haney and Jackson, 1996; Follows and Dutkiewicz, 2011) assuming that environmental variability at high frequency is not simulated.

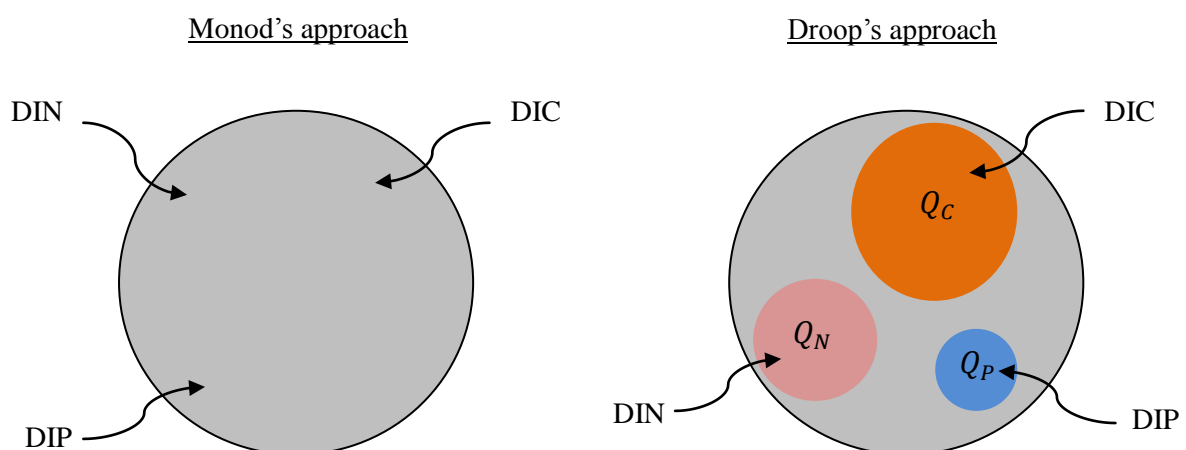


Figure 1.6: Monod and Droop approaches to phytoplankton physiology
Dissolved inorganic nutrients (DIP, DIN and DIC) and Quota (Q_P , Q_N and Q_C)
(Figure inspired by Follows and Dutkiewicz, 2011)

Alternatively, a more physiologically defensible (Grover, 1992, 1991), yet still highly idealized and not always accurate in many comparative studies (Flynn, 2005) is the Droop/Caperone ‘internal-stores’ approach (Droop 1968, Caperone 1968). It links growth to the internal nutrient pool (or quota) and provides a hyperbolic form of the growth curve using only two parameters – the minimum quota to sustain growth and a maximum theoretical growth rate at infinite quota. The decoupling between substrate uptake and growth via the internal store or quota (Q) of each biogeochemical cycle enables variation in the elemental ratios of organic matter in response to fast environmental changes (Thingstad & Pengerud 1985, Martinussen & Thingstad 1987) and a better capacity to simulate the resulting competition (Sunda et al., 2009; Grover, 1992; Smith, 1997).

1.6. Aims of the study

Alexandrium minutum has continued to proliferate in the region Bretagne ever since it was observed in 1988. Its presence leads to a ban on aquaculture activities, tourism and restrictions on the sale and consumption of sea food, all of which have negative economic consequences on the region. We focused on the Daoulas estuary which has so far experienced the maximum abundances and levels of toxicity in the bay as recorded in the French National Phytoplankton and Phycotoxins survey – REPHY (Réseau d'Observation et de Surveillance du Phytoplancton et des Phycotoxines). By doing this, we attempted to address the following questions -

- How does *A. minutum* out-compete other species? Does bloom occur under identical or different environmental conditions?
- What fraction of the seasonal and interannual variations at a decade scale in the abundance of species is explained by abiotic factors and resource competition?
- What parameters control species selection and phenology at seasonal scale and how do we place them in order of hierarchy?

To answer these questions, we surveyed and analyzed field data (abundance of species, temperature and concentration of nutrients) obtained from the study site (Daoulas estuary) since 2009-2018 and integrated them with a numerical model.

Chapter 2

In Situ Data Survey

2.1. Data Acquisition Strategy

The consequences of *A. minutum* bloom outbreak (2012) in the local economy triggered a long-term survey (*Alex-Breizh*), complementing already existing surveys (REPHY, SOMLIT and VELYGER). This bloom was followed by other blooms of less importance in subsequent years. As shown in figure 2.1, *A. minutum* abundances exhibited a very high spatial variability, with one hot spot located in the river of Daoulas. In this area, Pointe du Château was chosen for data acquisition.

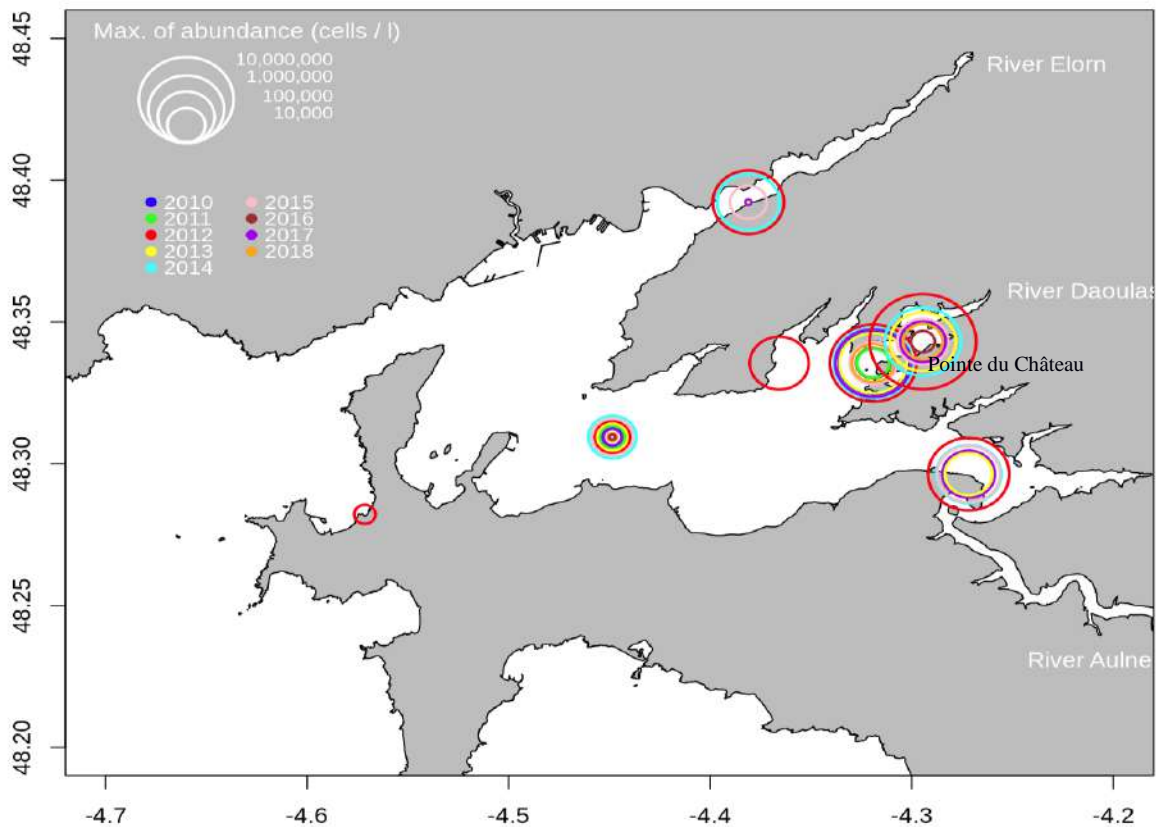


Figure 2.1: Maximum abundances of *A. minutum* recorded between 2010 and 2018 in the Bay of Brest. Data source: REPHY, VELYGER, modified and completed after Sourisseau et al., 2017.

Note that the circles are proportional to the log-scale presented and not to the absolute abundance values

2.1.1. Sampling Protocol (*Alex-Breizh*)

Nutrient concentrations and the composition of phytoplankton community were obtained from *Alex-Breizh*, a weekly sampling project that was launched in 2016. Water samples were collected at Pointe du Château (48.3350°N, -4.3194°W) at high tides ± 2 hours, at sub-surface using Niskin bottles and kayak. Samples were further analyzed in the laboratory. Determination of the abundances of species was performed by optical microscopy (for the microphytoplankton) and cytometry (CytoSub-CytoBuoy flow-cytometer with laser excitation at 488nm, for pico- and nano-phytoplankton size classes). Dissolved inorganic nutrient concentrations were analyzed following the method of Aminot and K  rouel (2004), with fluorimetry for ammonium (NH₄), and colorimetry for nitrate (NO₃), phosphate (PO₄) and silicate (Si(OH)₄). Same method was used to analyze Chlorophyll *a* concentrations with fluorimetry after acetone extraction and suspended matter (MES) using gravimetry. Water temperature and salinity were measured using a VTW-LF320 thermo-salinometer.

Alex-Breizh project was complemented by Daoulex monitoring (2013-2015) and the VELYGER monitoring program (water sampling for phytoplankton abundances by optical microscopy, as well as high-frequency survey of water temperature, salinity, pH, turbidity and chlorophyll *a*) which is dedicated to studying the factors that control oyster growth in the Bay of Brest since 2009. Sampling protocol and materials are written in French.

<u>Nutriments</u>	<u>Cytom��trie</u>	<u>Autres</u>
Flacon 15ml (pour Si)	Pipette P5000 Gilson	Support d'��criture
Flacons 60ml (pour NH ₄ ,NO ₃ et PO ₄)	C��nes de 5 ml	Feuille de terrain
Seringues 50ml	Cryotubes pr��-remplis avec Gluta et pluronic	��tiquettes/rouleau adh��sif
Filtre minisarts 0.22��m	Boite cartonn��e pour mettre les ��chantillons	Feutres/Marqueurs
Filtre Swinnex 200��m	Falcon de 50ml	Gants non poudr��s
	Entonnoir	2 bouteilles Niskin
<u>Abondance (microphyto)</u>	Pr��-filtre en nylon de 150 �� 200��m	Gilet de s��curit��
Doses de 1ml Lugol		Parapluie
Flacons de 1L et 500 mL	<u>Pigments (Chlorophylle fractionn��e)</u>	GPS/Camion
	Flacon de 1 litre	1 Bidon 5L
<u>Pr��l��vements terrains</u>	<u>Temp��rature/Salinit��</u>	Pains de glace /l'eau MilliQ
Speedoo	Sondes	Glaci��res 1 et 2, avec et sans produits toxiques
Kayak		

Table 2.1: List of *Alex-Breizh* field sampling materials

List of tasks to be completed immediately after sampling (return at land)

Pour salinité et température,

- Tremper la sonde T/S dans le reste de l'échantillon.
- Noter sur la fiche terrain la température et la salinité mesurées.
- Rincer la sonde utilisée avec de l'eau MilliQ

Pour nutriments,

- Préfiltrer l'eau de mer pour éliminer le zooplancton avec filtre 200µm
- Rincer les 2 flacons de 60ml 3 fois puis les remplir aux $\frac{3}{4}$.
- Rincer la seringue de 50ml en prélevant un peu d'eau de mer puis en la vidant.
- Prélever de l'eau de mer, fixer le minisart et le rincer en évacuant les premières gouttes.
- Rincer le flacon de 15 ml 3 fois avec l'eau de mer filtrée puis le remplir jusqu'à la gorge.
- Stocker les flacons nutriments debout dans la glacière N°2 jusqu'au laboratoire.

Pour chlorophylle et taxonomie pigmentaire,

- Sous-échantillonner dans les flacons de 1L et 0.5L. Mettre au frais et à l'abri de la lumière.

Pour abondance,

- Remplir 1 flacon avec 500mL d'eau de mer prélevé et ajouter une dose de lugol (1ml).
- Homogénéiser et stocker dans la glacière N°1.
- Remplir 1 flacon avec 500mL d'eau de mer prélevé dans 1 flacon de 1L pour comptage au laboratoire du phytoplancton frais.

Pour échantillons cytométrie,

- Identifier les 3 tubes (contenant le gluta et pluronic) avec la date et l'heure de prélèvement.
- Avec le filtre Swinnex de 200µm, échantillonner 50ml d'eau de mer dans un tube Falcon rincé.
- Immédiatement après, prélever dans le Falcon et remplir un cryotube avec 1.5ml. Remplir deux cryotubes avec l'eau de mer sans pré-filtrer. Agiter par plusieurs renversements.
- Les 3 cryotubes sont ensuite maintenue à l'obscurité, à température ambiante et stockés dans la glacière N°1. La congélation peut attendre le retour au laboratoire.

Pour les matières en suspension (MES),

- Mettre directement le bidon dans la glacière N°2

2.1.2. Laboratory Protocol

Filtration –

Chlorophylle fractionnée: Filtrer à l'abri de la lumière, à moins de 150mmHg.

- Chlorophylle totale: Filtrer environ 100 à 150 ml d'eau sur un filtre GFF (porosité 0.7 μm) de diamètre 25 mm. Le volume filtré doit être adapté à la charge en particules, ne jamais colmater le filtre, il doit être à peine coloré. Placer le filtre dans une boîte de Pétri de diamètre 52 mm, scotcher. Noter la date, CHLT et le volume filtré.
- Chlorophylle > 3 μm : Filtrer environ 100 à 150 ml d'eau sur un filtre de 25 mm de diamètre et porosité 3 μm . Le volume filtré doit être adapté à la charge en particules, ne jamais colmater le filtre, il doit être à peine coloré. Placer le filtre dans une boîte de Pétri de diamètre 52 mm, scotcher. Noter la date, CHL>3 μm et le volume filtré.
- Chlorophylle < 20 μm : Filtrer environ 100 à 150 ml d'eau sur 2 filtres en série, le premier filtre de diamètre 47 mm a une porosité 20 μm , le second placé dessous a une porosité de 0.7 μm (GFF) et un diamètre de 25 mm. Le volume filtré doit être adapté à la charge en particules, ne jamais colmater le filtre, il doit être à peine coloré. Placer le filtre GFF dans une boîte de Pétri de diamètre 52 mm, scotcher la boîte. Noter la date, CHL<20 μm et le volume filtré.
- Reporter les volumes filtrés et les porosités sur la fiche terrain

Taxonomie pigmentaire: Filtrer à l'abri de la lumière, à moins de 150mmHg.

- Filtrer environ 1 litre d'eau sur filtre 0.7 μm (GFF) de diamètre 47 mm, ne pas colmater le filtre, noter le volume filtré. Placer le filtre dans un cryotube et congeler à -80°C.

Matières en Suspension (MES)

- Homogénéiser l'échantillon en agitant fortement.
- Mesurer le volume à filtrer à l'aide d'une éprouvette.
- Placer un filtre (GFF) de diamètre 47 mm et le centrer sur le dispositif de filtration
- Verser l'échantillon sur le filtre puis appliquer le vide, sans créer une dépression supérieur à 0.2 bar. Filtrer progressivement tout le volume mesuré, en veillant à ne pas amener le filtre à sec avant la fin de la filtration.

- Dès que le filtre est à sec, ramener à pression normale. Rincer les parois de la tulipe avec 10 à 20ml d'eau déminéralisée puis remettre le système en dépression pour aspirer cette eau. Rincer une seconde fois de la même manière.
- Tout en maintenant l'aspiration sous vide, retirer l'entonnoir de filtration puis, à l'aide d'une pissette d'eau déminéralisée, rincer avec le plus grand soin la couronne du filtre qui était pincée entre la base et la tulipe du dispositif de filtration. Cette opération doit durer 20 à 30 secondes et nécessite 20ml d'eau environ. Terminer en rinçant à nouveau la totalité de la surface du filtre en la balayant de plusieurs fois avec le jet de la pissette (10-20 ml).
- Ramener à pression normale et remettre chaque filtre dans sa boîte numérotée.

Stockage des échantillons -

- Cyto et pigments: Les échantillons sont à congeler dans l'azote liquide si possible puis à stocker au -80°C dans la boîte prévu à cet effet.
- Abondance phytoplancton: L'échantillon fixé est stocké au réfrigérateur (4°C)
- Chlorophylle fractionnée: Les 3 boîtes contenant les filtres seront conservées à -20°C.
- Nutriments: Flacon de 60ml au congélateur (-25°C) et celui de 15ml au réfrigérateur (4°C)
- MES: Mettre les boîtes au frais et à l'abri de la lumière et conserver à -20°C

Maintenance rinçage des appareils -

- Les flacons utilisés ainsi que les soies, le porte-filtre et les poches de prélèvement sont à rincer à l'eau milliQ et à mettre à sécher. Les poches peuvent être mises dans une étuve.
- Ne pas oublier de rincer et de sécher à l'étuve la verrerie utilisée pour les filtrations.
- Bien rincer l'extérieur du kayak avec de l'eau douce après chaque sortie.

2.1.3. Available Data

The adopted data acquisition strategy together with the VELYGER monitoring program, gave rise to a number of data. All parameters were not recorded all along the time series. Indeed, nutrient analysis and chlorophyll *a* began in 2013, the year after the major *Alexandrium minutum* bloom and 2013, 2014 and 2015 were sampled only from May to August in a location 500 meters from Pointe du Château up to the river (River Daoulas station, Daouléx project). Nutrients at Pointe du Château and the use of flow-cytometer to determine pico and nanophytoplankton abundances began in 2016. Table 2.2 gives a resume of the different parameters time-series and the number of samples analyzed.

	Year	Abundance					Tempe.	Salinity	Nutrients			
		<i>Alex</i>	Pico	Nano	Micro	Chl a			NH ₄	NO ₃	PO ₄	Si
Availability	2009	✓	x	x	✓	x	✓	✓	x	x	x	x
	2010	✓	x	x	✓	x	✓	✓	x	x	x	x
	2011	✓	x	x	✓	x	✓	✓	x	x	x	x
	2012	✓	x	x	✓	✓	✓	✓	x	x	x	x
	2013	✓	x	x	✓	✓	✓	✓	✓	✓	✓	✓
	2014	✓	x	x	✓	✓	✓	✓	✓	✓	✓	✓
	2015	✓	x	x	✓	✓	✓	✓	✓	✓	✓	✓
	2016	✓	✓	✓	✓	✓	✓	✓	✓	✓	✓	✓
	2017	✓	✓	✓	✓	✓	✓	✓	✓	✓	✓	✓
	2018	✓	✓	✓	✓	✓	✓	✓	✓	✓	✓	✓
Number of data	2009	14	-	-	31	-	-	31	31	-	-	-
	2010	16	-	-	40	-	-	40	40	-	-	-
	2011	7	-	-	38	-	-	38	38	-	-	-
	2012	20	-	-	37	20	-	37	37	-	-	-
	2013	22	-	-	33	31	-	33	33	13	13	13
	2014	27	-	-	38	35	-	37	37	26	26	26
	2015	27	-	-	35	34	-	35	35	23	23	23
	2016	30	42	42	57	42	-	59	59	42	42	42
	2017	25	42	42	55	41	-	56	56	42	42	42
	2018	11	28	28	37	22	-	48	48	37	37	37

Table 2.2: Availability and frequency of *in situ* data of *Alex-Breizh* project at Pointe du Château. Nutrient concentrations between 2013 and 2015 were sampled at river Daoulas station.

In addition to the data obtained in *Alex-Breizh* project, there are also measurement stations e.g. SOMLIT-Portzic and REPHY-Lanveoc (Fig. 1.5) in the Bay of Brest that provide nutrient and environmental data on daily, weekly or monthly basis.

	Variable	Source	Availability	Frequency	Reference
Inorganic nutrients	In Daoulas river	BMO	2009 to 2018	Monthly	rade.brest.fr
	At Portzic station	SOMLIT		Weekly	-
	At Lanveoc station	REPHY		-	-
Organic nutrients	In Daoulas river	Slope function (PO ₄)		-	Andrieux-Loyer, F. 2008
		BMO (NH ₄)		-	rade.brest.fr
	In the Bay	SOMLIT		-	-
Others	Irradiance (PAR)	METEOSAT		Daily	Le Borgne et al. 2006
	River flow	HYDRO			hydro.eaufrance.fr
	Dilution	3D Model			Guallar et al. 2017
	Hydrology	MARS3D			Lazure and Dumas, 2008
	Weather conditions	Météo-France			Seity et al. 2011
	Kpar	OSI-SAF			Gohin et al. 2005
	Microphytoplankton	REPHY		-	-
	Tidal coefficient	VELYGER	2014-2018	-	Pouvreau et al. 2016

Table 2.3: Supplementary *in situ* data

BMO: Brest Metropole Océane ; SOMLIT: Service d'Observation en Milieu Littoral ; OSI-SAF: Satellite Application Facility on Ocean and Sea Ice ; REPHY: Réseau d'Observation et de Surveillance du Phytoplancton et des Phycotoxines ; VeLyGer: obserVer anaLyser et Gérer, Observatoire de la reproduction et du recrutement de l'huître en France ; Kpar: Light attenuation coefficient ; PAR: Photosynthetically Active Radiation

Furthermore, the renewal of water masses in Daoulas estuary was estimated. This renewal (hereafter called Dilution) depends on wind stress at surface, tides and river flow. It was first estimated between 2012 and 2014 using a hydrodynamic model (MARS3D, Lazure and Dumas, 2008) configured for the Bay of Brest at a resolution of 50 meters. For the other years (2009-2011 and 2015-2018), we used a multiple linear regression relationship found between the measured mean of daily wind speed, the log10 of river Daoulas daily mean flow, the tidal coefficient and the model derived Dilution (Guallar et al., 2017).

2.1.4. Data Analysis

Before analyzing all data, we considered their availability by year (2009 to 2018) and their availability by season (January 1 to December 31). For the seasonal variability of phytoplankton and environmental variables, the approach of Del Amo et al. (1997) was used to divide the annual cycle of the Bay of Brest into four seasons: Season I, Spring (March 1 to May 31); Season II, Summer (June 1 to August 31); Season III, autumn (September 1 to November 30); and Season IV, Winter (December 1 to February 28).

A Heatmap diagram is used to summarize the interannual variability of phytoplankton abundances, chlorophyll and nutrients concentrations. Here, each year is represented in a column and each variable is represented in a row. Scaled value (the color assigned to a variable) is a correlation distance or a normalization which is obtained by dividing the mean of each row by its standard deviation. Comparison can be made per variable per year for interannual variations.

To determine which years had wet or dry spring, the approach of Van-Rooy (1965) was used to analyze rainfall anomaly index (RAI). The same approach was equally used to determine light and temperature anomalies particularly for cold or warm spring. The following function was adopted:

$$\text{Daily anomaly, } D = \frac{X - \bar{N}}{\bar{N}}$$

Where X is the daily value of each year and
 \bar{N} is the average daily value between a range of several years e.g. 2006 to 2018 for temperature anomaly

The monthly anomalies, M, were then calculated as the sum of daily anomalies (D) for the corresponding month.

For the phenology of phytoplankton particularly *A. minutum*, we adopted the method of Rolinski et al. (2007). This method uses a Weibull function to determine, characterize and distinguish the different phases of *A. minutum* bloom. It was re-illustrated by Guallar et al. (2017).

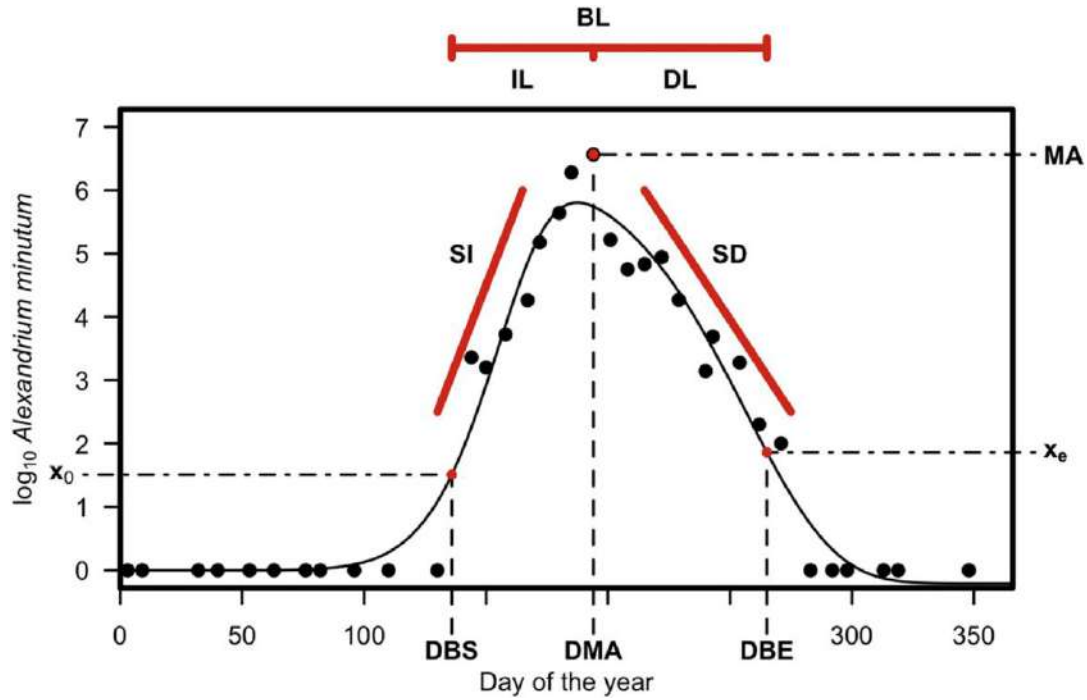


Figure 2.1b: Guallar et al. (2017) bloom analysis using Weibull. The curve is a Weibull function which is determined from observations - the points in black. Maximum abundance (MA), Date of MA (DMA), Date of bloom start (DBS), Date of bloom end (DBE), X_0 is the abundance at DBS, X_e is the abundance at DBE, Bloom length (BL), Increasing Length (IL), Decreasing Length (DL), Slope Increase (SI) and Slope Decrease (SD)

For the diversity of phytoplankton, over 109 taxa were recorded in the Bay of Brest during the study period. We retained only those whose annual maximum abundance (MA) is greater than 100 cells.L^{-1} (between 2009 and 2018) and classified them into three categories: $100 > \text{MA} < 1000$, $1000 > \text{MA} < 10000$ and $\text{MA} > 10000 \text{ cells.L}^{-1}$. The later were further grouped into diatoms and dinoflagellates (using REPHY classification standard) in order to overcome some of the difficulties associated with species identification (Hernandez et al., 2015). And the zooplankton were equally eliminated in order to strictly represent the phytoplankton.

2.2. Results of the Survey

2.2.1. Environmental variables

Environmental variables showed both intra (month to month) and inter-year variability (Figure 2.2). In the ten year period, anomalies calculated for the period of *A. minutum* bloom (May to August) show positive temperature anomalies in 2014 and 2018, negative anomalies in 2012; 2013 and 2016 except in the month of August. May 2011 was the hottest month of the time series followed by June 2017. The lowest overall temperature was recorded in 2013. Light anomalies varied greatly among the years. The summer period (May - August) exhibited neither consistent positive nor negative anomaly values. With river flow however, the anomalies are generally negative with a notable exception in year 2012 which was positive throughout the months. Year 2014 showed slight positive river flow anomalies while 2011 exhibited the lowest river flows in the time series.

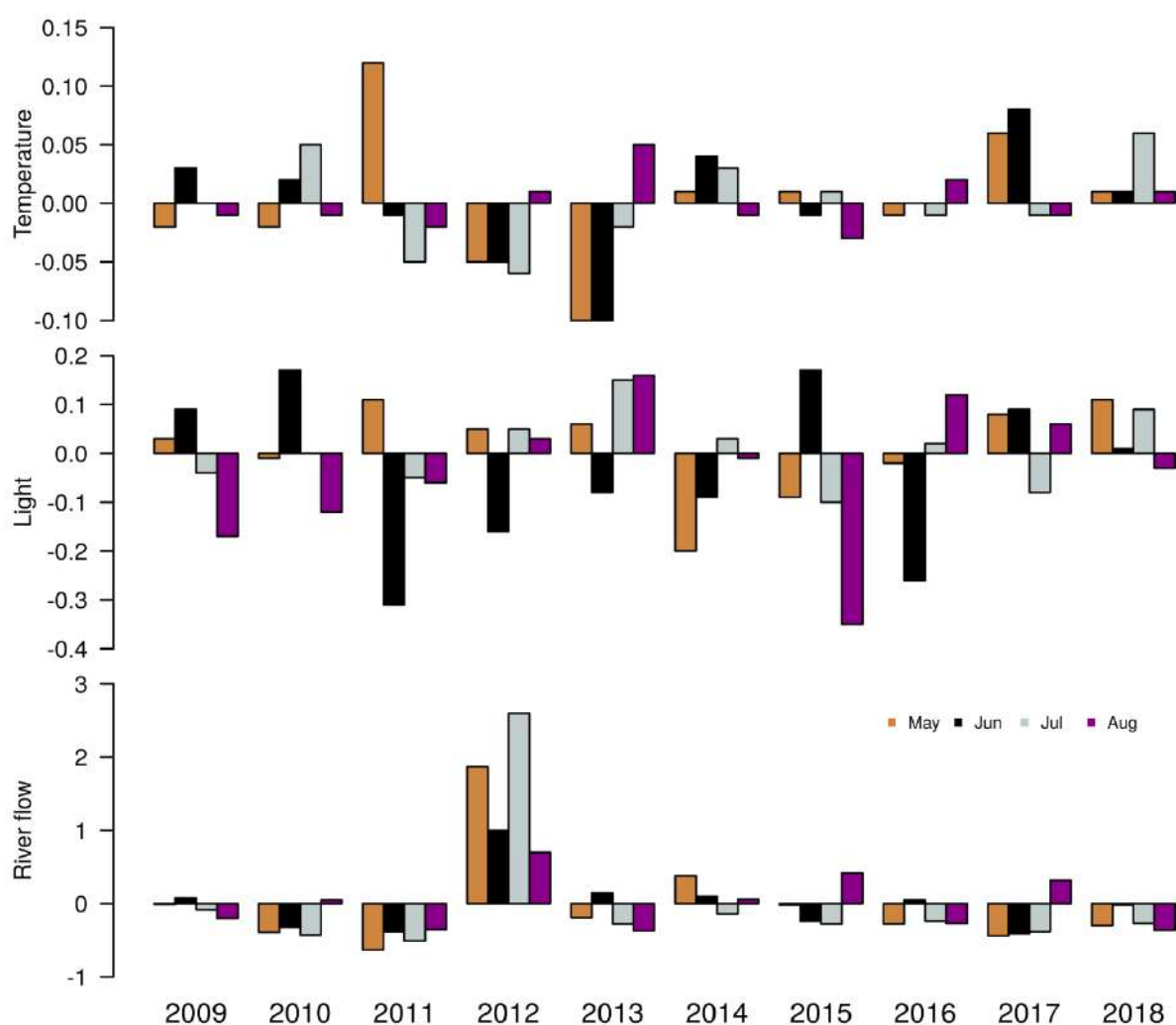


Figure 2.2: Interannual variability of environmental variables. Cumulative anomalies calculated in series for temperature (2006 – 2018), light (2000 – 2018) and river flow (1972 – 2018)

2.2.1.1. Daily temperature and light

As expected, temperature and light are highly correlated and showed similar seasonal variability (Figure 2.3). These two factors exhibit low values during winter and high values during the summer. Whatever the year considered, light for example was below $5\text{W}\cdot\text{m}^{-2}$ in winter and above $300\text{W}\cdot\text{m}^{-2}$ during summer though there were instances of very cloudy days when light fell below $5\text{W}\cdot\text{m}^{-2}$ during summer. Temperature on the other hand, was below 15°C between early November and end of March but remained above 15°C throughout the summer in most of the cases.

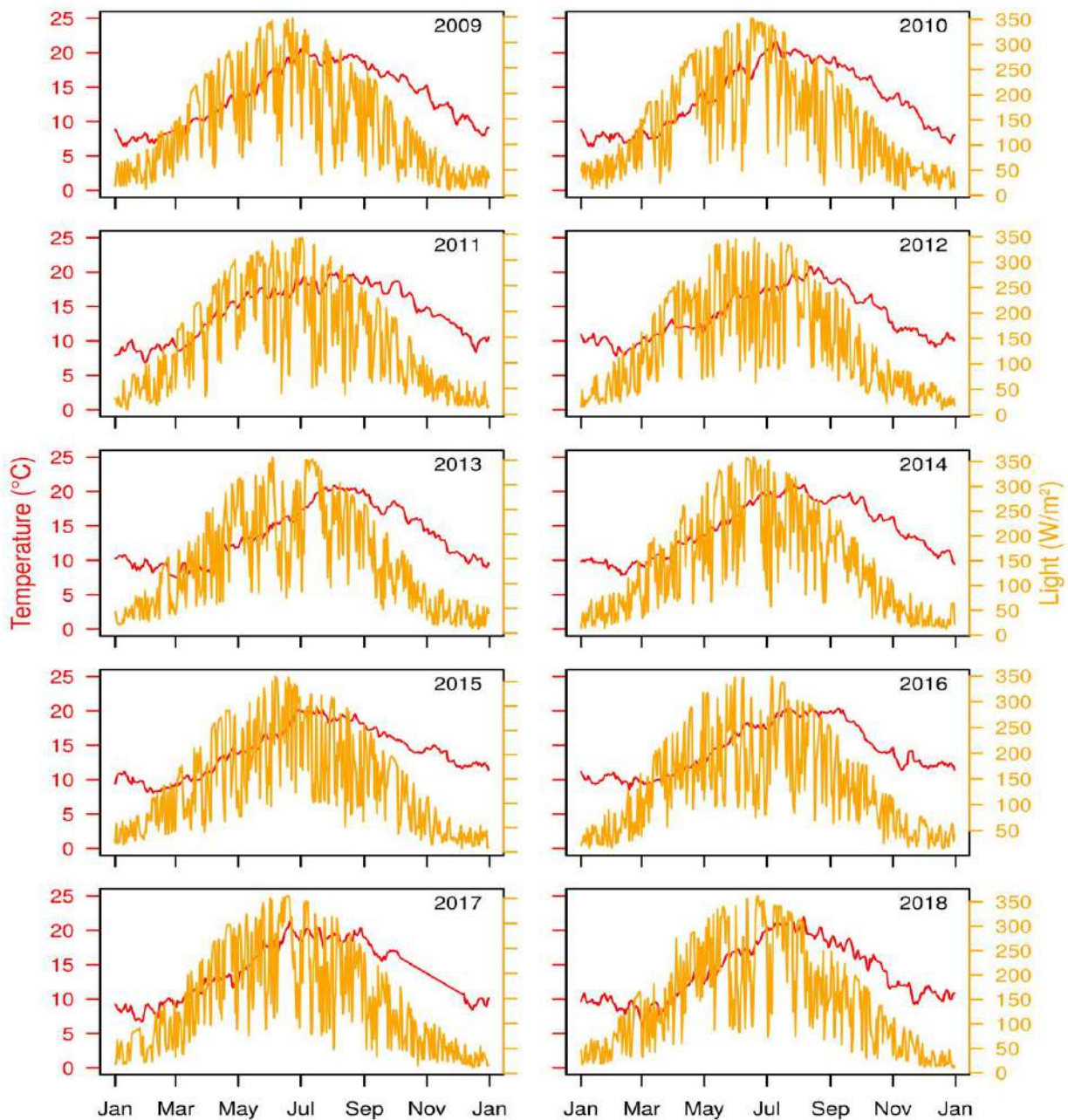


Figure 2.3: Daily temperature and light distribution over the study period

2.2.1.2. Daily river flow and salinity

River flows in Daoulas depend on rainfalls on the catchment area. Having high rainfalls in the winter and low in the summer, the Daoulas estuary is thus, characterized by high river inputs from November to March but less during the summer (Figure 2.4). As expected, salinity being influenced by river flow, we observed lower salinities between November and April when river flow is high and higher salinities between June and August when river flow is less.

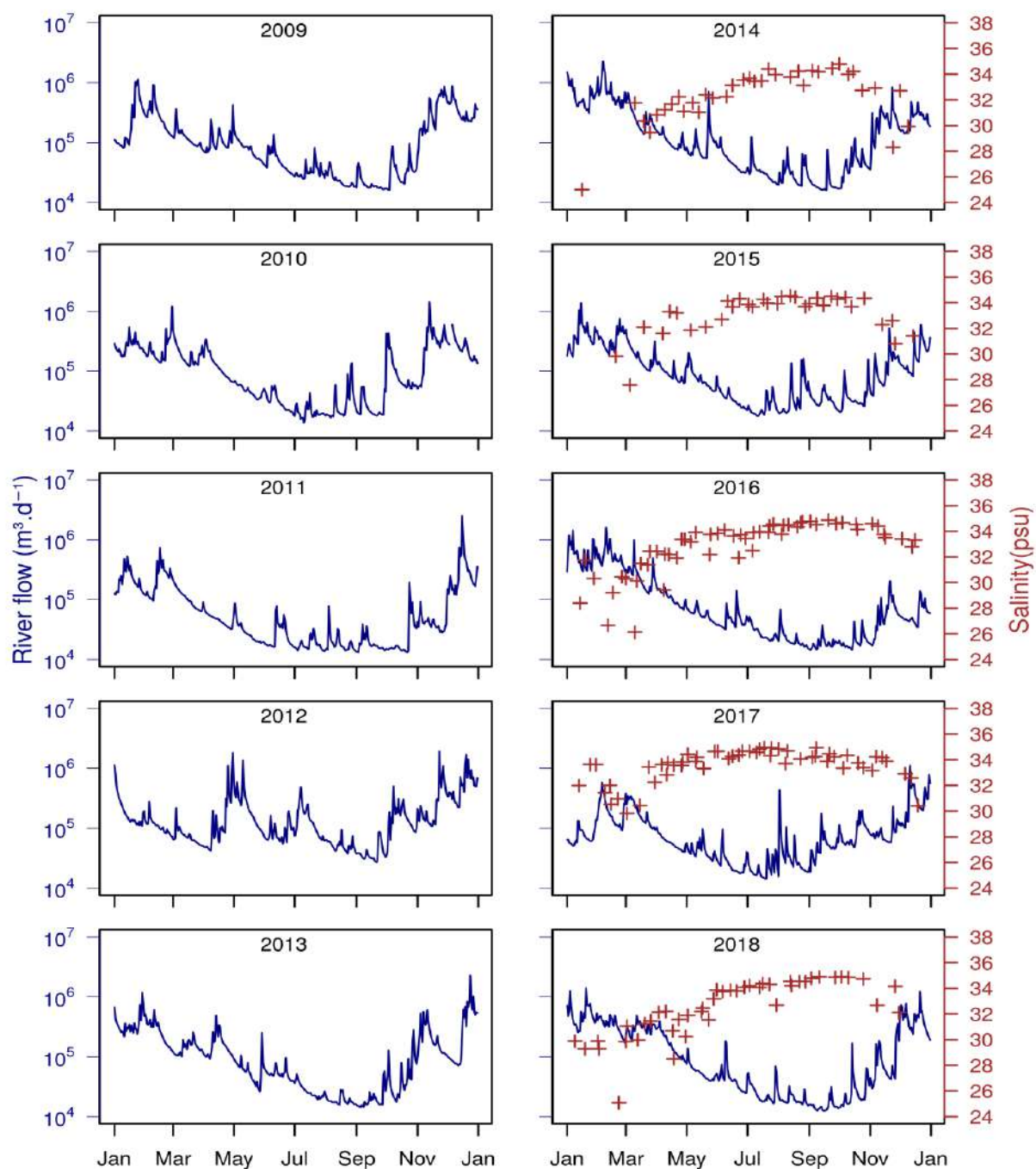


Figure 2.4: Daily river flow and salinity

2.2.1.3. Tidal coefficient and dilution

Tidal coefficient is a proxy for the tide amplitude (as a percentage of the highest amplitudes ranked 120 and the lowest possible amplitude ranked 20). It draws out the succession of spring and neap tides on a 14 day cycle (moon cycle) with maxima in the equinox between spring and autumn. Variations are not obvious seasonally but changes are observed on daily and weekly basis. Being influenced by tide, river flow and wind, dilution showed a similar seasonal behavior to river flow i.e. low dilution rates in the summer but much higher rates in the winter and a 14 day cycle linked to tides (higher dilution for spring tides).

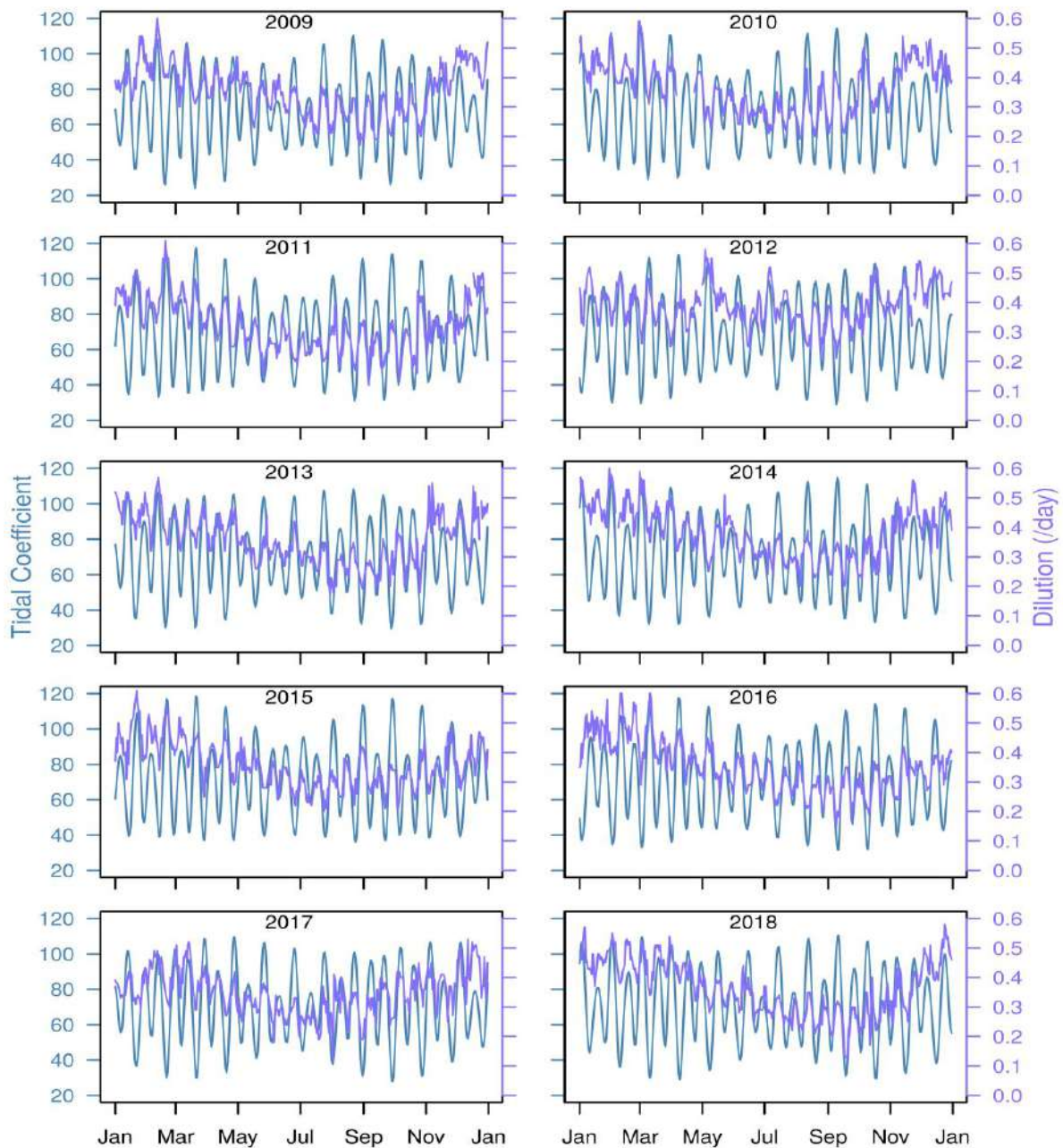


Figure 2.5: Tidal coefficient and dilution

2.2.1.4. Nutrients

The concentrations of all nutrients varied from one season to another. As expected in temperate north hemisphere, we observed high concentrations during the winter (between December and February), a decreasing trend in spring, low concentrations in summer and an increasing trend in autumn (Fig. 2.6).

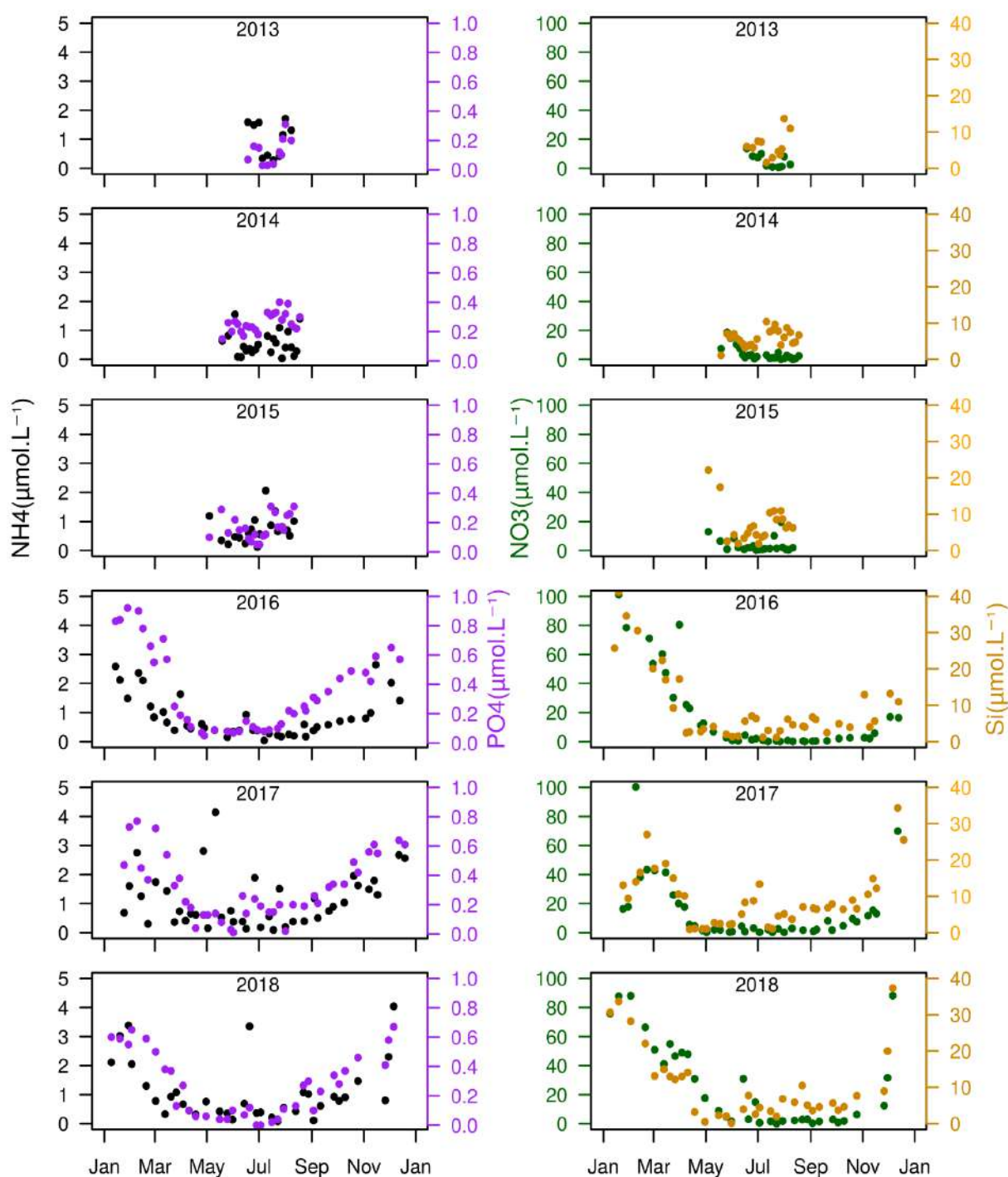


Figure 2.6: Concentration of inorganic nutrients in river Daoulas (2013-2015) and Pointe du Château (2016-2018)

When looking at the summer periods (2013 to 2018), minimum phosphate concentrations were recorded in 2018 while maximum summer concentrations were observed in 2014 but not at the same sampling points. Nitrogen in the form of NH_4 and NO_3 showed the highest summer concentrations in 2013 and the lowest in 2014. The minimum silicate summer concentration was recorded during 2017 and the highest in 2015.

	2009	2010	2011	2012	2013	2014	2015	2016	2017	2018
NH_4	-	-	-	-	0.28	0.04	0.12	0.04	0.09	0.08
NO_3	-	-	-	-	0.75	0.01	0.33	0.08	0.11	0.02
PO_4	-	-	-	-	0.030	0.150	0.050	0.050	0.013	0.004
Si(OH)_4	-	-	-	-	1.59	1.10	1.83	1.17	0.89	0.14

Table 2.4: Minimum concentrations (in $\mu\text{mol.L}^{-1}$) of inorganic nutrients in river Daoulas (2013-2015) and Pointe du Château (2016-2018)

2.2.1.5. Chlorophyll a

Phytoplankton possess *Chl a* pigments whose concentration in the ecosystem increases with increasing abundance of species. As shown in figure 2.7, we measured a relatively low and stable concentration (around $1\mu\text{g.L}^{-1}$) in the winter but an increase during the summer (above $13.9\mu\text{g.L}^{-1}$ in 2012) when phytoplankton growth occurs. Lowest values were detected between November and March whereas the highest values occurred between mid-April and end of July. Year 2012 recorded the highest value followed by 2018 whereas 2017 and 2016 had the lowest values (Table 2.5).

	2009	2010	2011	2012	2013	2014	2015	2016	2017	2018
<i>Chl a</i>	-	-	-	13.92	7.41	7.55	10.35	4.26	3.41	11.38

Table 2.5: Maximum concentration of chlorophyll a

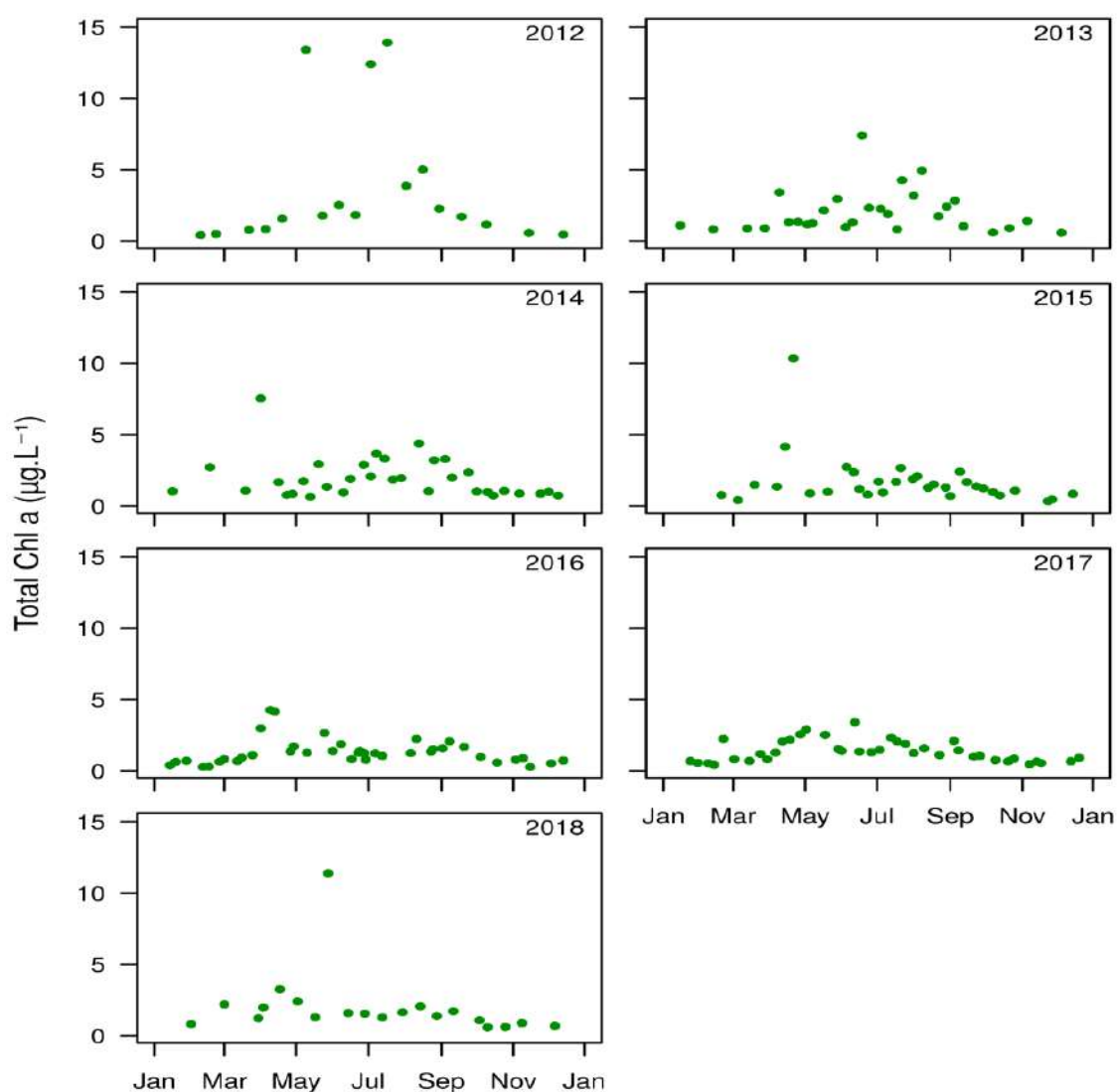


Figure 2.7: Concentration of Chlorophyll a from 2012 to 2018

2.2.2. *Alexandrium minutum*

Only the abundances greater than 100cells.L⁻¹ were taken into account following the detection threshold of REPHY monitoring program. From November to March, this threshold was never reached in Pointe du Château station. *A. minutum* begins to emerge in April but it is more obvious in May when abundance starts to increase. As a general pattern, maximum abundance (MA) is attained between June and August after which it begins to decrease until the end of October (Table 2.6 and Fig. 2.8). Though few data were available for certain years, extremely high MA is observed in 2012 and 2014. Lowest MA occurred in 2011 and 2016. The date of MA (DMA) is an important parameter for bloom analysis. Over the years, all MAs occurred in July except an early occurrence in 2011 (May) and late occurrence in 2016 (August) - these two years also had the lowest MA. Both years equally showed early bloom start and late bloom end. More than 10000cells.L⁻¹ were observed in eight of the ten years and 100000cells.L⁻¹ were exceeded in five different years (2010, 2012, 2013, 2014, 2017) with a bloom duration of 12 days (2010) to 26 days (2014).

Year	Actual Data		Weibull Data					
	MA	DMA	Bloom Start	Bloom End	Start Abund.	End Abund.	Bloom Duration	Cumulat. Abund.
2009	15 400	Jul 31	Jun 30	Aug 08	1 426	4 512	37	203 249
2010	432 600	Jul 5	Jun 27	Jul 10	78 547	100 808	12	2 875 937
2011	5 100	May 27	Apr 17	Dec 06	1 580	2 649	339	84 824
2012	3 675 330	Jul 12	Jun 27	Jul 18	336 041	920 348	23	41 336 152
2013	358 400	Jul 22	Jul 02	Jul 16	5 782	13 484	15	333 130
2014	1 496 480	Jul 22	May 29	Jun 24	21 552	71 614	26	2 783 118
2015	68 800	Jul 31	May 30	Sep 08	4 493	16 331	101	857 668
2016	6 000	Aug 10	Mar 02	Dec 25	202	298	346	11 135
2017	968 400	Jun 12	Jun 01	Jun 18	59 916	107 694	18	3 759 309
2018	17 500	Jul 23	Jun 28	Jul 14	963	1 192	16	38 196

Table 2.6: Bloom phenology of *Alexandrium minutum*

Weibull data show that the abundance of *A. minutum* at bloom end is always higher than the abundance at bloom start. Years 2009, 2012, 2013, 2014 and 2015 have bloom end abundances that are more than double the start abundances. Other years showed close start and end abundances.

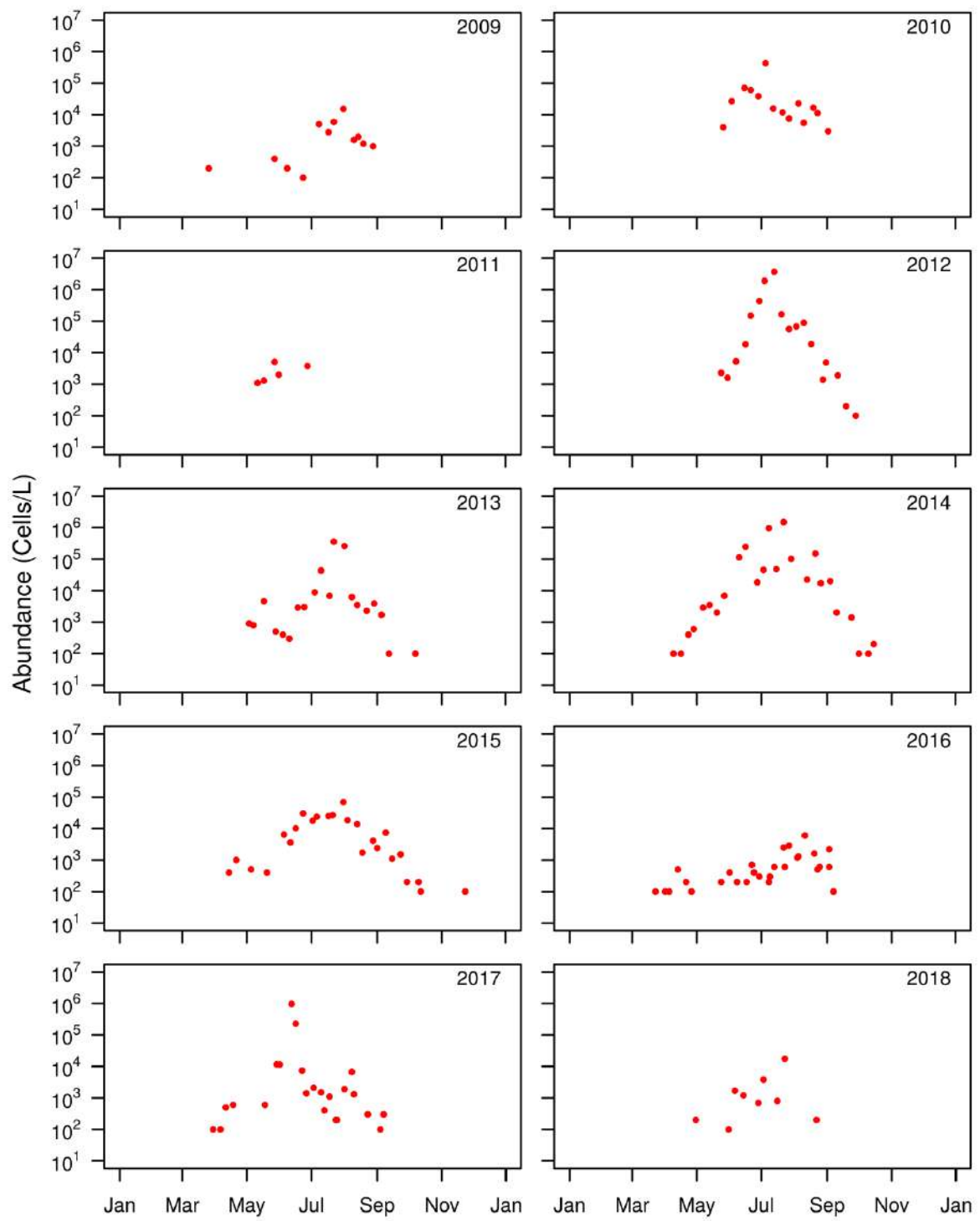


Figure 2.8: Abundances of *Alexandrium minutum*

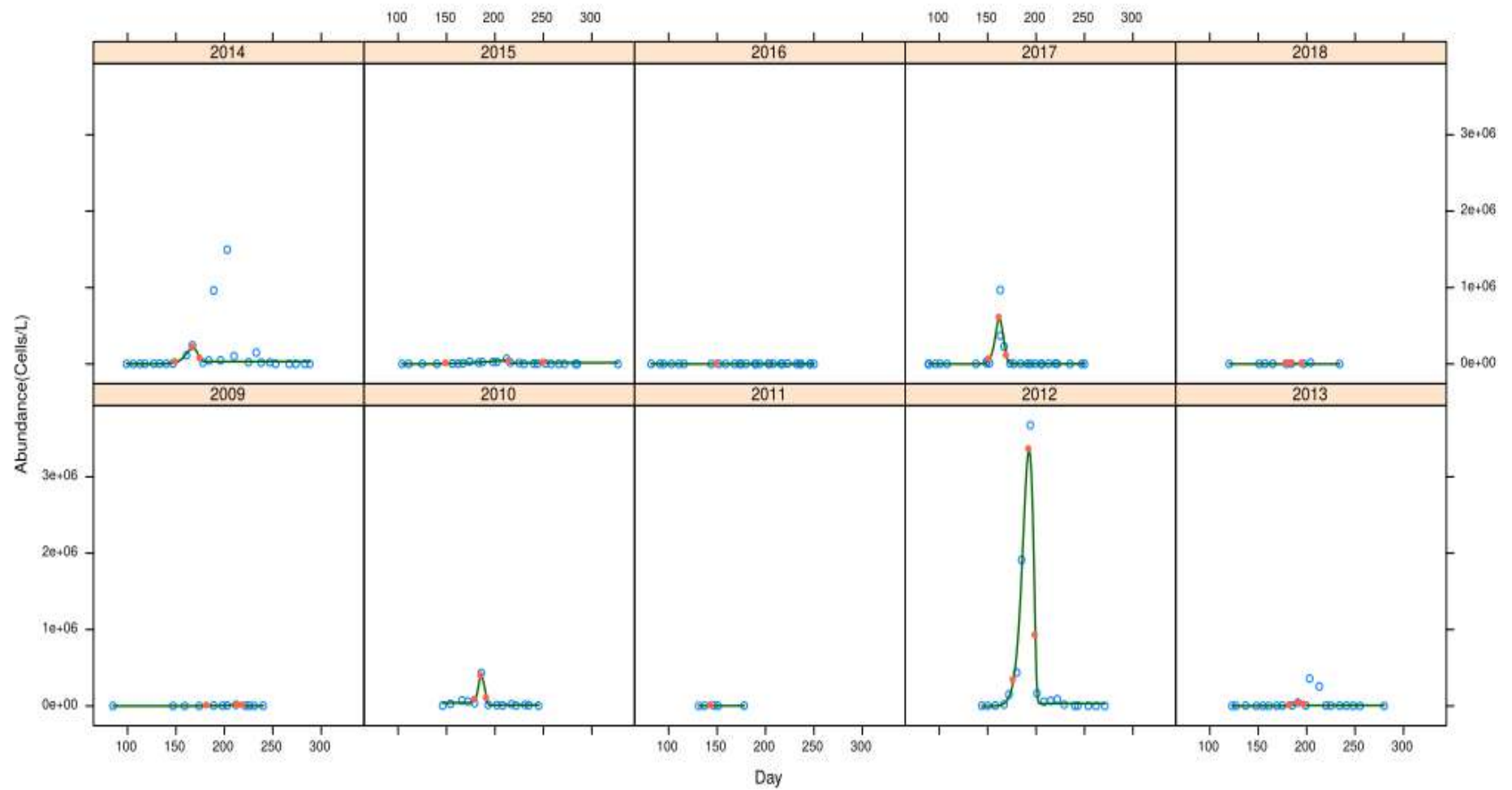


Figure 2.9: Weibull presentation of *Alexandrium minutum* abundances (blue dots). Green lines are the Weibull functions and the red points show the beginning, date of maximum abundance and end of bloom.

2.2.3. Phytoplankton

The abundance of each category (pico $\leq 2\mu\text{m}$, $2\mu\text{m}$ >nano< $20\mu\text{m}$ counted with flow cytometry and micro $>20\mu\text{m}$, counted with optical microscopy) of phytoplankton varied seasonally with low values in winter and high values in summer depending on the category. Results (Fig. 2.10) show that large cells (micro) are the first to experience growth in spring before smaller cells (pico and nano) and in most cases, the large cells also attain a maximum abundance before the smaller ones. Micro decreased quite rapidly in autumn while the abundance of pico can remain significant. Two micro spring/summer peaks are observable in 2010, 2012, 2014, 2016 and 2017 whereas other years have a single peak. Among the different categories, pico was observed to be more abundant than nano and micro throughout the seasons.

Interannually, between 2016 and 2018 (years of data availability for all categories), the highest MA of pico, nano and micro occurred in 2017. Over all years, micro recorded the highest MA in 2009 and lowest in 2016. Abundances at the beginning of bloom and at the end of bloom were similar from 2009 to 2015 and 2018 but 2016 showed higher bloom end abundance while 2017 showed lower bloom end abundance (Fig. 2.10). Pico and nano however showed higher bloom end abundance in 2018.

Year	Abundance		
	Pico	Nano	Micro
2009	-	-	4 909 700
2010	-	-	3 436 498
2011	-	-	1 841 408
2012	-	-	2 921 035
2013	-	-	4 490 923
2014	-	-	1 082 600
2015	-	-	1 579 687
2016	84 036 364	17 760 181	561 500
2017	99 594 046	19 052 774	2 676 800
2018	83 103 097	12 692 690	2 145 700

Table 2.7: Maximum abundance of phytoplankton

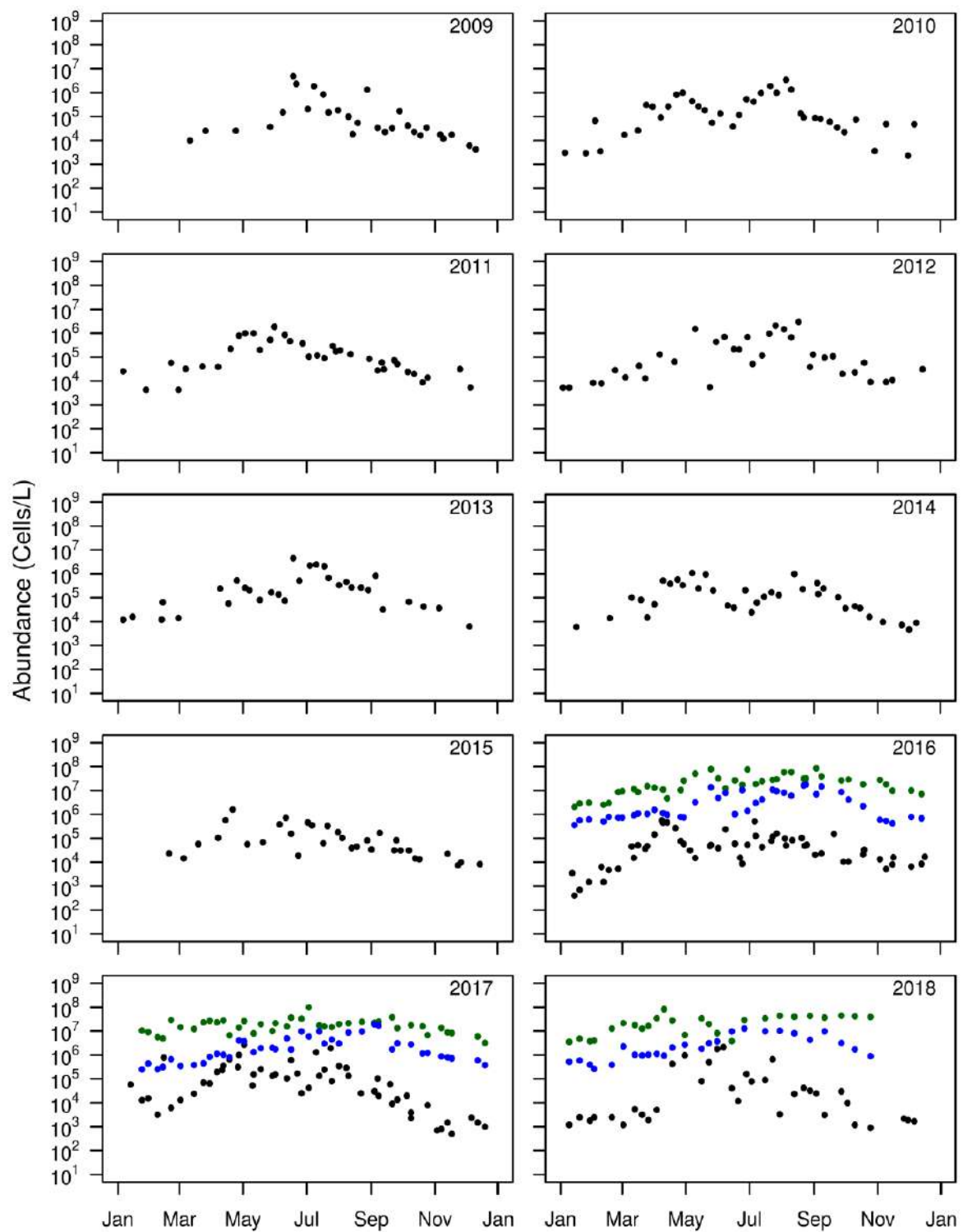


Figure 2.10: Abundance of phytoplankton by category.
Micro in black, nano in blue and pico in green

The interannual variability of phytoplankton, chlorophyll and nutrients is best described with scaled value patterns in a Heatmap diagram. It estimates the correlation distance (among years) in order to identify the cluster of rows of variables with similar patterns i.e. same score/color is assigned to years with similar values. Red corresponds to the year with the highest value while linen corresponds to a year with the lowest value. Shown in figure 2.11 are the minimum concentrations of nutrients, maximum of chlorophyll and abundance of phytoplankton.

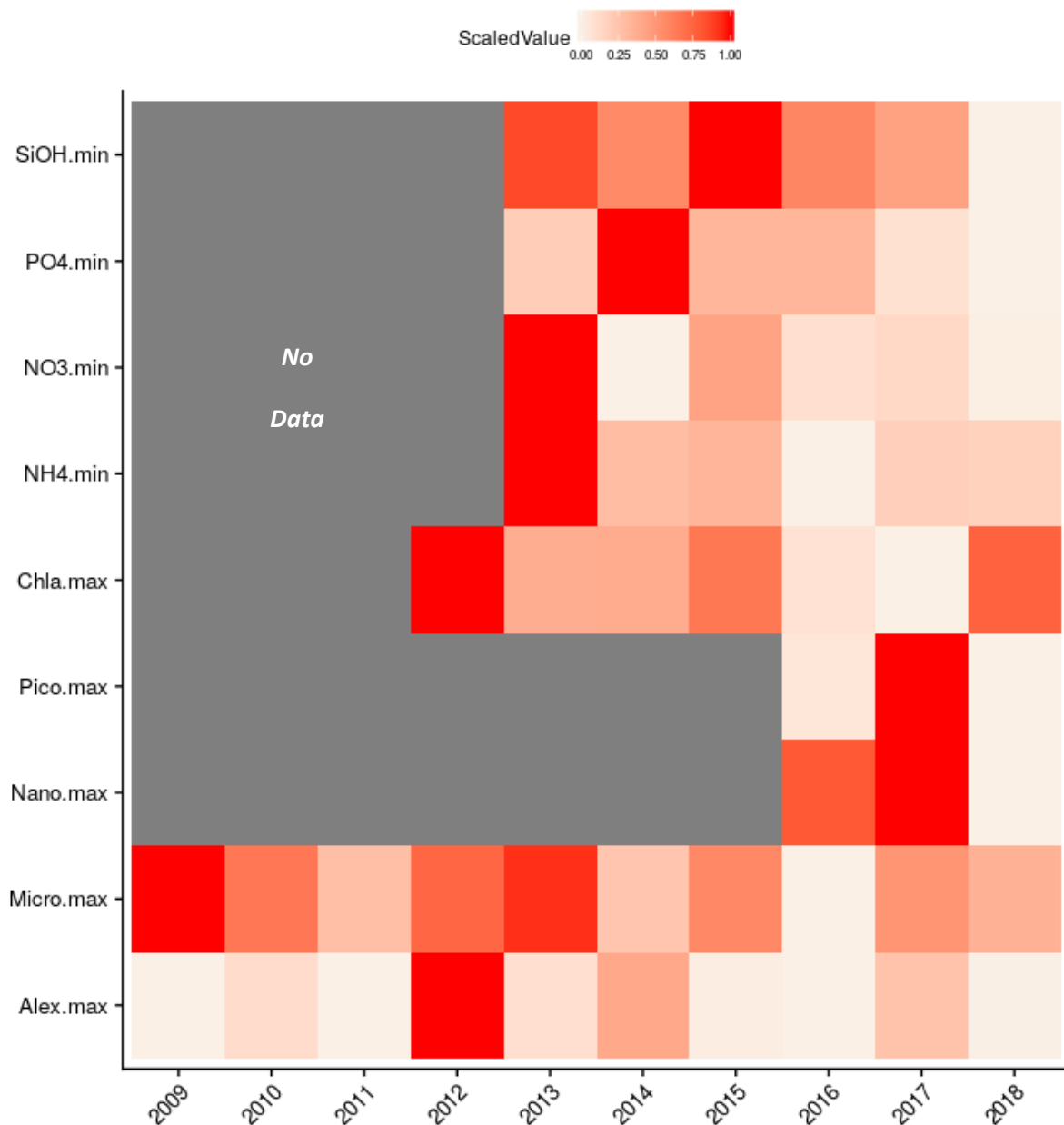


Figure 2.11: Heatmap diagram showing the interannual variations in field survey for minimum concentration of nutrients, maximum of chlorophyll and maximum abundances of phytoplankton

Nutrients: Although there are not enough data for some of the years studied, we found interannual variations in the minimum concentration of nutrients. Looking at the annual minimum concentrations on Heatmap, years 2013 to 2015 (sampled at river Daoulas) showed rather high scores (with 2013 housing the highest minimum concentrations) and, 2016, 2017 and 2018 (sampled at Point du Château) showed lower scores (with 2018 being the year with lowest minimum concentrations).

Chlorophyll: Higher *Chl a* concentrations were recorded between 2012 and 2015 (with the maximum score in 2012). These years correspond to periods of higher nutrient concentrations. In the same way, 2016 and 2017 exhibited low maximum (with 2017 showing the lowest score) but surprisingly, 2018 exhibited a high score even with quite low nutrient concentrations. This is probably due to a high value (above $10\mu\text{g.L}^{-1}$) recorded in May 2018.

Alexandrium minutum: During the study periods, higher abundances were recorded in 2012, 2014 and 2017. Other years especially 2011 and 2016 had very low abundances.

Phytoplankton community: The maximum abundance of micro was observed in 2009 followed by 2013. Similar MA occurred in 2010, 2012, 2015 and 2017 and the lowest score was in 2016. With visibility on the last three years (2016-2018) of study, pico and nano recorded their maximum abundances in 2017 although nano also had a significant abundance in 2016 and their minimum scores in 2018.

2.2.4. Phytoplankton Diversity

A. minutum is not the only species of phytoplankton that proliferates in the Bay of Brest. At least 109 taxons have been observed from 2009 to 2018. They correspond to species seen by optical microscopy i.e. above 10µm in Equivalent Spherical Diameter (ESD). With a minimum annual MA threshold of 100cells.L⁻¹, the taxons were classified into three categories: A, B and C, corresponding to 100≥MA<1000, 1000≥MA<10000 and MA>10000cells.L⁻¹ respectively (Table 2.8).

Focusing on category C (where *A. minutum* is found), the dominant taxon was the diatom *Chaetoceros* with MA of over 4.8×10^6 cells per liter in the ten year period. The least dominant taxon was *Ditylum brightwellii* (another diatom) whose MA was less than 13000 cells per liter.

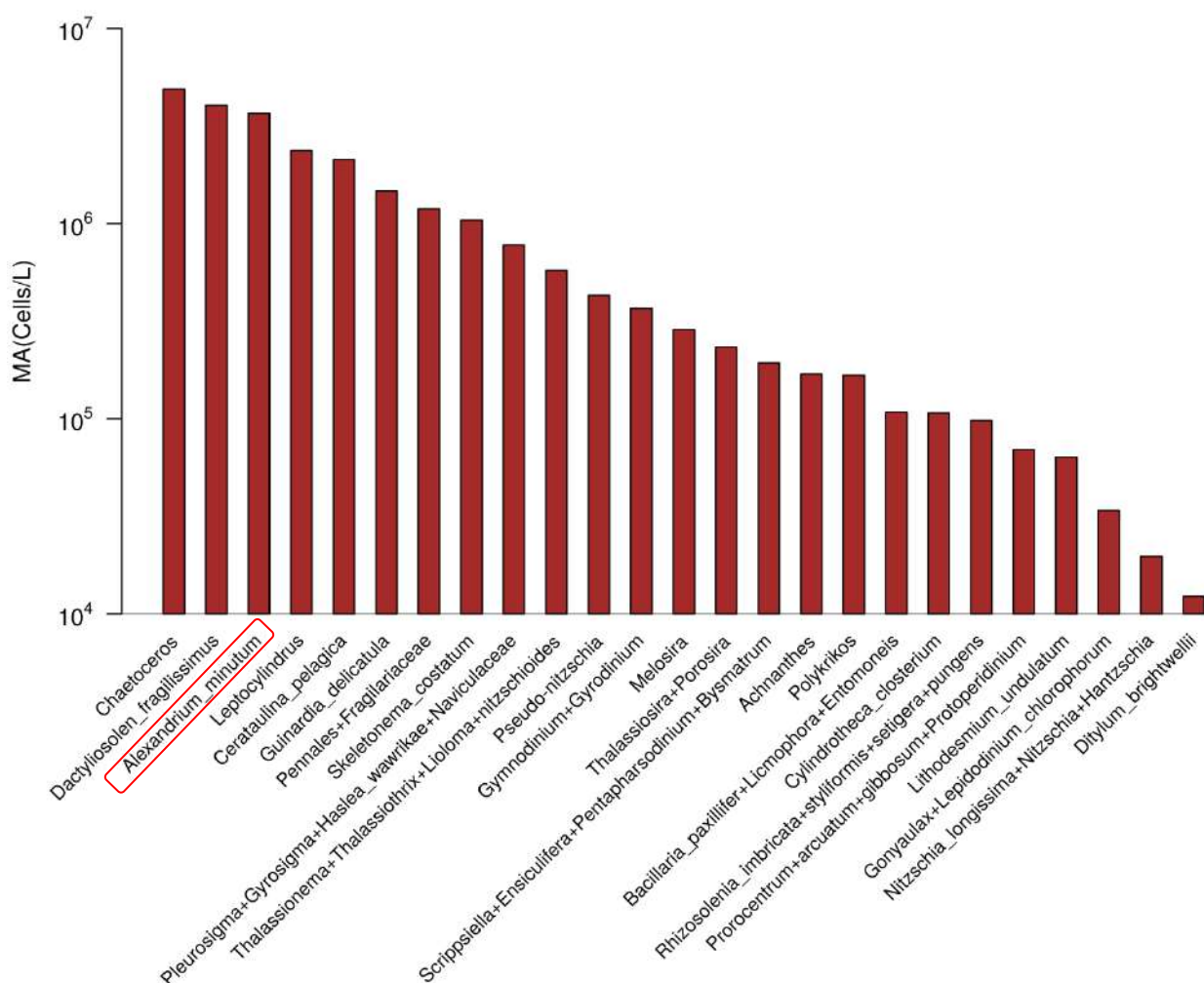


Figure 2.12: Most dominant taxa with maximum abundance greater than 10 000 cells per liter in Daoulas estuary (2009-2018)

Phytoplankton Diversity

Category A			Category B			Category C		
100 > Maximum Abundance < 1 000 Cells/L			1 000 > Maximum Abundance < 10 000 Cells/L			Maximum Abundance > 10 000 Cells/L		
Taxon	MA	Mean MA	Taxon	MA	Mean MA	Taxon	MA	Mean MA
<i>Pyrocystaceae</i>	800	700	<i>Paralia</i>	8 900	1 369	<i>Chaetoceros</i>	4 897 600	201 955
<i>Diatomophyceae</i>	700	450	<i>Fragilariaceae + Toxariaceae</i>	8 500	1 992	<i>Dactyliosolen fragilissimus</i>	4 040 223	76 927
<i>Scenedesmus</i>	700	157	<i>Dinophyceae</i>	7 600	1 001	<i>Alexandrium minutum</i>	3 675 330	73 597
<i>Eucampia + Climacodium</i>	600	600	<i>Biddulphia + Odontella + Trigonium + Trieres</i>	6 600	1 640	<i>Leptocylindrus</i>	2 369 437	15 456
<i>Peridinales</i>	600	233	<i>Lauderiaceae + Melosiraceae + Paraliaceae</i>	6 200	1 966	<i>Cerataulina pelagica</i>	2 129 000	70 597
<i>Dinophysis + Phalacroma</i>	500	183	<i>Cymbellaceae</i>	6 100	2 560	<i>Guinardia delicatula</i>	1 469 800	47 969
<i>Lithodesmiaceae</i>	500	500	<i>Dictyocha</i>	6 000	514	<i>Pennales + Fragilariaceae</i>	1 190 800	6 925
<i>non applicable</i>	400	400	<i>Nitzschiaceae</i>	6 000	1 562	<i>Skeletonema costatum</i>	1 043 000	40 178
<i>Ceratiaceae</i>	400	400	<i>Cymatosiraceae + Plagiogrammaeae</i>	5 900	2 940	<i>Pleurosigma + Gyrosigma + Haslea wawriake + Naviculaceae</i>	778 500	7 462
<i>Coscinodiscus + Stellarima</i>	400	250	<i>Closterium</i>	5 600	656	<i>Thalassionema + Thalassiothrix + Lioloma + nitzschioides</i>	576 000	6 334
<i>Diploneis</i>	300	136	<i>Dinobryon</i>	5 200	745	<i>Pseudo-nitzschia</i>	429 800	11 889
<i>Karlodinium</i>	300	300	<i>Centriques</i>	5 100	687	<i>Gymnodinium + Gyrodinium</i>	367 900	3 687
<i>Staurodesmus</i>	300	300	<i>Lauderia + Detonula</i>	4 800	1 378	<i>Melosira</i>	286 800	14 954
<i>Warnowiaceae</i>	300	300	<i>Heterocapsa</i>	4 700	809	<i>Thalassiosira + Porosira</i>	233 200	9 387
<i>Amphidomataceae</i>	200	200	<i>Cocconeis</i>	4 200	2 100	<i>Scripsiella + Ensiculifera + Pentapharsodinium + Bysmatrum</i>	193 600	3 822
<i>Noctiluca</i>	200	200	<i>Katodin</i>	4 000	591	<i>Achnanthes</i>	169 700	16 221
<i>Oxytoxum + Corythodinium</i>	200	200	<i>Thalassiosiraceae</i>	4 000	1 542	<i>Polykrikos</i>	167 200	29 150
<i>Proboscia alata var. alata</i>	200	150	<i>Warnovia + Nematodinium + Nematopsides</i>	4 000	855	<i>Bacillaria paxillifer + Licmophora + Entomoneis</i>	108 200	1 622
<i>Coccolithaceae</i>	100	100	<i>Rhizosoleniaceae</i>	3 800	882	<i>Cylindrotheca closterium</i>	107 200	6 312
<i>Cyanobacteria</i>	100	100	<i>Ceratium + Neoceratium + Tripos</i>	3 700	933	<i>Rhizosolenia imbricata + styliformis + setigera + pungens</i>	98 000	3 433
<i>Diatoma + Fragilaria</i>	100	100	<i>Striatella</i>	3 600	1 880	<i>Prorocentrum + arcuatum + gibbosum + Protoperidinium</i>	69 500	2 339
<i>Pediastrum</i>	100	100	<i>Synedra + Toxarium</i>	3 300	1 700	<i>Lithodesmium undulatum</i>	63 600	3 103
<i>Phacus</i>	100	100	<i>Amphora</i>	3 100	1 420	<i>Gonyaulax + Lepidodinium chlorophorum</i>	33 900	529
<i>Pyramimonas</i>	100	100	<i>Dinophysiaceae</i>	3 000	1 733	<i>Nitzschia longissima Nitzschia + Hantzschia</i>	19 700	905
<i>Rhabdonema</i>	100	100	<i>Grammatophora</i>	3 000	373	<i>Ditylum brightwellii</i>	12 300	1 868
-	-	-	<i>Cymatosiraceae</i>	2 900	1 350	-	-	-
-	-	-	<i>Chlorophyceae</i>	2 700	513	-	-	-
-	-	-	<i>Achnanthaceae</i>	2 300	2 100	-	-	-
-	-	-	<i>Diplopsalis + Diplopelta + Preperidinium</i>	1 900	574	-	-	-
-	-	-	<i>Asterionellopsis</i>	1 700	1 060	-	-	-
-	-	-	<i>Corethron</i>	1 700	742	-	-	-
-	-	-	<i>Karenia</i>	1 600	266	-	-	-
-	-	-	<i>Ebria</i>	1 300	700	-	-	-
-	-	-	<i>Amphidinium</i>	1 100	544	-	-	-
-	-	-	<i>Leptocylindraceae</i>	1 100	1 100	-	-	-
-	-	-	<i>Surirella</i>	1 100	600	-	-	-

Table 2.8: Phytoplankton diversity and MA over ten year period (2009-2018)

Distinguishing siliceous from non-siliceous cells in category C, *Alexandrium minutum* dominated in dinoflagellates while *Chaetoceros* dominated in diatoms (Table 2.9).

Class	Phenotype	Size range (µm)	Size range (Reference)
Non-Siliceous (Dinoflagellate)	<i>Alexandrium minutum</i>	17 – 29	Balech E. (1995); Bolch et al. (1991); Steidinger K. & Tangen K. (1996)
	<i>Gymnodinium</i> + <i>Gyrodinium</i>	7.5 – 92	Olenina et al. (2006)
	<i>Scrippsiella</i> + <i>Ensiculifera</i> + <i>Pentaparsodinium</i> + <i>Bysmatrum</i>	15 – 30	'
	<i>Polykrikos</i>	100 – 150	Dodge J. D. (1982); Drebes G. (1974)
	<i>Prorocentrum</i> + <i>arcuatum</i> + <i>gibbosum</i> + <i>Protoperdinium</i>	10 – 60	Olenina et al. (2006)
	<i>Gonyaulax</i> + <i>Lepidodinium chlorophorum</i>	20 – 70	'
Siliceous (Diatom)	<i>Chaetoceros</i>	4 – 30	'
	<i>Dactyliosolen fragilissimus</i>	42 – 300	Cupp E. (1943); Drebes G. (1974); Hasle G. & Syvertsen E. (1996)
	<i>Leptocylindrus</i>	3 – 100	Olenina et al. (2006)
	<i>Cerataulina pelagica</i>	55 – 120	Drebes G. (1974); Hasle G. & Syvertsen E. (1996)
	<i>Guinardia delicatula</i>	27 – 110	Cleve P. (1900); Drebes G. (1974); Hasle G. & Syvertsen E. (1996)
	<i>Pennales</i> + <i>Fragilariaceae</i>	4 – 100	Olenina et al. (2006)
	<i>Skeletonema costatum</i>	3 – 18	'
	<i>Pleurosigma</i> + <i>Gyrosigma</i> + <i>Haslea wawriake</i> + <i>Naviculaceae</i>	17 – 75	'
	<i>Thalassionema</i> + <i>Thalassiothrix</i> + <i>Lioloma</i> + <i>nitzschoides</i>	4 – 500	'
	<i>Pseudo-nitzschia</i>	10 – 150	'
	<i>Melosira</i>	8 – 20	'
	<i>Thalassiosira</i> + <i>Porosira</i>	7 – 110	'
	<i>Achnanthes</i>	3 – 35	'
	<i>Bacillaria paxillifer</i> + <i>Licmophora</i> + <i>Entomoneis</i>	6 – 120	'
	<i>Cylindrotheca closterium</i>	3 – 35	'
	<i>Rhizosolenia imbricata</i> + <i>styliformis</i> + <i>setigera</i> + <i>pungens</i>	2.5 – 57	Hasle G. & Syvertsen E. (1996); Sundström B. (1986)
	<i>Lithodesmium undulatum</i>	37 – 93	Cupp E. (1943); Hasle G. & Syvertsen E. (1996); Hendey N. (1964)
	<i>Nitzschia longissima</i> <i>Nitzschia</i> + <i>Hantzschia</i>	4 – 155	Olenina et al. (2006)
	<i>Ditylum brightwellii</i>	80 – 130	Delgado M. & Fortuno J. (1991); Drebes G. (1974)

Table 2.9: Diatoms and dinoflagellates whose MA > 10000 cells.L⁻¹ in river Daoulas

Alexandrium minutum and *Chaetoceros* did not dominate during the same years (Table 2.10). Interannually, *Chaetoceros* had the highest MA in 2009 and the lowest in 2016. *A. minutum* dominated other taxons in 2012 and 2014, *Dactyliosolen fragilissimus* in 2013, *Leptocylindrus* in 2015 and *Cerataulina pelagic* in 2018. The DMA varied interannually for each taxon and among taxons (Table 2.11) but the major blooms > 1M cells.L⁻¹ occurred from June to mid-August except for *Pennales* + *Fragilariaceae* that bloomed mid-February in 2017. The average MA over the ten year period equally varied among the taxons (Fig. 2.15).

Phenotype	Maximum Abundance									
	2009	2010	2011	2012	2013	2014	2015	2016	2017	2018
<i>Chaetoceros</i>	4 897 600	3 269 198	1 826 408	2 837 135	2 410 236	655 800	269 300	457 900	1 882 900	967 000
<i>Dactyliosolen fragilissimus</i>	1 800	20 200	8 600	28 100	4 040 223	167 100	30 900	161 500	2 554 600	32 200
<i>Alexandrium minutum</i>	15 400	432 600	5 100	3 675 330	358 400	1 496 480	68 800	6 000	968 400	17 500
<i>Leptocylindrus</i>	21 200	140 300	117 500	184 600	66 400	204 200	2 369 437	37 300	288 600	48 300
<i>Cerataulina pelagica</i>	18 800	190 200	73 600	5 500	28 600	461 700	3 500	24 300	7 800	2 129 000
<i>Guinardia delicatula</i>	14 100	776 286	7 100	1 469 800	4 900	46 900	1 423 187	50 700	63 500	25 500
<i>Pennales</i> + <i>Fragilariaceae</i>	13 300	4 700	5 500	6 200	45 100	25 900	20 400	49 500	1 190 800	25 200
<i>Skeletonema costatum</i>	3 600	3 700	724 800	833 600	1 043 000	461 400	27 400	39 900	78 000	-
<i>Pleurosigma</i> + <i>Gyrosigma</i> + <i>Haslea wawriake</i> + <i>Naviculaceae</i>	13 700	141 200	38 100	27 800	112 200	20 600	49 900	37 100	778 500	1 500
<i>Thalassionema</i> + <i>Thalassiothrix</i> + <i>Lioloma</i> + <i>nitzschoides</i>	32 300	133 500	61 100	171 100	169 900	37 100	19 000	136 600	78 800	576 000
<i>Pseudo-nitzschia</i>	5 800	35 600	85 500	40 900	429 800	38 200	106 700	22 200	108 100	1 200
<i>Gymnodinium</i> + <i>Gyrodinium</i>	10 600	19 300	367 900	22 300	7 500	22 500	9 900	6 900	20 700	200
<i>Melosira</i>	600	1 700	10 800	-	-	18 200	106 500	8 400	286 800	400
<i>Thalassiosira</i> + <i>Porosira</i>	21 700	21 900	74 800	35 400	149 500	233 200	60 800	89 900	48 600	72 000
<i>Scrippsiella</i> + <i>Ensiculifera</i> + <i>Pentapharsodinium</i> + <i>Bysmatrum</i>	4 600	86 900	193 600	24 700	21 700	15 900	4 000	12 600	7 900	8 200
<i>Achnanthes</i>	-	300	-	-	-	14 800	169 700	26 400	72 100	200
<i>Polykrikos</i>	100	1 900	-	167 200	-	1 800	-	-	-	-
<i>Bacillaria paxillifer</i> + <i>Licmophora</i> + <i>Entomoneis</i>	5 200	21 500	10 700	4 800	108 200	7 500	11 400	15 900	4 100	5 400
<i>Cylindrotheca closterium</i>	1 900	26 500	14 900	88 000	107 200	93 600	11 900	44 400	9 600	46 800
<i>Rhizosolenia imbricata</i> + <i>styliformis</i> + <i>setigera</i> + <i>pungens</i>	900	98 000	-	5 400	31 100	10 900	84 700	93 500	43 300	15 700
<i>Prorocentrum</i> + <i>arcuatum</i> + <i>gibbosum</i> + <i>Proto-peridinium</i>	18 300	17 800	12 200	31 700	36 000	69 500	11 500	11 300	25 200	59 200
<i>Lithodesmium undulatum</i>	3 800	3 200	4 400	3 400	21 300	27 700	8 900	7 300	63 600	2 300
<i>Gonyaulax</i> + <i>Lepidodinium chlorophorum</i>	8 500	7 100	4 400	33 900	1 000	25 900	7 700	4 400	2 700	1 600
<i>Nitzschia longissima</i> <i>Nitzschia</i> + <i>Hantzschia</i>	3 000	19 700	12 700	16 700	12 900	3 200	-	1 200	400	600
<i>Ditylum brightwellii</i>	2 200	-	-	-	-	3 000	1 100	12 300	3 700	2 100

Table 2.10: Interannual MA of phytoplankton category C

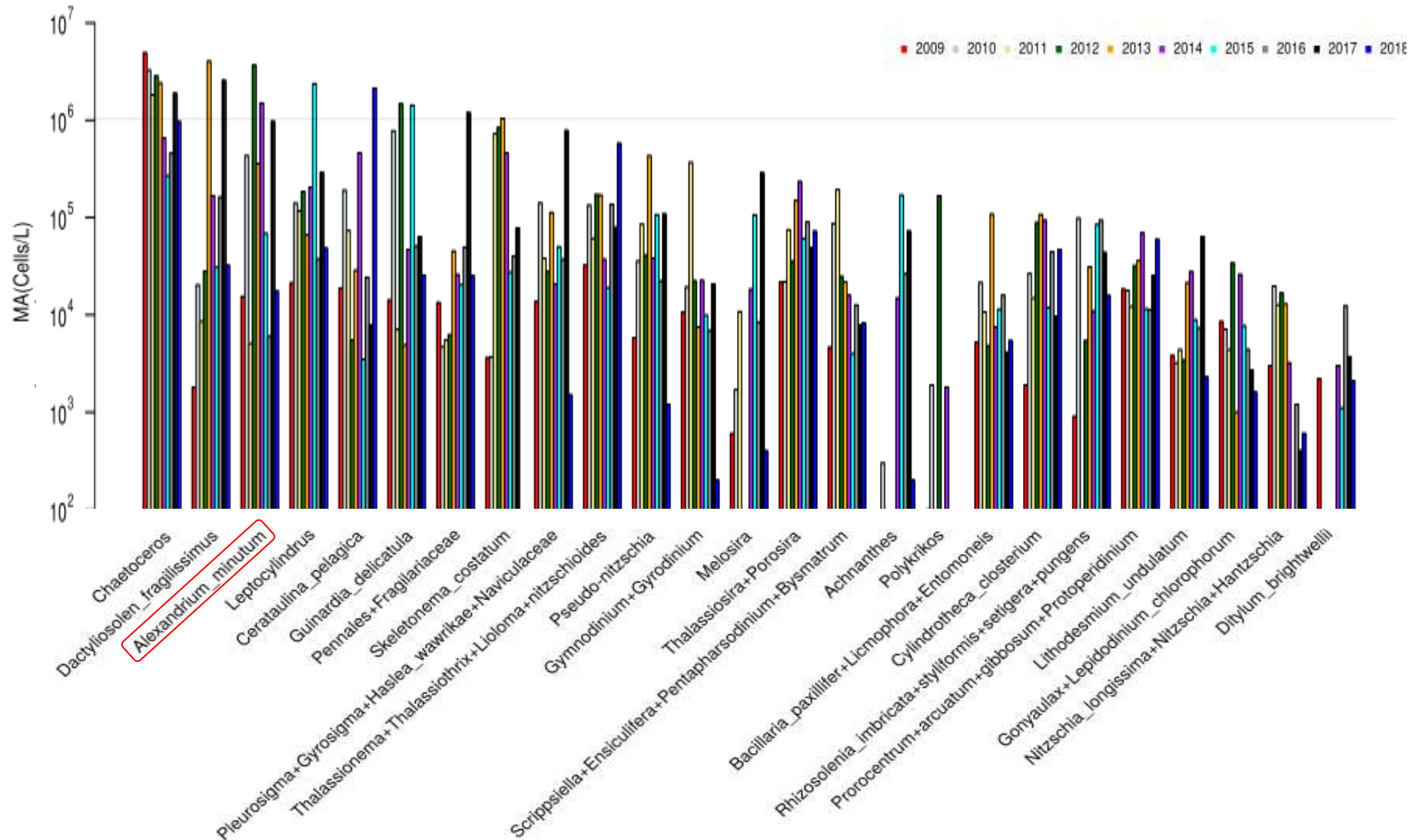


Figure 2.13: Interannual MA of phytoplankton category C

Phenotype	Date of Maximum Abundance									
	2009	2010	2011	2012	2013	2014	2015	2016	2017	2018
<i>Chaetoceros</i>	169	217	151	228	191	140	156	187	205	120
<i>Dactyliosolen fragilissimus</i>	145	118	123	179	169	140	162	159	122	143
<i>Alexandrium minutum</i>	212	186	147	193	203	203	212	223	163	104
<i>Leptocylindrus</i>	271	172	131	200	248	140	162	111	138	157
<i>Cerataulina pelagica</i>	114	127	131	129	248	127	156	103	149	157
<i>Guinardia delicatula</i>	271	118	178	129	225	140	111	168	122	197
<i>Pennales + Fragilariaceae</i>	264	222	166	347	148	238	78	98	45	33
<i>Skeletonema costatum</i>	344	97	192	200	220	233	64	91	30	-
<i>Pleurosigma + Gyrosigma + Haslea wawriake</i>	264	89	52	291	99	238	78	98	45	33
<i>Thalassionema + Thalassiothrix + Lioloma + nitzschioides</i>	203	217	207	207	225	225	187	208	167	104
<i>Pseudo-nitzschia</i>	169	139	131	207	248	140	104	98	108	165
<i>Gymnodinium + Gyrodinium</i>	212	202	178	221	169	203	266	194	199	165
<i>Melosira</i>	222	313	6	-	-	328	78	350	45	171
<i>Thalassiosira + Porosira</i>	145	208	178	253	220	225	252	266	220	108
<i>Scrippsiella + Ensiculifera + Pentapharsodinium + Bysmatrum</i>	344	154	184	207	123	184	162	103	61	171
<i>Achnanthes</i>	-	39	-	-	-	48	78	98	45	334
<i>Polykrikos</i>	189	217	-	200	-	233	-	-	-	-
<i>Bacillaria paxillifer + Licmophora + Entomoneis</i>	85	179	109	214	148	133	240	98	191	143
<i>Cylindrotheca closterium</i>	279	89	109	200	99	225	125	98	116	143
<i>Rhizosolenia imbricata + styliformis + setigera + pungens</i>	159	127	-	95	169	106	111	103	250	143
<i>Prorocentrum + arcuatum + gibbosum + Protoperidinium</i>	203	179	214	228	203	203	225	232	173	104
<i>Lithodesmium undulatum</i>	231	222	256	242	220	255	212	266	220	238
<i>Gonyaulax + Lepidodinium chlorophorum</i>	226	266	207	221	213	189	187	223	167	171
<i>Nitzschia longissima Nitzschia + Hantzschia</i>	222	118	166	242	213	118	-	144	266	120
<i>Ditylum brightwellii</i>	85	-	-	-	-	91	64	91	83	108

Table 2.11: Interannual DMA of phytoplankton category C

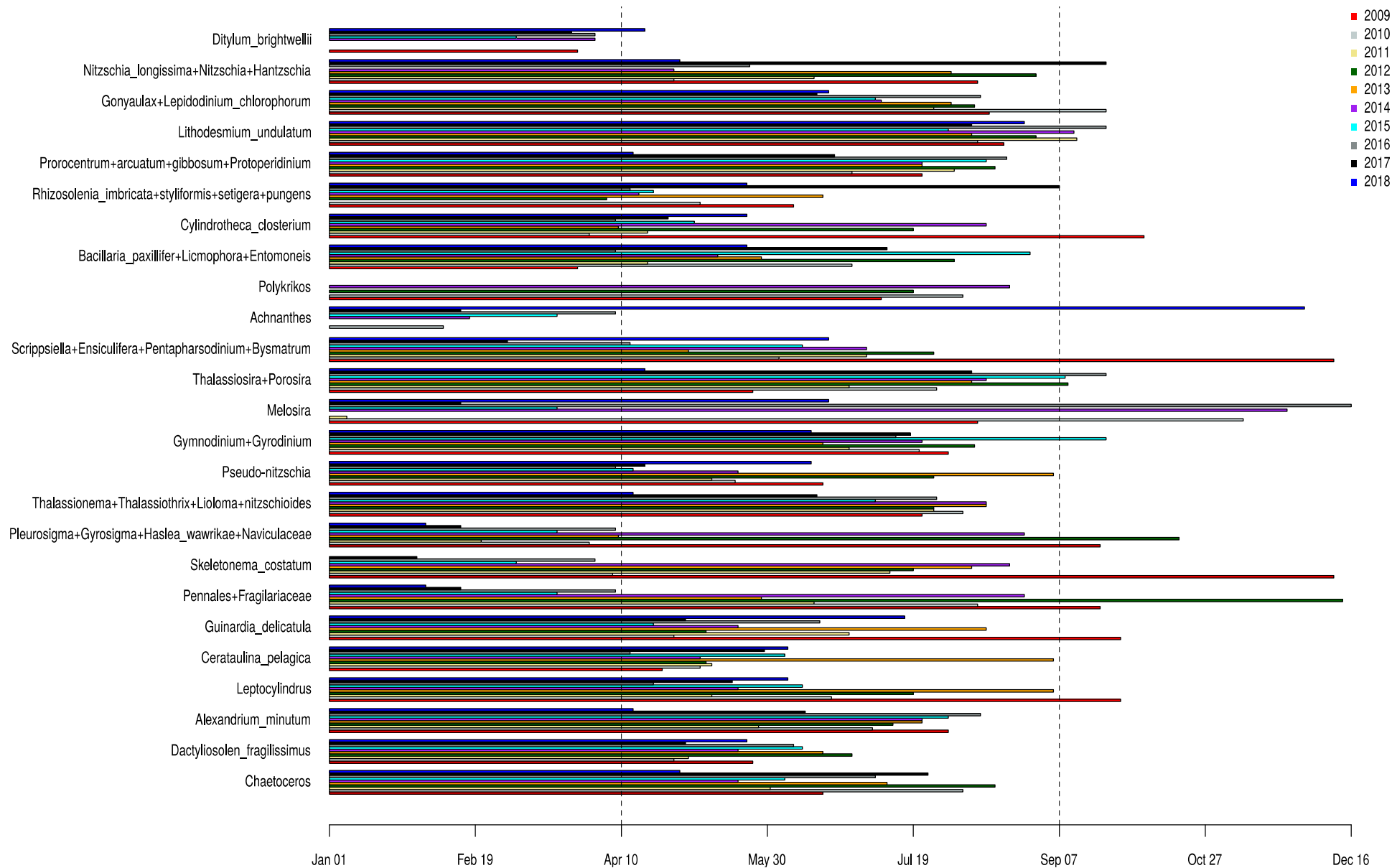


Figure 2.14: Interannual DMA of phytoplankton category C

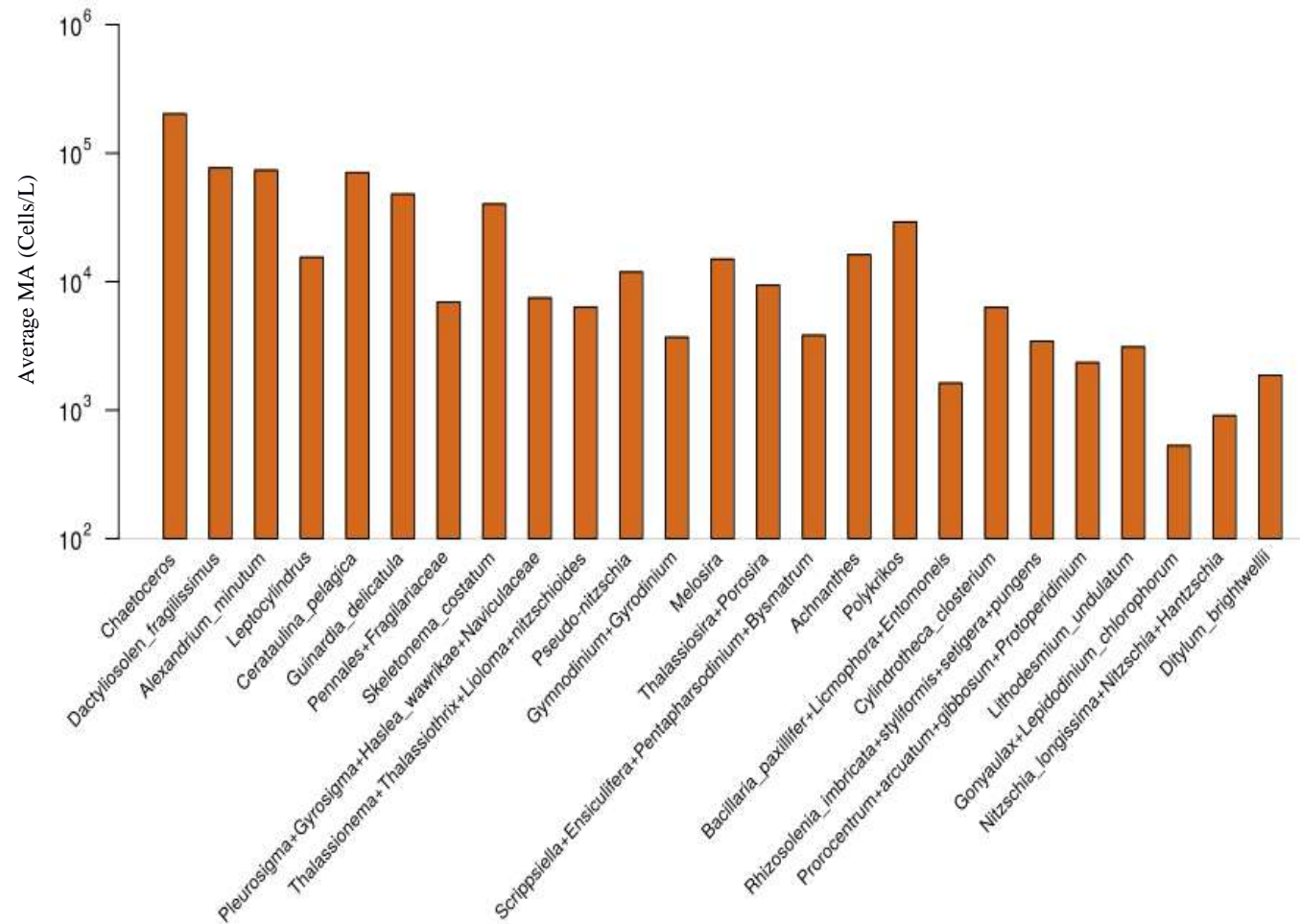


Figure 2.15: Average MA (2009-2018) of phytoplankton category C

2.3. Discussion

2.3.1. *A. minutum* and environmental variables

Year	2009	2010	2011	2012	2013	2014	2015	2016	2017	2018
Date @ 15°C	May 22	May 21	Apr 22	May 25	Jun 01	May 16	May 11	May 17	May 13	May 07
Ave. Temperature	12.1	11.6	13.6	12.4	10.8	12.7	12.6	12.1	13.1	11.8
Spring	-	-	Warm	-	Cold	Warm	-	-	Warm	-
Ave. River Flow	108 253	127 834	62 712	194 247	125 920	165 054	122 693	144 888	99 337	178 963
Spring	-	-	Dry	Wet	-	Wet	-	-	-	Wet

Table 2.12: Interannual variability in temperature dates at 15°C, average temperature and river flow and spring (March 1 to May31) conditions.

Cold/Warm and Dry/Wet are determined by the interannual differences.

Temperature and light: These factors have similar seasonal and sometimes, interannual behaviors. They have the lowest values in the winter but highest in the summer. It has been demonstrated that light can limit the development of *A. minutum* (Chang and McClean, 1997) but in the Bay of Brest, this factor can be considered minor compared to others for explaining the interannual variabilities (Chapelle, 2008). Temperature however, is more significant and it has been shown that blooms of *A. minutum* are always initiated when water temperature is above 15°C (Guallar et al. 2017). During the study period, 2011 was the first year to attain this threshold (April, 22) and 2013 was the last (June, 1), marking a difference of more than a month (39 days). The earliest *A. minutum* maximum occurred May 27, 2011 (Table 2.6) and June 22, 2013 – a difference of 26 days. In fact, temperature gives an indication of early bloom start but does not actually influence the MA of species.

River flow: The noticeable high increase in river flow during the summer of 2012 and slight increases in the summer of 2014 and 2017 (Fig. 2.2) correspond to the years with the highest *A. minutum* bloom (Table 2.6). River flow has 2 effects on *A. minutum* bloom (Guallar et al 2017), a positive effect by bringing nutrients, and a negative effect by enhancing the dilution rate. In summer, flow is low and so dilution is lower and *A. minutum* growth can be favored by high light and temperature but limited by the scarcity of nutrients. The effect of positive river flow is then more effective during this period. Our data show that high river flow during the period of *A. minutum* bloom development (i.e. when temperature is above 15°C) is probably responsible for higher maximum abundance. Year 2012 for example, had the highest river flow as well as MA.

Nutrients: The concentration of nutrients in general is high in the winter but low in the summer. This is directly linked to the river flow since the river is the main source of nutrients in coastal ecosystems (Tréguer et al. 2014) as observed in the Bay of Brest. Furthermore, nutrients are absorbed in higher concentrations during the period of vegetative growth of phytoplankton in summer than in winter when there is little or no growth. Interannually, there is not much change in nutrient variations. However, we noticed a slightly higher concentration of Silicate during the summers of 2015 and 2017 compared to other years. Being the first limiting nutrient in the area (Andrieux-Loyer et al. 2008), PO_4 had the highest summer concentration in 2014 thereby, boosting the abundance of *A. minutum*. Similarly, NO_3 concentration was highest in the summer of 2018. NH_4 has similar interannual trend but with a difference in the spring of 2017 where it showed a higher concentration.

2.3.2. *Alexandrium minutum* and Phytoplankton

Abundances of *A. minutum* above 100cells.L⁻¹ were not observed between end of October and mid-March in all the years surveyed except 2015 which had an abundance of 100cells.L⁻¹ in early November. *A. minutum* growth in the Daoulas estuary is a balance between net growth and dilution. In autumn, winter and beginning of spring, dilution rate is usually higher than net growth which is limited by temperature and light. In late spring and summer, dilution decreases but growth becomes limited by nutrients due to less input from the river and competition with the phytoplankton community. Interannually, differences exist in the MA across the years but 2009, 2011, 2015 and 2018 showed similar patterns (Fig. 2.11). Ideally, *Chl a* concentration increases with increasing abundance of phytoplankton. This is true for years 2012 and 2014 which had high species abundances.

Chaetoceros dominated other species in most of the years. This is in line with the findings of Beucher et al. (2004) and Del Amo et al. (1997) who observed that diatoms dominate the Bay of Brest phytoplankton community. With over 10⁶ cells per liter, *Dactyliosolen fragilissimus* dominated in 2013, *Leptocylindrus* in 2015, *Ceratualina pelagic* in 2018 but *A. minutum*, a dinoflagellate dominated in 2012 and 2014 (Fig. 2.13). These years showed higher river flows in end spring and higher nutrient (phosphorus) concentration is measured in 2014 (no data in 2012). This domination by *A. minutum* may be linked to its ability to assimilate and store more phosphorus than other species (Labry et al. 2008; Andrieux-Loyer et al. 2008; Yamamoto and Tarutani, 1999), giving it an advantage in the competition for nutrients.

Chapter 3

Simulations 0D

3.1. Simulated Area

The Daoulas estuary was considered homogeneous in surface and depth with a river inflow (Riv) and dilution rate due to wind, river flow and the tidal inflow/outflow with the Bay of Brest (Rad). Both flows are accompanied by the macronutrients (PO_4 , NH_4 , NO_3 and $\text{Si}(\text{OH})_4$) which are commonly known to drive phytoplankton dynamics in coastal waters. Nutrient concentrations in river Daoulas were interpolated from monthly data measured by Brest Metropole Océane while those of ‘Rad’ were interpolated from weekly data provided by the Service d’Observation en Milieu Littoral (SOMLIT) situated at the Portzic station (Fig. 3.1). Data on light and temperature were provided by METEOSAT Second generation satellites and Meteo-France respectively. The rate of dilution was calculated using a hydrodynamic model (MARS3D, Lazure and Dumas, 2008) with a realistic configuration of the Bay of Brest from 2012 to 2014. Then, a multiple linear relationship was found between the tidal coefficient, the log10 of river flow, the wind speed and the calculated dilution (Guallar et al., 2017). This relationship was used to estimate the dilution for years 2009-2011 and 2015-2018. The daily Daoulas river flow data were provided by HYDRO – a government environmental database.

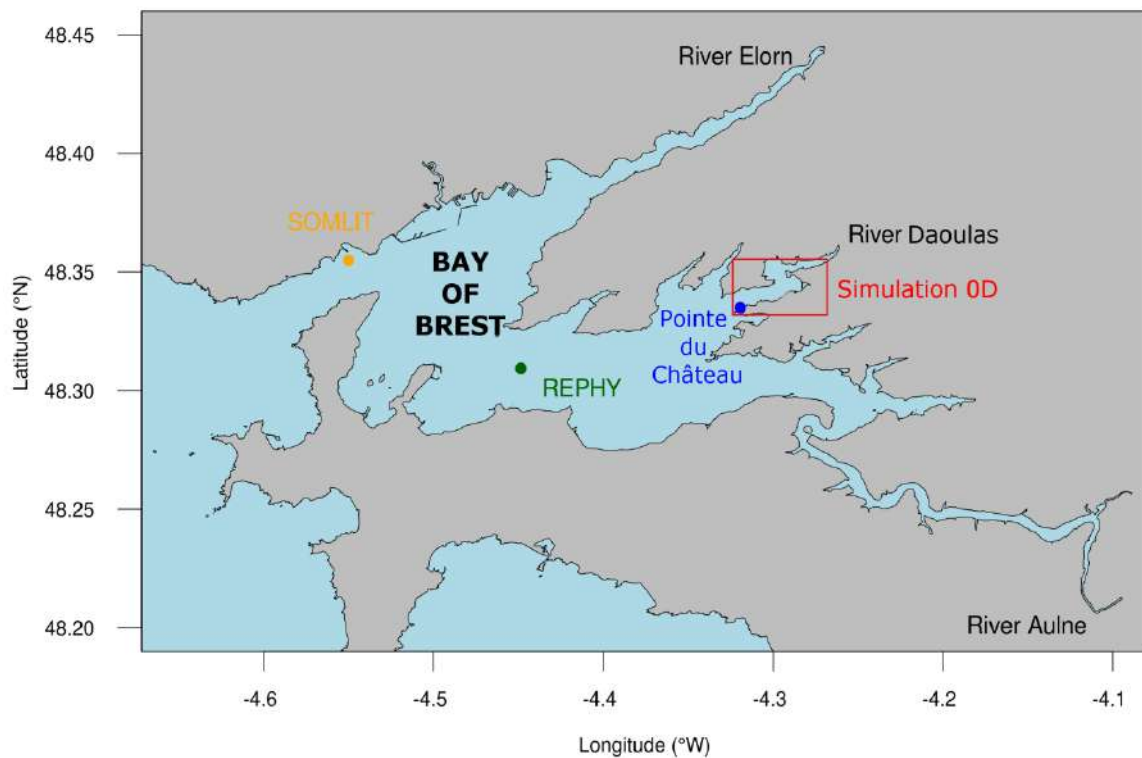


Figure 3.1: The Bay of Brest showing simulated area

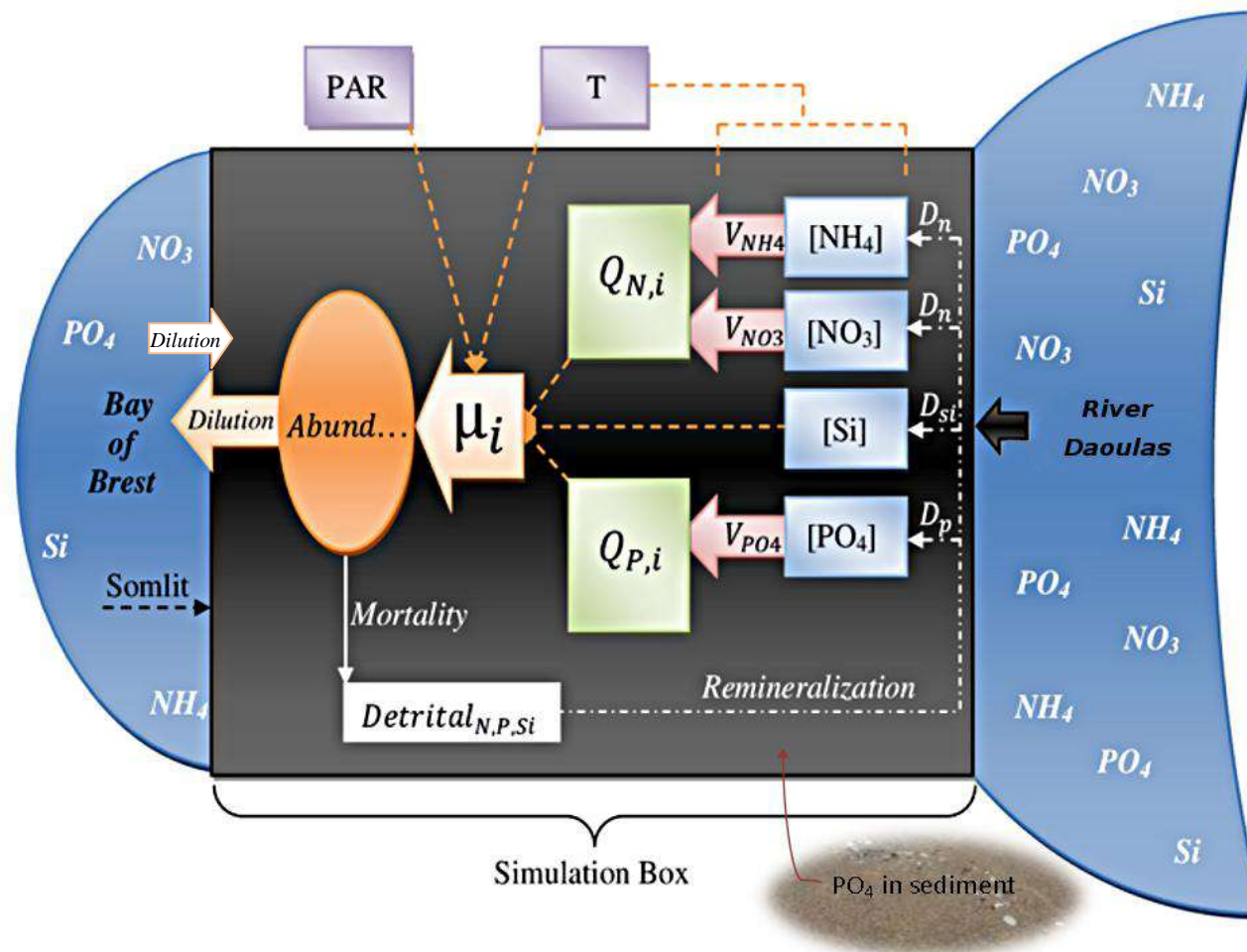


Figure 3.2: Concept of the model describing the simulated area

3.2. Model Equations

Differential equations governing the dynamics of the system have been presented in Sourisseau et al. (2017). This system refers to state variables such as nutrient concentration, abundance of species and intracellular cell quotas whose evolution with time is expressed with mathematical equations. These equations were applied in the model in order to obtain the abundance of each species (φ_i), their growth (μ_i), the concentration ($[\text{PO}_4]$, $[\text{NH}_4]$, $[\text{NO}_3]$ and $[\text{Si}]$) and absorption of nutrients ($V_{P,i}$ and $V_{N,i}$) and lastly, the intracellular cell quotas of phosphorus ($Q_{P,i}$) and nitrogen ($Q_{N,i}$).

3.2.1. Abundance of species

$$\frac{\partial \varphi_i}{\partial t} = \mu_i \varphi_i - D \varphi_i - m \varphi_i$$

Where i represents each species, μ_i the growth (d^{-1}), D the dilution rate (d^{-1}) and m the mortality rate (d^{-1})

The abundance of *A. minutum* is described in the same manner –

$$\begin{aligned} \frac{\partial Alex}{\partial t} &= \mu_{Alex} - D_{Alex} - m_{Alex} \\ &= \text{Growth} - \text{Dilution} - \text{Mortality} \end{aligned}$$

Dilution varied from 0.17 to 0.6d^{-1} and mortality is equal for all species (0.02d^{-1}). A minimal abundance was considered in order to avoid the extinction of species due to dilution and mortality. It was determined as Sourisseau et al. (2017) in a way that the minimal volume occupied by each species is $10^6 \mu\text{m}^3 \text{L}^{-1}$. This implies a minimal abundance of 3.8cells.L^{-1} for the largest cells ($64 \mu\text{m}$), 10^6cells.L^{-1} for the smallest cells ($1 \mu\text{m}$) and 171cells.L^{-1} for *A. minutum* ($18 \mu\text{m}$) similar to the detection threshold for microphytoplankton (100cells.L^{-1}) used in the protocol of REPHY monitoring program.

3.2.2. Growth of species

Growth itself is a function of limiting factors and therefore, can be expressed with Liebig's law (Legovic and Cruzado, 1997) as –

$$\mu_i = \mu_{max_i} \cdot f_{T,i} \cdot f_{min}(L_{L,i} L_{N,i} L_{P,i} L_{Si,i})$$

$$\mu_{Alex} = \mu_{max_{Alex}} \cdot f_{T,alex} \cdot f_{min}(L_{L,alex} L_{N,alex} L_{P,alex})$$

Where $f_{T,i}$ is the temperature function on growth, f_{min} is minimum limitation for: Light ($L_{L,i}$), Nitrogen ($L_{N,i}$), Phosphorus ($L_{P,i}$) and Silicon ($L_{Si,i}$)

Maximum growth rate ($\mu_{max,i}$) defines the competition among species within the ecosystem of a model. It has a relationship with optimal temperature and can be simulated with a global exponential law according to Eppley, 1972.

$$\mu_{max,i} = \mu_{max,ref} * e^{(K_T * T_{opt,i})}$$

Where $\mu_{max,ref}$ ($0.58d^{-1}$) is the growth rate at $0^\circ C$ without limitations and K_T (0.063 per $^\circ C$) is the temperature coefficient for growth rate

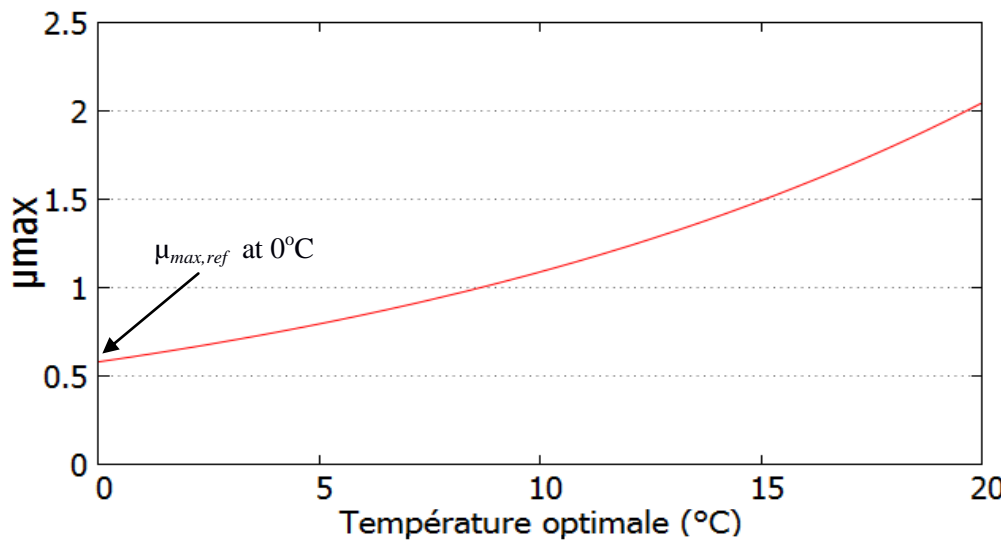


Figure 3.3: Maximum growth rate as a function of optimal temperature defined for each species (Eppley, 1972)

3.2.3. Concentration of nutrients

The simulated area has two nutrient sources - the river (Riv) and the Bay (Rad).

$$\frac{\partial[PO_4]}{\partial t} = [PO_4]_{Riv} \frac{F}{V} + [PO_4]_{Rad} \left(D - \frac{F}{V} \right) + fTmi(K_{remiP}D_P) - \sum_{i=1}^{N_s} V_{PO_4,i} \varphi_i - D[PO_4]$$

$$\frac{\partial[NH_4]}{\partial t} = [NH_4]_{Riv} \frac{F}{V} + [NH_4]_{Rad} \left(D - \frac{F}{V} \right) - K_{nitriF}[NH_4] + fTmi(K_{remiN}D_N) - \sum_{i=1}^{N_s} V_{NH_4,i} \varphi_i - D[NH_4]$$

$$\frac{\partial[NO_3]}{\partial t} = [NO_3]_{Riv} \frac{F}{V} + [NO_3]_{Rad} \left(D - \frac{F}{V} \right) + K_{nitriF}[NH_4] - \sum_{i=1}^{N_s} V_{NO_3,i} \varphi_i - D[NO_3]$$

$$\frac{\partial[Si]}{\partial t} = [Si]_{Riv} \frac{F}{V} + [Si]_{Rad} \left(D - \frac{F}{V} \right) + fTmi(K_{dissSi}D_{Si}) - \sum_{i=1}^{N_s} Q_{Si,i} \varphi_i - D[Si]$$

Organic detrital – nitrogen D_N , phosphorus D_P , silicon D_{Si} . D_N and D_P are mineralized in NH_4 for N and PO_4 for P. D_{Si} is dissolved in Si. NH_4 is nitrified in NO_3 .

$$\frac{\partial[D_P]}{\partial t} = -D * D_P + fTmi \left(\sum_{i=1}^{N_s} m Q_{P,i} \varphi_i - K_{miP} D_P \right)$$

$$\frac{\partial[D_N]}{\partial t} = -D * D_N + fTmi \left(\sum_{i=1}^{N_s} m Q_{N,i} \varphi_i - K_{miN} D_N \right)$$

Symbol	Description	Unit
φ_i	Abundance of species	Cell.L ⁻¹
μ_i	Growth of species	d ⁻¹
μ_{\max_i}	Maximum growth rate of species	d ⁻¹
$Q_{P,i}$	Phosphorus cell quota	$\mu\text{mol.cell}^{-1}$
$Q_{N,i}$	Nitrogen cell quota	"
$Q_{\min P,i}$	Minimum phosphorus cell quota	"
$Q_{\min N,i}$	Minimum nitrogen cell quota	"
$Q_{\max P,i}$	Maximum phosphorus cell quota	"
$Q_{\max N,i}$	Maximum nitrogen cell quota	"
D_P	Organic phosphorus	$\mu\text{mol.L}^{-1}$
D_N	Organic nitrogen	"
D_{Si}	Detrital silicon	"
$[\text{PO}_4]$	Concentration of phosphate	"
$[\text{NH}_4]$	Concentration of ammonium	"
$[\text{NO}_3]$	Concentration of nitrate	"
$[\text{Si}]$	Concentration of silicate	"
$[\text{PO}_4]_{\text{Riv}}$	Phosphate concentration in the river	"
$[\text{NH}_4]_{\text{Riv}}$	Ammonium concentration in the river	"
$[\text{NO}_3]_{\text{Riv}}$	Nitrate concentration in the river	"
$[\text{Si}]_{\text{Riv}}$	Silicate concentration in the river	"
$[\text{PO}_4]_{\text{Rad}}$	Phosphate concentration in the bay	"
$[\text{NH}_4]_{\text{Rad}}$	Ammonium concentration in the bay	"
$[\text{NO}_3]_{\text{Rad}}$	Nitrate concentration in the bay	"
$[\text{Si}]_{\text{Rad}}$	Silicate concentration in the bay	"
$V_{\text{PO}_4,i}$	Absorption of phosphate	$\mu\text{mol.cell}^{-1}.\text{d}^{-1}$
$V_{\text{NH}_4,i}$	Absorption of ammonium	"
$V_{\text{NO}_3,i}$	Absorption of nitrate	"
$V_{\max \text{PO}_4,i}$	Maximum absorption of phosphate	"
$V_{\max \text{NH}_4,i}$	Maximum absorption of ammonium	"
$V_{\max \text{NO}_3,i}$	Maximum absorption of nitrate	"

Symbol	Description	Unit
fT_i	Limitation by temperature	-
fL_i	Limitation by light	-
fP_i	Limitation by phosphorus	-
fN_i	Limitation by nitrogen	-
fSi_i	Limitation by silicon	-
f_{min}	Minimum limitation	-
$K_{P,i}$	Phosphorus half-saturation constant	$\mu\text{mol.L}^{-1}$
$K_{N,i}$	Nitrogen half-saturation constant	$\mu\text{mol.L}^{-1}$
K_{par}	Light attenuation coefficient	m^{-1}
K_{nitrif}	Nitrification constant	d^{-1}
K_{remiP}	Phosphate remineralization rate	d^{-1}
K_{remiN}	Nitrate remineralization rate	d^{-1}
K_{dissSi}	Organic silica dissolution rate	d^{-1}
fT_{mi}	Temperature effect Q_{10}	$^{\circ}\text{C}^{-1}$
T	Temperature	$^{\circ}\text{C}$
T_{opt}	Optimal temperature	$^{\circ}\text{C}$
I_o	PAR at sea surface	W.m^{-2}
I	PAR at depth	W.m^{-2}
D	Dilution rate	d^{-1}
m	Mortality rate	d^{-1}
F	River flow	$\text{m}^3.\text{d}^{-1}$
V	Volume of sea water	m^3

Table 3.1: Table of symbols

Sediment also contains concentrations of organic matter and nutrients and therefore, may be a secondary nutrient source in shallow waters that release irregular phosphate and nitrogen (Andrieux-Loyer et al., 2008). This additional nutrients input from sediment enhances the growth of species like *A. minutum* which is able to store phosphate in high quantities (Yamamoto and Tarutani, 1999) thereby, making it appear more like a ‘storage specialist’ that uptakes PO_4 pulses for luxury consumption (storage) and then, utilizes the stored PO_4 for cell growth (Labry et al. 2008). Phosphates fluxes from the sediment were obtained with the slope:

$$f(x) = 5.9 * e^{(0.1*T)}$$

Where $f(x)$ is the PO_4 flux (in $\mu\text{molL}^{-1}\text{d}^{-1}$) and T is temperature (in $^{\circ}\text{C}$). This relationship was determined by Andrieux-Loyer (2008) for marine coastal sediments.

Nitrogen sediment fluxes were not included here. Trommer et al. (2013) found that the phytoplankton community in the Bay of Brest generally experience longer P limitation than N limitation. They equally found a significantly increased growth rate in all samples containing P additions.

3.2.4. Absorption of nutrients

Species compete for nutrients whose uptake increases with an increasing external pool following Michaelis-Menten equation, but decreases when cell quota approaches maximum. NH_4 is assimilated preferentially from NO_3 .

$$\begin{aligned}
 & \begin{array}{ccc}
 & \text{Michaelis-Menten} & \text{Quota limit} \\
 & \underbrace{\hspace{1.5cm}} & \underbrace{\hspace{1.5cm}} \\
 V_{P,i} = V_{maxPO_4,i} \frac{[PO_4]}{K_{P,i} + [PO_4]} & \left(\frac{Q_{maxP,i} - Q_{P,i}}{Q_{maxP,i} - Q_{minP,i}} \right) & fTmi
 \end{array} \\
 \\
 V_{N,i} = V_{maxNH_4,i} \frac{[NH_4]}{K_{N,i} + [NH_4]} & \left(\frac{Q_{maxN,i} - Q_{N,i}}{Q_{maxP,i} - Q_{minN,i}} \right) fTmi \\
 \\
 V_{N,i} = V_{maxNO_3,i} \frac{[NO_3]}{K_{N,i} + [NO_3]} & \left(\frac{Q_{maxN,i} - Q_{N,i}}{Q_{maxP,i} - Q_{minN,i}} \right) \left(1 - \frac{[NH_4]}{K_{N,i} + [NH_4]} \right) fTmi
 \end{aligned}$$

3.2.5. Cell quota: Nutrient storage capacity which influences nutrient absorption, growth and metabolism.

$$\frac{\partial Q_{N,i}}{\partial t} = V_{N,i} - \mu_i Q_{N,i}$$

$$\frac{\partial Q_{P,i}}{\partial t} = V_{P,i} - \mu_i Q_{P,i}$$

3.2.6: Allometric Relationship

The functional traits used to simulate phytoplankton diversity follow different distribution types (Sourisseau et al., 2017) therefore, allometric relationship is necessary for proper definition of the key physiological parameters such as minimum/maximum quota, maximum nutrient absorption rate and half-saturation coefficient that all dependant on power function of the cell size.

$$Q_{minN,i} = Q_{minN,ref} \cdot V_i^{\alpha1} \qquad Q_{maxN,i} = Q_{maxN,ref} \cdot V_i^{\beta1}$$

$$Q_{minP,i} = Q_{minP,ref} \cdot V_i^{\alpha2} \qquad Q_{maxP,i} = Q_{maxP,ref} \cdot V_i^{\beta2}$$

$$Q_{Si,i} = Q_{Si,ref} \cdot V_i^{\alpha3}$$

$$V_{maxNH4,i} = Q_{maxNH4,ref} \cdot V_i^{\gamma1} \qquad K_{N,i} = K_{N,ref} \cdot V_i^{\delta1}$$

$$V_{maxNO3,i} = Q_{maxNO3,ref} \cdot V_i^{\gamma2} \qquad K_{P,i} = K_{P,ref} \cdot V_i^{\delta2}$$

$$V_{maxP,i} = Q_{maxP,ref} \cdot V_i^{\gamma3} \qquad K_{N,i} = K_{Si,ref} \cdot V_i^{\delta3}$$

Cells with larger volume generally possess a higher cell quota and V_{max} . The small cells have reversely higher affinity ($1/K_{N,i}$, $1/K_{P,i}$). As a consequence, small cells will out-compete the large ones in conditions of limited nutrient supply.

Symbol	Description	Value
α^1	$Q_{\min N}$	0.84
α^2	$Q_{\min P}$	0.84
α^3	Q_{Si}	0.84
β^1	$Q_{\max N}$	0.92
β^2	$Q_{\min P}$	0.92
γ^1	$V_{\max NH_4}$	0.97
γ^2	$V_{\max NO_3}$	0.97
γ^3	$V_{\max P}$	0.97
δ^1	K_N	0.33
δ^2	K_P	0.33
δ^3	K_{Si}	0.33

Table 3.2: Coefficient of Allometry (Sourisseau et al. 2017)

3.2.7. Limitation

This is an important aspect of species growth and development. It simply refers to the factors which are insufficient at a certain period. For the phytoplankton, we consider temperature, light and nutrients particularly, nitrogen and phosphorus as limiting factors. In addition to N and P, Si is taken into account for the diatoms. In terms of light, we consider the Photosynthetically Available Radiation (PAR).

Limitation in our model is a dimensionless function ranging between 0 (full limitation or maximum) and 1 (no limitation at all). The limiting factors were thus determined as follows –

Temperature limitation: Rathaille and Raine, 2007

$$IF (T_{opt,i} - 10) < T < T_{opt,i}$$

$$fT_i = 0.1 * \{T - (T_{opt,i} - 10)\}$$

$$IF T < (T_{opt,i} - 10) ; fT_i = 0$$

$$IF T > T_{opt,i} ; fT_i = 1$$

Light limitation: Jassby and Platt, 1976

$$fL_i = \tanh \left(\frac{I}{I_{opt,i}} \right)$$

$$\text{With } I = I_{opt} * e^{-(K_{par} * depth)}$$

Nitrogen limitation: Droop, 1973

$$fN_i = \frac{Q_{maxN,i}}{Q_{maxN,i} - Q_{minN,i}} \left(1 - \frac{Q_{minN,i}}{Q_{N,i}} \right)$$

$$\text{IF } Q_{N,i} \leq Q_{minN,i} \quad ; \quad fN_i = 0$$

$$\text{IF } Q_{N,i} \geq (Q_{maxN,i}) \quad ; \quad fN_i = 1$$

Phosphorus limitation: Droop, 1973

$$fP_i = \frac{Q_{maxP,i}}{Q_{maxP,i} - Q_{minP,i}} \left(1 - \frac{Q_{minP,i}}{Q_{P,i}} \right)$$

$$\text{IF } Q_{P,i} \leq Q_{minP,i} \quad ; \quad fP_i = 0$$

$$\text{IF } Q_{P,i} \geq (Q_{maxP,i}) \quad ; \quad fP_i = 1$$

Silicon limitation: Monod, 1942

$$fSi = \frac{[Si]}{K_{Si} + [Si]}$$

Only diatoms are concerned.

3.3. Phenotypic Variability

Using the Droop approach, simulations were performed with a trait-based model (Litchman et al. 2012) that includes a phenotypic variability of different parameter sets (Barton et al. 2010; Dutkiewicz et al. 2009).

3.3.1. Number of Species

The number of species (NS) is very important in every competition related model. By doubling NS, we lose about fifty per cent of the abundance of species. This means that the presence of more phytoplankton reduces the concentration of available nutrients, increases the competition and thus, reduces the abundance of each species too.

	NS =25	NS =50	NS =100	NS =200
2012	4 855 354	2 799 620	1 456 161	386 398
2013	551 428	216 879	66 951	24 878
2014	2 095 205	866 550	340 026	141 860




Table 3.3: Simulated abundance of *A. minutum* as a function of NS

The ideal NS to be used in a model is therefore, one which has a closer relationship with actual field observation. For this reason, different numbers of phenotypes (e.g. 25, 50, 72, 100 and 200) were placed in competition with *A. minutum* under the same environmental conditions. Within a reasonable computing time, a total of 73 species (i.e. 72 plus *A. minutum*) showed the best fit or resemblance with *in situ* data.

3.3.2. Characteristics of species

Phenotypic variability was determined based on three relevant and independent physiological traits: cell size (a continuous trait in ESD, Equivalent Spherical Diameter), cell cover (a categorical trait: siliceous or not) and optimal temperature (a continuous trait in degree Celsius). The selected configuration includes 36 siliceous and 36 non-siliceous phenotypes with size distribution on log scale from 1 to 64 μm of ESD (Fig. 3.4). In characterizing them, the picophytoplankton (pico) was represented by phenotypes of 1 and 2 μm , nanophytoplankton (nano) by 5 and 18 μm and microphytoplankton (micro) by 28 and 64 μm (Table 3.4). For *A. minutum*, 18 μm (Maranon et al., 2013) is attributed to its mean length since its shape is considered sub-spherical (Balech, 1989), spherical (Probert, 1999) or ellipsoidal (Hillebrand et al., 1999).

Temperature being a major environmental parameter that regulates metabolic rates such as photosynthesis, respiration, growth, resource acquisition and motility (Sourisseau et al., 2017; Litchman and Klausmeier, 2008; Eppley, 1985), this dependence may be simulated with an optimal temperature (T_{opt}). T_{opt} in the configuration was linearly distributed from 10 to 20°C to cover the temperature range of seawater in the bay. *A. minutum* was assigned a T_{opt} of 18°C because its optimum growth occurs between 17 and 20°C (Bill et al., 2016) and also because its maximum bloom densities in Bretagne (Penzé and Rance) have been observed when water temperatures were between 16 and 20°C (Chapelle et al., 2007).

Category	Size (µm)	Phenotype		Topt	µmax	Iopt	Qmin N	Qmin P	Qmax N	Qmax P	Qsi	Kn	Kp	Ksi	Mort	Vmax		
		Dino	Diat													NH ₄	NO ₃	PO ₄
Pico	1	2	38	10	1.09	100	2.9E-09	1.4E-10	2.00	2.00	0	0.23	0.01	0	0.02	0.38	0.19	0.38
		8	44	12	1.24													
		14	50	14	1.40													
		20	56	16	1.59													
		26	62	18	1.80													
		32	68	20	2.05													
	2	3	39	10	1.09	84	2.3E-08	1.1E-09	2.46	2.46	0	0.53	0.03	0	0.02	0.53	0.265	0.53
		9	45	12	1.24													
		15	51	14	1.40													
		21	57	16	1.59													
		27	63	18	1.80													
		33	69	20	2.05													
Nano	5	4	40	10	1.09	54	1.9E-07	9.0E-09	3.03	3.03	0	1.21	0.06	0	0.02	0.73	0.36	0.73
		10	46	12	1.24													
		16	52	14	1.40													
		22	58	16	1.59													
		28	64	18	1.80													
		34	70	20	2.05													
	18	Alex	-	18	1.80	24	4.1E-06	2.0E-07	6.62	7.38	0	3.93	0.28	0	0.02	1.16	0.58	1.86
		5	41	10	1.09													
		11	47	12	1.24													
		17	53	14	1.40													
		23	59	16	1.59													
		29	65	18	1.80													
		35	71	20	2.05													
Micro	28	6	42	10	1.09	12	1.2E-05	5.7E-07	4.60	4.60	0	6.41	0.31	0	0.02	1.43	0.71	1.43
		12	48	12	1.24													
		18	54	14	1.40													
		24	60	16	1.59													
		30	66	18	1.80													
		36	72	20	2.05													
	64	7	43	10	1.09	8	9.5E-05	4.6E-06	5.66	5.66	0	14.72	0.70	0	0.02	2.00	1.00	2.00
		13	49	12	1.24													
		19	55	14	1.40													
		25	61	16	1.59													
		31	67	18	1.80													
		37	73	20	2.05													

Table 3.4: Characteristics of species

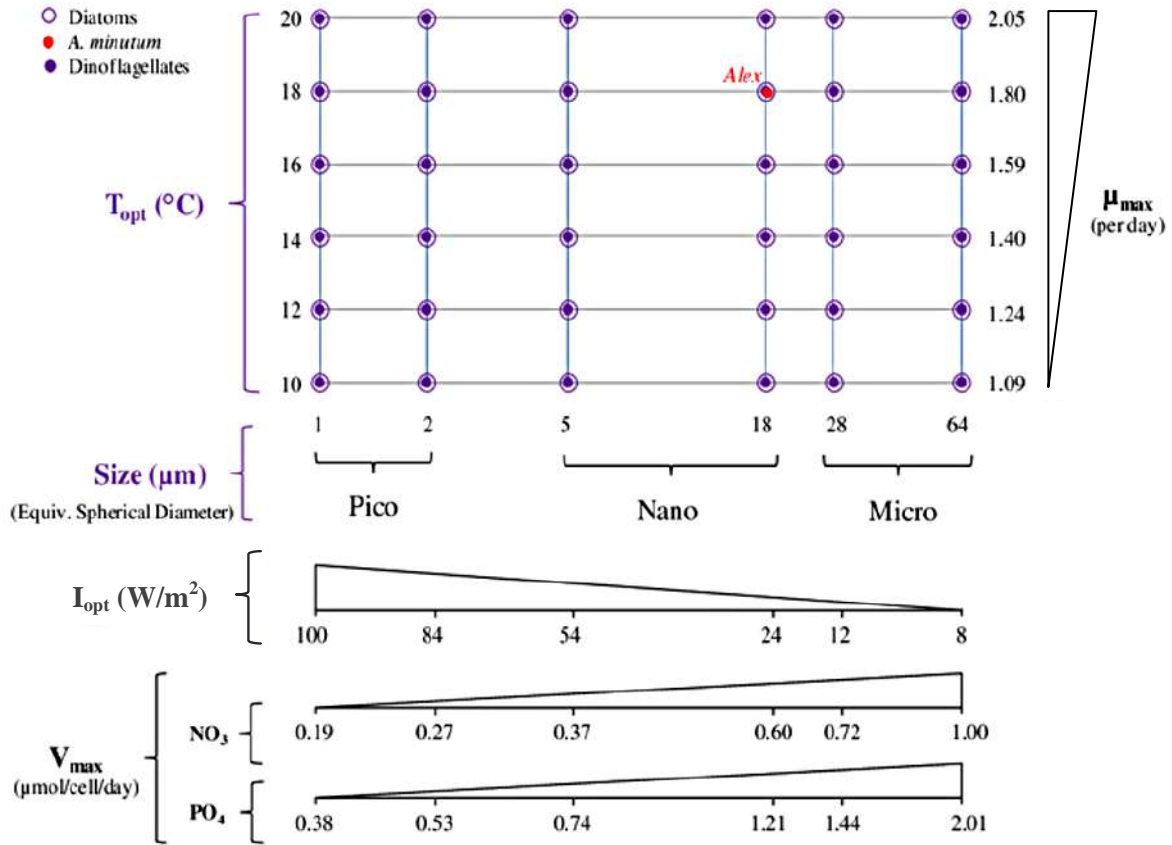


Figure 3.4: Distribution of 73 Species (*A. minutum*, 36 diatoms and 36 dinoflagellates)

The parameterization of these traits was accompanied by relevant trade-offs that are well defined for phytoplankton groups (Litchman and Klausmeier, 2008). The size of a cell is very important in classifying and modeling photosynthetic rates in phytoplankton (Tang, 1995; Agusti, 1991; Joint and Pomroy, 1988). Cullen et al. (1993) suggested that cell size should be included in the description of phytoplankton growth intended for biogeochemical models. Trade-offs were then determined based on the relationships between the cell size and – (i) the maximum growth rate of species i ($\mu_{max,i}$), (ii) the speed of nutrient absorption (V_{max}), (iii) the nutrient storage capacity (cell quota; Litchman et al., 2007; Finkel, 2001; Kooijman 2001; Tang, 1995; Banse, 1982; Laws, 1975), and (iv) the optimal irradiance (I_{opt} , the quantity and quality of pigment content in a cell, Edwards et al. 2015; Finkel, 2001). Using an I_{opt} of $100\mu\text{mol.m}^{-2}.\text{s}^{-1}$ or 24W.m^{-2} (FiNAL, 2008; Chang and McClean, 1997) for *A. minutum* and a cell size of $18\mu\text{m}$ as points of reference, I_{opt} was assigned to other phenotypes based on their cell size (Table 3.4). It was distributed from 8 to 100W.m^{-2} in our configuration to cover the Photosynthetically Available Radiation (PAR) observed in the Bay of Brest.

3.4. Simulation Analysis

The approaches - Heatmap correlation distance, Weibull analysis (Rolinski et al. 2007), rainfall anomaly index (Van-Rooy, 1965), annual seasonal cycle of the Bay of Brest (Del Amo et al. 1997) - used in analyzing field data of nutrients, phytoplankton and environmental variables were equally used to analyze the results of the model. In addition to these approaches, Taylor diagrams (Taylor, 2001) were used to summarize the relationship (correlation and deviation) between model and field data in order to evaluate the overall quantitative performance of the model in relation to the phenology of *A. minutum*.

3.5. Results of the simulations

3.5.1. Seasonal variability

All environmental variables change with respect to season and the three categories of phytoplankton showed the same global seasonal phenological trend over the study period. We therefore, used the data of year 2016 to illustrate the seasonal variations because it is one of the years with more phytoplankton observed data.

3.5.1.1. Environmental variables

Temperature and light follow strong and similar seasonal patterns with low values of 8.6°C and 15W.m^{-2} in the winter respectively in January and December but high values in the summer with a maximum 20.5°C in August and 349W.m^{-2} in July (Fig. 3.5). River flow is highest ($10^6\text{m}^3\cdot\text{d}^{-1}$) in the winter and lowest ($10^4\text{m}^3\cdot\text{d}^{-1}$) in the summer. Dilution rate follows the seasonal pattern of river flow being maximum in the winter and minimum in the summer. Furthermore, tide variations (neap and spring) affect dilution rate in an interval of seven days. Out of the productive periods (from January to March), rainfall influences the concentration of nutrients which increases with increasing river flow. From April to October, nutrients remain low due to less river flow and high productivity of phytoplankton. The model closely followed the trends of field data especially those of NO_3 and Si. PO_4 was however underestimated by the model in the summer and beginning of autumn. Reversely, between January and June, the model overestimated NH_4 field data but slightly followed the trend from November to December.

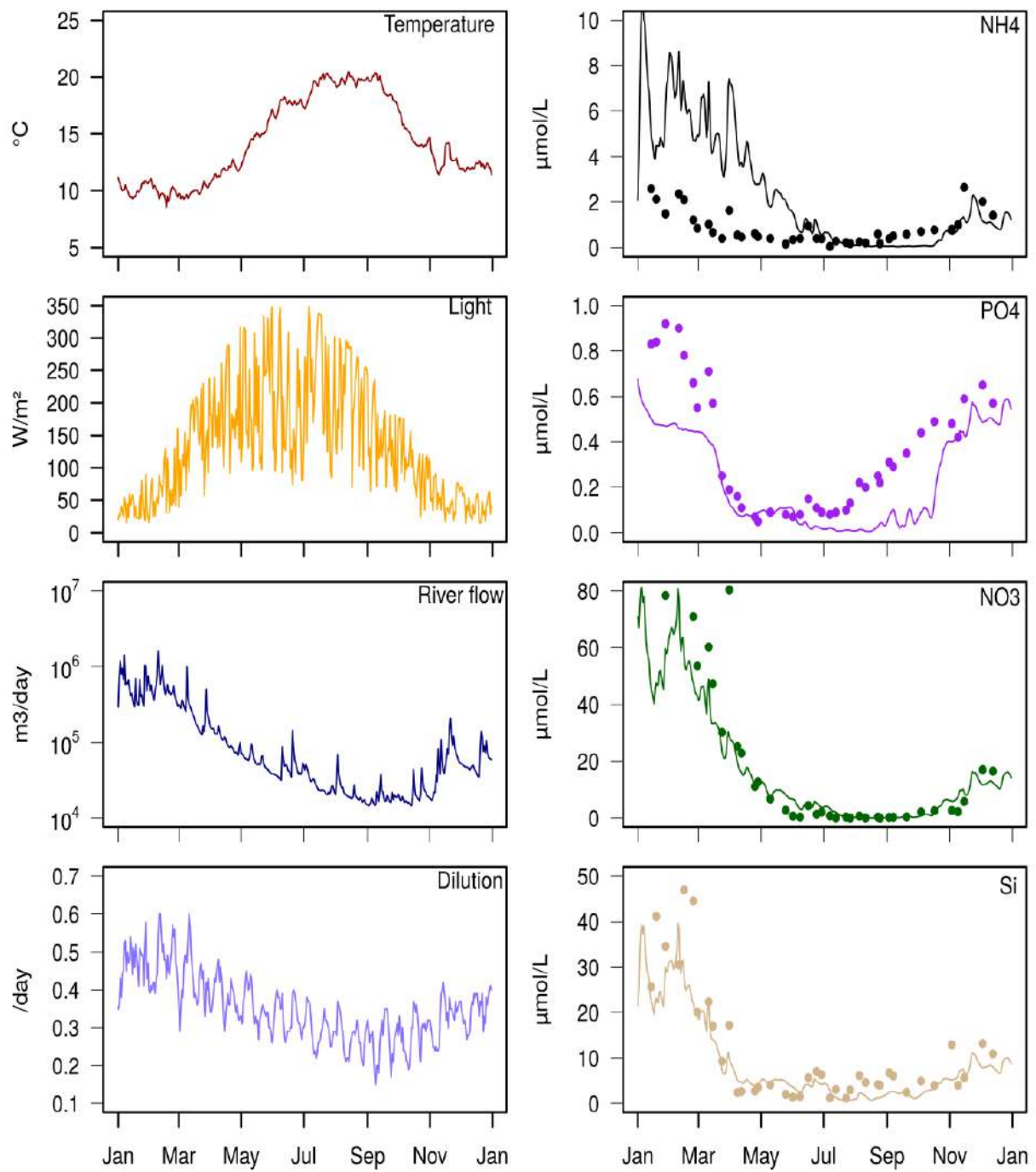


Figure 3.5: Seasonal variability of environmental variables. Observed nutrients are points while simulated are lines

N/P ratios are regularly over 16 (Redfield, 1958), which signifies that N is in excess of P. Only in end of summer did the ratio drop below Redfield (Fig 3.5b). At this period, N concentration reached low values which may imply possible N limitation on phytoplankton growth. The ecosystem was highly limited in P during late spring and summer when N/P ratio was well above 16 and concentrations low.

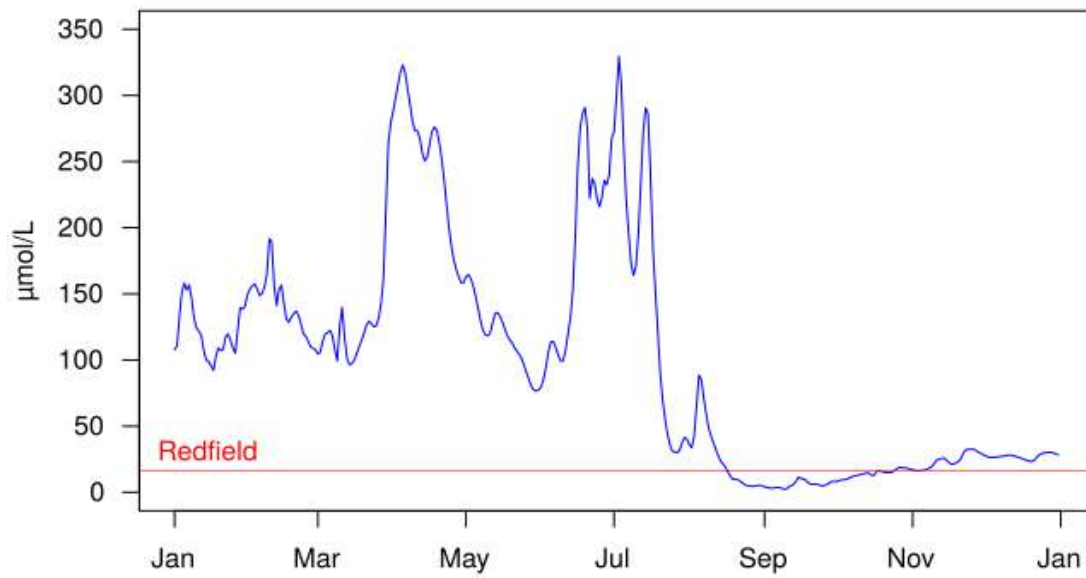


Figure 3.5b: Simulated ratio (in blue) of Nitrogen to Phosphorus, 2016

3.5.1.2. Phytoplankton community

December to the end of April showed a stable abundance of simulated phytoplankton which corresponds to the minimal values fixed in the model (Fig. 3.6.A). In May, there is first – a gradual increase of micro and nano and slight increase of pico. The micro reached its maximum abundances first ($5 \times 10^2 \text{ cells.L}^{-1}$) followed by the nano ($10^6 \text{ cells.L}^{-1}$) in June and pico (over $10^9 \text{ cells.L}^{-1}$) in October. At the end of June, the microphytoplankton size fraction had decreased to its lowest abundance whereas, nano is about its maximum but pico is still on the increase. By September, pico continued to increase in abundance but no further net growth is simulated in nano and micro size fractions. The abundance of pico remained relatively stable until late October and early November when it experienced a sharp decrease. The same period is marked by a slight increase in the abundance of micro before the last decrease.

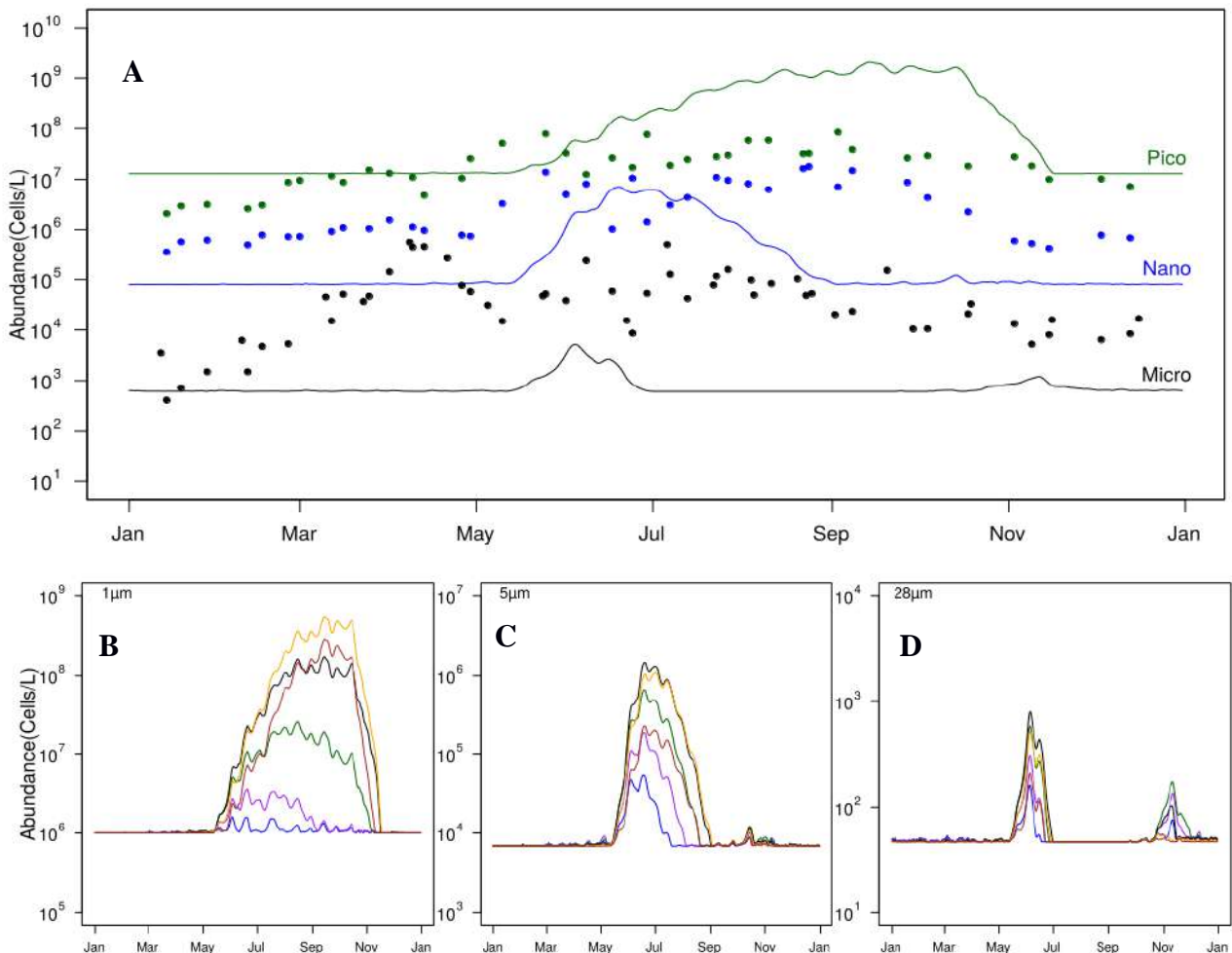


Figure 3.6.A: Field and model seasonal variability of phytoplankton abundance in 2016. B, C and D show the variability in the simulated abundance of species of same size as a function of optimal temperature in 2016: blue (10°C), purple (12°C), green (14°C), black (16°C), orange (18°C), and brown (20°C).

There are also seasonal variations in the abundance of each phenotype of the same size with regards to their optimal temperature. Among those of 1 μ m (Fig. 3.6.B), species of 10°C have the lowest abundance while species of 16°C to 20°C have the highest abundance. Those of 16°C were the first to bloom, 18°C being the most abundant and 20°C having an MA below those of 18°C but above those of 16°C. With species of 5 μ m (Fig. 3.6.C), there is a similar timing of bloom increase and all the species have a good summer peak. Their peaks started to decrease at the same period but species of lower T_{opt} were the first to completely decrease. For the 28 μ m (Fig. 3.6.D), species of 16°C are the most abundant in the summer bloom but those of 14°C dominated in autumn bloom.

With *in situ* data, field abundances of pico, nano and micro appeared steady in the winter but increased earlier in spring with a slightly faster increase for the micro size fraction from March. Pico and nano experienced high abundances in June whereas micro decreased in the same month. Micro however, showed two maxima – one in April and another from June to August and then, decreased in October. Nano remained stable all summer but decreased in September to reach winter abundances. Pico decreased in late October and early November. At this period, there is a slight increase in micro which might represent the autumn peak. Final densities of the micro size fraction in December 2016 are different from the initial conditions in January 2016 thereby, indicating some interannual variability of this seasonal cycle. There is a difference in the timing of abundance increase and decrease between field and model in several cases. For example, the comparison of model and observation shows underestimation of micro, nano and pico in winter/spring but good timing in summer micro bloom. Nano showed similar increasing time in May, pico and micro showed similar decreasing time in November. The model closely followed *in situ* pico between March and mid-June after which, it overestimated observation until mid-November to December when both showed similar abundances.

3.5.1.3. *Alexandrium minutum*

Observed *A. minutum* blooms occurred during summer between May and August with MA between June and the end of August (Fig. 3.7). By the end of September, abundances dropped to the lowest levels and consequently disappearing during the winter. Simulated *A. minutum* also has similar dynamics. Despite sometimes, a slight delay of the abundance increase compared to observations (e.g. in 2013 and 2014), the model showed a good timing in the beginning of the bloom but its MA occurred much earlier in some of the years (2010, 2012 2013, 2014 and 2015). Between August and mid-October, no significant net growth was noted in the model. In November however, another bloom (autumn peak) was detected in the model but none was observed in the field. Finally, from December until the end of April, growth was absent in both field and model. To evaluate what environmental factors control *A. minutum* growth, the maximum limiting factors (T, L, P, and N) are shown in figure 3.8. *A. minutum* is first limited by temperature at the beginning of the year then it becomes limited by nutrients – first by P and then N from May to October. The end of the year is marked by temperature and light limitations.

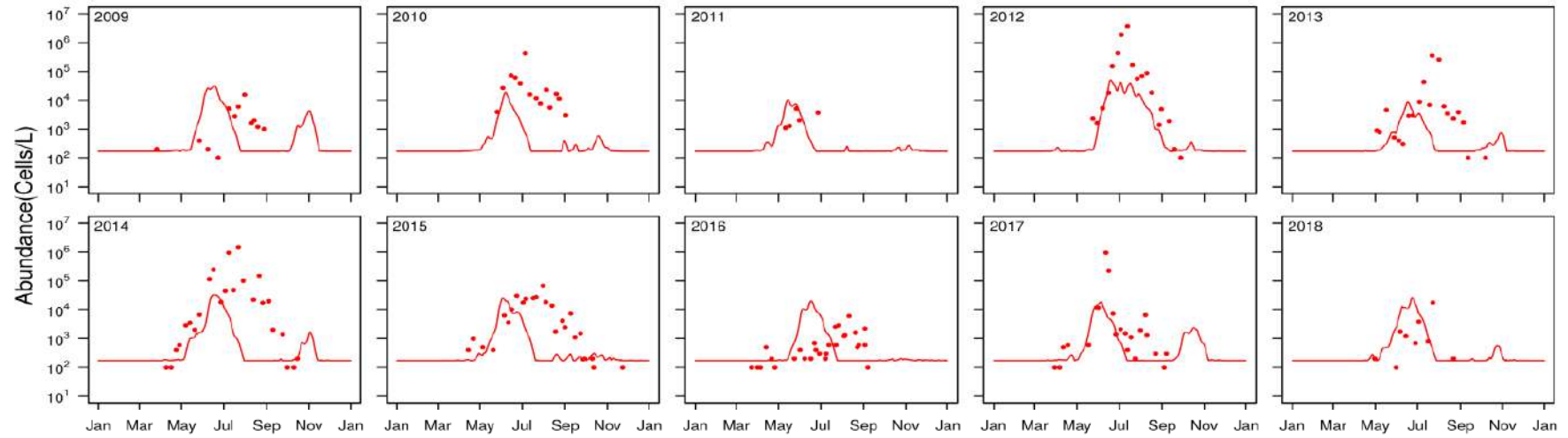


Figure 3.7: Field (points) and model (line) seasonal and interannual variability in the abundances of *A. minutum*

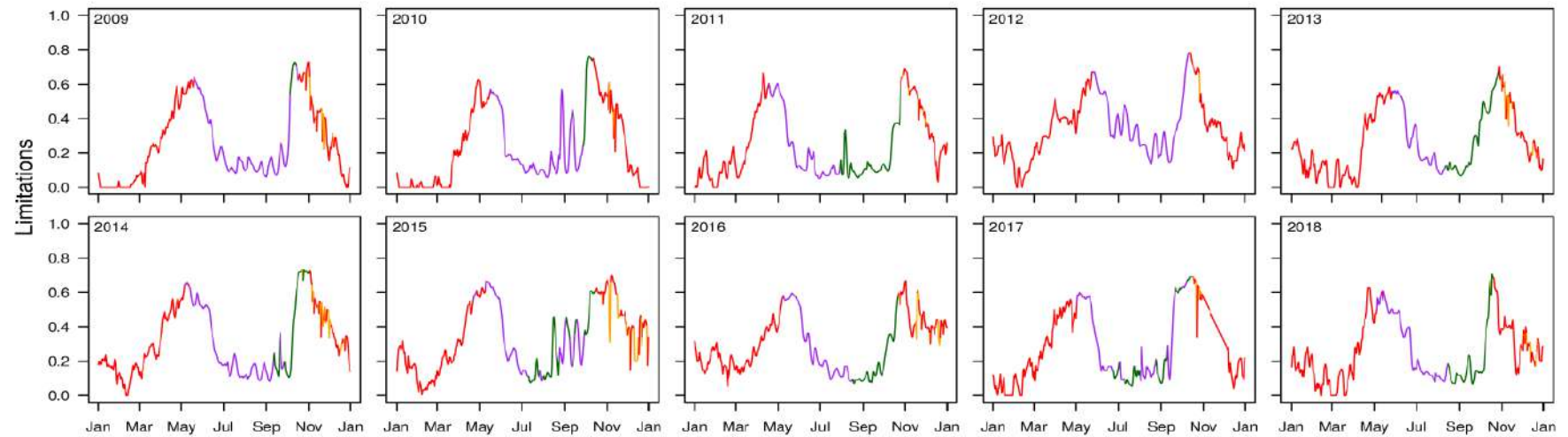


Figure 3.8: Maximum limitations on the growth of *A. minutum*. Temperature in red, Light in orange, N in green and P in purple

	Year	Field					Model				
		MA	DMA	Bloom (Weibull)			MA	DMA	Bloom (Weibull)		
				Start	End	Duration			Start	End	Duration
A. <i>minutum</i>	2009	15 400	Jul 31	Jun 30	Aug 08	37	31 600	Jun 11	May 27	Jun 29	33
	2010	432 600	Jul 04	Jun 27	Jul 10	12	19 030	Jun 05	May 27	Jun 21	25
	2011	5 100	May 22	Apr 17	Dec 06	339	10 450	May 14	May 05	Jun 06	32
	2012	3 675 330	Jul 11	Jun 27	Jul 18	23	49 810	Jun 18	Jun 10	Aug 11	62
	2013	358 400	Jul 09	Jul 02	Jul 16	15	8 728	Jun 15	Jun 03	Jul 11	38
	2014	1 496 480	Jun 16	May 29	Jun 24	26	33 130	Jun 14	Jun 05	Jul 05	30
	2015	68 800	Aug 02	May 30	Sep 08	101	25 770	Jun 01	May 25	Jun 29	35
	2016	6 000	May 29	Mar 02	Dec 25	346	19 760	Jun 15	May 26	Jul 04	39
	2017	968 400	Jun 12	May 31	Jun 18	18	18 660	Jun 05	May 17	Jun 16	31
	2018	17 500	Jul 23	Jun 26	Jul 14	16	26 320	Jun 23	May 27	Jul 06	40
Pico	2009	-	-	-	-	-	2 596 800 000	Sep 15	Jun 25	Oct 25	122
	2010	-	-	-	-	-	2 407 200 000	Sep 04	Jun 06	Oct 05	121
	2011	-	-	-	-	-	2 398 560 000	Sep 22	May 11	Oct 30	172
	2012	-	-	-	-	-	513 600 000	Sep 14	Jul 27	Oct 10	75
	2013	-	-	-	-	-	1 563 120 000	Sep 17	Jul 06	Oct 29	115
	2014	-	-	-	-	-	1 843 920 000	Sep 23	Jun 21	Oct 21	121
	2015	-	-	-	-	-	2 139 840 000	Aug 26	Jun 15	Oct 19	126
	2016	84 036 364	Sep 03	Feb 14	Apr 14	59	2 069 520 000	Sep 14	Jun 20	Oct 25	127
	2017	99 594 046	Jul 03	Jan 02	Dec 18	351	1 885 200 000	Aug 02	Jan 02	Dec 18	351
	2018	83 103 097	Apr 10	Mar 23	Apr 18	22	1 991 520 000	Sep 21	Mar 27	Apr 18	22
Nano	2009	-	-	-	-	-	8 786 400	Jun 20	May 28	Jul 24	57
	2010	-	-	-	-	-	8 488 800	Jun 08	May 27	Jul 14	49
	2011	-	-	-	-	-	6 712 800	May 27	May 03	Jun 26	54
	2012	-	-	-	-	-	8 440 800	Aug 14	May 30	Oct 01	124
	2013	-	-	-	-	-	8 937 600	Jul 04	May 28	Aug 04	78
	2014	-	-	-	-	-	7 524 000	Jun 27	Jun 04	Jul 29	54
	2015	-	-	-	-	-	8 652 000	Jun 27	May 17	Jul 22	66
	2016	17 760 181	Aug 24	May 06	Jun 13	38	6 991 200	Jun 19	Jun 01	Jul 29	58
	2017	19 052 774	Sep 04	-	-	-	9 300 000	Jun 06	-	-	-
	2018	12 692 690	Jun 23	May 22	Oct 16	147	6 616 800	Jun 24	May 22	Oct 16	147
Micro	2009	4 909 700	Jun 18	Jun 08	Jun 25	17	8 981	Jun 07	May 22	Jun 20	29
	2010	3 436 498	Aug 05	Apr 08	May 10	32	8 813	Jun 06	May 09	Jun 12	34
	2011	1 841 408	May 31	Apr 14	May 16	32	5 930	May 13	Apr 21	May 19	29
	2012	2 921 035	Jul 13	Apr 19	May 20	31	12 257	Jun 18	Jun 03	Jun 27	24
	2013	4 490 923	Jun 18	Apr 17	May 07	20	5 213	Jun 16	May 15	Jun 22	38
	2014	1 082 600	Jul 22	Feb 16	Mar 24	35	5 830	Nov 03	-	-	-
	2015	1 579 687	Jun 11	Mar 05	Apr 07	32	12 053	Jun 02	May 22	Jun 12	21
	2016	561 500	Apr 08	Feb 25	Mar 11	13	5 222	Jun 04	May 26	Jun 21	27
	2017	2 676 800	May 02	Feb 08	Feb 19	11	2 808	May 25	Feb 08	Feb 19	11
	2018	2 145 700	Jun 06	Apr 03	Apr 27	23	1 872	Oct 27	Apr 04	Apr 24	23

Table 3.5: Field and model interannual variability in the MA, DMA and bloom characteristics of phytoplankton

3.5.2. Interannual variability

3.5.2.1. *Alexandrium minutum*

Highest MA in the field ($3\,675\,330\text{ cells.L}^{-1}$) and model ($49\,810\text{ cells.L}^{-1}$) occurred in 2012 which has not just the highest MA but also the longest bloom duration in the model (Table 3.5). In 2010, 2012, 2013, 2014 and 2015 (Fig. 3.7), both model and field increased simultaneously but model declined before field data – leading to lower MA and early date of maximum abundance. DMA is quite close in 2011. Years 2009 and 2016 are not properly represented by the model as MA was overestimated and occurred much earlier in the model. Regarding environmental limitations, year 2012 showed exceptional less nutrient limitation in summer with only a P limitation over 0.2 (Fig. 3.8).

The interannual variability in the abundance of *A. minutum* is described with scaled value patterns (Fig. 3.9). There appears to be an obvious similarity in the temporal patterns on the MA of *A. minutum* (in both field and model) with higher scores in 2012 and 2014 in contrast to 2011 and 2013, having lower scores. In the same manner, some similarities were observed in the cumulative abundance, DMA, bloom start and end of *A. minutum*.

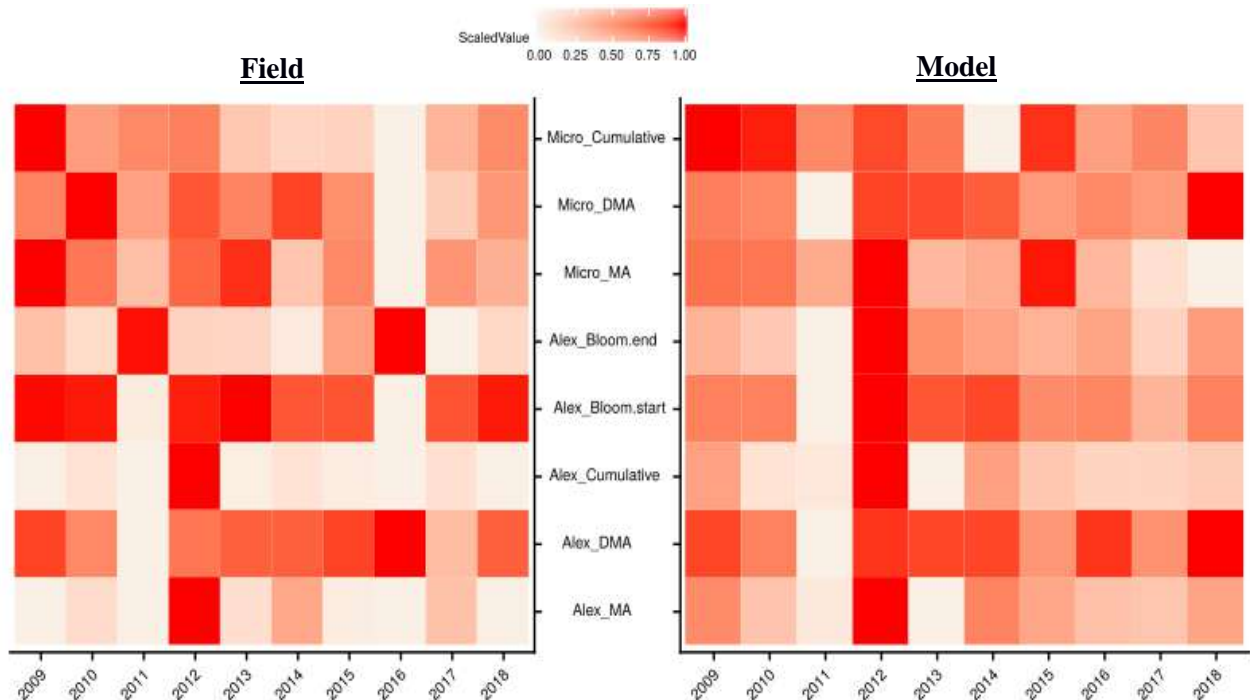


Figure 3.9: Heatmap comparing interannual field and model variables of phytoplankton in the years studied. All variables are directly extracted from actual data except Alex_Bloom.Start, Alex_Bloom.End, Alex_Cumulative and Micro_Cumulative which were obtained with the fitting of a Weibull function.

The overall quantitative performance of the model in relation to the abundance of *A. minutum* is summarized in Taylor diagram (Fig. 3.10.A) where the simulations of 2010, 2012, 2014, 2015 and 2017 are much closer to the observations with positive correlation coefficient and similar variability than other years especially 2011 which is the most poorly simulated year. Over the ten year period, having the lowest mean square difference, the DMA appears to be better represented (Fig. 3.10.B) than other variables of *A. minutum*. Despite a good representation of the DMA, the bloom start, end and duration are not consistently simulated over the period.

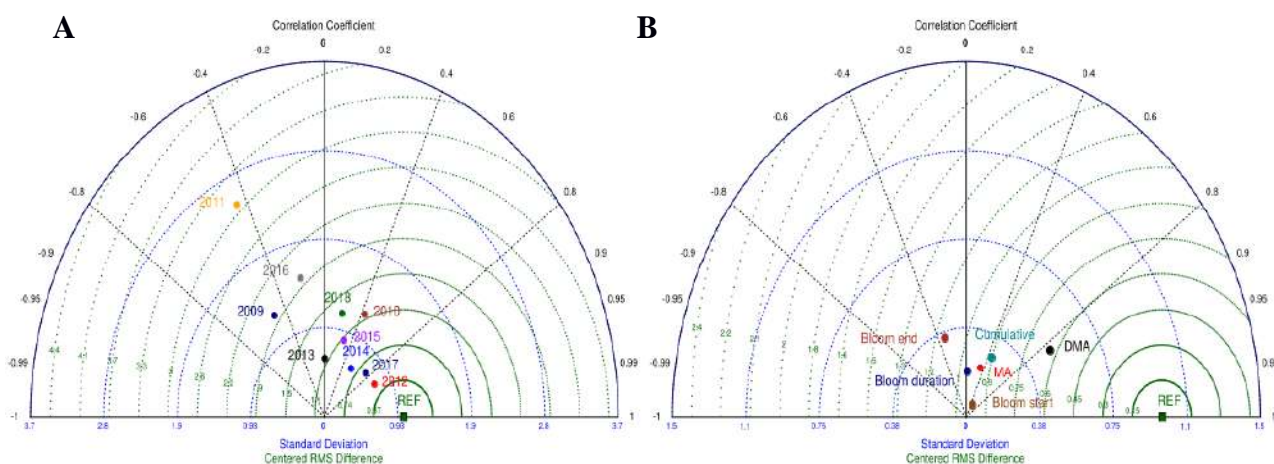


Figure 3.10.A: Taylor diagram of log *A. minutum* abundance of each simulated year. B: Sum of each variable over the ten year period - MA, DMA and Cumulative are actual values whereas Bloom start, end and duration were determined with Weibull. REF is the field data equivalence of each simulated variable.

3.5.2.2. Phytoplankton community

Over all simulated years, an average MA of approximately $10^9 \text{ cells.L}^{-1}$ was noted for the picophytoplankton which appeared to be the most abundant phytoplankton group. It showed a long duration in 2011 (the year with little growth in large cells) and a very short duration in 2012 (the year with high growth in large cells) – Table 3.5. These years (2011 and 2012) respectively showed the lowest and highest river flows and nutrient supplies. The nanophytoplankton on the other hand, had an average MA of $10^6 \text{ cells.L}^{-1}$, with the longest duration in 2012 and short durations in 2010 and 2011. Comparing field and model, there is a similar indication in the MA of micro in 2010 and in its cumulative abundances in 2009, 2011 and 2012 (Fig. 3.9). Their DMAs correspond only in 2009 and 2015. As a global evaluation, highest values were recorded in 2012 for most of the variables. Micro also had very short

durations with low average MA of $10^3 \text{ cells.L}^{-1}$ over the ten simulated years. It showed significant secondary peaks over the years except in 2012 and equally underestimated field data in most cases (Fig. 3.11).

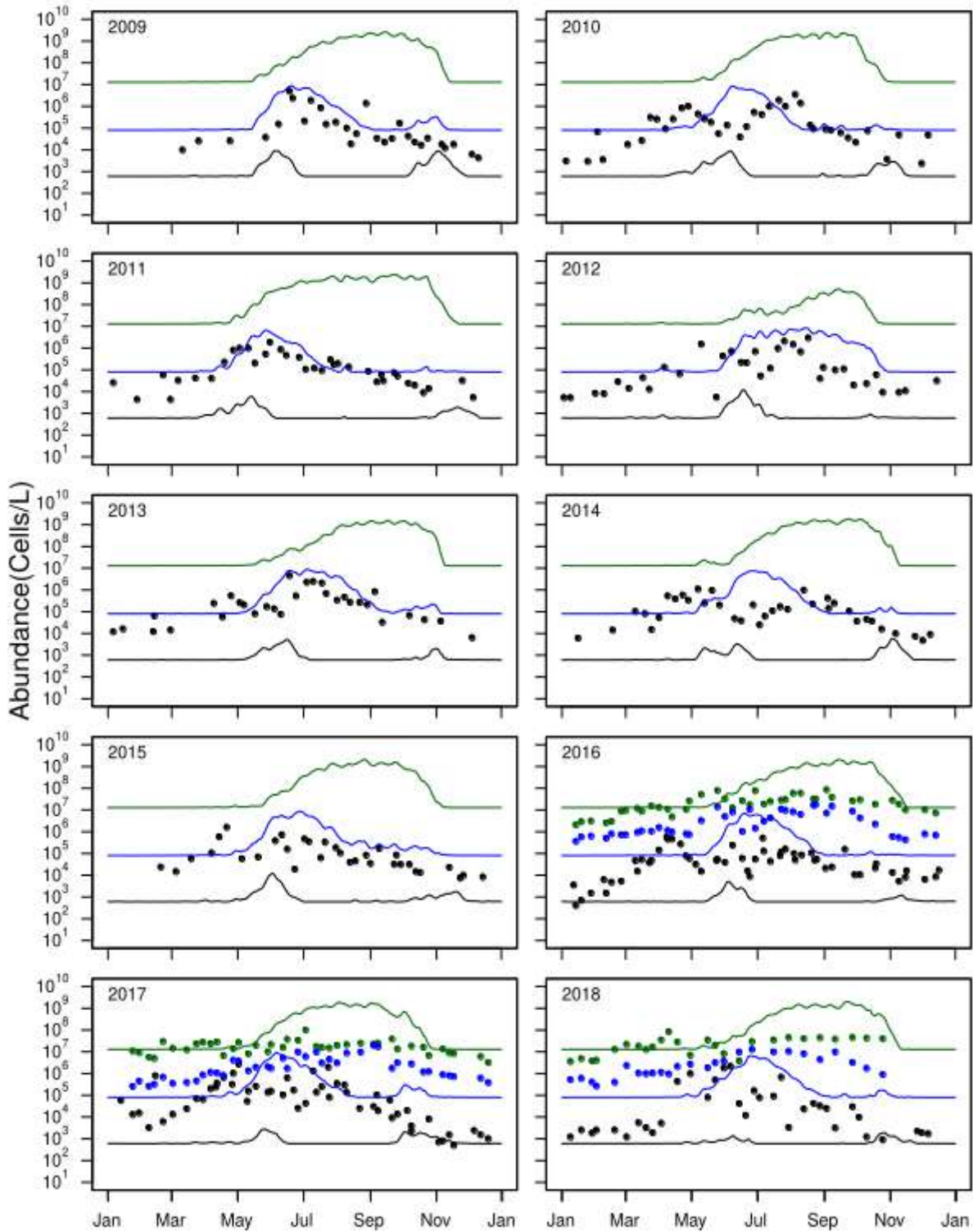


Figure 3.11: Field and model interannual variability of phytoplankton abundances. Pico in green, nano in blue and micro in black. Observed abundances are points while simulated are lines

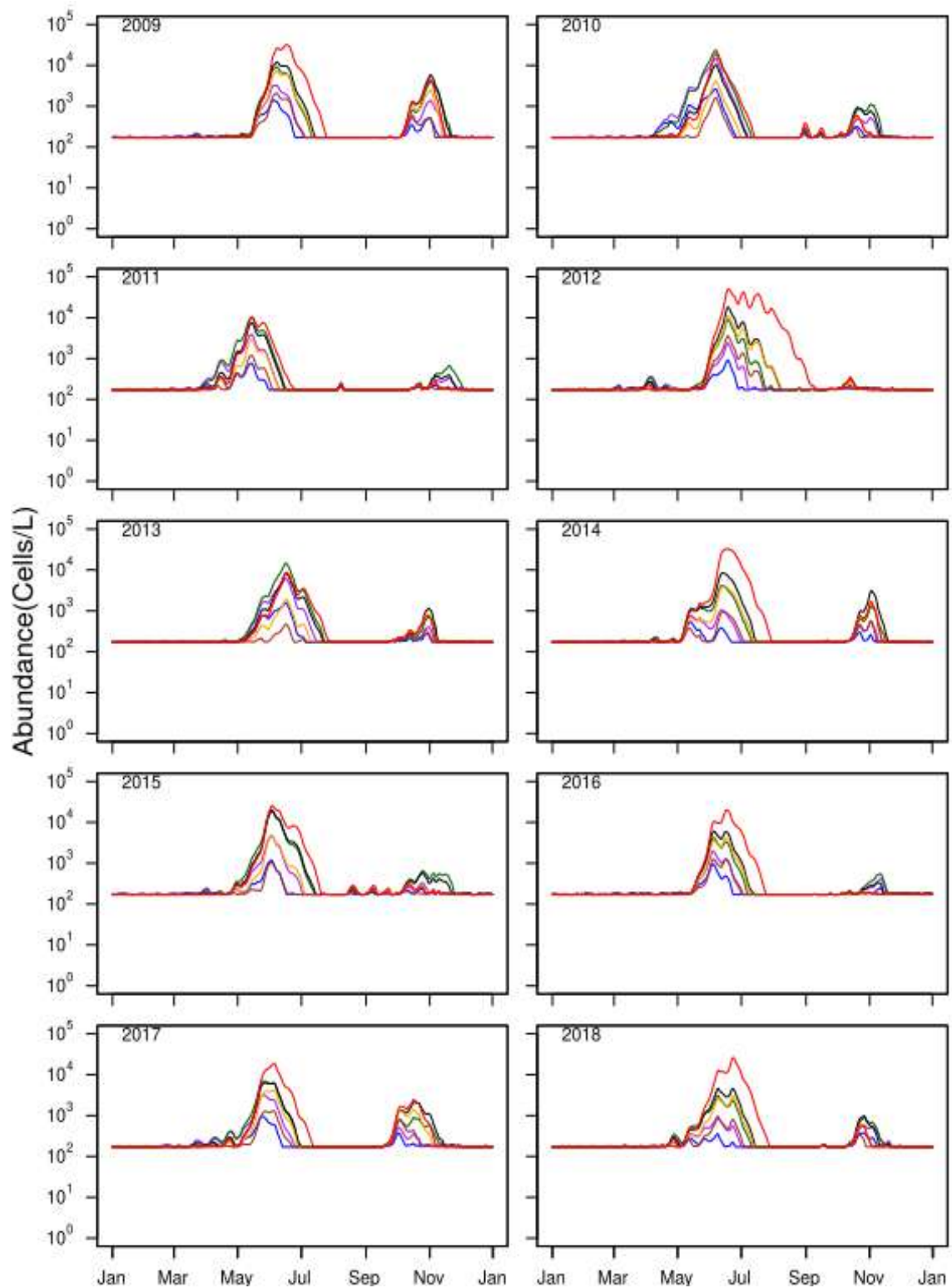


Figure 3.12: Simulated abundances of phytoplankton phenotypes of 18μm in relation to optimal temperature: Blue (10°C), purple (12°C), green (14°C), black (16°C), orange (18°C), red (18°C) and brown (20°C)

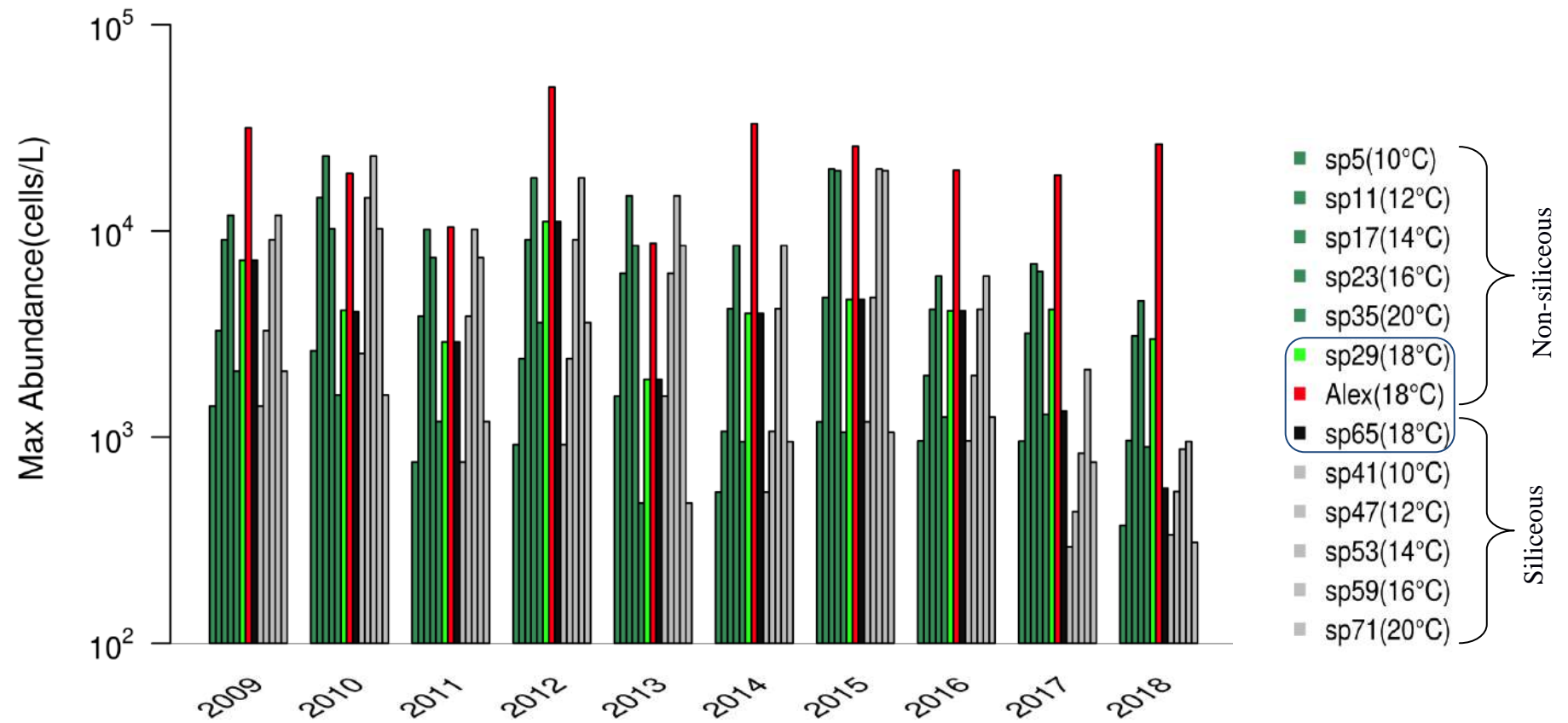


Figure 3.12: Simulated abundances of phytoplankton phenotypes of 18µm in relation to optimal temperature

Category	Size (µm)	Phenotype	Topt	Maximum Abundance (Model)									
				2009	2010	2011	2012	2013	2014	2015	2016	2017	2018
Pico	1	2	10	1745 000	3816 000	4496 000	1590 000	2292 000	1495 000	2807 000	1632 000	3315 000	1729 000
		8	12	7060 000	16220 000	18220 000	1883 000	11050 000	3876 000	10120 000	3644 000	14270 000	3338 000
		14	14	38180 000	71430 000	90340 000	3389 000	74510 000	14130 000	45160 000	25520 000	77090 000	26870 000
		20	16	234700 000	222800 000	425600 000	18270 000	239500 000	64260 000	201100 000	171500 000	318200 000	162400 000
		26	18	727200 000	723600 000	662700 000	92750 000	324000 000	342800 000	487700 000	545500 000	587400 000	518100 000
		32	20	299700 000	558500 000	120700 000	42730 000	162700 000	520000 000	311200 000	284300 000	379600 000	336000 000
	2	3	10	371 500	556 200	663 900	181 100	510 200	195 000	309 800	339 000	593 900	159 500
		9	12	1374 000	2633 000	1879 000	431 900	2928 000	459 500	1265 000	1154 000	3097 000	918 500
		15	14	6789 000	10220 000	6705 000	1259 000	21050 000	3686 000	8965 000	5045 000	13630 000	6692 000
		21	16	20880 000	18410 000	18130 000	15310 000	35330 000	17380 000	18710 000	19650 000	25150 000	28260 000
		27	18	23270 000	12690 000	12100 000	69440 000	11840 000	18680 000	17280 000	23900 000	25470 000	27330 000
		33	20	6559 000	6347 000	2362 000	13960 000	2607 000	10350 000	5144 000	5015 000	7858 000	8256 000
Nano	5	4	10	65 790	123 200	58 510	34 890	128 500	19 800	42 560	54 670	83 630	32 480
		10	12	225 600	813 600	223 800	95 500	661 100	98 530	203 400	185 300	439 500	186 600
		16	14	955 500	1635 000	962 700	402 900	2128 000	647 800	1472 000	657 300	1520 000	1216 000
		22	16	1832 000	1184 000	1484 000	1415 000	1637 000	1916 000	2193 000	1452 000	1685 000	3081 000
		28	18	1221 000	459 500	587 400	2550 000	263 200	1101 000	524 000	1088 000	977 200	1859 000
		34	20	261 900	152 800	163 700	382 400	30 840	173 200	86 730	226 300	242 700	255 900
	18	Alex	18	31 600	19 030	10 450	49 810	8 728	33 130	25 770	19 760	18 660	26 320
		5	10	1 417	2 624	759	919	1 579	540	1 189	957	956	374
		11	12	3 290	14 510	3 851	2 409	6 232	1 065	4 761	1 989	3 188	961
		17	14	9 069	23 080	10 180	9 071	14 770	4 196	19 990	4 159	6 930	3 093
		23	16	11 900	10 250	7 430	18 110	8 489	8 494	19 620	6 036	6 352	4 594
		29	18	7 199	4 117	2 899	11 130	1 906	3 983	4 659	4 100	4 153	2 996
		35	20	2 088	1 603	1 193	3 590	478	951	1 053	1 255	1 293	898
Micro	28	6	10	252	259	123	169	162	128	209	162	155	113
		12	12	513	1 193	472	393	474	218	607	306	301	187
		18	14	1 211	1 725	1 084	1 137	1 012	517	2 169	583	574	266
		24	16	1 660	936	742	2 233	661	1 229	2 094	797	741	339
		30	18	948	416	373	1 561	192	670	705	515	490	217
		36	20	317	230	180	575	100	229	193	211	210	122
	64	7	10	8	8	7	5	6	7	6	6	6	8
		13	12	13	20	14	7	8	14	8	7	8	11
		19	14	30	47	28	11	13	29	16	8	10	16
		25	16	37	29	16	19	16	64	16	10	13	15
		31	18	20	15	7	16	11	37	10	8	13	11
		37	20	10	7	5	8	7	14	8	7	10	7

Table 3.6: Interannual variability in the maximum abundance of each dinoflagellate phenotype

Interannually variability exists not only among pico, nano and micro but also among phenotypes of similar size (Table 3.6). Among those of 18µm, *A. minutum* appeared to be dominant in most of the years simulated, even out-competing a phenotype with the same T_{opt} of 18°C. This is obvious in the year 2012 where it showed a higher abundance and longer bloom duration (Fig. 3.12). The MAs of these phenotypes varied from one year to the other but phenotype of 10°C appeared to be the least dominant. We equally observed autumn peaks for most of the species especially in 2009 and 2014 which had abundances close to those of the summer peak. The peak is however, insignificant in 2012 compared to other years. There was a very close competition between *A. minutum* and phenotype of 14°C in 2010 and 2011. Phenotype of 14°C however, dominated other phenotypes in terms of MA in 2013 being a cold spring/summer. The same phenotype was also dominant in autumn in most of the years except in 2012.

3.5.2.3. Environmental variables

Cumulative anomalies of the measured variables (from May to August) show interannual variations (Fig. 2.2). Year 2011 was the first to reach a temperature of 15°C while 2013 was the last, in a difference of 39 days (Table 2.12). Positive temperature values in 2014 from May to July and negative values in 2013 during the same period, were also observed on the anomalies thereby, giving an indication of warm spring/summer in 2014 and cold spring/summer in 2013. Irradiance equally varied interannually with lowest values in 2014 and high values in 2012 and 2013.

Interannual variability exists in nutrient concentrations. During the periods of availability (Figs. 3.13 - 3.16), there is a good Si relation between field and model especially in 2016. The relation with NH_4 is also close only that field data was overestimated by model in the spring of 2016 and 2018. NO_3 has very close relation in most of the years. With PO_4 however, there is closeness between field and model in the beginning of spring but the model underestimated the field data from June to October in all years.

Being the source of nutrients, the river flow in 2012 (from May to August) was exceptionally high (Fig. 2.2). Years 2014 and 2015 were slightly wet in May and August respectively. On the contrary, 2011 showed negative river flow anomalies during the same period - indicating a dry spring and summer. The flow in other years varied with mainly negative anomalies except in 2014.

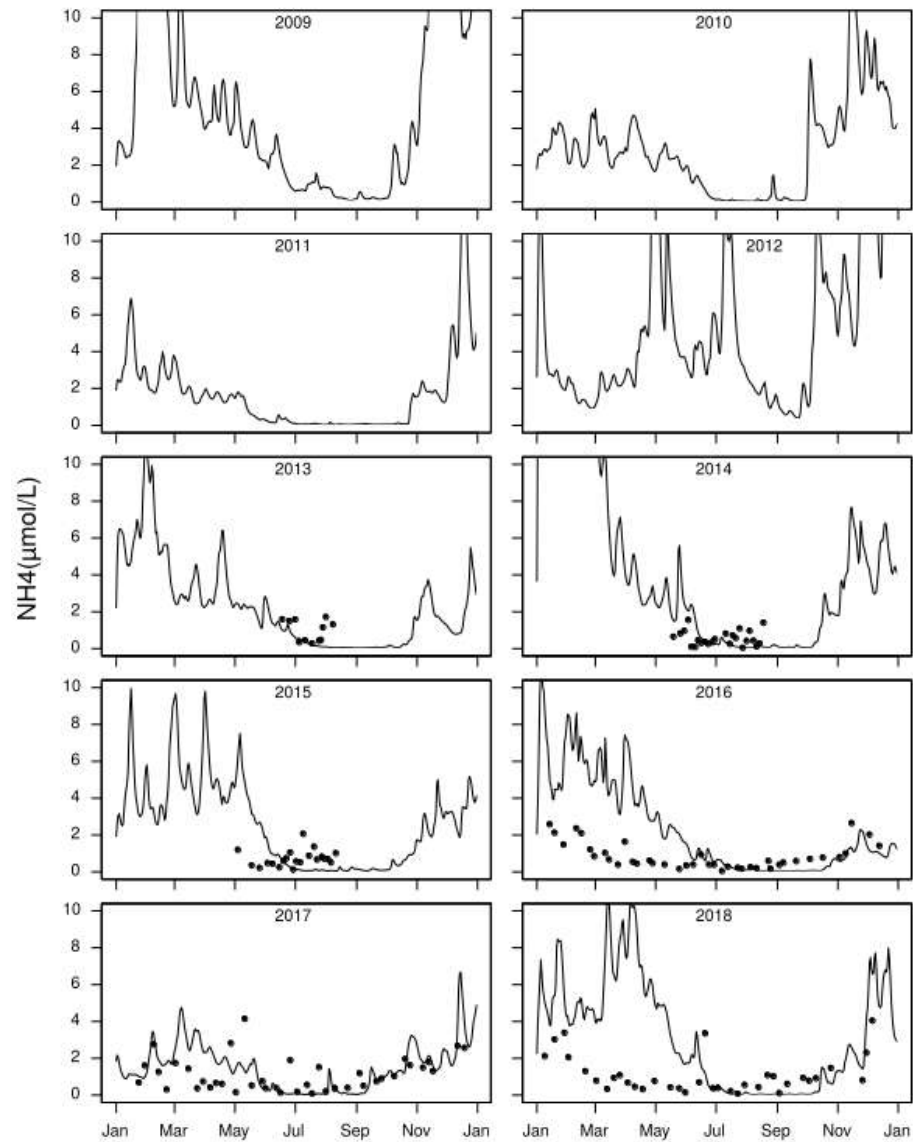


Figure 3.13: NH_4 concentrations in field (points) and model (line)

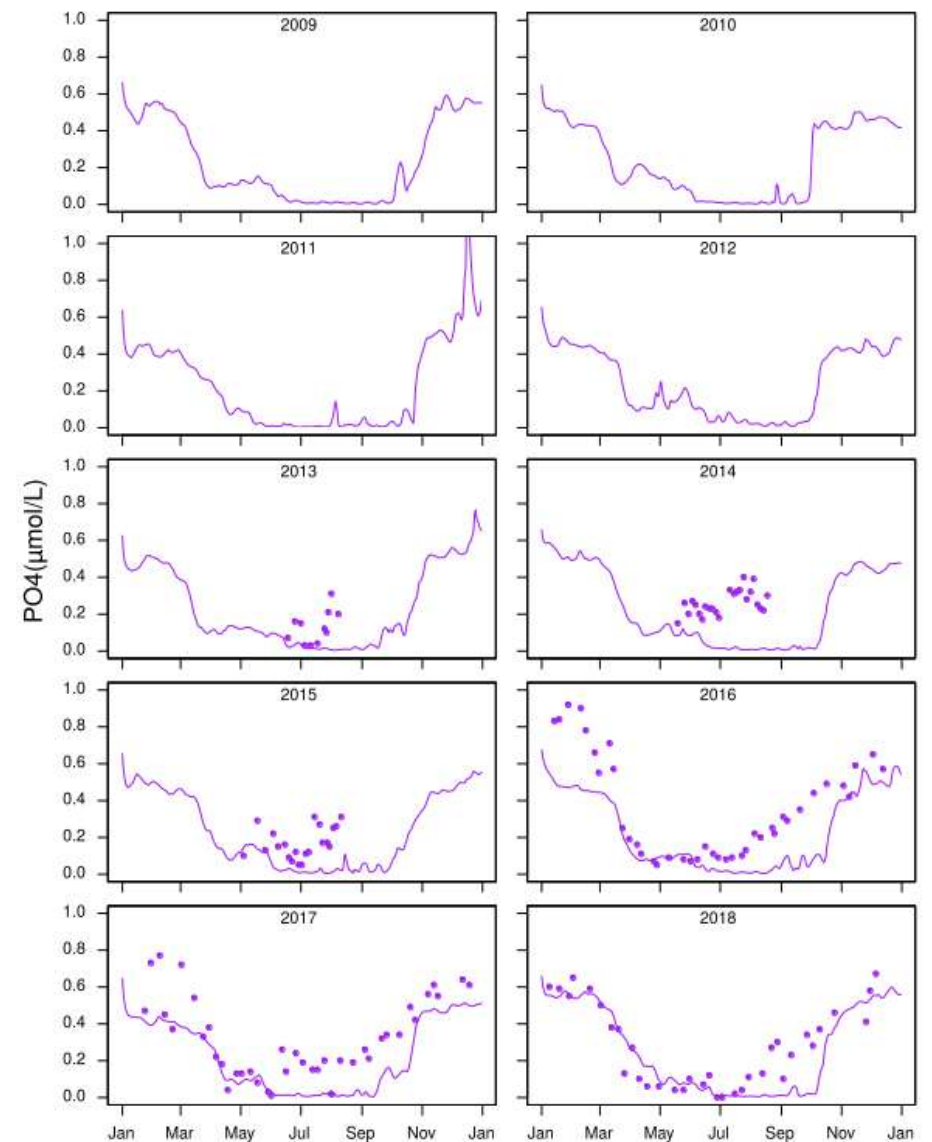


Figure 3.14: PO_4 concentrations in field (points) and model (line)

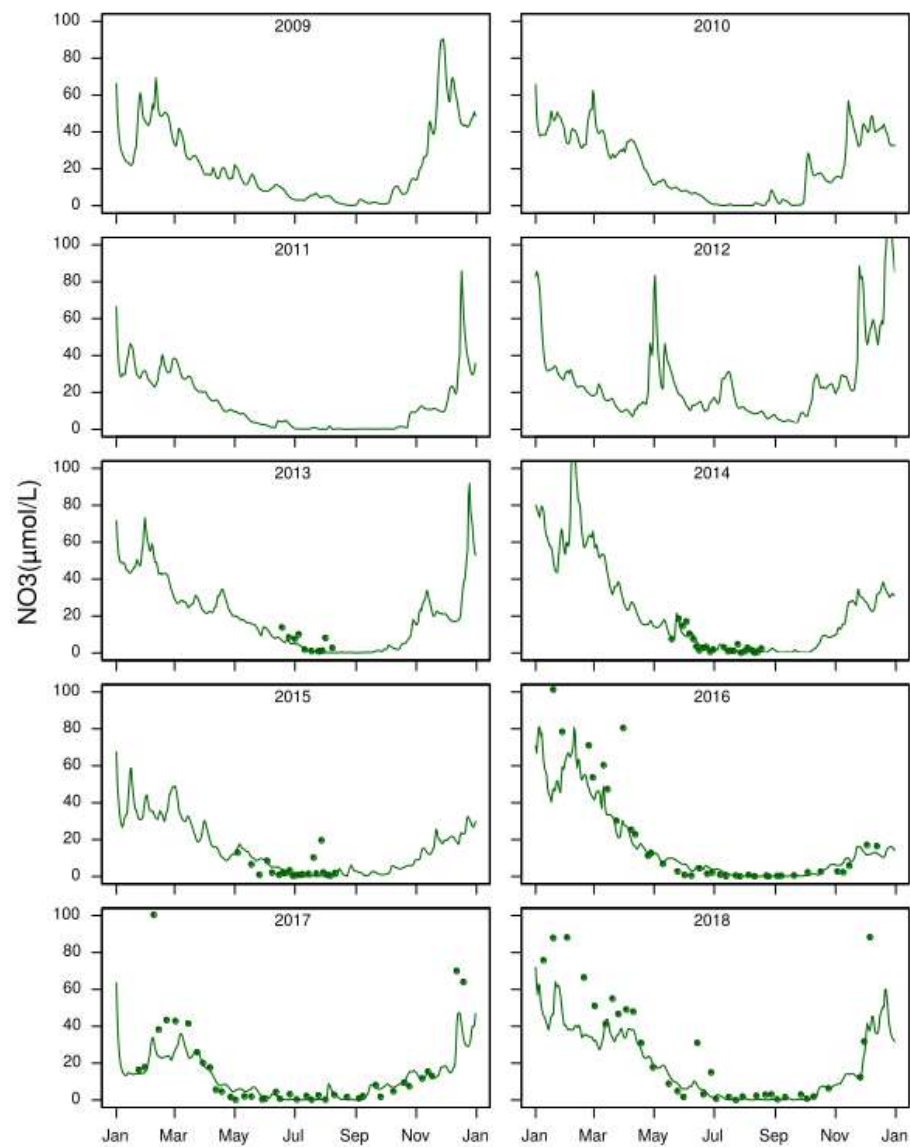


Figure 3.15: NO_3 concentrations in field (points) and model (line)

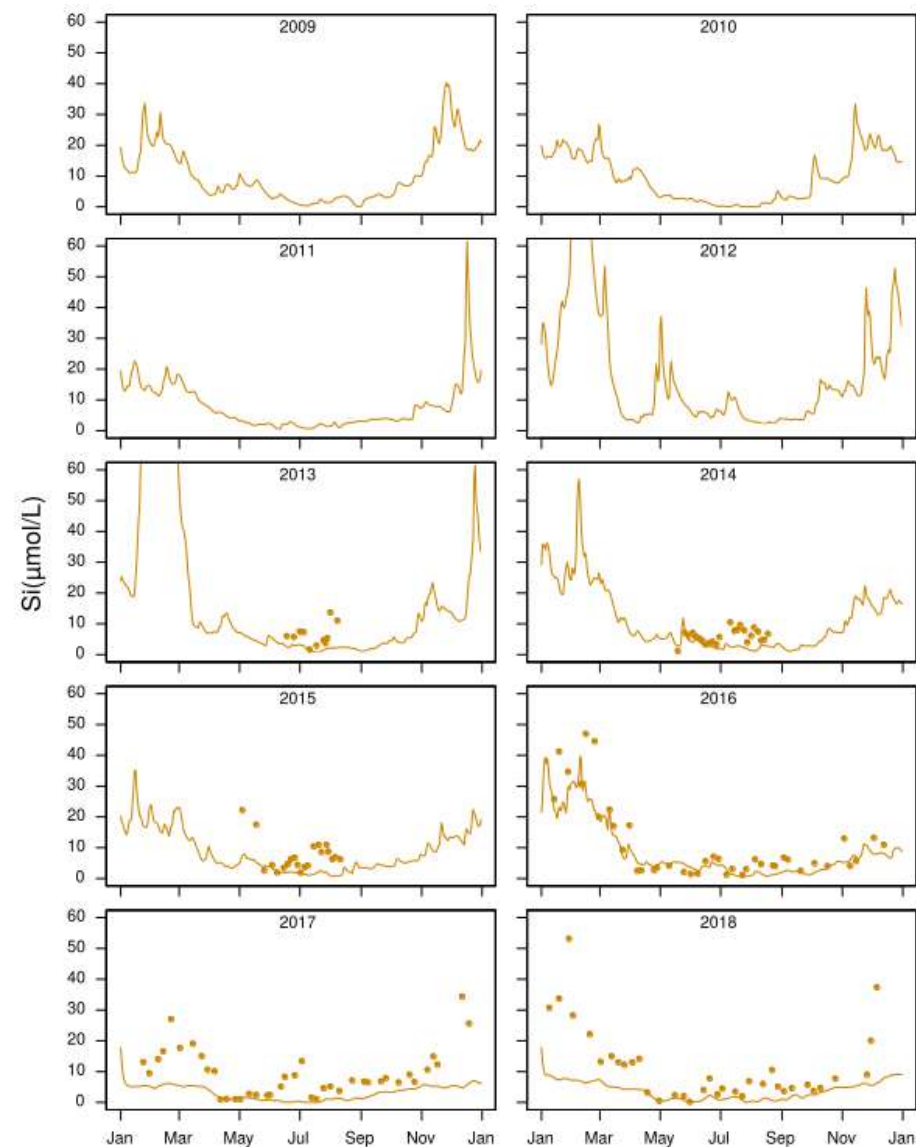


Figure 3.16: Si(OH)_4 concentrations in field (points) and model (line)

Simulated N/P ratios showed similar seasonal evolution in all years but 2009, 2010 and 2012 were never below the Redfield ratio (Fig. 3.17). Redfield N/P ratio equivalence was observed mid-July 2017 and 2015, beginning of August 2011, mid-August 2016, end-August 2013, beginning September 2018 and mid-September 2016. Years 2011, 2016 and 2017 are the years with the lowest N/P ratios and longest period where N/P is below 16.

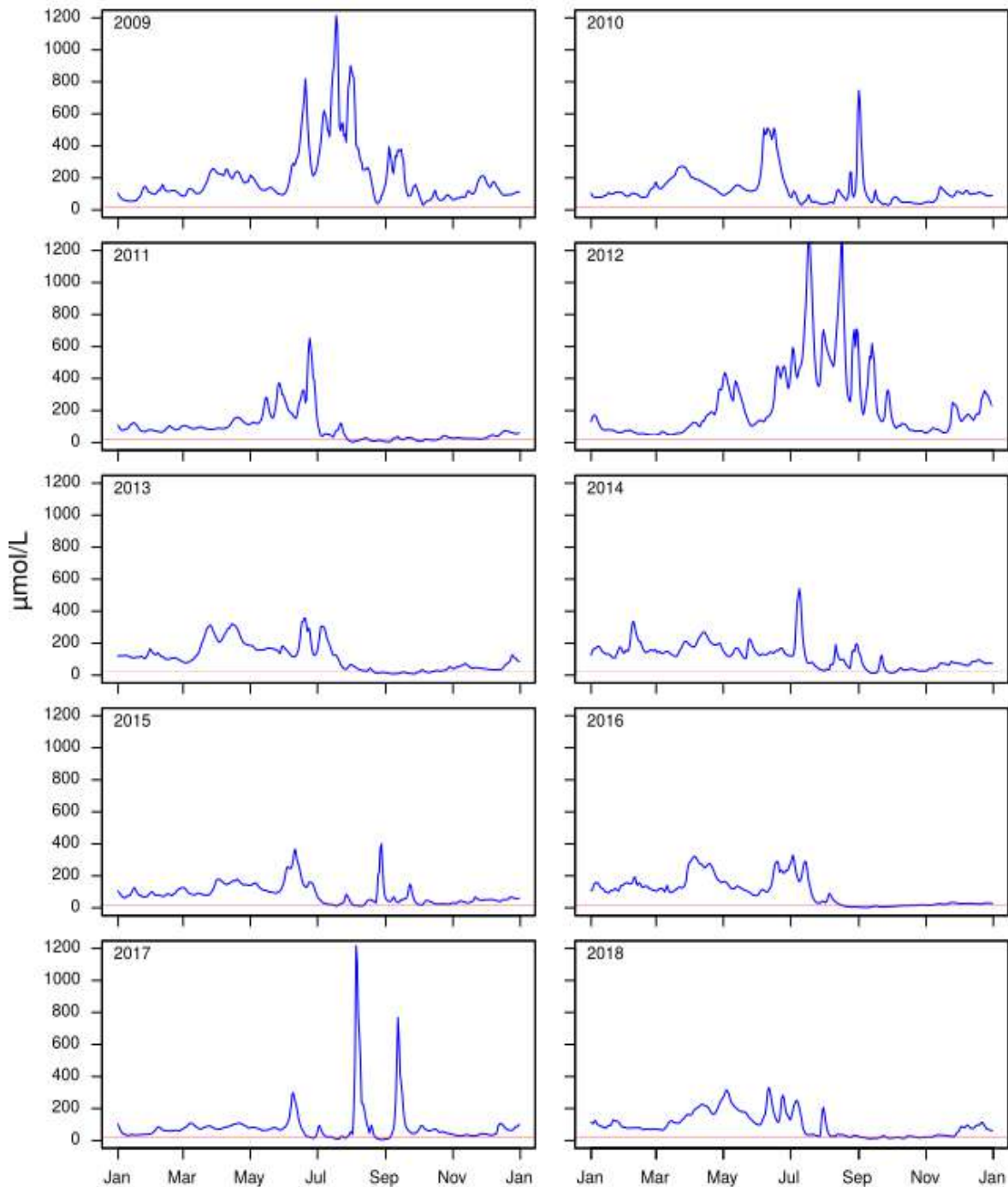


Figure 3.17: Interannual variability in simulated N/P ratio (blue) to Redfield ratio (red)

3.6. Discussion

Bloom definition in the present study follows the criteria established by Smayda (1997) regarding HABs, i.e. when species experience growth in the ecosystem and exceed certain cell concentrations which result in harmful consequences. Unlike Valbi et al. (2019), the originality of this study (model) is not to accurately predict bloom or reproduce past bloom events but to act as a tool which can evaluate the impact of potential drivers on seasonal and interannual variability together with bloom occurrences. The current study went beyond Sourisseau et al. (2017) by incorporating light trait, selecting phenotypes uniformly and studying (for a 10 year period not 3) the competition for resources not just among the different size fractions but also between phenotypes of the same size.

3.6.1. Methodological challenges

The first assumption of using 0D model is that it only tackles how local growth can modulate observed bloom events. All migration processes were neglected whereas numerous studies have shown that such physical-biological interactions could create strong cell accumulations in local areas and from several origins (Crespo et al. 2011). In our case, the possibility of another *A. minutum* source such as the Aulne estuary cannot be excluded from observations (Fig. 2.1). However, this source is probably limited because the biomass observed in this part of the bay is not explained by aggregation processes only. In addition, it accounts for a small part of the phytoplankton growth during the spring. We already know that a strong phytoplankton production occurs over the Bay of Brest (Del Amo et al., 1997) in summer for all the other taxons. A great bias was probably introduced by considering the same dilution rates for all phenotypes describing the community in the model.

The second assumption is the model's capacity to reproduce a consistent competition for resources with the integrated phytoplankton diversity. The initial model (Sourisseau et al. 2017) was based on random selection and consisted of 200 phenotypes with 100 simulations, assuming that each phenotype represented one species through one mean traits composition. By using this approach, the initial model was able to produce some consistent simulations for a period of 3 years (from 2012 to 2014). Here, a uniform distribution over the traits space was used to reduce the duration of simulation for a longer time series. Several simulations with different numbers of phenotypes (e.g. 25, 50, 72, 100 and 200) were obviously conducted but with the same minimal density per phenotype. Those with less number of phenotypes had

lower minimal cumulated-abundance but higher maximal abundance per phenotype. Despite the selection of the configuration with 72 phenotypes due to a closer fit with *in situ* data, the simulated densities were considered semi-quantitative and the behavior of the model is more relevant than a direct comparison with *in situ* data (Figs. 3.9 and 3.10). For the same periods (2012-2014), this new configuration produced similar dynamics but with lower densities.

A third assumption was the absence of intraspecific variability of *A. minutum*, which is more and more described for a lot of species (Menden-Deuer and Rowlett, 2014; Rynearson and Menden-Deuer, 2016; Pigliucci, 2001; Whitlock et al., 2007; Vellend, 2006). Using a fixed phenotype evaluated from a single strain to define species fitness also limits the capacity of species to adapt to the environment and, despite a successful first attempt by Sourisseau et al. (2017) in a three year period, is probably an increasing limitation with increased simulation period (2009-2018).

There was equally a challenge in analyzing the bloom phenology of *A. minutum* using the method of Rolinski et al. (2007) because of the smoothing property of the curve fitting procedures (Ji et al., 2010) and the irregular shape of the abundances. The presence of a good peak makes it possible to efficiently analyze the bloom of *A. minutum* with Weibull function e.g. in 2010, 2012, 2014 and 2017 (Fig. 2.9). In these years, bloom start; bloom end and bloom duration can easily be determined. In other years e.g. 2009 and 2011 however, the nature of the peaks does not permit an efficient analysis. Bloom durations of field data were sometimes exaggerated e.g. in 2011, 2015 and 2016 (Table 3.5).

Lastly, most data were obtained on weekly or monthly instead of daily basis and in some cases, less than 10 data points were sometimes available out of a possible 365 points for several years. Linear interpolation is the procedure to avoid these gaps but it might be inaccurate if high variabilities occurred. The real natural variability is probably underestimated.

3.6.2. *Alexandrium minutum* and environmental variables

Previous studies (Labry et al., 2008; Chapelle et al., 2007) on the analysis of *A. minutum* blooms in closed areas such as the Penzé estuary located on the coast of French Brittany, as well as in other coastal areas have shown that light, temperature and nutrients are the first abiotic factors controlling the blooms, with light being less important. Our own study shows similar abiotic conditions where irradiance was found to have little effect on *A. minutum* growth despite the implicit seasonal link between light, heat fluxes and water temperature. During the winter until late spring, the local growth in the Daoulas bay is thus reduced by temperature as also noted in Sourisseau et al. (2017). In the same period, dilution is high and exceeds growth. A lot of statistical analyses based on *in-situ* observations at local or larger scale also found sea surface temperature to be an important predictive variable for the occurrence, bloom initiation and possibly, the magnitude of *A. minutum* blooms (Valbi et al., 2019; Figueroa et al., 2007; Lim et al., 2006; Guallar et al., 2017; Chapelle et al., 2015; Raine, 2014; Bravo et al., 2008; Giacobbe et al., 1996; Delgado et al., 1990). More precisely, Guallar et al. (2017) noted that *A. minutum* bloom starts when water temperature is up to 15°C and this value remains stable at regional scale. Cosgrove et al. (2014) also observed that bloom initiation occurs after the first large spring tide in June when water column temperatures are above this threshold. The simulated dynamic also respects this pattern with 2011 being the first year to exceed 15°C in April and year 2013 the last to cross it in June thus, confirming the late and early bloom start respectively in 2013 and 2011 (Table 2.12). Furthermore, temperature limitation just before the end of spring in 2013 was quite high and longer compared to 2011 (Fig. 3.8).

When temperature no longer reduces *A. minutum*, its growth becomes quickly limited by nutrients usually in late spring and throughout summer. Nutrients are quite abundant before the growth of *A. minutum* but decrease in concentration during its growth due to reduced inputs by the river (Figs. 2.4 and 3.13 – 3.16), which is the main source of nutrients in coastal ecosystems (Tréguer et al., 2014; Del Amo, 1997), and also assimilation by phytoplankton leading a competition for resources (Laanaia et al., 2013; Labry et al., 2008; Ignatiades et al., 2007; Guisande et al., 2002). In line with Labry et al. (2008), our model shows that phosphorus is the first limiting nutrient. Later in the summer is nitrogen (after the *A. minutum* blooming period) which might be potentially limiting when concentrations fall below $2\mu\text{mol.L}^{-1}$. N/P river input ratio greater than 16/1 (Krom et al., 1992), gives an indication that

nitrogen is never limiting during periods with a significant river flow. Reversely, when river flow decreases, N concentrations decrease as well. A significant fraction of the interannual variability of the MA appeared related to this enrichment.

Year	2009	2010	2011	2012	2013	2014	2015	2016	2017	2018
f_N	0.54	0.17	0.05	0.65	0.07	0.1	0.08	0.07	0.05	0.07
f_P	0.06	0.06	0.05	0.14	0.07	0.08	0.09	0.08	0.09	0.08

Table 3.7: Annual highest N and P limitations (i.e. lowest f_N and f_P) on *A. minutum*

When river flow was quite high in summer 2012 (Fig. 2.2), P limitation was less severe (at 0.14) and N limitation was almost absent (at 0.65, Table 3.7 and Fig. 3.8), causing the most intense bloom – both simulated and observed over this period. The opposite is recorded in 2011 which had a dry summer, low river flow anomaly, low nutrient concentration and least intense bloom. The dominance of *A. minutum* in the phytoplankton community during low P conditions (after the growth of larger cells and with N/P ratio over 100 on the date of its maximum abundance in all the years, Fig. 3.18) can be explained by higher PO_4 uptake capacity and its ability to store P for a delayed or progressive growth (Labry et al. 2008). These abilities are thus specific advantages to face competition at local scale and probably contribute significantly to its capacity to dominate the community in this environment.

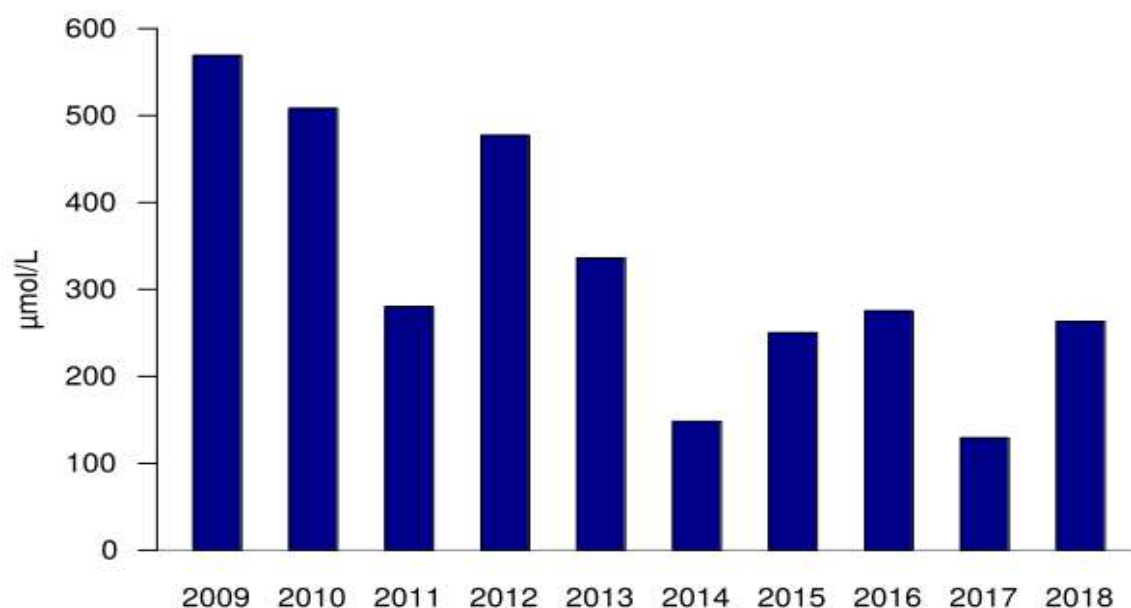


Figure 3.18: N/P ratio on the DMA of *A. minutum*

A good representation of *A. minutum* blooms by the model (in 2012 and 2014) and the high degree of agreement between REF and simulations of MA, DMA, cumulative abundance and bloom start of *A. minutum* in the ten year period (Fig. 3.10.B) indicates that the considered factors explained a great part of the interannual variability. However, some significant differences between simulated and observed *A. minutum* remain (Fig. 3.7). For example, early declines leading to early DMAs and lower MA were simulated. These are probably due to an excessive P limitation. In addition to the limitations previously described in the methodological challenges, only few factors controlling the bloom termination are simulated. With the exception of the competition effect, light and temperature effects do not appear to be strong drivers of bloom termination. Our results thus show that other biological processes like sexual reproduction (Brosnahan et al., 2015) or parasitism by eukaryotes and grazing by micro-zooplankton (Montagnes et al., 2008) may have occurred in the observed bay and therefore, explain some interannual variability of bloom occurrence.

3.6.3. Phytoplankton community and environmental variables

The phytoplankton dynamic in the Bay of Brest (out of the considered box) was well described by previous work (Beucher et al., 2004; Del Amo et al., 1997) with a first bloom dominated by diatoms, occurring in April. This first bloom is next, (often) followed along the summer by secondary blooms developed under low nutrient concentrations. The first bloom, leading to a strong decrease in Si, is not simulated by our model (neither in microphytoplankton biomass nor Si reduction). Observed in the center of the Bay of Brest, the bloom is thus not driven by a local growth in the Daoulas bay but probably occurs downstream in the Bay of Brest. It explains also the inability of the model to simulate correctly the timing of the first micro-phytoplankton bloom. According to this observation, our model probably slightly overestimated the competition by the siliceous phenotypes and limited the growth capacities of *A. minutum* and non-siliceous phenotypes.

The model also overestimated the competition for resources, with phosphorus being underestimated in summer of all years despite the added fluxes from the sediment. This results in a strong selection towards the smallest cell size fraction in the model. If the pico-size fraction is well represented in the phytoplankton community at the end of spring (Fig. 3.6.A), there is still a significant fraction of the nano- size fraction (50% of the total phytoplankton densities in September). It is thus difficult to assume that this observation was only due to a migration process. This bulk of species, simulated only by several phenotypes, develop complex interactions (commensalism, mutualism etc.) that are not integrated in the model and are probably of great relevance for resource access.

Very low growth was noted among species with an optimal temperature of 10°C and 12°C both seasonally and interannually (Figs. 3.6.B, C and D). The difference between these species and those of higher T_{opt} is their maximum growth (Table 3.4) which is lower. In winter and early spring when water temperature is 10°C or 12°C, dilution is high due to high river flow and species of low T_{opt} have insufficient growth to compensate dilution losses even though temperature is more adapted. This may also explain part of the non simulation of early spring blooms.

Chapter 4

Scenarios of Nutrient Reduction

4.1. Context

Having seen the effects of nutrient limitations on *A. minutum* bloom intensity as well as the possible link between high bloom and high river inputs, a test to reduce river nutrient inputs was conducted. The only way to change the nutrient fluxes into the bay is to reduce the river concentrations. This might be applied in agricultural practices since it has been shown that agricultural sources are responsible for the main part of nitrogen and phosphorus presence in rivers. Besides, these concentrations have highly increased for 50 years, being responsible for eutrophication effects (Le Pape and Menesguen, 1997). The actual interest is on the effects of nutrient reduction on *A. minutum* blooms. A model is a perfect tool to test such scenarios.

4.2. Method

The scenarios chosen were to reduce river nutrient concentrations by 50 per cent while maintaining the configuration of the model i.e. 73 species uniformly selected in the traits space. In doing this, three reduction scenarios were applied -

- (i) A reduction in nitrogen only (N50%)
- (ii) A reduction in phosphorus only (P50%) and
- (iii) A reduction in both nitrogen and phosphorus (NP50%)

And the results obtained were compared to the simulated reference (REF) without reduction for a 10 year period.

The concentration of phosphorus in the simulation box is that of PO_4 while nitrogen is the sum of NO_3 and NH_4 . Nutrient concentration in the box (model) is never constant due to continuous river inputs, dilution and the assimilation by phytoplankton.

4.3. Results

Looking at the annual cumulative concentrations of N and P for each year compared to the reference (Table 4.1), 50% N reduction in the river input gives between 76% and 81% reduction of N compared to the reference. 50% P reduction gives between 90% and 97% reduction of P compared to the reference simulation. Results for NP50% reduction are equivalent. It can be noticed that the N scenario reduction leads to a P cumulative increase and the P reduction scenario to a slight N cumulative increase. Furthermore, with N reduction, N minimum (N_{\min}) in the summer had the highest reduction in 2016 and the lowest reductions in 2009 and 2014, of the initial reference value. When P was reduced by 50%, P_{\min} showed a different result with more or less no reduction in the minimum value.

Year	N50%		P50%		NP50%	
	N	P	N	P	N	P
2009	81%	100%	101%	95%	81%	95%
2010	77%	101%	101%	95%	77%	95%
2011	79%	103%	101%	90%	80%	93%
2012	78%	100%	100%	95%	79%	95%
2013	78%	103%	100%	94%	79%	98%
2014	81%	101%	100%	96%	81%	97%
2015	79%	104%	101%	96%	80%	98%
2016	76%	104%	100%	93%	77%	97%
2017	77%	102%	100%	97%	78%	98%
2018	79%	102%	100%	96%	79%	98%

Table 4.1: % change in the annual cumulative concentration of nutrients for each reduction scenario compared to the reference

N or P reduction reduces the cumulative concentration of the considered nutrient, more for N than for P (Fig. 4.1). This is more evident in winter than in summer.

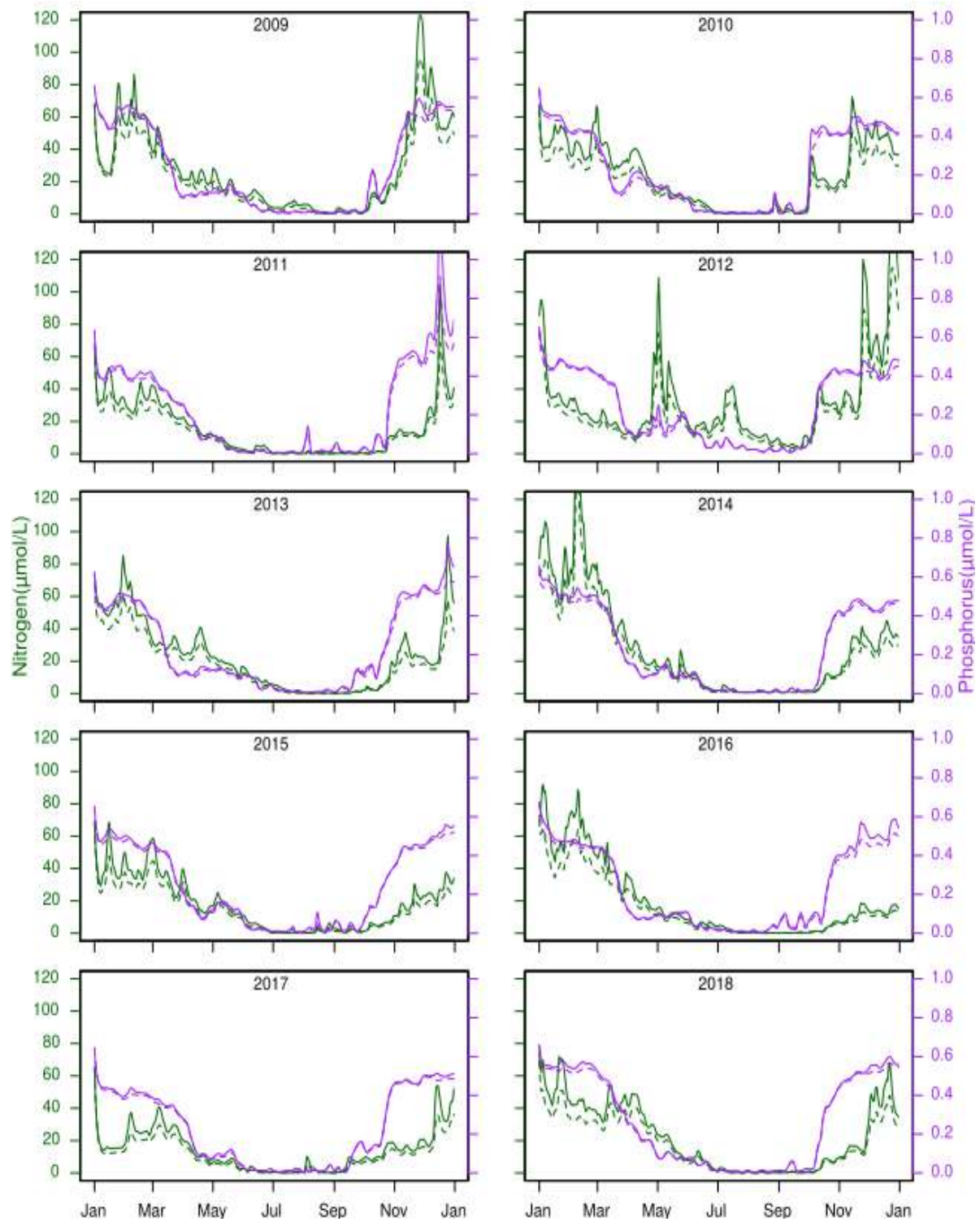


Figure 4.1: N (only) and P (only) reduction by 50 per cent.
Thick line is the reference without reduction

Reducing nutrient inputs from the river had an effect on *A. minutum*. However, a reduction in N50% only did not change the maximum abundance of *A. minutum* (Fig. 4.2) except a slight reduction in 2011. On the contrary, a reduction in P50% only or NP50% reduced the MA of *A. minutum* by 7 to 32%. The highest reductions in MA were in 2011 and 2015 while the weakest were in 2010 and 2018 (Fig. 4.3).

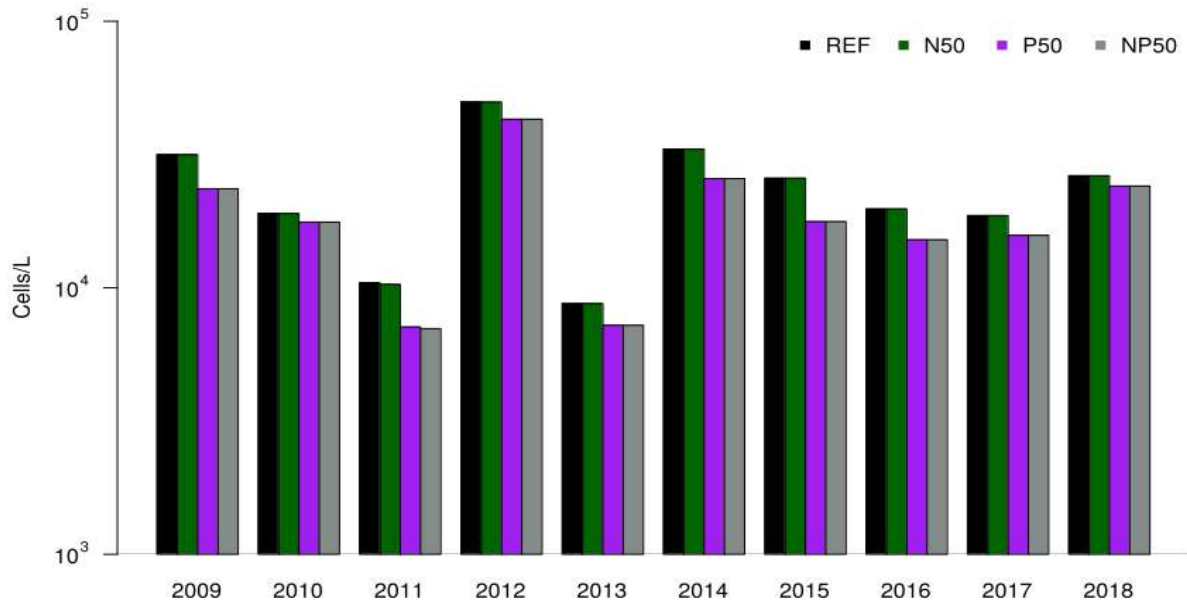


Figure 4.2: Changes in the MA of *A. minutum* following a reduction in nutrients

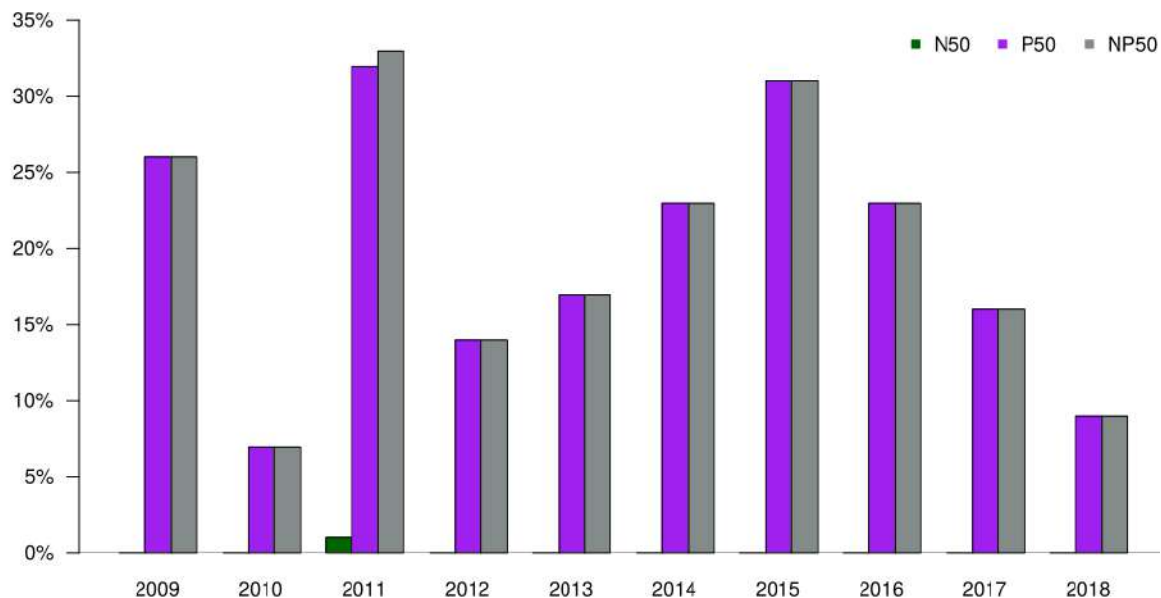


Figure 4.3: Percentage reduction in the MA of *A. minutum*

No change was observed in the date of maximum abundance (DMA) of *A. minutum* with N reduction and just a slight delay by one day in 2009 and 2014 with P reduction (Table 4.2).

Year	2009	2010	2011	2012	2013	2014	2015	2016	2017	2018
REF	168	158	135	170	168	168	154	168	156	174
N50%	168	158	135	170	168	168	154	168	156	174
P50%	169	158	135	170	168	169	154	168	156	174
NP50%	169	158	135	170	168	169	154	168	156	174

Table 4.2: DMA of *A. minutum* with N and P reductions

The cumulative abundance of *A. minutum*, nano and microphytoplankton showed similar response to nutrient reductions i.e. less impact with N50 than P50 or NP50 (Tab 4.3). On the contrary, pico responded more to N reduction than P.

		2009	2010	2011	2012	2013	2014	2015	2016	2017	2018
N50%	Alex	99%	100%	99%	100%	98%	100%	99%	100%	96%	100%
	Pico	100%	93%	88%	100%	89%	90%	90%	88%	92%	86%
	Nano	100%	100%	100%	100%	96%	99%	92%	99%	93%	97%
	Micro	98%	100%	99%	100%	98%	99%	97%	99%	99%	99%
P50%	Alex	78%	88%	77%	82%	87%	77%	74%	82%	83%	90%
	Pico	95%	94%	98%	98%	101%	99%	99%	100%	98%	100%
	Nano	88%	86%	86%	92%	88%	89%	86%	90%	88%	95%
	Micro	89%	84%	89%	93%	92%	94%	86%	95%	95%	99%
NP50%	Alex	77%	88%	76%	82%	85%	76%	73%	82%	80%	90%
	Pico	95%	90%	87%	98%	89%	90%	89%	88%	90%	86%
	Nano	88%	86%	86%	92%	86%	89%	81%	90%	82%	93%
	Micro	89%	84%	88%	93%	91%	93%	82%	94%	94%	98%

Table 4.3: % cumulative abundance of *A. minutum* and phytoplankton after nutrient reduction with respect to the reference

As for cumulative abundance, the maximum of micro and nano are more reduced with a P reduction than with N reduction (Fig. 4.4). Maximum abundance of pico is more reduced by P in 2009, 2010 and 2015 and by N in 2011, 2013, 2015, 2016 and 2018. The coupled N and P reductions led to a reduction of all maxima. Maximum abundance of micro is more reduced than nano and pico, with the highest reduction (62%) observed in 2011.

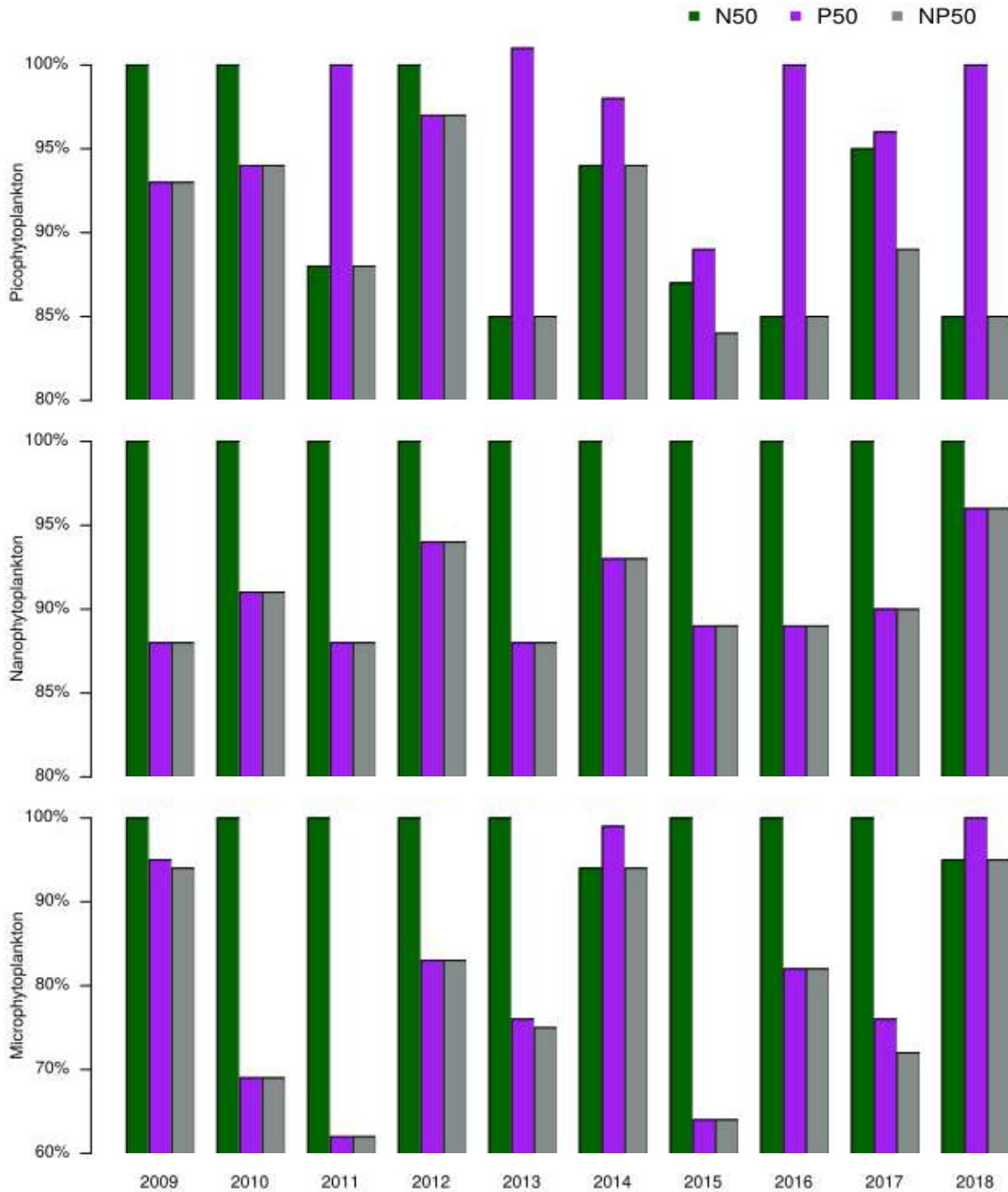


Figure 4.4: Percentage reduction in the cumulative abundance of pico, nano and micro with respect to the reference under the 3 reduction scenarios.

4.4. Discussion

Alexandrium minutum is not greatly affected by a reduction in N because its growth was mainly limited by P than N irrespective of the year. This is supported by N/P ratio >16:1 in river Daoulas (Redfield, 1958). Concentrations of both nutrients increase with an increase in river flow (Chapter 2). The observed seasonal and interannual variations in river flow make it possible to classify flow rates into four categories (Table 4.4).

Season	2009	2010	2011	2012	2013	2014	2015	2016	2017	2018
Winter	Low	Low	Low	Very low	Low	Very high	High	Very high	Low	High
Spring	Low	Low	Very low	Very high	Low	Low	Low	Low	Very low	Low
Summer	Low	Low	Very low	Very high	Low	Low	High	Low	High	Very low

Table 4.4: Seasonal and interannual conditions of river flow in Daoulas estuary

In 2011, the year with ‘very low’ river input and negative anomalies in spring/summer, P concentrations were very less and thus, less species abundance – in line with our findings in nutrient reduction scenarios. However, with ‘very high’ river input in 2012, positive anomalies as well as more species abundances were observed. This is the only year with outstanding minima in N concentration, more than ten times in other years (Fig. 4.5). It is also the year with the largest P minimum after a reduction by 50%. If the scenario of nutrient reduction can reduce species abundance, it means that a scenario of nutrient increase will inevitably increase abundance but that is not in our interest.

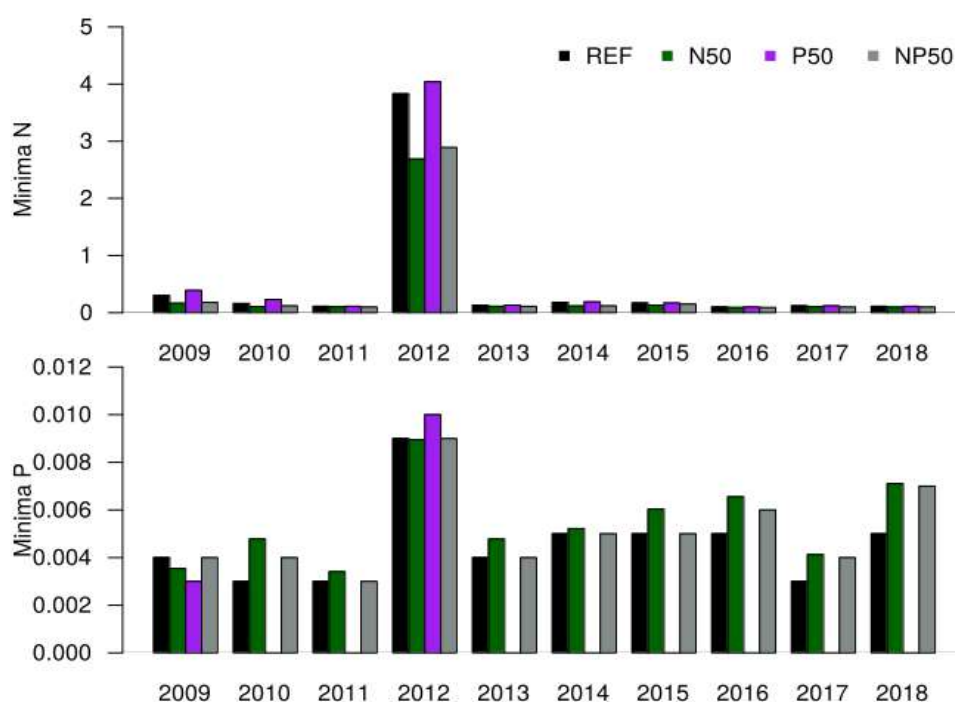


Figure 4.5: Minimum concentrations (μmolL⁻¹) of N and P before and after reduction

It can be noticed also that whatever the nutrient reduced, 50% reduction never leads to 50% reduction of any group of phytoplankton, neither *A. minutum* (cumulative or maximum abundance) nor nutrient concentration. In fact, the reduction in the inputs is distributed in the nutrient biogeochemical cycles within the estuary, following non linear relationships.

Among the years, 2011 showed a greater P reduction impact (32%) on *A. minutum* than 2012 (14%). This could be linked to the summer of 2011 which was a dry summer, leading to low P concentration and a high P limitation, compared to 2012 which had a very rainy summer. This scheme is not so obvious for the other years nevertheless. Nano and micro showed the same response, being more reduced by P in 2011 than 2012. For pico, N reduction was equally severe in 2018 while P reduction was highest in 2010 with respectively 14% and 6% reductions in cumulative abundance (Table 4.3). This could be explained by the fact that pico grows later in the season when N becomes more limiting. Pico is then much affected by N reduction than the other phytoplankton groups. This is obvious in 2011 where N limitation was greater than in 2012, leading to a greater pico bloom reduction. In 2012, N was not really limiting for all phytoplankton (not even pico). In general, the three categories of phytoplankton respond differently to N and P limitations (Fig. 4.6). They show opposite limitations mainly in summer and autumn.

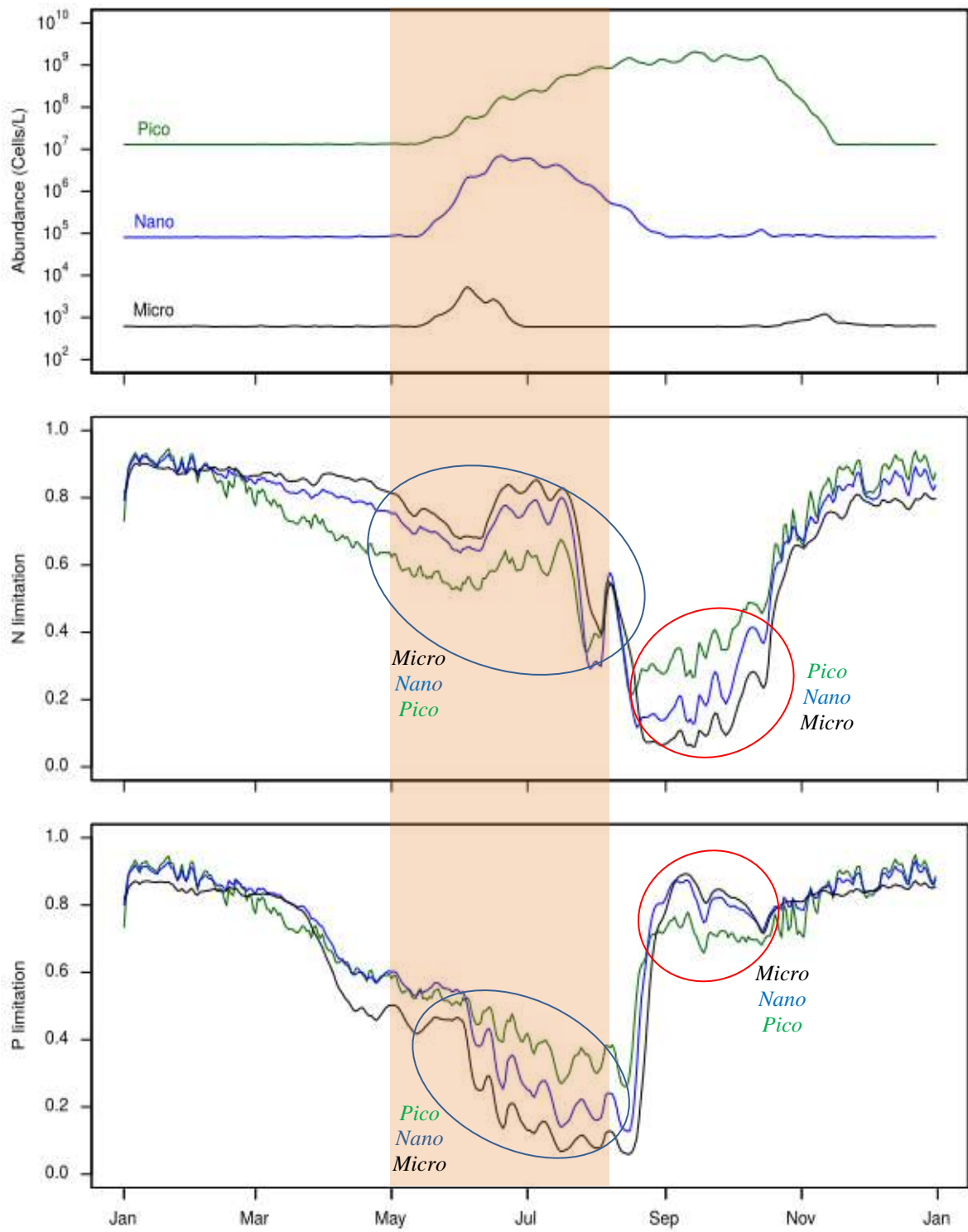


Figure 4.6: Phytoplankton responses to N and P limitations

Chapter 5

Summary

5.1. First Year

The start of this PhD thesis in December 2016 consisted of a comprehensive literature review on phytoplankton, harmful algal blooms and the genus *Alexandrium* particularly *Alexandrium minutum*. A large bloom of the species was in fact detected at Pointe du Château in the Bay of Brest in 2012 thereby, raising sanitary; touristic and economic concerns in the local region (Bretagne). Several blooms also occurred during the following years and they were still located in the same area of the bay, indicating some local and favorable environmental conditions. Interest was given to *A. minutum* because its ability to cause Paralytic Shellfish Poisoning (PSP) led to some important monitoring effort. We raised several scientific questions regarding the species such as why/when some species become dominant in the phytoplankton community; is the occurrence/frequency of toxic events related to human activity etc. Responses to these questions were relevant in the *Alex-Breizh* project (funded by Agence de l'eau Loire Bretagne) which is dedicated to studying the factors that control the proliferation of toxic algae particularly *A. minutum* in the Bay of Brest ecosystem. Literature review on *A. minutum* was made to define its physiology and nutrition, diversity and biogeography, spatial distribution and interannual variability etc. The aims were to understand how *A. minutum* sometimes, successfully competes with other phytoplankton including diatoms and dinoflagellates under different environmental conditions. We tried to identify and place in order of hierarchy, the key environmental factors responsible for its seasonal and interannual variations at a decade scale.

Two approaches were adopted. First was analyzing field data (abundance of species, temperature and concentration of nutrients) obtained at Pointe du Château since 2009 to 2016 and participate in subsequent surveys that involved weekly field sampling at the site. The second approach was to use a numerical model to integrate the existing interactions between the physical and biological processes in the ecosystem by using a model developed to evaluate the species growth with respect to environmental factors such as light, temperature and nutrients (PO_4 , NH_4 , NO_3 and Si) while competing with other species. This approach was developed by Sourisseau et al. (2017) who studied the main drivers of species selection using a trait-based model that keeps phenotypic variability through physiological trait parameterization.

Using such a mechanistic model in our study was relevant to understand the classification of the environmental drivers within the observed variability. Some studies have previously shown that a model can demonstrate high fidelity at reproducing observations at seasonal and inter-annual scales. Even if the parameterization and stability of these models can be questioned, they provide potential and realistic scenarios that are sometimes used for weekly nowcasts and forecasts (looking forward 3 or 4 days). They are useful tools to test scenarios like nutrient reduction inputs or to unravel local growth rate and local diffusion blooms. This study focused on hindcast mode (past observations) with a model including resource competition and simulations were compared with *in situ* data. Having field data for the years 2009 to 2016, simulations covered the same period.

The method previously used to simulate the phenotypic variability for resource competition was based on random selection of phenotypic size ranging from 1-100 μ m of Equivalent Spherical Diameter (ESD), allometric relationships (quota, nutrient absorption and half-saturation concentrations), random selection of optimal temperature ranging from 10-20°C and an average of 100 simulations with 51 species of both siliceous and non-siliceous cells. The abiotic and biogeochemical forcings (river flow, dilution, light, temperature, nutrients etc.) were integrated for a virtual simulation box that represented the Daoulas bay ecosystem. Simulations enabled us to obtain the growth of species (μ), maximum growth rate of species (μ_{max}), abundance of species (ϕ) and concentration of nutrients (NH_4 , NO_3 , PO_4 and Si). Species limitations by nutrients (fN , fP and fS), light (fL) and temperature (fT) were also determined.

Results obtained in these simulations showed seasonal and interannual variations in the abundance of *A. minutum* and other phytoplankton. The model was able to reproduce bloom occurrence but was not consistent in all the years. Some species experienced high growths while others especially the largest species, had no growth.

5.2. Second Year

Participation continued in the *Alex-Breizh* project.

A number of tests were performed while looking for ways to improve our model. First was the introduction of light influence (photoinhibition) into the model (Annex 3). First year's simulations adopted the equation of Jassby and Platt (1976) to determine light limitation without taking photoinhibition into account. Function was therefore replaced with Steele (1962) and found species growth to be highly limited by light. Lacroix (2002) was introduced in place of Steele but the microphytoplankton was unable to grow due to a lower optimal irradiance. The equation of Jassby and Platt was thus kept.

Changes to initial configuration

Simulation was intended for a longer period at Pointe du Château but also for the entire Bay of Brest with a 3D numerical model. Conducting 100 simulations on 3D for eight to ten different years would require unrealistic computing time. We therefore modified the initial configuration to use 1 instead of 100 simulations in order to accommodate 3D. This was done with species being selected uniformly in the traits space, instead of randomly, following continued bibliographic research. Changes were thus made in the initial configuration of the traits space for cell size, optimal temperature, optimal irradiance and number of species.

Cell Size: The size range of 1-100µm of the initial configuration was first sampled by 5 phenotypes of phytoplankton – one pico (1µm), two nano (3 and 10µm) and two micro (32 and 100µm). However, species of the largest size fraction (especially those of 100µm) showed no local net growth. We finally decided to have 6 classes ranging from 1 - 64µm to incorporate at least two classes for each category of phytoplankton. They were thus - 1 and 2µm for pico, 5 and 18 µm for nano, 28 and 64µm for micro size fraction. One advantage of this size range is having a phenotype which has the same characteristics (in terms of size, T_{opt} and I_{opt}) as *A. minutum*. This enabled us to study the competition of *A. minutum* not just with pico, nano or micro but also with phenotypes of exactly the same size.

Optimal irradiance (I_{opt}) is a parameter that was common to all phenotypes in previous simulations. New parameterization of light was evaluated following an intensive study on photoinhibition. The addition of this trait seemed necessary in determining light limitation on each phenotype that competes for resources with different adaptations. I_{opt} has a direct relationship with cell size such that the smaller the cell, the higher the I_{opt} and vice-versa. We thus fixed 6 values ranging from 8 to 100W.m^{-2} from the largest to the smallest size. Optimal temperature was equally modified in order to accommodate the number of species in the simulations but in the same range [10-20°C] that corresponds to the sea water temperature in temperate systems.

The number of species was fixed to 51 in the initial configuration using random communities. For the new configuration with fixed community structure, different numbers of uniformly selected species (25, 50, 72, 100 and 200) in competition with *A. minutum* were tested and the best representation of field data with a reasonable computing time was obtained with 72. This corresponded to a matrix of 6*6*2 respectively the number of sizes, optimal temperature and silicate use. The uniform selection showed no significant difference in abundance when compared to random selection with 100 simulations.

Further changes were made by verifying the initial configuration and adding parameters which were not used in first year's simulations – all in attempt to further improve our model. One error was detected for the initial V_{max} that should be at 0°C for all species. After verification and further bibliographic study, V_{max} (NH_4 , NO_3 and PO_4) of phytoplankton was at 0°C while that of *A. minutum* was actually at 18°C. This detected error gave *A. minutum* a more competitive advantage over other species in the previous configuration. Correction was done by converting the V_{max} at 18°C to V_{max} at 0°C in order to have an equal competition field for all species.

Another modification was done by adding a new source of nutrient. River is still the main source of inorganic nutrients but after the observed underestimation of nutrients by the model, a potential nutrient source (sediment) was added. The remineralization in the sediments produced inorganic nutrient flux from the sediment particularly for PO_4 which was the most limiting nutrient. Significant changes were observed both in growth and modeled nutrient following the flux addition.

Results of a uniform simulation from 2009-2016 were very similar to those obtained with 100 simulations at random selection. They equally showed seasonal and interannual variations in the abundance of *A. minutum* together with the phytoplankton community (pico, nano and micro). No growth was found among the species at the beginning and end of each year. Growth was observed between March and September with the highest abundance occurring in the months of June and July when temperatures were relatively high. The micro was the first to dominate followed by the nano and then picophytoplankton which had the highest abundance. Results also showed the expected seasonal nutrient variability. In winter, species growth was limited by temperature and light but in the summer, they were limited by nutrients particularly phosphorus. These results were presented at an International Conference on harmful Algae (ICHA) in October 2018. A scientific paper (Article) on the seasonal and interannual variability of *A. minutum* in the Bay of Brest was also in preparation.

5.3. Third Year

Some scenarios of input nutrient reduction were tested as proposed in the *Alex-Breizh* project to evaluate its growth limitations on *A. minutum*. First, only the concentration of nitrogen was reduced by 50 per cent while other nutrients remained unmodified, after which we did the same reduction with phosphorus alone. The result obtained showed that a reduction in nitrogen inputs does not affect the growth of *A. minutum*, microphytoplankton and nanophytoplankton phenotypes but phosphorus reduction did. For picophytoplankton phenotypes, both nitrogen or phosphorus reductions reduced the maximum abundance, with nitrogen reduction effect being higher.

The difference between our model and field data with regards to nutrients in the winter was investigated (Annex 1). The position of the model in the field (river Daoulas) was compared to the position where field data were obtained (Pointe du Château). The latter was more saline due to its location near the bay. Nutrient field data measured at Pointe du Chateau in winter were thus interpolated using the mean salinity of the model and the sampling salinity (keeping in mind that nutrients are conserved in winter) and the result obtained showed a better homogeneity between field and model. We also investigated nutrient data from Lanveoc and Portzic stations in order to evaluate the importance of data at sea limits. Although Lanveoc is closer to Pointe du Chateau, all our simulations used Portzic data (which are more complete) and in some cases, field data were underestimated in Portzic station compared to Lanveoc station. Using the nutrient concentrations of Lanveoc or Portzic, simulations showed no much difference within the estuary. We thus continued to use data from the Portzic station.

Two additional years (2017 and 2018) were also added to the simulation following the new availability of *in situ* data (abundance of species and concentration of nutrients) via the *Alex-Breizh* project. The study of seasonal and interannual variability of *A. minutum* was thus conducted over a ten year period. Field and model showed the highest MA of *A. minutum* in 2012. The model worked quite well in reproducing observations of *A. minutum* in 2011, 2014 and 2017 with close date of MA. It also followed the trend of field data in 2012, 2014, 2015 and 2017 but some bias were observed for 2009 and 2016. At a larger scale, the phytoplankton (micro) was underestimated although it gave a close indication on the date of summer MA in 2009, 2011, 2013, 2015 and 2018. In the other years, this date occurred much earlier in the model. Nano field data were also underestimated in the summer of 2016, 2017 and 2018 except in winter. Pico was well reproduced in spring but was overestimated in

summer in the years of available data. With regards to nutrients, our model is very good at simulating NO_3 and Si. NH_4 was well simulated except in winter/spring of 2016 and 2018 where the model overestimated field data. In 2016, 2017 and 2018, the model closely followed the trend of PO_4 but in 2013, 2014 and 2015; it slightly underestimated the overall concentration of PO_4 and in general, all years in summer despite the introduction of PO_4 fluxes from the sediment.

Among the three categories of phytoplankton, simulation results showed the classical distribution with a decrease of abundance from pico to the micro-phytoplankton. Species of 18°C dominated the two size classes ($1\mu\text{m}$ and $2\mu\text{m}$) of the pico size fraction with MA of 727×10^6 and $23 \times 10^6 \text{ cells.L}^{-1}$ respectively in 2009. Both phenotypes were also slightly less limited in phosphorus than phenotypes of the same size range. Nano being represented by phenotypes of 5 and $18\mu\text{m}$, those with an optimal temperature of 16°C and 18°C dominated in $5\mu\text{m}$ with an average MA of $1.5 \times 10^6 \text{ cells.L}^{-1}$ in 2018 whereas *A. minutum* dominated among the $18\mu\text{m}$ with the highest MA of $49810 \text{ cells.L}^{-1}$ in 2012. The phenotypes of microphytoplankton (28 and $64\mu\text{m}$) displayed MA of just 2233 and 64 cells.L^{-1} respectively in 2012 and 2014 with phenotypes of 16°C dominating.

The remarkable difference observed between cells according to their size, was that small cells were active from June to late October whereas large cells became active mainly in November as seen in autumn peaks. Small cells were more limited by light than large cells due to their relationship with optimal irradiance. They were equally more limited by nitrogen than large cells during the summer due to reduced input from the river but we found the opposite with phosphorus limitation where small cells were less limited than large cells due to assimilation capacity. There is also a difference in the abundance of species of similar size. Having looked at the phenology of phytoplankton by cell size, we compare *A. minutum* and sp29 – a phenotype which has the same T_{opt} , I_{opt} and cell size as *A. minutum* (Annex 4). Both species are dinoflagellates but *A. minutum* dominated sp29 because it had a higher ability to absorb phosphorus than sp29 in each of the ten simulated years. *A. minutum* also dominated among the dinoflagellates in field observations whereas *Chaetoceros* dominated among diatoms, as seen in phytoplankton diversity (Chapter 2).

Some springs/summers were found to be hotter/colder or more dry/wet than others (Annex 2). Distinguishing them was useful in understanding the interannual variability of phytoplankton and why species with the same parameters had different abundances. We found the wet summer (2012) – the year with the highest rainfall during the summer to be rich in nutrients and species abundance and have the highest *A. minutum* bloom both *in situ* and in the model. With regards to species of the same size having different abundances, species with high T_{opt} are more favored in warm conditions whereas others (with low T_{opt}) are favored in cold conditions.

5.4. Conclusion

The present study provides information on the seasonal and interannual variability of *A. minutum* and phytoplankton in the Daoulas estuary from 2009 to 2018. This ecosystem is exposed to high rainfalls and river flows during the winter, giving rise to high dilution and high nutrient concentrations but also low temperatures which prevent bloom initiation. The opposite is however, observed in the summer – leading to bloom outbreaks. With species in resource competition with *A. minutum*, we observed differences in MA both seasonally and interannually. These differences are linked to changes in environmental conditions because some of the years simulated were found to be hotter/colder or more dry/wet than others thereby, having an influence on the degree of limitation and on the species competitiveness. The year (2012) with the highest river flow in spring/summer for example, was found to have less nutrient limitations, high species growth and abundance and favored *A. minutum* development when compared to a year (2011) with low river flow in the same season. Although some results of our model did not correspond with field data in certain cases, the model is certainly able to point out the conditions that are necessary, though not sufficient, to trigger HAB events. Thus, it can improve some models which are able to correctly predict real-world instances of *A. minutum* presence or absence. This could support the implementation of predictive models focused on providing early warnings to prevent the impacts of HABs on public health and economic activities.

5.5. Perspective

While our model was tested only locally, the same procedure can be applied to simulate spatial variability. This will require an advanced version of the model in 2D or 3D in order to go beyond the limitations (local growth without species migration) associated with the current 0D model and by incorporating new processes like parasitism, predation, cyst germination and other forms of competition. The ultimate goal, obviously, is a model which can be tested and validated on a larger scale.

Bibliographic References

-A-

- Agusti, S. (1991). Allometric Scaling of Light-Absorption and Scattering by Phytoplankton Cells. *Canadian Journal of Fisheries and Aquatic Sciences*, 48(5), 763-767. <https://doi.org/10.1139/f91-091>
- Aminot, A., & K  rouel, R. (2004). Hydrologie des   cosyst  mes marins ; param  tres et analyses / 2004 / Actualit   / infos / envlit / Ifremer—Envlit. Consult   29 octobre 2019,    https://envlit.ifremer.fr/infos/actualite/2004/hydrologie_des_ecosystemes_marins_parametres_et_analyses
- Anderson, D. M., Alpermann, T. J., Cembella, A. D., Collos, Y., & Montresor, M. (2012). *The globally distributed genus Alexandrium : Multifaceted roles in marine ecosystems and impacts on human health*. 55.
- Anderson, D. M., Glibert, P. M., & Burkholder, J. M. (2002). Harmful algal blooms and eutrophication : Nutrient sources, composition, and consequences. *Estuaries*, 25(4), 704-726. <https://doi.org/10.1007/BF02804901>
- Andrieux-Loyer, F., Philippon, X., Bally, G., K  rouel, R., Youenou, A., & Le Grand, J. (2008). Phosphorus dynamics and bioavailability in sediments of the Penz   Estuary (NW France) : In relation to annual P-fluxes and occurrences of *Alexandrium minutum*. *Biogeochemistry*, 88(3), 213-231. <https://doi.org/10.1007/s10533-008-9199-2>

-B-

- Balech, E. (1989). Redescription of *Alexandrium minutum* Halim (Dinophyceae) type species of the genus *Alexandrium*. *Phycologia*, 28(2), 206-211. <https://doi.org/10.2216/i0031-8884-28-2-206.1>
- Balech, E. (1995). The genus *Alexandrium* Halim (*Dinoflagellata*). pp. 1-151. Sherkin Island: Sherkin Island Marine Station, Cork, Ireland.
- Banse, K. (1982). Cell Volumes, Maximal Growth-Rates of Unicellular Algae and Ciliates, and the Role of Ciliates in the Marine Pelagial. *Limnology and Oceanography*, 27(6), 1059-1071. <https://doi.org/10.4319/lo.1982.27.6.1059>
- Barton, A. D., Dutkiewicz, S., Flierl, G., Bragg, J., & Follows, M. J. (2010). Patterns of Diversity in Marine Phytoplankton. *Science*, 327(5972), 1509-1511. <https://doi.org/10.1126/science.1184961>
- Belin, C. (1993). *Distribution of Dinophysis spp. And Alexandrium minutum along French coasts since 1984 and their DSP and PSP toxicity levels*. (T. J. Smayda,   d.). Consult      l'adresse <https://search.proquest.com/asfa/docview/16668127/253C39E1E0064A97PQ/5>

- Beucher, C., Treguer, P., Corvaisier, R., Hapette, A. M., & Elskens, M. (2004). Production and dissolution of biosilica, and changing microphytoplankton dominance in the Bay of Brest (France). *Marine Ecology Progress Series*, 267, 57-69. <https://doi.org/10.3354/meps267057>
- Bill, B. D., Moore, S. K., Hay, L. R., Anderson, D. M., & Trainer, V. L. (2016). Effects of temperature and salinity on the growth of *Alexandrium* (Dinophyceae) isolates from the Salish Sea. *Journal of phycology*, 52(2), 230-238. <https://doi.org/10.1111/jpy.12386>
- Bolch, C.J., Blackburn, S. I., Cannon, J. A. & Hallegraeff, G. M. (1991). The resting cyst of the red-tide dinoflagellate *Alexandrium minutum* (Dinophyceae), *Phycologia*, 30:2, 215-219, <https://doi.org/10.2216/i0031-8884-30-2-215.1>
- Bravo, I., Vila, M., Masó, M., Figueroa, R. I., & Ramilo, I. (2008). *Alexandrium catenella* and *Alexandrium minutum* blooms in the Mediterranean Sea : Toward the identification of ecological niches. *Harmful Algae*, 7(4), 515-522. <https://doi.org/10.1016/j.hal.2007.11.005>
- Brosnahan, M. L., Velo-Suárez, L., Ralston, D. K., Fox, S. E., Schein, T. R., Shalapyonok, A., Anderson, D. M. (2015). Rapid growth and concerted sexual transitions by a bloom of the harmful dinoflagellate *Alexandrium fundyense* (Dinophyceae). *Limnology and Oceanography*, 60(6), 2059-2078. <https://doi.org/10.1002/lno.10155>
- Burkholder, J. M., Glibert, P. M., & Skelton, H. M. (2008). Mixotrophy, a major mode of nutrition for harmful algal species in eutrophic waters. *Harmful Algae*, 18.

-C-

- Caperone, J. (1968). Population Growth Response of *Isochrysis Galbana* to Nitrate Variation at Limiting Concentrations. *Ecology*, 49(5), 866-872. <https://doi.org/10.2307/1936538>
- Chambouvet, A., Morin, P., Marie, D., & Guillou, L. (2008). Control of Toxic Marine Dinoflagellate Blooms by Serial Parasitic Killers. *Science*, 322(5905), 1254-1257. <https://doi.org/10.1126/science.1164387>
- Chang, F. H., & McClean, M. (1997). Growth responses of *Alexandrium minutum* (Dinophyceae) as a function of three different nitrogen sources and irradiance. *New Zealand Journal of Marine and Freshwater Research*, 31(1), 1-7. <https://doi.org/10.1080/00288330.1997.9516740>
- Chapelle, A. (2016). Modélisation du phytoplancton dans les écosystèmes côtiers. Application à l'eutrophisation et aux proliférations d'algues toxiques. Consulté à l'adresse <https://archimer.ifremer.fr/doc/00360/47141/>

- Chapelle, A., Andrieux, F., Fauchot, J., Guillaud, J.-F., Labry, C., Sourisseau, M., & Verney, R. (2007). Comprendre, Prédire et Agir sur les efflorescences toxiques. Jusqu'où peut-on aller aujourd'hui dans le cas d'*Alexandrium minutum* en Penzé ? Consulté à l'adresse <https://archimer.ifremer.fr/doc/00105/21651/>
- Chapelle, A., Le Gac, M., Labry, C., Siano, R., Quere, J., Caradec, F., ... Gouriou, J. (2015). The Bay of Brest (France), a new risky site for toxic *Alexandrium minutum* blooms and PSP shellfish contamination. *Harmful Algae News*, 51, 4-5.
- Cleve, P. T. (1900). The plankton of the North Sea, the English Channel, and the Skagerak in 1898. *K. Svenska Vet. Akad. Handl.* 32:1-53.
- Collos, Y., Bec, B., Jauzein, C., Abadie, E., Laugier, T., Lautier, J., Vaquer, A. (2009). Oligotrophication and emergence of picocyanobacteria and a toxic dinoflagellate in Thau lagoon, southern France. *Journal of Sea Research*, 61(1), 68-75. <https://doi.org/10.1016/j.seares.2008.05.008>
- Cosgrove, S., Rathaille, A. N., & Raine, R. (2014). The influence of bloom intensity on the encystment rate and persistence of *Alexandrium minutum* in Cork Harbor, Ireland. *Harmful Algae*, 31, 114-124. <https://doi.org/10.1016/j.hal.2013.10.015>
- Crespo, L. G. M. (2011, septembre 18). *Uncertainty Analysis via Failure Domain Characterization : Polynomial Requirement Functions*. Présenté à ESREL 2011 Annual Conference, Troyes, France. Consulté à l'adresse <https://ntrs.nasa.gov/search.jsp?R=20110015880>
- Cullen, J. J., Geider, R. J., Ishizaka, J., Kiefer, D. A., Marra, J., Sakshaug, E., & Raven, J. A. (1993). Towards a General Description of Phytoplankton Growth for Biogeochemical Models. In G. T. Evans & M. J. R. Fasham (Éd.), *Towards a Model of Ocean Biogeochemical Processes* (p. 153-176). Springer Berlin Heidelberg.
- Cupp, E. E. (1943). Marine plankton diatoms of the west coast of North America. *Bulletin of the Scripps Inst. Oceanography of the University of California*. 5: 1-237.

-D-

- Del Amo, Y., Quéguiner, B., Tréguer, P., Breton, H., & Lampert, L. (1997). Impacts of high-nitrate freshwater inputs on macrotidal ecosystems. II. Specific role of the silicic acid pump in the year-round dominance of diatoms in the Bay of Brest (France). *Marine Ecology Progress Series*, 161, 225-237. <https://doi.org/10.3354/meps161225>
- Delgado, M. and J.M. Fortuno. (1991). Atlas de fitoplancton del Mar Mediterráneo. *Sci. Mar.*, 55 (Supl. 1): 1-133.

- Delgado, M., Estrada, M., Camp, J., Fernández, J. V., Santmartí, M., & Lletí, C. (1990). *Development of a toxic Alexandrium minutum Halim (Dinophyceae) bloom in the harbour of Sant Carles de la Ràpita (Ebro Delta, northwestern Mediterranean)*. Consulté à l'adresse <https://digital.csic.es/handle/10261/28581>
- Dodge J.D. (1982). Marine Dinoflagellates of the British Isles. H.M.S.O., London, VI + 303p.
- Drebes, C. G. (1974). Marines Phytoplankton, Eine Auswahl der Helgoländer Planktonalgen (Diatomeen, Peridinee). Georg Thieme Verlag, Stuttgart. 186 pp.
- Droop, M. R. (1968). Vitamin B12 and Marine Ecology. IV. The Kinetics of Uptake, Growth and Inhibition in Monochrysis Lutheri. *Journal of the Marine Biological Association of the United Kingdom*, 48(3), 689-733. <https://doi.org/10.1017/S0025315400019238>
- Droop, M. R. (1973). Some Thoughts on Nutrient Limitation in Algae1. *Journal of Phycology*, 9(3), 264-272. <https://doi.org/10.1111/j.1529-8817.1973.tb04092.x>
- Droop, M. R. (2003). In defence of the Cell Quota model of micro-algal growth. *Journal of Plankton Research*, 25(1), 103-107. <https://doi.org/10.1093/plankt/25.1.103>
- Dutkiewicz, S., Follows, M. J., & Bragg, J. G. (2009). Modeling the coupling of ocean ecology and biogeochemistry. *Global Biogeochemical Cycles*, 23, GB4017. <https://doi.org/10.1029/2008GB003405>

-E-

- Edwards, K. F., Thomas, M. K., Klausmeier, C. A., & Litchman, E. (2015). Light and growth in marine phytoplankton : Allometric, taxonomic, and environmental variation. *Limnology and Oceanography*, 60(2), 540-552. <https://doi.org/10.1002/lno.10033>
- Eppley, R. (1985). Citation Classic—Temperature and Phytoplankton Growth in the Sea. *Current Contents/Agriculture Biology & Environmental Sciences*, (37), 20-20.
- Eppley, R. W. (1972). Temperature And Phytoplankton Growth In The Sea | Scientific Publications Office. Consulté 29 octobre 2019, à l'adresse <https://spo.nmfs.noaa.gov/content/temperature-and-phytoplankton-growth-sea>
- Erard-Le Denn, E. (1997). “*Alexandrium minutum*,” in *Efflorescences Toxiques Des Eaux Cotieres Francaises*. Ifremer, Plouzané: Reperes Ocean.

-F-

- Fauchot, J., Saucier, F. J., Levasseur, M., Roy, S., & Zakardjian, B. (2008). Wind-driven river plume dynamics and toxic Alexandrium tamarense blooms in the St. Lawrence estuary (Canada) : A modeling study. *Harmful Algae*, 7(2), 214-227. <https://doi.org/10.1016/j.hal.2007.08.002>

- Field, C. B., Behrenfeld, M. J., Randerson, J. T., & Falkowski, P. (1998). Primary Production of the Biosphere : Integrating Terrestrial and Oceanic Components. *Science*, 281(5374), 237-240. <https://doi.org/10.1126/science.281.5374.237>
- Figuerola, R. I., Garcés, E., & Bravo, I. (2007). Comparative study of the life cycles of *Alexandrium tamutum* and *Alexandrium minutum* (Gonyaulacales, Dinophyceae) in culture1. *Journal of Phycology*, 43(5), 1039-1053. <https://doi.org/10.1111/j.1529-8817.2007.00393.x>
- FiNAL. (2008). *Forecasting the Initiation of Harmful Algal Blooms. Ecophysiological models of Alexandrium and Pseudo-nitzschia*.
- Finkel, Z. V. (2001). Light absorption and size scaling of light-limited metabolism in marine diatoms. *Limnology and Oceanography*, 46(1), 86-94. <https://doi.org/10.4319/lo.2001.46.1.0086>
- Flynn, K. J. (2003). Modelling multi-nutrient interactions in phytoplankton; balancing simplicity and realism. *Progress in Oceanography*, 56(2), 249-279. [https://doi.org/10.1016/S0079-6611\(03\)00006-5](https://doi.org/10.1016/S0079-6611(03)00006-5)
- Flynn, K. J. (2005). Modelling marine phytoplankton growth under eutrophic conditions. *Journal of Sea Research*, 54(1), 92-103. <https://doi.org/10.1016/j.seares.2005.02.005>
- Follows, M. J., & Dutkiewicz, S. (2011). *Modeling Diverse Communities of Marine Microbes*. 27.
- G-
- Giacobbe, M. G., Oliva, F. D., & Maimone, G. (1996). Environmental Factors and Seasonal Occurrence of the Dinoflagellate *Alexandrium minutum*, a PSP Potential Producer, in a Mediterranean Lagoon. *Estuarine, Coastal and Shelf Science*, 42(5), 539-549. <https://doi.org/10.1006/ecss.1996.0035>
- Gohin, F., Loyer, S., Lunven, M., Labry, C., Froidefond, JM., Delmas, D., Huret, M., Herbland, A. (2005). Satellite-derived parameters for biological modelling in coastal waters: Illustration over the eastern continental shelf of the Bay of Biscay. *Remote Sensing of Environment*, Volume 95, Issue 1. Pages 29-46, ISSN 0034-4257, <https://doi.org/10.1016/j.rse.2004.11.007>
- Grover, J. P. (1991). Resource Competition in a Variable Environment : Phytoplankton Growing According to the Variable-Internal-Stores Model. *The American Naturalist*, 138(4), 811-835. <https://doi.org/10.1086/285254>
- Grover, J. P. (1992). Constant- and variable-yield models of population growth : Responses to environmental variability and implications for competition. *Journal of Theoretical Biology*, 158(4), 409-428. [https://doi.org/10.1016/S0022-5193\(05\)80707-6](https://doi.org/10.1016/S0022-5193(05)80707-6)

Guallar, C., Bacher, C., & Chapelle, A. (2017). Global and local factors driving the phenology of *Alexandrium minutum* (Halim) blooms and its toxicity. *Harmful Algae*, 67, 44-60. <https://doi.org/10.1016/j.hal.2017.05.005>

Guisande, C., Frangopulos, M., Maneiro, I., Vergara, A. R., & Riveiro, I. (2002). Ecological advantages of toxin production by the dinoflagellate *Alexandrium minutum* under phosphorus limitation. *Marine Ecology Progress Series*, 225, 169-176. <https://doi.org/10.3354/meps225169>

-H-

Halim, Y. (1960). *Alexandrium minutum*, n. Gen. N. Sp. Dinoflagellé provocant des « eaux rouges » (Vie et Milieu 11: 102-105.).

Hallegraeff, G. (1993). A Review of Harmful Algal Blooms and Their Apparent Global Increase. *Phycologia*, 32(2), 79-99. <https://doi.org/10.2216/i0031-8884-32-2-79.1>

Hallegraeff, G. M. (2010). Ocean Climate Change, Phytoplankton Community Responses, and Harmful Algal Blooms : A Formidable Predictive Challenge1. *Journal of Phycology*, 46(2), 220-235. <https://doi.org/10.1111/j.1529-8817.2010.00815.x>

Haney, J. D., & Jackson, G. A. (1996). Modeling phytoplankton growth rates (vol 18, pg 63, 1996). *Journal of Plankton Research*, 18(7), 1269-1269. <https://doi.org/10.1093/plankt/18.7.1269>

Hasle, G. R. & Syvertsen, E. E. (1996). Identifying Marine Diatoms and Dinoflagellates. Academic Press, San Diego, CA, pp. 5-385.

He, R., & McGillicuddy, D. J. (2008). Historic 2005 toxic bloom of *Alexandrium fundyense* in the west Gulf of Maine : 1. In situ observations of coastal hydrography and circulation. *Journal of Geophysical Research-Oceans*, 113(C7), C07039. <https://doi.org/10.1029/2007JC004601>

Hendey, N. I. (1964). An introductory account of the smaller algae of British coastal waters. Part 5: Bacillariophyceae (Diatoms). Her Majesty's Stationery Office, London, 317 pp.

Hernandez, A. Q., Gnanasambandam, S.-N., Zhao, S., Lee, H., Voll, W., Morey, G., & Cacciola, D. (2015). Multi-source contextual information item grouping for document analysis. *United States Patent N° US9165053B2*. Consulté à l'adresse <https://patents.google.com/patent/US9165053B2/en>

Hillebrand, H., Dürselen, C.-D., Kirschtel, D., Pollinger, U., & Zohary, T. (1999). Biovolume Calculation for Pelagic and Benthic Microalgae. *Journal of Phycology*, 35(2), 403-424. <https://doi.org/10.1046/j.1529-8817.1999.3520403.x>

-I-

Ignatiades, L., Gotsis-Skretas, O., & Metaxatos, A. (2007). Field and culture studies on the ecophysiology of the toxic dinoflagellate *Alexandrium minutum* (Halim) present in Greek coastal waters. *Harmful Algae*, 6(2), 153-165. <https://doi.org/10.1016/j.hal.2006.04.002>

-J-

Jassby, A., & Platt, T. (1976). Mathematical Formulation of Relationship Between Photosynthesis and Light for Phytoplankton. *Limnology and Oceanography*, 21(4), 540-547. <https://doi.org/10.4319/lo.1976.21.4.0540>

Ji, R., Edwards, M., Mackas, D. L., Runge, J. A., & Thomas, A. C. (2010). Marine plankton phenology and life history in a changing climate : Current research and future directions. *Journal of Plankton Research*, 32(10), 1355-1368. <https://doi.org/10.1093/plankt/fbq062>

Joint, I., & Pomroy, A. (1988). Allometric Estimation of the Productivity of Phytoplankton Assemblages. *Marine Ecology Progress Series*, 47(2), 161-168. <https://doi.org/10.3354/meps047161>

-K-

Kooijman S.A.L.M. (2001). Quantitative aspects of metabolic organization : A discussion of concepts. *Philosophical Transactions of the Royal Society of London. Series B: Biological Sciences*, 356(1407), 331-349. <https://doi.org/10.1098/rstb.2000.0771>

Krom, M. D., Brenner, S., Kress, N., Neori, A., & Gordon, L. I. (1992). Nutrient dynamics and new production in a warm-core eddy from the Eastern Mediterranean Sea. *Deep Sea Research Part A. Oceanographic Research Papers*, 39(3), 467-480. [https://doi.org/10.1016/0198-0149\(92\)90083-6](https://doi.org/10.1016/0198-0149(92)90083-6)

-L-

Laanaia, N., Vaquer, A., Fiandrino, A., Genovesi, B., Pastoureaud, A., Cecchi, P., & Collos, Y. (2013). Wind and temperature controls on *Alexandrium* blooms (2000–2007) in Thau lagoon (Western Mediterranean). *Harmful Algae*, 28, 31-36. <https://doi.org/10.1016/j.hal.2013.05.016>

Labry, C., Erard-Le Denn, E., Chapelle, A., Fauchot, J., Youenou, A., Crassous, M., Lorgeoux, B. (2008). Competition for phosphorus between two dinoflagellates : A toxic *Alexandrium minutum* and a non-toxic *Heterocapsa triquetra*. *Journal of Experimental Marine Biology and Ecology*, 358(2), 124-135. <https://doi.org/10.1016/j.jembe.2008.01.025>

- Lacroix, G., & Grégoire, M. (2002). Revisited ecosystem model (MODECOGeL) of the Ligurian Sea : Seasonal and interannual variability due to atmospheric forcing. *Journal of Marine Systems*, 37(4), 229-258. [https://doi.org/10.1016/S0924-7963\(02\)00190-2](https://doi.org/10.1016/S0924-7963(02)00190-2)
- Laws, E. A. (1975). The Importance of Respiration Losses in Controlling the Size Distribution of Marine Phytoplankton. *Ecology*, 56(2), 419-426. <https://doi.org/10.2307/1934972>
- Lazure, P., and Dumas, F. (2008). An external–internal mode coupling for a 3D hydrodynamical model for applications at regional scale (MARS). *Advances in Water Resources*, 31(2), 233-250. <https://doi.org/10.1016/j.advwatres.2007.06.010>
- Le Borgne, P., Legendre, G., and Marsouin, A. (2006). “Validation of the OSI SAF radiative fluxes,” in Proceedings of the 2006 EUMETSAT Meteorological Satellite Conference (Helsinki).
- Le Pape, O., & Menesguen, A. (1997). Hydrodynamic prevention of eutrophication in the Bay of Brest (France), a modelling approach. *Journal of Marine Systems*, 12(1), 171-186. [https://doi.org/10.1016/S0924-7963\(96\)00096-6](https://doi.org/10.1016/S0924-7963(96)00096-6)
- Legović, T., & Cruzado, A. (1997). A model of phytoplankton growth on multiple nutrients based on the Michaelis-Menten-Monod uptake, Droop’s growth and Liebig’s law. *Ecological Modelling*, 99(1), 19-31. [https://doi.org/10.1016/S0304-3800\(96\)01919-9](https://doi.org/10.1016/S0304-3800(96)01919-9)
- Li, Y., He, R., McGillicuddy, D. J., Anderson, D. M., & Keafer, B. A. (2009). Investigation of the 2006 Alexandrium fundyense bloom in the Gulf of Maine : In-situ observations and numerical modeling. *Continental Shelf Research*, 29(17), 2069-2082. <https://doi.org/10.1016/j.csr.2009.07.012>
- Lim, P.-T., Leaw, C.-P., Usup, G., Kobiyama, A., Koike, K., & Ogata, T. (2006). Effects of Light and Temperature on Growth, Nitrate Uptake, and Toxin Production of Two Tropical Dinoflagellates : Alexandrium Tamiyavanichii and Alexandrium Minutum (dinophyceae)1. *Journal of Phycology*, 42(4), 786-799. <https://doi.org/10.1111/j.1529-8817.2006.00249.x>
- Litchman, E., & Klausmeier, C. A. (2008). Trait-Based Community Ecology of Phytoplankton. *Annual Review of Ecology, Evolution, and Systematics*, 3, 615-639.
- Litchman, E., Edwards, K. F., Klausmeier, C. A., & Thomas, M. K. (2012). Phytoplankton niches, traits and eco-evolutionary responses to global environmental change. *Marine Ecology Progress Series*, 470, 235-248. <https://doi.org/10.3354/meps09912>
- Litchman, E., Klausmeier, C. A., Schofield, O. M., & Falkowski, P. G. (2007). The role of functional traits and trade-offs in structuring phytoplankton communities : Scaling from cellular to ecosystem level. *Ecology Letters*, 10(12), 1170-1181. <https://doi.org/10.1111/j.1461-0248.2007.01117.x>

-M-

- Maguer, J. F., Wafar, M., Madec, C., Morin, P., & Erard-Le Denn, E. (2004). Nitrogen and phosphorus requirements of an *Alexandrium minutum* bloom in the Penze Estuary, France. *Limnology and Oceanography*, 49(4), 1108-1114. <https://doi.org/10.4319/lo.2004.49.4.1108>
- Marañón, E., Cermeño, P., López-Sandoval, D. C., Rodríguez-Ramos, T., Sobrino, C., Huete-Ortega, M., ... Rodríguez, J. (2013). Unimodal size scaling of phytoplankton growth and the size dependence of nutrient uptake and use. *Ecology Letters*, 16(3), 371-379. <https://doi.org/10.1111/ele.12052>
- Martinussen, I., & Thingstad, T. F. (1987). Utilization of N, P and organic C by heterotrophic bacteria. 11. Comparison of experiments and a mathematical model. *Mar. Ecol. Prog. Ser.*, 9.
- McGillicuddy, D. J., Anderson, D. M., Solow, A. R., & Townsend, D. W. (2005). Interannual variability of *Alexandrium fundyense* abundance and shellfish toxicity in the Gulf of Maine. *Deep-Sea Research Part II-Topical Studies in Oceanography*, 52(19-21), 2843-2855. <https://doi.org/10.1016/j.dsr2.2005.06.020>
- McGillicuddy, D. J., Townsend, D. W., He, R., Keafer, B. A., Kleindinst, J. L., Li, Y., ... Anderson, D. M. (2011). Suppression of the 2010 *Alexandrium fundyense* bloom by changes in physical, biological, and chemical properties of the Gulf of Maine. *Limnology and Oceanography*, 56(6), 2411-2426. <https://doi.org/10.4319/lo.2011.56.6.2411>
- Menden-Deuer, S., & Rowlett, J. (2014). Many ways to stay in the game: Individual variability maintains high biodiversity in planktonic microorganisms. *Journal of The Royal Society Interface*, 11(95), 20140031. <https://doi.org/10.1098/rsif.2014.0031>
- Menesguen, A., Le Pape, O., & Leblond, I. (2003). Nutrient loadings and eutrophication risks in the Bay of Brest. In *Coastal Zones and Environmental Issues: Methodological Reflections* (Vol. 27, p. 163-175). Paris: Inst Oceanographique.
- Monbet, Y., & Bassoullet, P. (1989). *Bilan des connaissances océanographiques en rade de Brest*. (Rapport IFREMER/DERO/EL-89.23).
- Monod, J. (1942). *Recherches sur la croissance des cultures bactériennes* (2^e éd.). Hermann.
- Montagnes, Chambouvet, A., Guillou, L., & Fenton. (2008). Responsibility of microzooplankton and parasite pressure for the demise of toxic dinoflagellate blooms. *Aquatic Microbial Ecology*, 53, 211-225. <https://doi.org/10.3354/ame01245>

-O-

Olenina. I, Hajdu. S, Edler. L, Andersson. A, Wasmund. N, Busch. S, Göbel. J, Gromisz. S, Huseby. S, Huttunen. M, Jaanus. A, Kokkonen. P, Ledaine. I, Niemkiewicz. E (2006). Biovolumes and size-classes of phytoplankton in the Baltic Sea. HELCOM Baltic Sea Environment Proceedings No. 106

-P-

Pigliucci, M. (2001). *Phenotypic Plasticity: Beyond Nature and Nurture*. Johns Hopkins University Press.

Pouvreau, S., Daniele, M., Auby, I., Lagarde, F., Le Gall, P., Cochet, H., et al. (2016). VELYGER Database: The Oyster Larvae Monitoring French Project. SEANOE. <https://doi.org/10.17882/41888>

Probert, I. (1999). *Sexual reproduction and ecophysiology of the marine dinoflagellate Alexandrium minutum Halim* (University of Westminster). Consulté à l'adresse <https://archimer.ifremer.fr/doc/00104/21512/>

-R-

Raine, R. (2014). A review of the biophysical interactions relevant to the promotion of HABs in stratified systems: The case study of Ireland. *Deep Sea Research Part II: Topical Studies in Oceanography*, 101, 21-31. <https://doi.org/10.1016/j.dsr2.2013.06.021>

Rathaille, A. N., & Raine, R. (2007). *Predicting Alexandrium blooms in Cork harbour*. Galway: Marine Institute.

Redfield, A. C. (1958). The Biological Control Of Chemical Factors In The Environment. *American Scientist*, 46(3), 230A - 221. Consulté à l'adresse JSTOR.

Roberts, E.M., Bowers, D.G., Davies, A.J. (2014). Springs-neaps cycles in daily total seabed light: Daylength-induced changes. School of Ocean Sciences, Bangor University, Menai Bridge, Anglesey LL59 5AB, UK. *Journal of Marine Systems* 132 (2014) 116-129

Rolinski, S., Horn, H., Petzoldt, T., & Paul, L. (2007). Identifying cardinal dates in phytoplankton time series to enable the analysis of long-term trends. *Oecologia*, 153(4), 997-1008. <https://doi.org/10.1007/s00442-007-0783-2>

Rynearson, T. A., & Menden-Deuer, S. (2016). Drivers That Structure Biodiversity in the Plankton. In P. M. Glibert & T. M. Kana (Éd.), *Aquatic Microbial Ecology and Biogeochemistry: A Dual Perspective* (p. 13-24). https://doi.org/10.1007/978-3-319-30259-1_2

-S-

- Seity Y., Brousseau P., Malardel S., Hello G., Benard P., Bouttier F., et al. (2011). The AROME-France convective-scale operational model. *Mon. Weather Rev.* 139, 976–991. <https://doi.org/10.1175/2010MWR3425.1>
- Smayda, Theodore J. (1997). What is a bloom? A commentary. *Limnology and Oceanography*, 42(5part2), 1132-1136. https://doi.org/10.4319/lo.1997.42.5_part_2.1132
- Smith, H. L. (1997). The periodically forced Droop model for phytoplankton growth in a chemostat. *Journal of Mathematical Biology*, 35(5), 545-556. <https://doi.org/10.1007/s002850050065>
- Sourisseau M., Le Guennec V., Le Gland G., Plus M., Chapelle A. (2017): Resource competition Affects Plankton Community Structure; Evidence from Trait-Based Modeling. *Front. Mar. Sci.*, 04 April 2017. <https://doi.org/10.3389/fmars.2017.00052>
- Spatharis, S., Tsirtsis, G., Danielidis, D. B., Chi, T. D., & Mouillot, D. (2007). Effects of pulsed nutrient inputs on phytoplankton assemblage structure and blooms in an enclosed coastal area. *Estuarine, Coastal and Shelf Science*, 73(3), 807-815. <https://doi.org/10.1016/j.ecss.2007.03.016>
- Steele, J. H. (1962). Environmental Control of Photosynthesis in the Sea. *Limnology and Oceanography*, 7(2), 137-150. <https://doi.org/10.4319/lo.1962.7.2.0137>
- Steidinger K.A. and Tangen K. (1996). Dinoflagellates. In: Tomas C.R. (ed), *Identifying Marine Phytoplankton*. Academic Press, San Diego. pp. 387-584
- Stock, C. A., McGillicuddy, D. J., Solow, A. R., & Anderson, D. M. (2005). Evaluating hypotheses for the initiation and development of *Alexandrium fundyense* blooms in the western Gulf of Maine using a coupled physical–biological model. *Deep Sea Research Part II: Topical Studies in Oceanography*, 52(19), 2715-2744. <https://doi.org/10.1016/j.dsr2.2005.06.022>
- Sunda, W. G., Shertzer, K. W., & Hardison, D. R. (2009). Ammonium uptake and growth models in marine diatoms : Monod and Droop revisited. *Marine Ecology Progress Series*, 386, 29-41. <https://doi.org/10.3354/meps08077>
- Sundstrom, B. G. (1986). The marine diatom genus *Rhizosolenia*: a new approach to the taxonomy. Ph.D. dissertation, Lund University, Lund, Sweden, 117 pp.

-T-

- Tang, E. P. Y. (1995). The allometry of algal growth rates. *Journal of Plankton Research*, 17(6), 1325-1335. <https://doi.org/10.1093/plankt/17.6.1325>
- Taylor, K. E. (2001). Summarizing multiple aspects of model performance in a single diagram. *Journal of Geophysical Research: Atmospheres*, 106(D7), 7183-7192. <https://doi.org/10.1029/2000JD900719>
- Thingstad, T., & Pengerud, B. (1985). Fate and effect of allochthonous organic material in aquatic microbial ecosystems An analysis based on chemostat theory. *Marine Ecology Progress Series*, 21, 47-62. <https://doi.org/10.3354/meps021047>
- Townsend, D. W., Pettigrew, N. R., & Thomas, A. C. (2005). On the nature of Alexandrium fundyense blooms in the Gulf of Maine. *Deep Sea Research Part II: Topical Studies in Oceanography*, 52(19), 2603-2630. <https://doi.org/10.1016/j.dsr2.2005.06.028>
- Tréguer, P., Goberville, E., Barrier, N., L'Helguen, S., Morin, P., Bozec, Y., ... Quémener, L. (2014). Large and local-scale influences on physical and chemical characteristics of coastal waters of Western Europe during winter. *Journal of Marine Systems*, 139, 79-90. <https://doi.org/10.1016/j.jmarsys.2014.05.019>
- Trommer, G., Leynaert, A., Klein, C., Naegelen, A., & Beker, B. (2013). Phytoplankton phosphorus limitation in a North Atlantic coastal ecosystem not predicted by nutrient load. *Journal of Plankton Research*, 35(6), 1207-1219. <https://doi.org/10.1093/plankt/fbt070>

-V-

- Valbi, E., Ricci, F., Capellacci, S., Casabianca, S., Scardi, M., & Penna, A. (2019). A model predicting the PSP toxic dinoflagellate *Alexandrium minutum* occurrence in the coastal waters of the NW Adriatic Sea. *Scientific Reports*, 9(1), 4166. <https://doi.org/10.1038/s41598-019-40664-w>
- Van-Rooy, M. P. (1965). A Rainfall Anomaly Index independent of time and space. In *Monthly Weather Review: Vol. 105. Subtropical droughts and cross-equatorial energy transports*.
- Vellend, M. (s. d.). The Consequences Of Genetic Diversity In Competitive Communities - Vellend—2006—Ecology—Wiley Online Library. Consulté 20 septembre 2019, à l'adresse <https://esajournals.onlinelibrary.wiley.com/doi/full/10.1890/05-0173>

-W-

- Whitlock, R., Grime, J. P., Booth, R., & Burke, T. (2007). The role of genotypic diversity in determining grassland community structure under constant environmental conditions. *Journal of Ecology*, 95(5), 895-907. <https://doi.org/10.1111/j.1365-2745.2007.01275.x>
- Wyatt, T., & Jenkinson, I. R. (1997). Notes on *Alexandrium* population dynamics. *Journal of Plankton Research*, 19(5), 551-575. <https://doi.org/10.1093/plankt/19.5.551>

-Y-

- Yamamoto, T., & Tarutani, K. (1999). Growth and phosphate uptake kinetics of the toxic dinoflagellate *Alexandrium tamarense* from Hiroshima Bay in the Seto Inland Sea, Japan. *Phycological Research*, 47(1), 27-32. <https://doi.org/10.1046/j.1440-1835.1999.00149.x>

Annexes

Annex 1

Nutrients in the Bay of Brest

A1.1. Pointe du Château and river Daoulas

There exists a link between nutrients (Nitrogen, Phosphorus and Silicon) and the growth of phytoplankton. Generally, growth is observed under optimal conditions – usually in the summer and spring when temperatures are relatively high and dilution rates low. At this moment, nutrients are absorbed by the species in order to facilitate their growth. During cold and low light periods however, growth is not observed and nutrients are thus not absorbed. For this reason, nutrients can be considered as conservative during the winter. Their concentrations are linked to the salinity gradient in estuaries, with the gradient being mainly governed by the mixing of fresh and oceanic waters (Aminot and Kerouel, 2004). Aminot and Kerouel showed a decrease in nutrients with an increase in salinity.

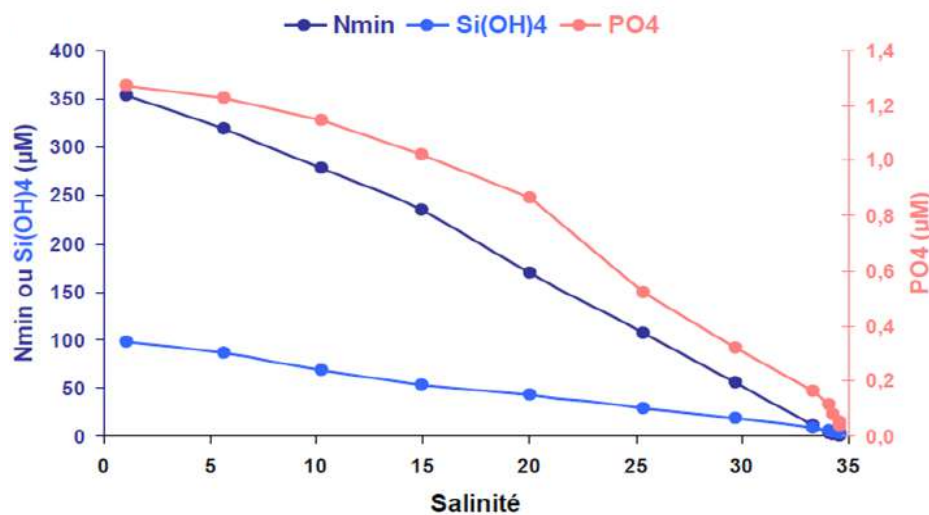


Figure A1.1: Nutrients-salinity relationship
Source: Alex-Breizh

In the case of the Bay of Brest, fresh water from Daoulas river contains high nutrient concentrations while sea water from the bay contains little nutrients. The mixing of both waters causes nutrient dilution in the estuarine system following the salinity gradient. In our case, we used a model to simulate the concentration of nutrients within the Daoulas estuary. The simulated section has two nutrient sampling points - Pointe du Château and River Daoulas (sampled only in summer so, doesn't follow the conservation hypothesis). However, we considered nutrient concentrations to be homogeneous in the model in the whole estuary. Do the nutrient data at Pointe du Château in winter represent those in the simulation box? We need to take this question into consideration because the points of measurement particularly Pointe du Château is quite close to the bay and therefore, cannot be a representation of the whole simulation box.

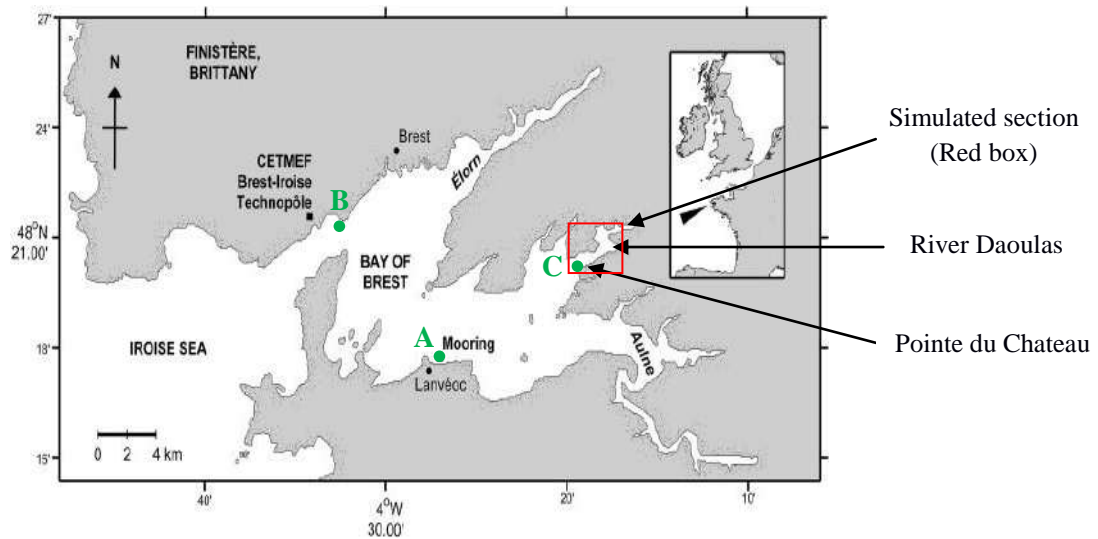


Figure A1.2: Daoulas estuary

The figures below show the relationship between model and nutrient field data in Pointe du Château (14 January to 06 July, 2016) and river Daoulas (04 May to 11 August, 2015.)

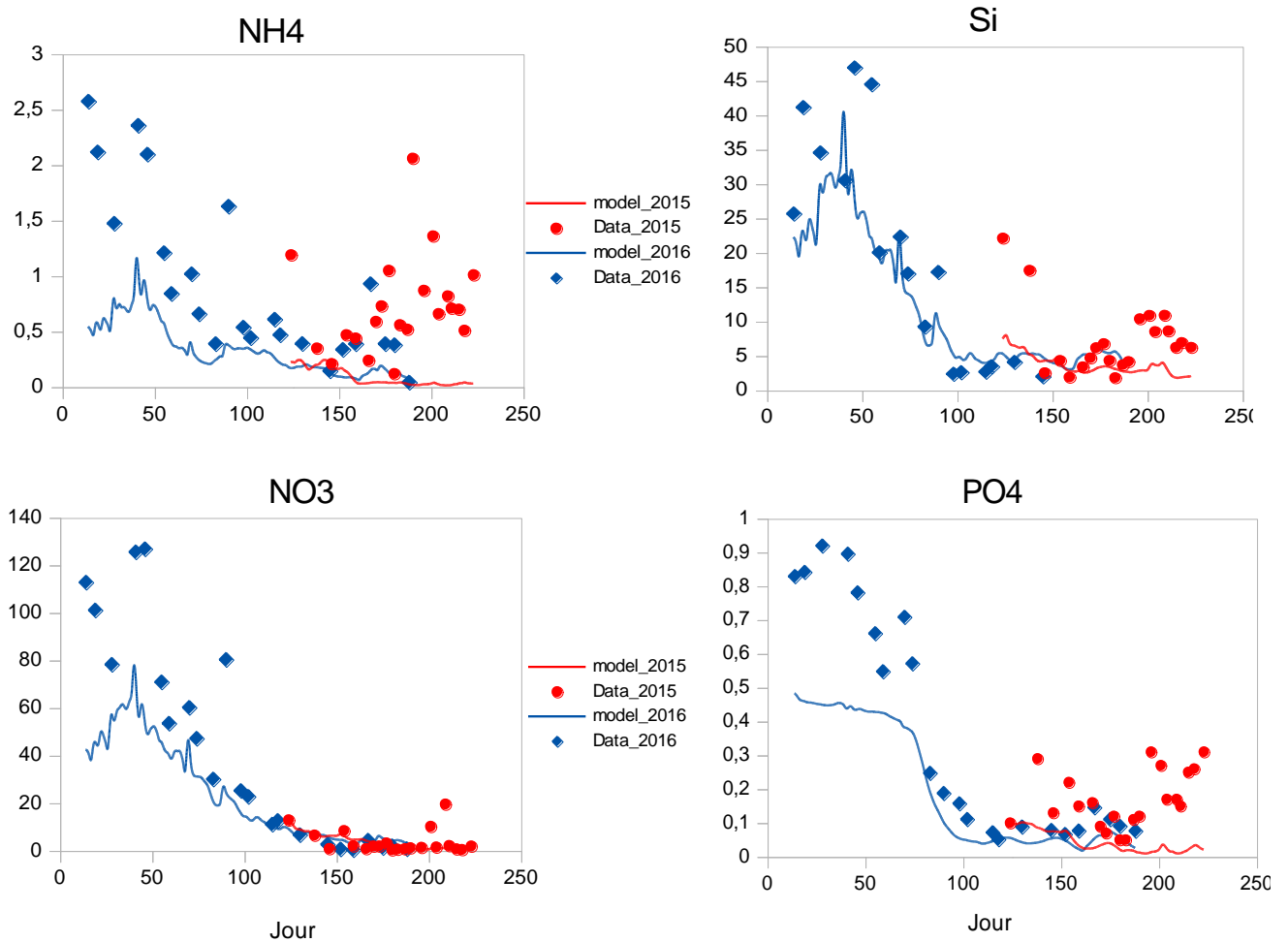


Figure A1.3: Nutrient variation in River Daoulas and Pointe du Château

In winter 2016, model underestimated nutrient concentrations. This may be the result of comparing the sampling point Pointe du Château to the modeled mean estuary concentration. This hypothesis is tested by calculating the new field data with the salinity of the model, using the dilution conservative equations.

To do this, we interpolated the field data at Pointe du château from November to March (2016-2017) with the following functions $-9.06 * \gamma + 327.26$, $-0.037 * \gamma + 1.73$ and $-1.45 * \gamma + 61.22$ for N, P and Si respectively where γ =mean salinity. This interpolation is only valid during nutrient conservation period (November to March), when they are not absorbed by the phytoplankton.

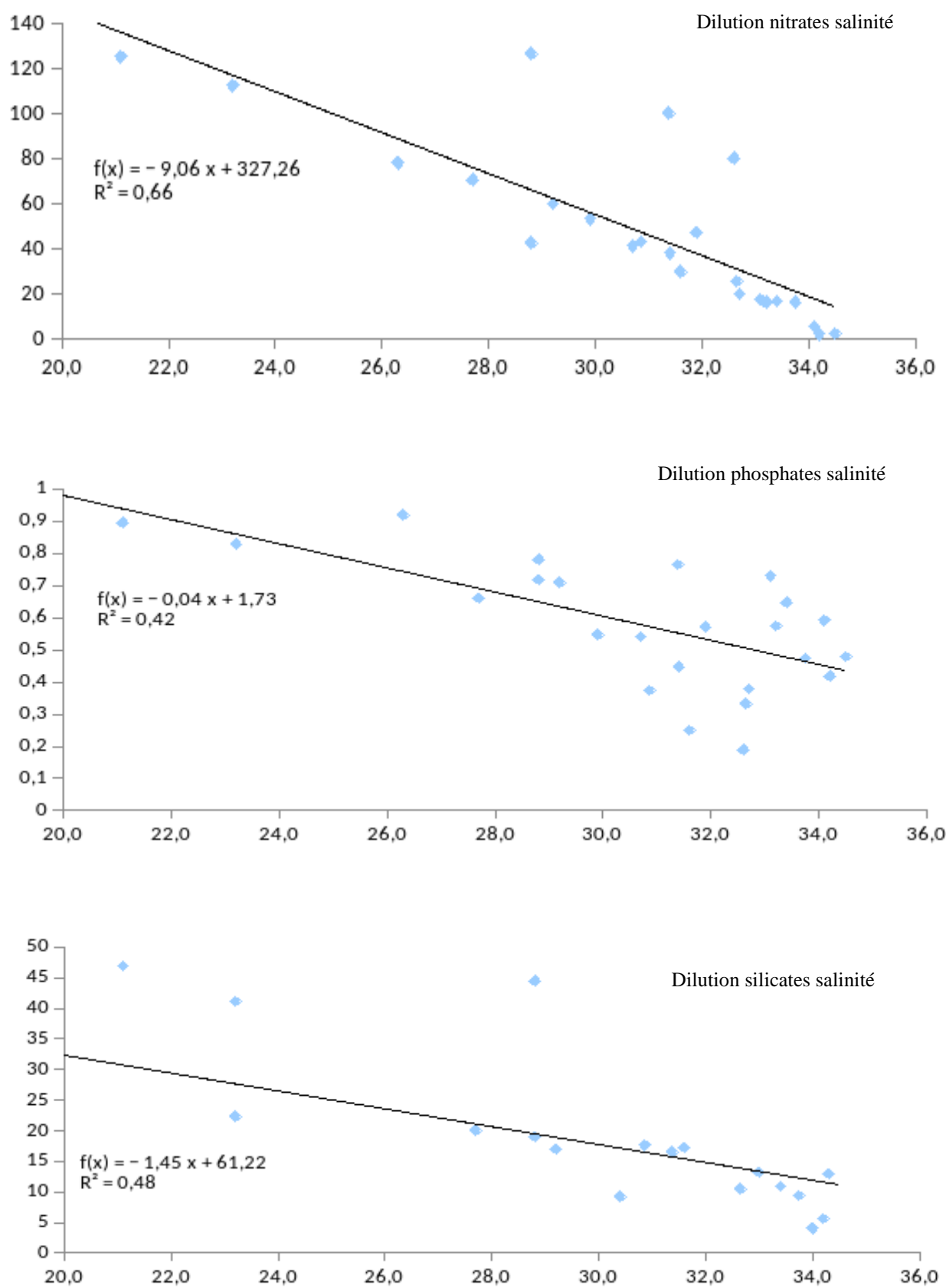


Figure A1.4: Dilution of nutrients with respect to salinity

Having the model salinity for 2016, we interpolated the field data in Pointe du Château. The interpolated result shows lower concentrations of nutrient data in winter which are closer to the model. But the model is still less than data except with silicon between January and March.

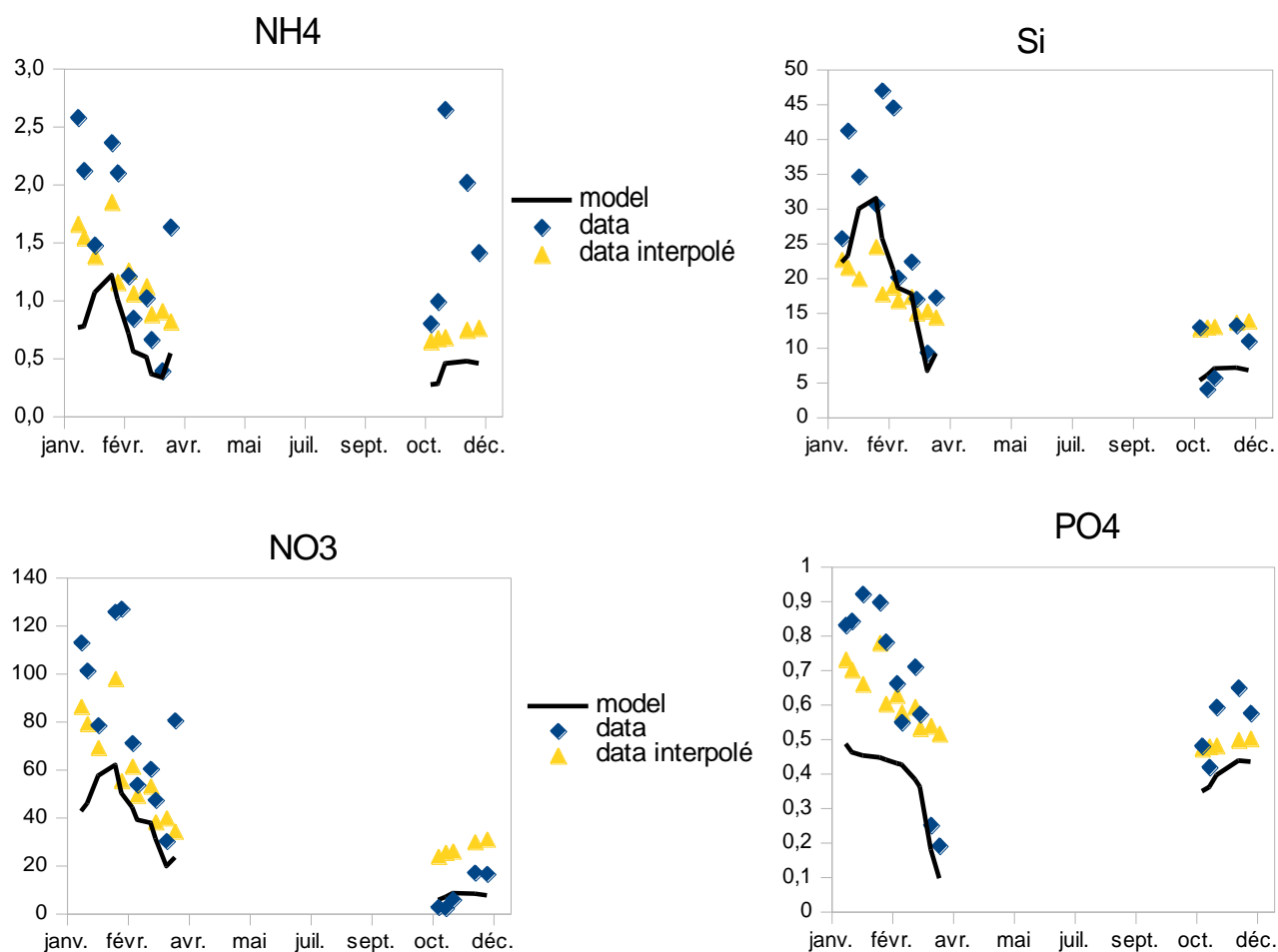
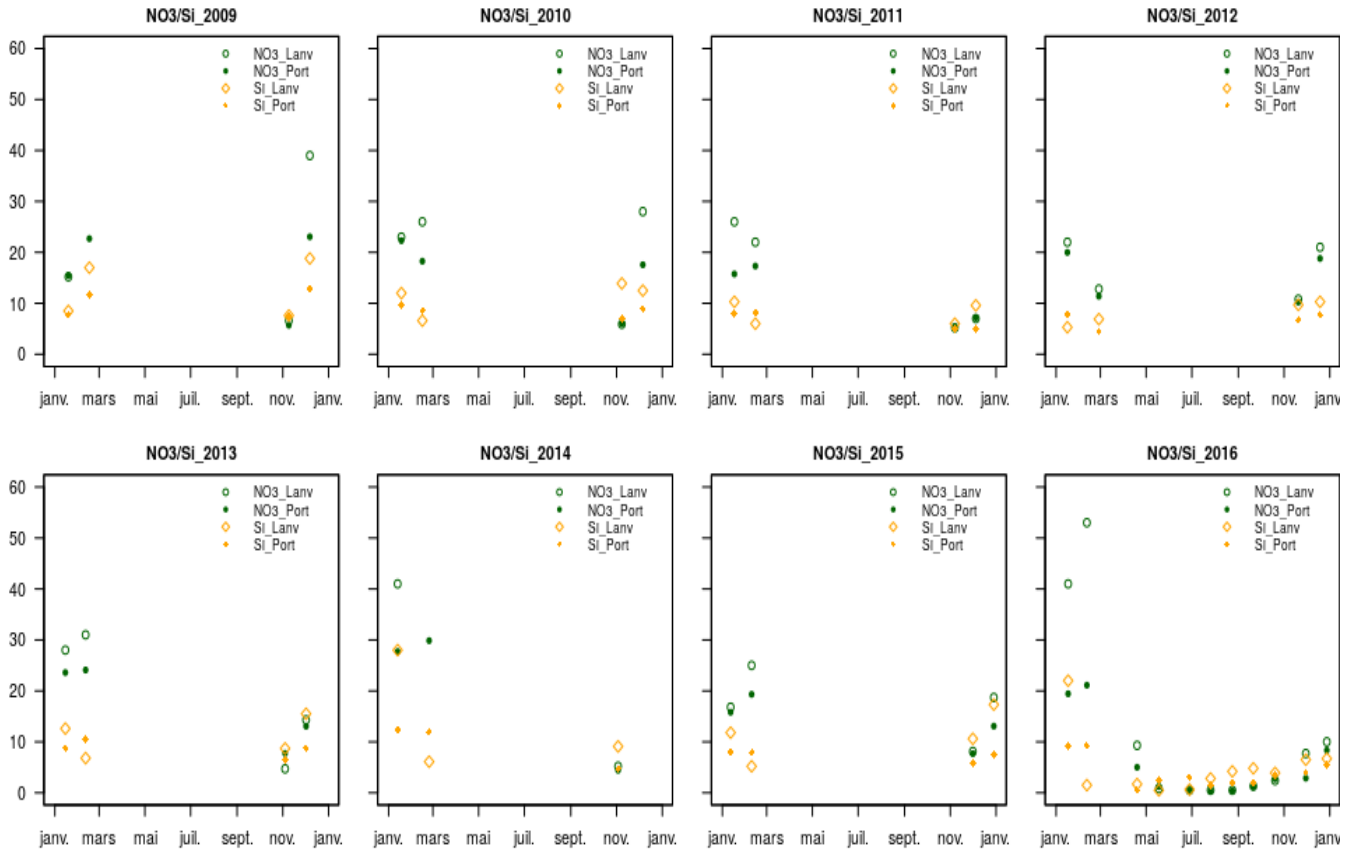


Figure A1.5: Interpolated nutrient data in Pointe du Château

Another possible reason for the variation is that the model takes the daily nutrient average whereas the field data provide value at the time of measurement, mainly high tide and not an average of the whole day. This can also underestimate the concentration of nutrients in the field.

A1.2. Nutrients at Lanveoc and Portzic

In addition to river Daoulas and Pointe du Château, there are measurement stations that provide data on nutrient concentrations within the Bay of Brest. Two of such stations are Lanveoc (A) and Portzic (B) which are at different distances from Pointe du Château (C) where our simulation box is located (Fig. A1.2). Portzic data are more detailed than Lanveoc and although Lanveoc is much closer to Daoulas than Portzic, we used data from Portzic in all our simulations. However, when we found that our model did not properly reproduce the nutrient field data particularly NH_4 and PO_4 ; we decided to see if there was a great difference in nutrient concentrations between the two measurement stations. Figure A1.6 shows the concentration of nutrients (in μmolL^{-1}) in Lanveoc and Portzic. In most cases, it indicates that both concentrations are similar or that Portzic is slightly lower. This is quite logical because Portzic is closer to the sea and therefore, more influenced by sea water - although we found Portzic to be higher than Lanveoc at some point in 2016. The comparison did not indicate much difference in both stations and we consequently, continued our simulations with Portzic data.



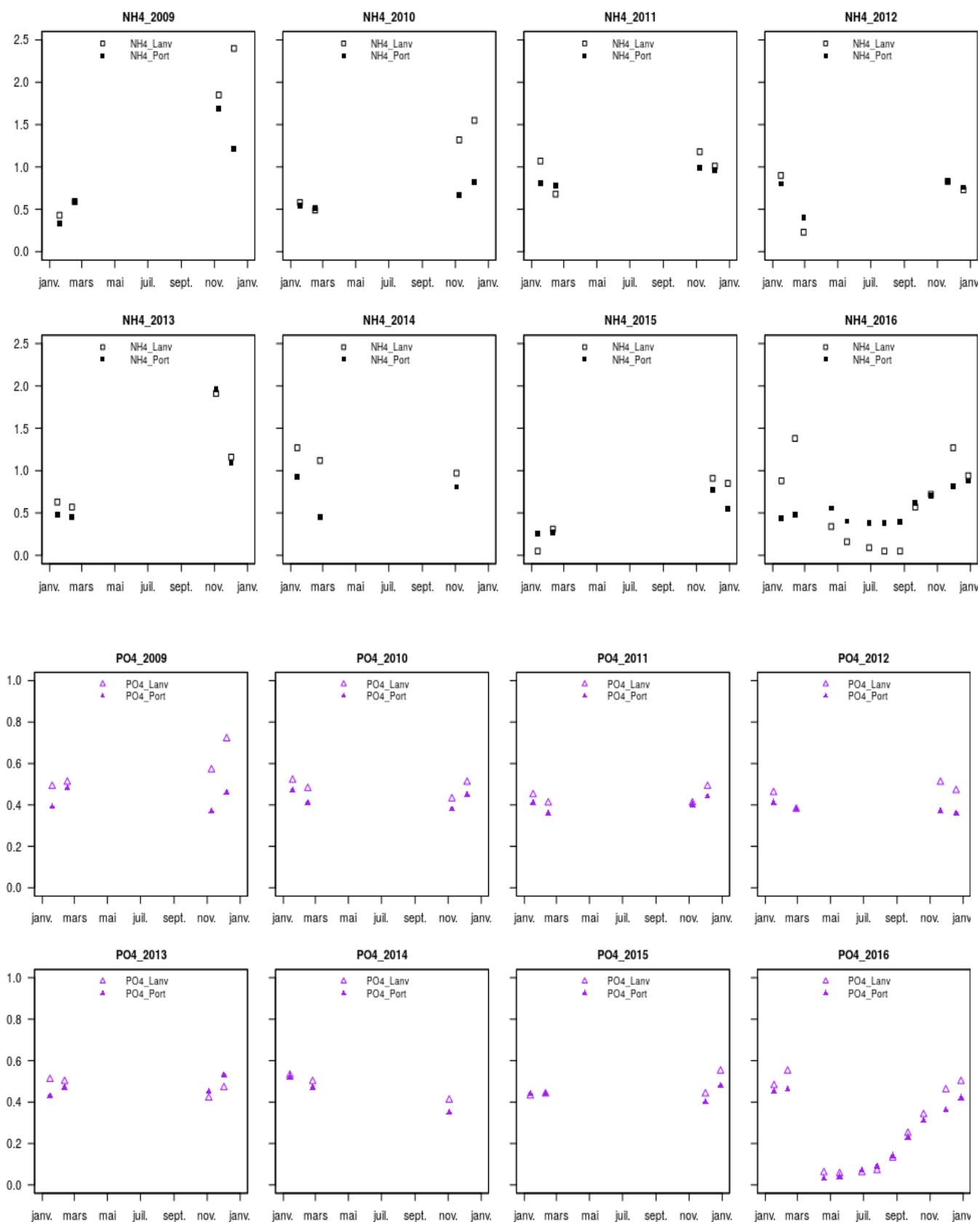


Figure A1.6: Nutrient concentrations in Lanveoc and Portzic stations

Annex 2

Summer Conditions

A2.1. Context

Environmental conditions in summer vary from one year to another and thus, it was necessary to evaluate their interannual variations in order to discuss their link to phytoplankton variability. Two parameters namely temperature and rainfall were chosen for a better understanding on how their variations relate to species growth as well as abundance.

A2.2. Warm/cold summer: Knowing that some species are favored during cold climates and some others in warm climates, we distinguished warm spring/summer from cold spring/summer in our simulations by comparing the average of minimum and maximum temperatures. As 15°C is a key temperature threshold for *A. minutum* growth intuition (Guallar et al, 2017), the date at which 15°C is surpassed is considered.

In figure A2.1 below, year 2011 was the first to exceed 15°C in the month of May. Every other year exceeded this temperature at some point but year 2013 was the last to cross it in the month of June. Between May and end of June, 2011 was already warm whereas 2013 was still cold. 2011 was also warmer than 2013 even in the month of July. With this in mind, we therefore believe that 2011 was a warm year and 2013 was a cold year. However, we do not necessarily expect species abundance in 2011 to be higher than 2013 because there are other factors to be considered.

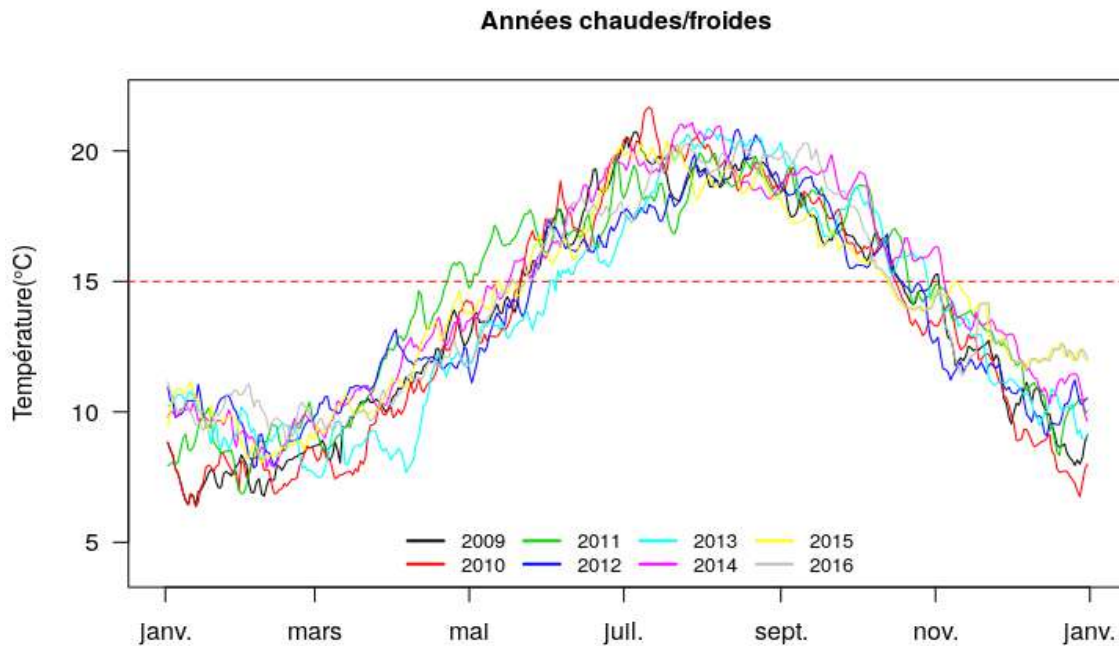


Figure A2.1: Warm and cold summer

A2.3. Wet/dry summer: Rainfall is another factor which influences growth and abundance of species. Its effect is not trivial in the sense that heavy rain increases the rate of dilution thus, reducing species abundance. On the contrary, it increases river nutrient input. Just like temperature, the amount of rainfall varied from season to season and year to year.

Keeping in mind that *A. minutum* growth is mainly from May to September; figure A2.2 below shows that 2012 had the overall maximum flow whereas 2011 had the lowest during this period. We therefore believe that 2012 was a wet summer and 2011 was a dry summer. Once again, this fact cannot single handedly determine the growth rate and abundance of species. However, it played a very significant role because the highest maximum abundance of *A. minutum* was observed in 2012 and the lowest was seen in 2011.

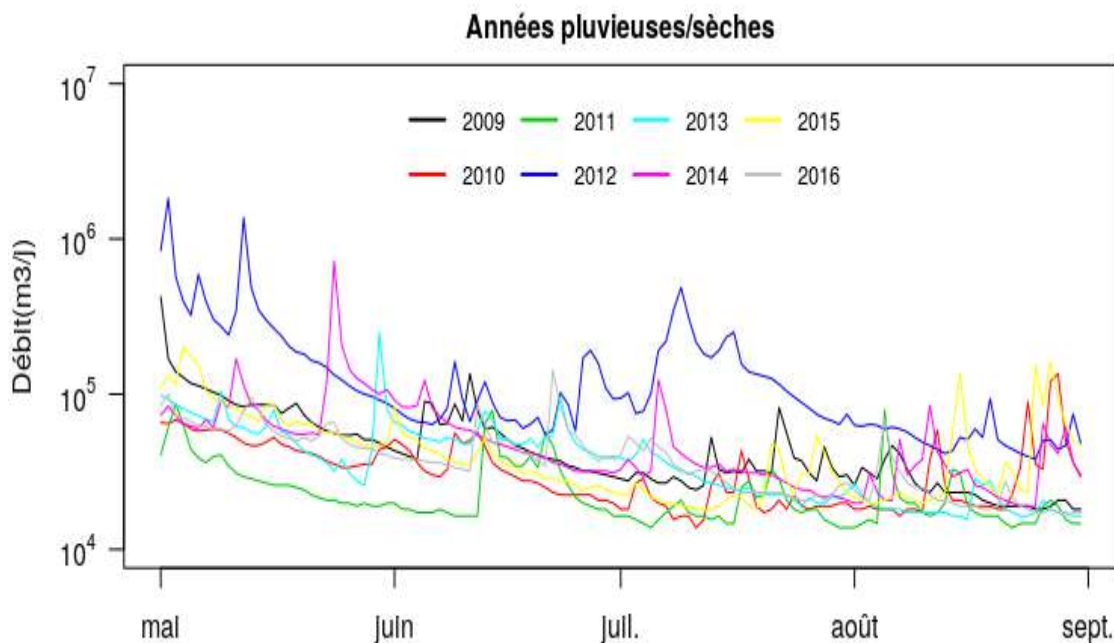


Figure A2.2: Wet and dry summer

Annex 3

Photoinhibition on phytoplankton

A3.1. Context

Photoinhibition is normally a light-induced reduction in the capacity of alga to photosynthesis. Species are photoinhibited when the light intensity is above their optimal irradiance (I_{opt}). In our first simulation, we used the same I_{opt} of 20W.m^{-2} for all the species. This option followed the equation of Jassby and Platt (1976) which does not take photoinhibition into account. We therefore, decided to introduce light trait to distinguish light effect among species and because photoinhibition is a well accepted process in the bay of Brest (Roberts et al, 2014).

To do this, we needed to assign an I_{opt} to each species. We looked at the field data containing most of the species that have been detected in the bay of Brest and then carried out a bibliographic study to find their optimal irradiance. Obviously, the I_{opt} of all species could not be found. The ones we found were either in $\mu\text{mol.m}^{-2}.\text{s}^{-1}$ or $\text{Einsteins.m}^{-2}.\text{d}^{-1}$ which we converted to W.m^{-2} using the following expressions -

$$1 \mu\text{Ein} = 1 \mu\text{moles of photons.m}^{-2}.\text{s}^{-1}$$

$$1 \mu\text{Ein.m}^{-2}.\text{s}^{-1} = 0.0864 \text{ Ein.m}^{-2}.\text{d}^{-1}$$

$$1 \mu\text{Ein.m}^{-2}.\text{s}^{-1} = 0.2409 \text{ W.m}^{-2}$$

$$1 \text{ W.m}^{-2} (\text{PAR}) = 0.3586 \text{ Ein.m}^{-2}.\text{d}^{-1}$$

$$1 \text{ W.m}^{-2} (\text{PAR}) = 4.1504 \mu\text{Ein.m}^{-2}.\text{s}^{-1}$$

Classe	Species	Iopt	Iopt (W.m ⁻²)	Reference
Dinophyceae	<i>A. minutum</i>	100 µmol.m ⁻² .s ⁻¹	23.8	Grzebyk et al., 2003; FiNAL, 2008; Laabir et al., 2010
	<i>Dinophyceae</i>	-	-	-
	<i>Dinophysiaceae</i>	-	-	-
	<i>Dinophysis acuminata</i>	-	-	-
	<i>Gymnodiniales</i>	-	-	-
	<i>Polykrikos</i>	-	-	-
	<i>Peridinales</i>	-	-	-
	<i>Ceratium fusus</i>	-	-	-
	<i>Ceratium lineatum</i> + <i>minutum</i>	-	-	-
	<i>Gonyaulax</i>	-	-	-
	<i>Diplopsalis</i> + <i>Diplopelta</i>	-	-	-
	<i>Peridiniaceae</i>	-	-	-
	<i>Peridinium quinquecorne</i>	-	-	-
	<i>Protoperidinium</i> + <i>Peridinium</i>	-	-	-
	<i>Scrippsiella</i> + <i>Enciculifera</i>	-	-	-
	<i>Prorocentrum</i>	-	-	-
	<i>Prorocentrum micans</i> + <i>arcuatum</i>	-	-	-
Chlorophyceae	<i>Closterium</i>	-	-	-
	<i>Scenedesmus</i>	-	-	-
	<i>Staurodesmus</i>	-	-	-
Diatomophyceae	Centrales	-	-	-
	<i>Cerataulina pelagica</i>	-	-	-
	<i>Eucampia zodiacus</i>	-	-	-
	<i>Chaetoceros</i>	20 à 450 µmol.m ⁻² .s ⁻¹	4,8 à 107	Kristian Spilling et al., 2015
	<i>Coscinodiscus</i>	-	-	-
	<i>Odontella aurita</i>	-	-	-
	<i>Leptocylindrus danicus</i> + <i>curvatus</i>	-	-	-
	<i>Ditylum brightwellii</i>	-	-	-
	<i>Lithodesmium undulatum</i>	-	-	-
	<i>Melosira</i>	-	-	-
	<i>Paralia sulcata</i>	-	-	-
	<i>Dactyliosolen fragilissimus</i>	-	-	-
	<i>Guinardia delicatula</i>	-	-	-
	<i>Rhizosolenia imbricata</i> + <i>styliformis</i>	-	-	-
	<i>Rhizosolenia setigera</i> + <i>pungens</i>	-	-	-
	<i>Skeletonema costatum</i>	-	-	-
	<i>Thalassiosira rotula</i>	-	-	-
	Pennales	-	-	-
	<i>Achnanthes</i>	-	-	-
	<i>Cocconeis</i>	-	-	-
	<i>Amphora</i>	-	-	-
	<i>Entomoneis</i>	-	-	-
	<i>Fragilariaceae</i>	-	-	-
	<i>Licmophora</i>	-	-	-
	<i>Thalassionema nitzschioides</i>	-	-	-
	<i>Navicula arenaria</i>	2,5 à 5 Ein.m ⁻² .d ⁻¹	6,9 à 13,9	Admiraal W., 1976
	<i>Pleurosigma</i> + <i>Gyrosigma</i>	-	-	-
	<i>Bacillaria paxillifer</i>	-	-	-
	<i>Cylindrotheca closterium</i>	-	-	-
	<i>Nitzschia sigma</i>	2,5 à 5 Ein.m ⁻² .d ⁻¹	6,9 à 13,9	Admiraal W., 1976
	<i>Nitzschia c. f. dissipata</i>	"	"	"
	<i>Pseudo-nitzschia</i>	-	-	-

Table A3.1: Identified optimal irradiance of some species present in the Bay of Brest.

Optimal Irradiance: The average light intensity in our model ranges from an average of 15 to 300W.m⁻² while the Photosynthetically Available Radiation (PAR) varies from 6 to 140W.m⁻².

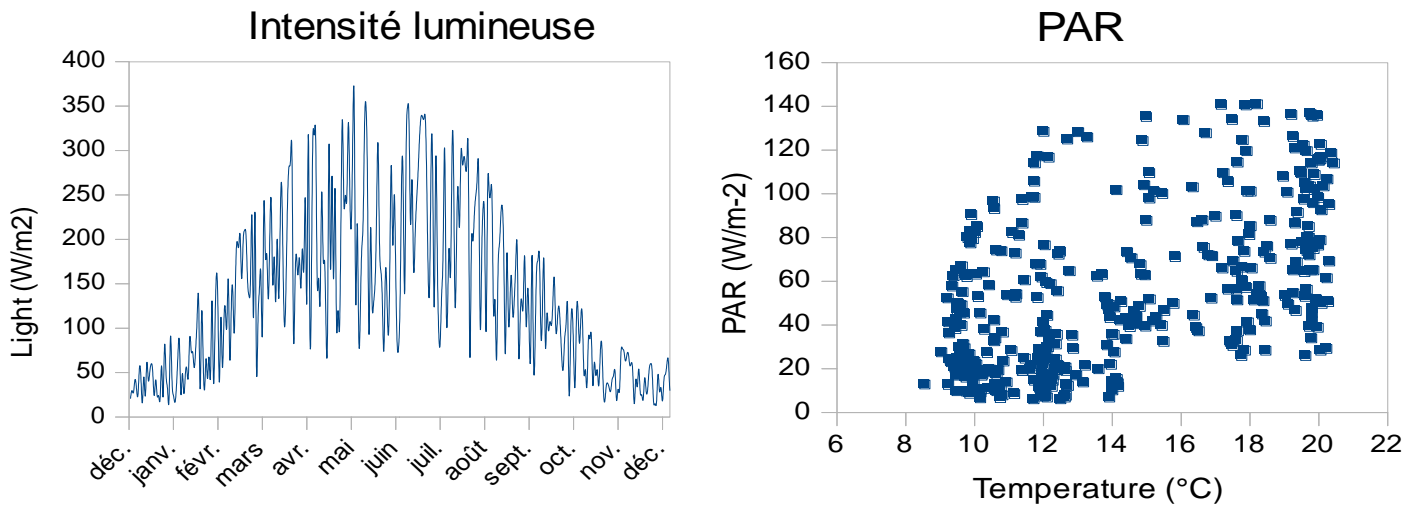


Figure A3.1: Light intensity and Photosynthetically Available Radiation (PAR)

Unlike using a general I_{opt} for all species, we introduce a range of I_{opt} which relates to the size of the species because I_{opt} decreases with an increasing cell size (Finkel 2001). With the previous size range, we looked at an I_{opt} of 10 to 150W.m⁻² which we found to be on a high side. Secondly, we looked at 3 to 150W.m⁻² which would have been an ideal I_{opt} range but unfortunately, the interval did not correspond with *A. minutum*. Lastly, we settled with an I_{opt} of 8 to 100W.m⁻² which has a better interval and covers both small and large species including *A. minutum*.

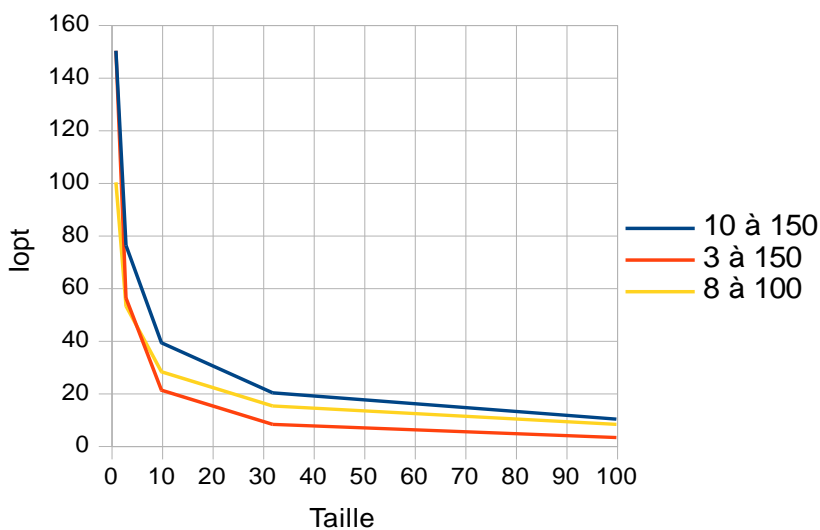


Figure A3.2: Relationship between cell size and I_{opt}

Taille (µm)	Iopt (W/m²)		
	10 à 150	3 à 150	8 à 100
100	10	3	8
32	20	8	15
Alex (18)	24	24	24
10	39	21	28
3	76	56	53
1	150	150	100

Category	Taille(µm)	Iopt(W/m²)
Pico	1	100
Pico	2	84
Nano	5	54
Nano	18	24
Micro	28	12
Micro	64	8

Table A3.2: Cell size and I_{opt}

In the light intensity shown above, this phenomenon will favor the growth of large cells before the small cells. In other words, as light intensity increases; the large cells dominate until the I_{opt} of small cells is reached. In assigning an I_{opt} to the species in our simulation, we made the allocation based on cell size and using *A. minutum* as point of reference. With initially defined cell size of 1 to 100 μ m (although the current range is now 1 to 64 μ m), we obtained the corresponding I_{opt} for pico, nano and microphytoplankton.

A3.2. Light limitation without photoinhibition

Previously, we used Jassby and Platt (1976) where –

$$\text{Light limitation} = \tanh \left(\frac{PAR}{I_{opt}} \right)$$

But no matter the I_{opt} , the species were not photoinhibited (top) but light limited (bottom) as shown in the figure below.

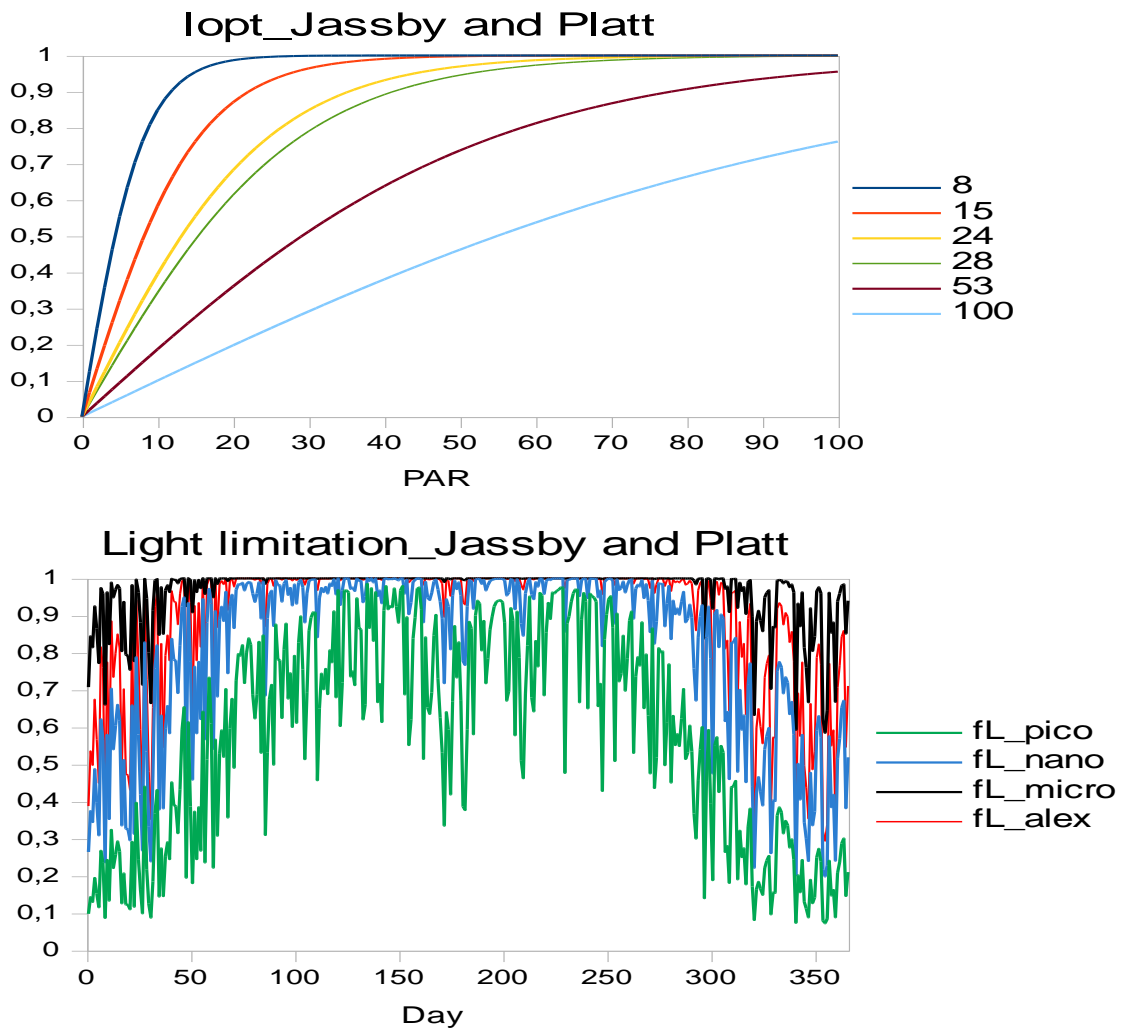


Figure A3.3: Light limitation by Jassby and Platt (1976)

Effect of Jassby and Platt on the growth of species: No significant effect was observed because the growth of species was not limited by light. The abundance shown in the figure below is the simulation of the year 2016.

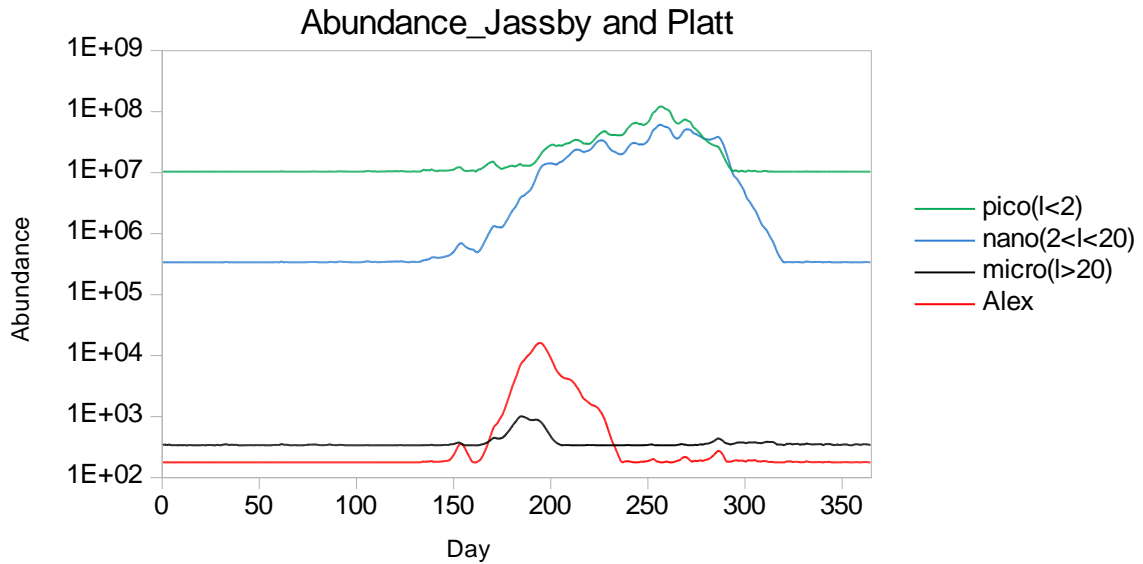


Figure A3.4: Abundance of species using Jassby and Platt equation

A3.3. Light limitation with photoinhibition

We intended to introduce light trait into our model because as mentioned earlier, it is a possible phenomenon in the bay of Brest and therefore, we tested different equations which incorporated photoinhibition.

The equation of Steele (1962):

$$\frac{G}{G_{max}} = \frac{PAR}{I_{opt}} \exp \left[1 - \frac{PAR}{I_{opt}} \right]$$

Where G is growth and G_{max} is the maximum growth achieved by definition, at the optimum light intensity (I_{opt}). Unlike Jassby and Platt, all species are photoinhibited using Steele's equation as shown in the figure below.

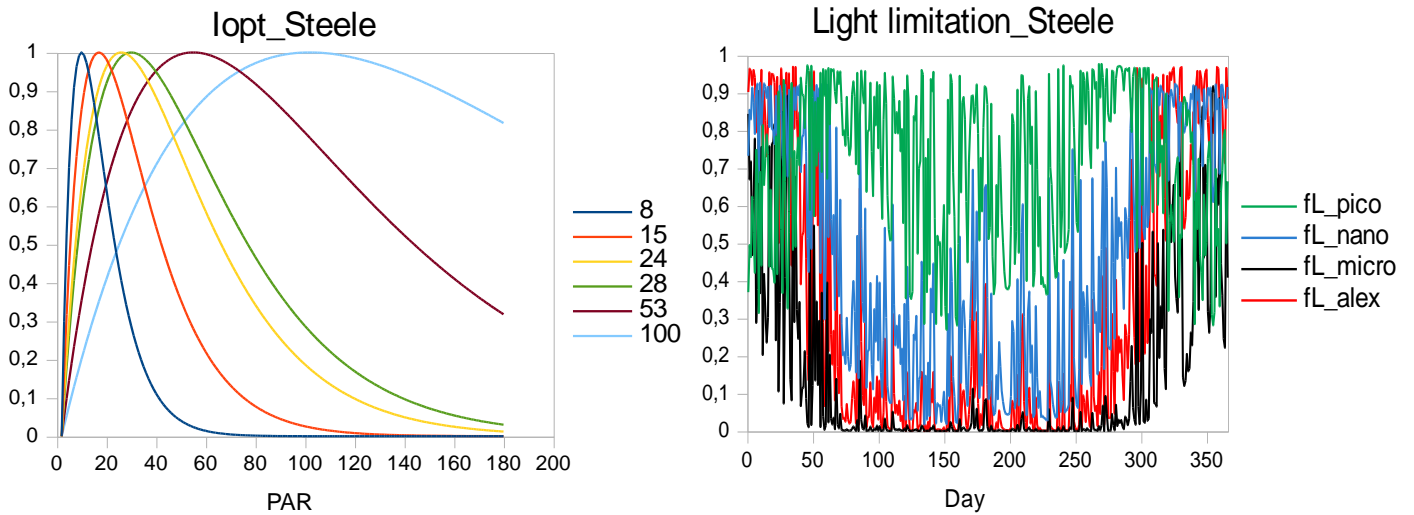


Figure A3.5: Light limitation by Steele (1962)

Effect of Steele on the growth of species: Steele's equation predicts growth relative to the maximum as a function of the ratio of the incident and optimum light intensity, PAR/I_{opt} . This equation remains one of the more simple and remarkably versatile (Kremer and Nixon, 1978). However, our species are almost completely photoinhibited and thus, experienced little or no growth as shown in the figure below.

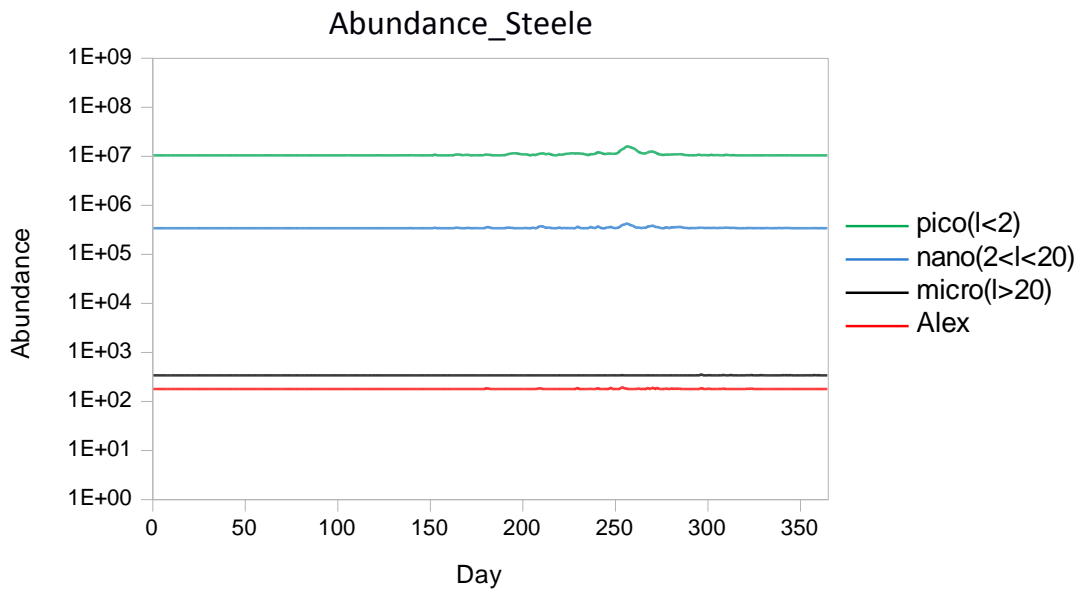


Figure A3.6: Abundance of species using Steele's equation

The equation of Lacroix (2002):

$$\text{Light limitation} = \frac{2(1+\beta) \left(\frac{PAR}{I_{opt}} \right)}{\left(\frac{PAR}{I_{opt}} \right)^2 + 2 \left(\frac{PAR}{I_{opt}} \right) \beta + 1}$$

Lacroix used this equation to compute as accurate as possible, the decrease of light intensity with depth. Limitation by light was calculated using β , a shape factor for the photoinhibition curve.

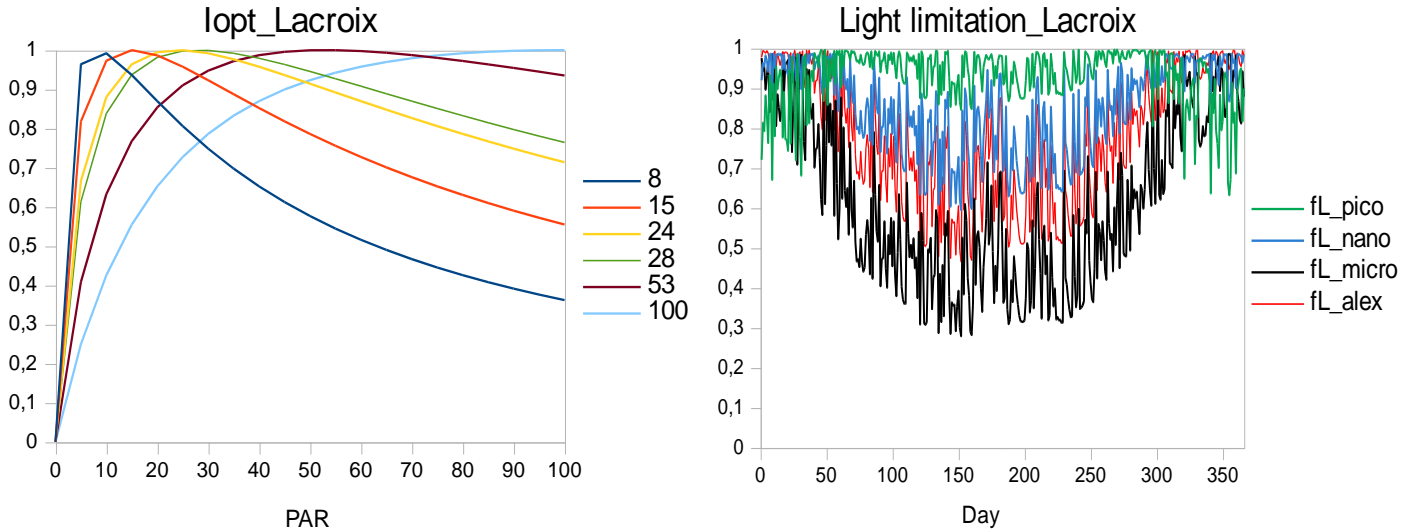


Figure A3.7: Light limitation by Lacroix (2002)

Effect of Lacroix on the growth of species: Here, we still observe a high level of light limitation especially for *A. minutum* and the microphytoplankton.

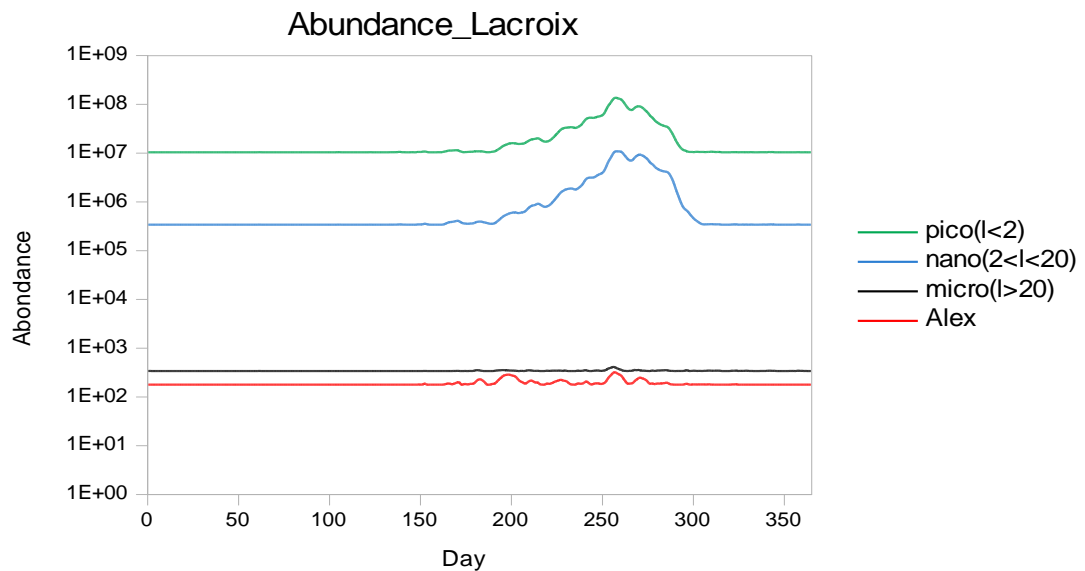


Figure A3.8: Abundance of species using Lacroix's equation

Having seen the effects of light limitation on the growth of species, we decided to suspend photoinhibition but retain the equation of Jassby and Platt and light trait or I_{opt} which corresponds to the size of each species.

Annex 4

Simulated phenology of phytoplankton (2009-2016)

A4.1. Phenology by category

The abundance of pico, nano and micro phytoplankton together with *A. minutum*

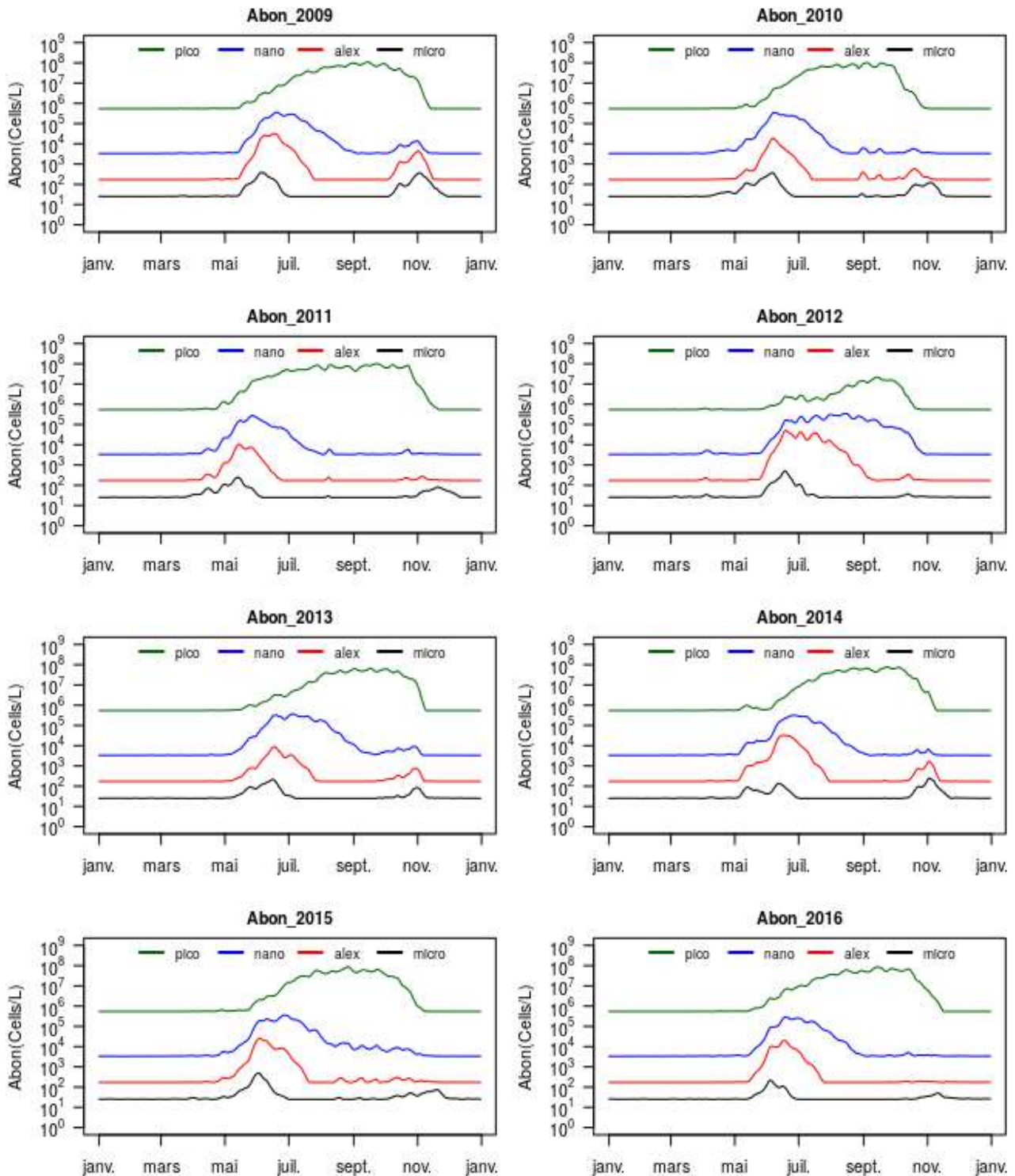


Figure A4.1: Phenology of phytoplankton

N limitation on phytoplankton: Nitrogen is one of the limiting nutrients in the growth of phytoplankton. The level of limitation depends on its availability as well as the cell quota of the species. Phenotype of large cells tend to be more advantaged than those of small cells in terms of nitrogen assimilation and are thus, less limited in nitrogen than small cells just before the month of July. We observed similar limitation at the beginning of each year except with *A. minutum* which showed little or no limitation mainly between January and March. From March to September 2012, the pico is more limited in N than nano and micro. In other years, the micro is more limited in the month of September.

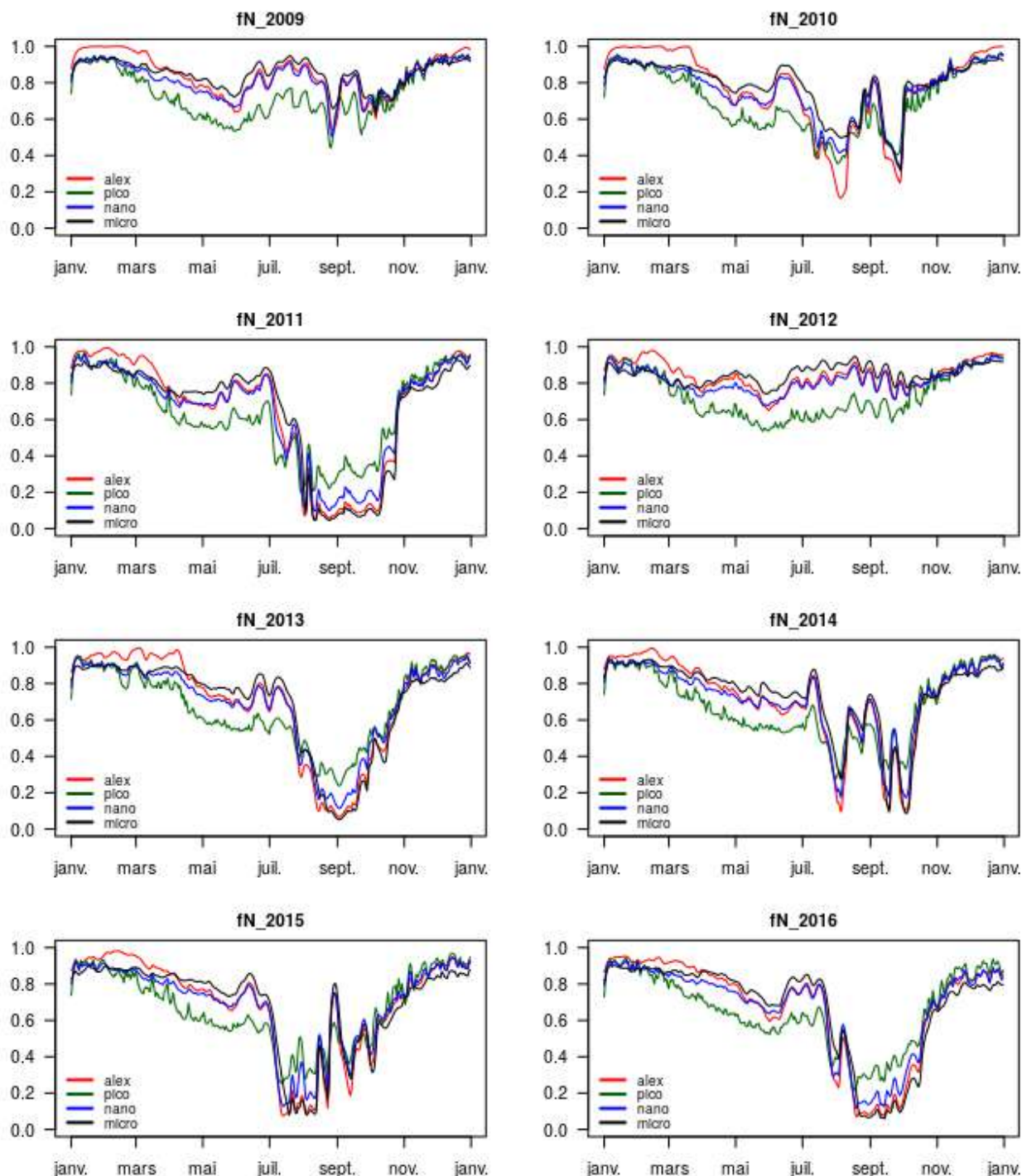


Figure A4.2: Nitrogen limitation on phytoplankton

P limitation on phytoplankton: This nutrient is naturally less abundant and quite limiting in the growth of phytoplankton. Competition for phosphorus is very high especially in the summer when species experience growth. During this period, we observed the inverse of nitrogen limitation i.e. pico is less limited while micro is more limited. Same scenario is present in each year. Unlike nitrogen, phosphorus is readily assimilated by small cells and this explains why micro and nano have the highest limitation in phosphorus. *A. minutum* has a limitation similar to nano and is still more limited than pico. In all cases, phosphorus limitation is at its highest between June and August.

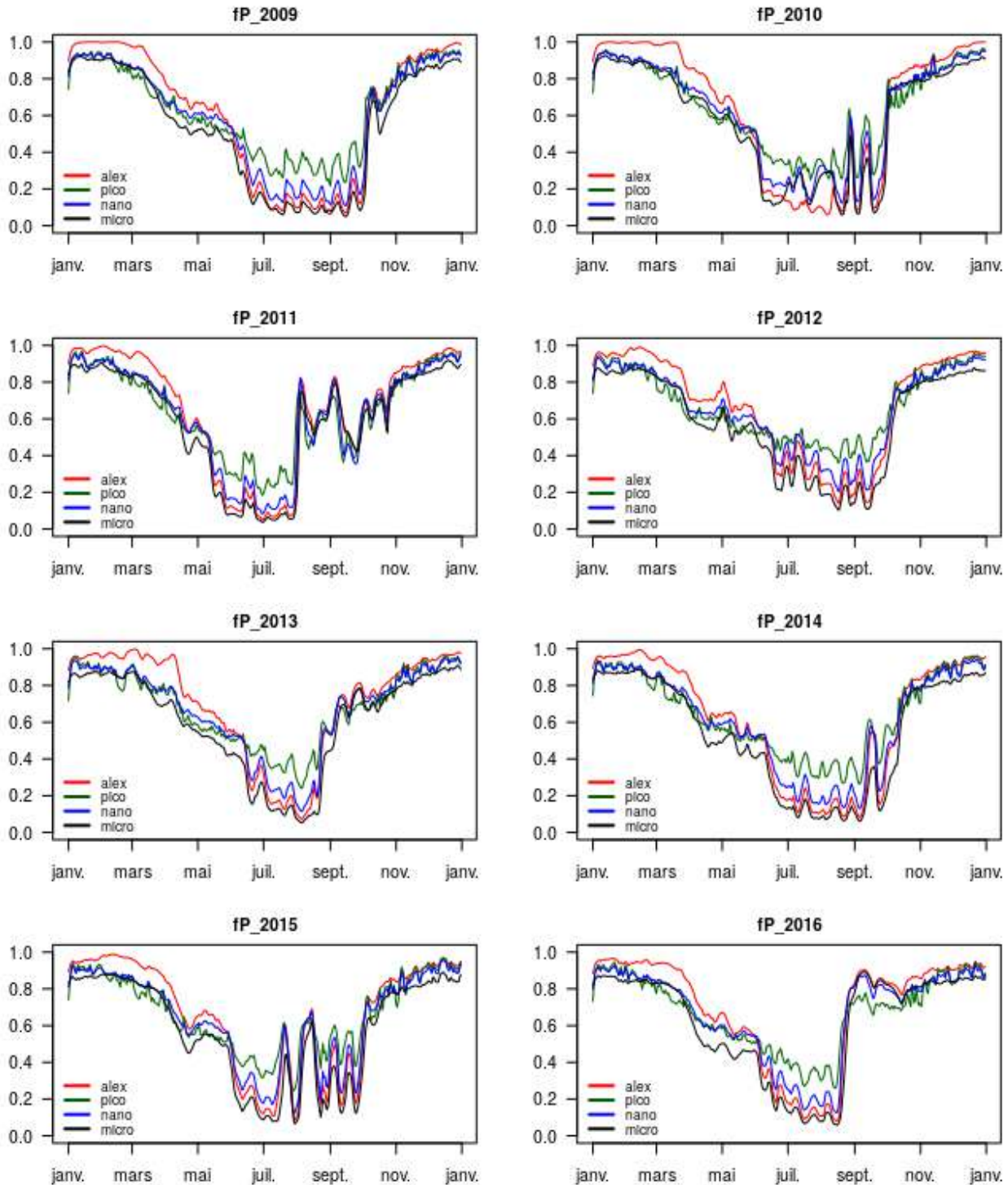


Figure A4.3: Phosphorus limitation on phytoplankton

Si limitation on phytoplankton: Limitation by silicon is only applicable to diatoms. The pico, nano and micro shown in the figure below are those of siliceous species. The figure equally shows *A. minutum* which in this case, represents all dinoflagellate species and it clearly shows that they are not in any way limited by silicon. On the other hand, Si limitation is directly linked to cell size such that the larger the cell; the more the need for silicon and vice versa. In our simulations, we observed that micro is more limited in silicon than pico.

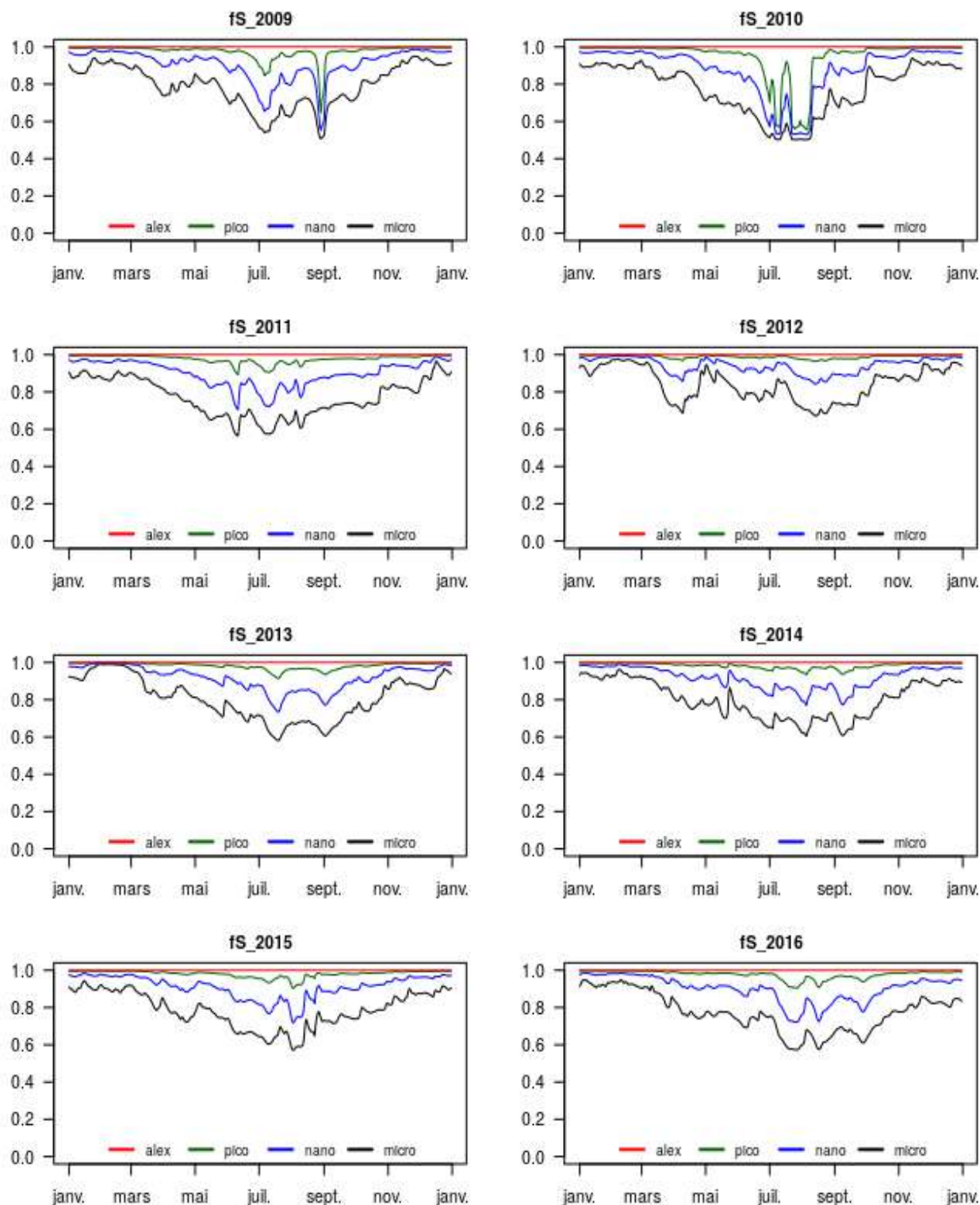


Figure A4.4: Silica limitation on phytoplankton

T and L limitations on phytoplankton: In addition to nutrients, temperature and light are also factors that can limit the growth of phytoplankton. In terms of temperature, limitation is highest in the winter but much less in the summer. This limitation has no relationship whatsoever with cell size but the T_{opt} of the species. In the figure below, we present $fT \cdot \mu_{max}$ because maximum growth is dependent on temperature. Pico, nano and micro show the same limitation because they share the same variation in μ_{max} as shown in the characteristics of uniform species. *A. minutum* on the other hand, appears to be different because it is a single species whereas other categories are a collection of several species. We shall see temperature limitation in more details.

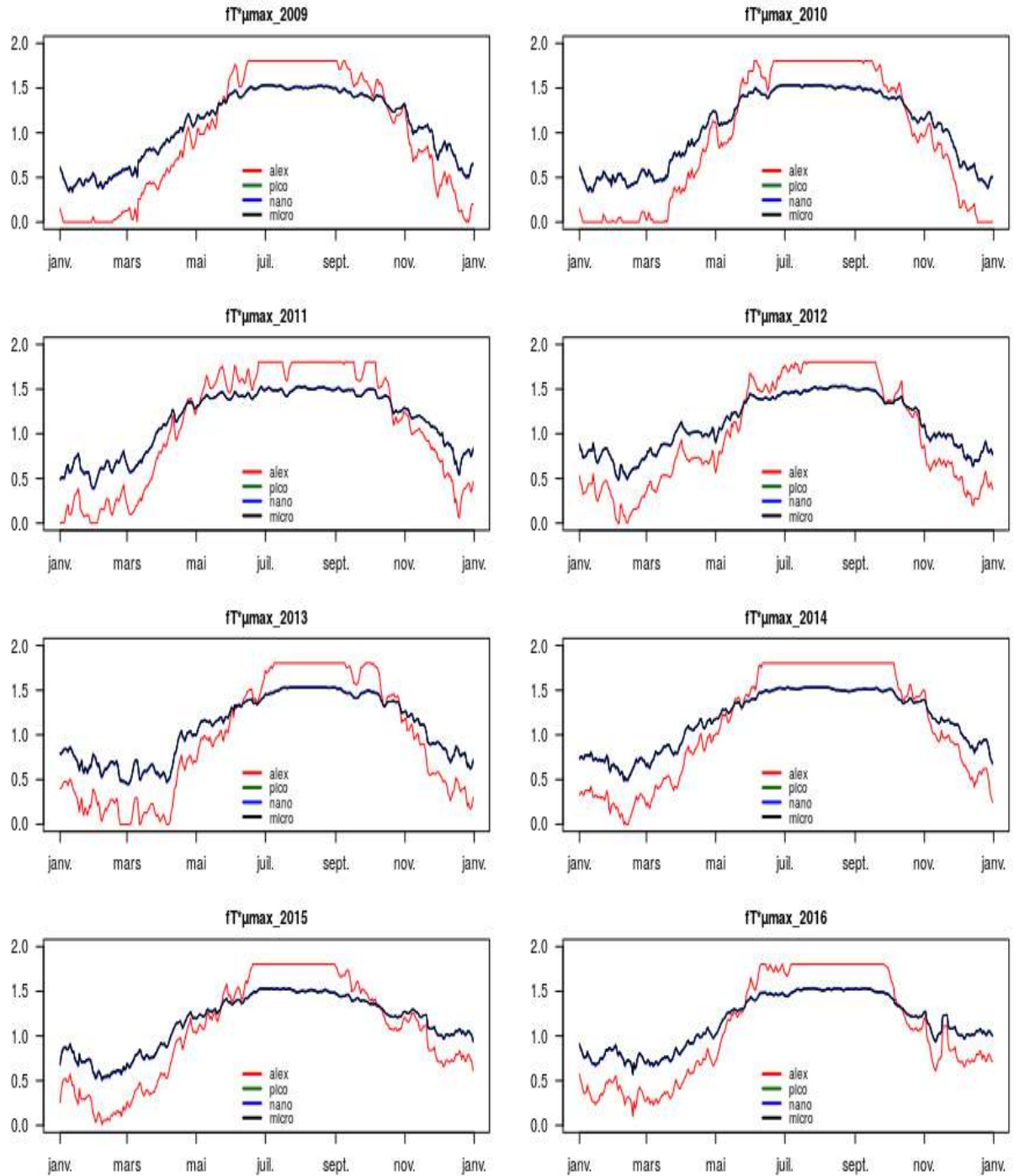


Figure A4.5: Temperature limitation on phytoplankton

In terms of light, limitation is linked to the optimal irradiance of the species and therefore; indirectly related to cell size. In other words, the larger the cell size; the smaller the saturating light intensity or I_{opt} and vice versa. In the figure below, we see the micro (having lower I_{opt}) with less light limitation and the pico (having higher I_{opt}) with a greater light limitation. We shall also see light limitation in more details.

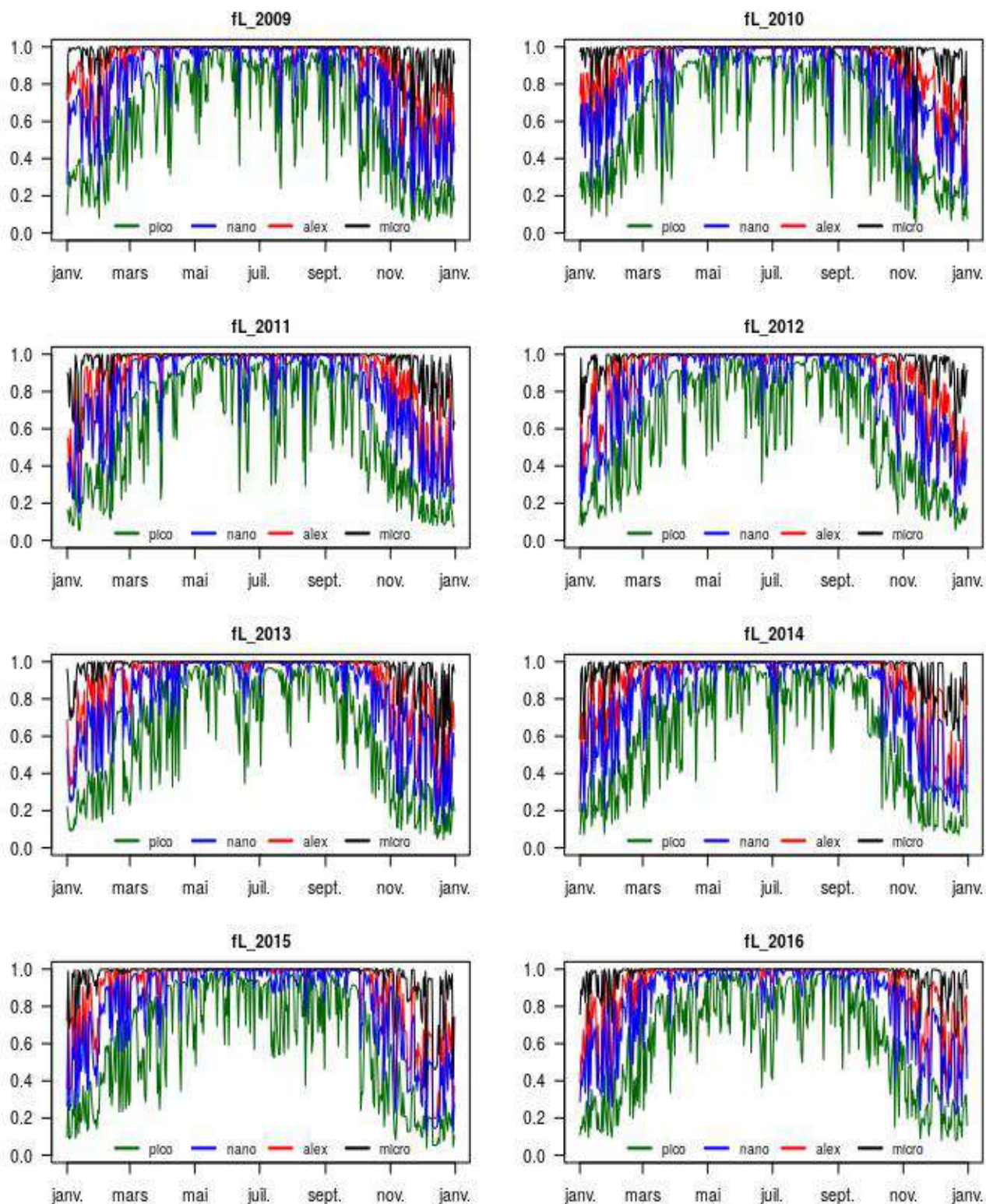


Figure A4.6: Light limitation on phytoplankton

A4.2. Phenology by cell size

In as much as large cells compete with small cells, they also compete among themselves. We therefore, looked at the competition among species of the same size consisting of diatoms and dinoflagellates. They share similar parameters other than optimal temperature.

Species of 1 μ m: These species represent the category of picophytoplankton. Though their sizes are the same, their abundances are completely different; indicating that some are more advantaged than others. In the figure below, we see the dominance of species with a T_{opt} of 18°C in all simulated years. It is closely followed by species of 20°C and 16°C. One remarkable observation is that these dominating species have a T_{opt} greater than 15°C. The least dominant species has a T_{opt} of 10°C.

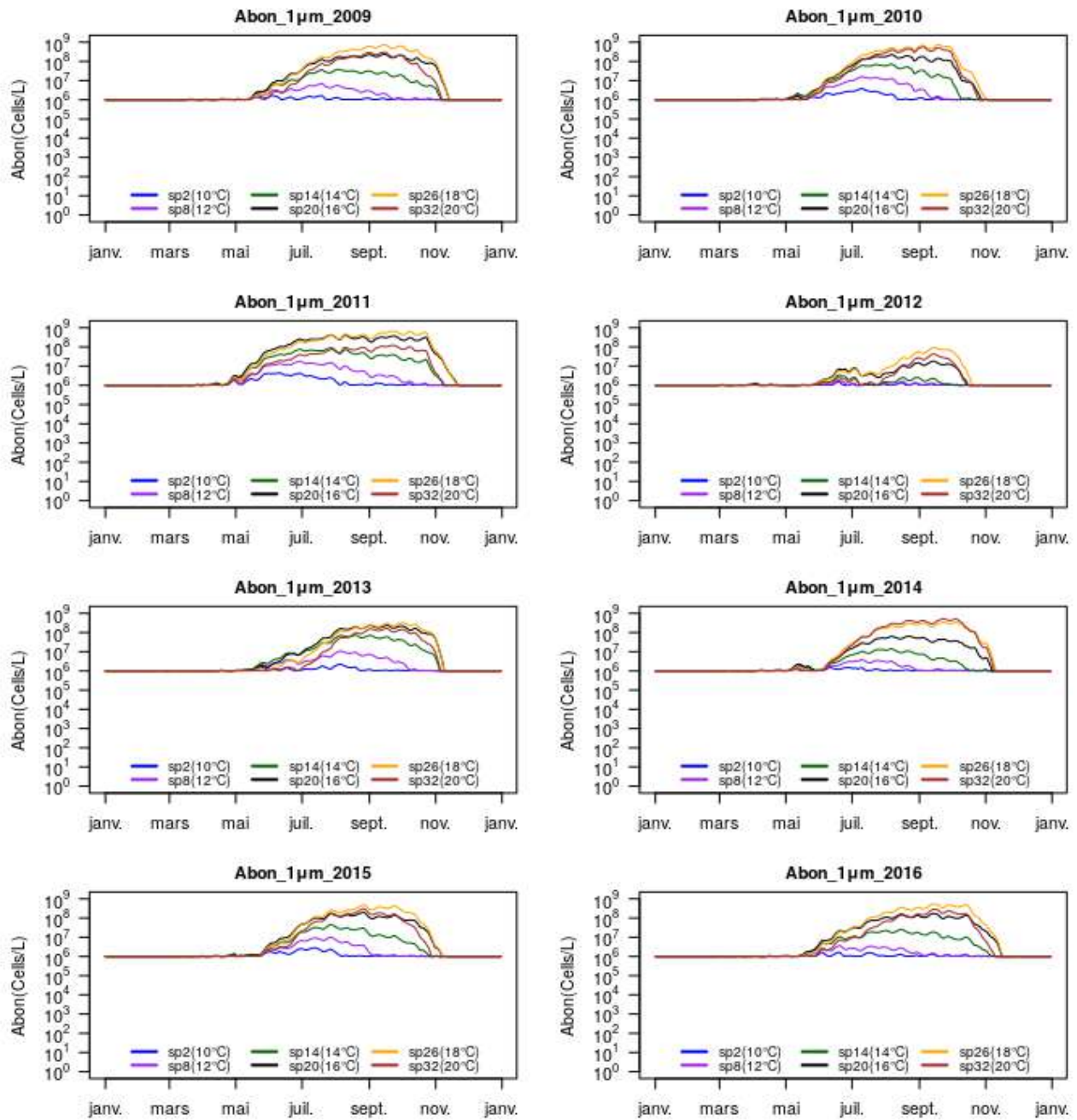


Figure A4.7: Species of 1 μ m

Species of 2µm: These are also picophytoplankton and they demonstrate a similar scenario with those of 1µm. Here, species with T_{opt} above 15°C still dominate but we observe a close competition by sp15 (14°C) in 2013. Despite the closeness, sp27 and sp33 had maximum abundances greater than one million cells per liter. Sp3 and sp9 with 10°C and 12°C respectively remain less dominant at abundances less than 1 000 000cellsL⁻¹.

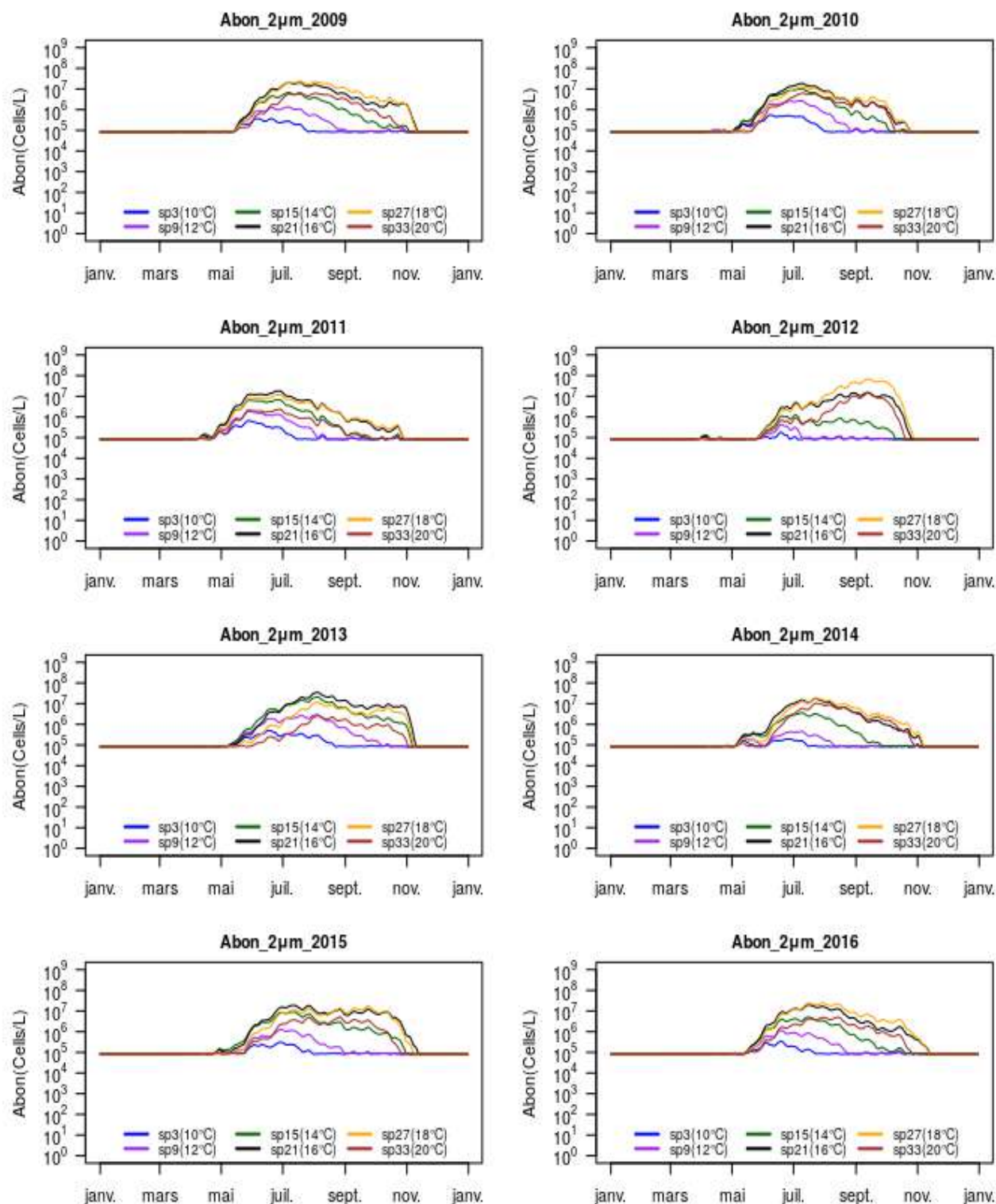


Figure A4.8: Species of 2µm

Species of 5µm: These species are under the category of nanophytoplankton. They are usually less abundant than the picophytoplankton. Their maximum abundance in our model for certain species is about $10^6 \text{ cells.L}^{-1}$. Sp4 with T_{opt} of 10°C has the lowest abundance whereas sp22, sp28 and sp34 with T_{opt} over 15°C competed very closely with each other. These species also showed the longest duration from the month of June to the end of August in the year 2012 when compared to other years. We equally observed slight November peaks in all years except 2012 whose summer peak continued till November.

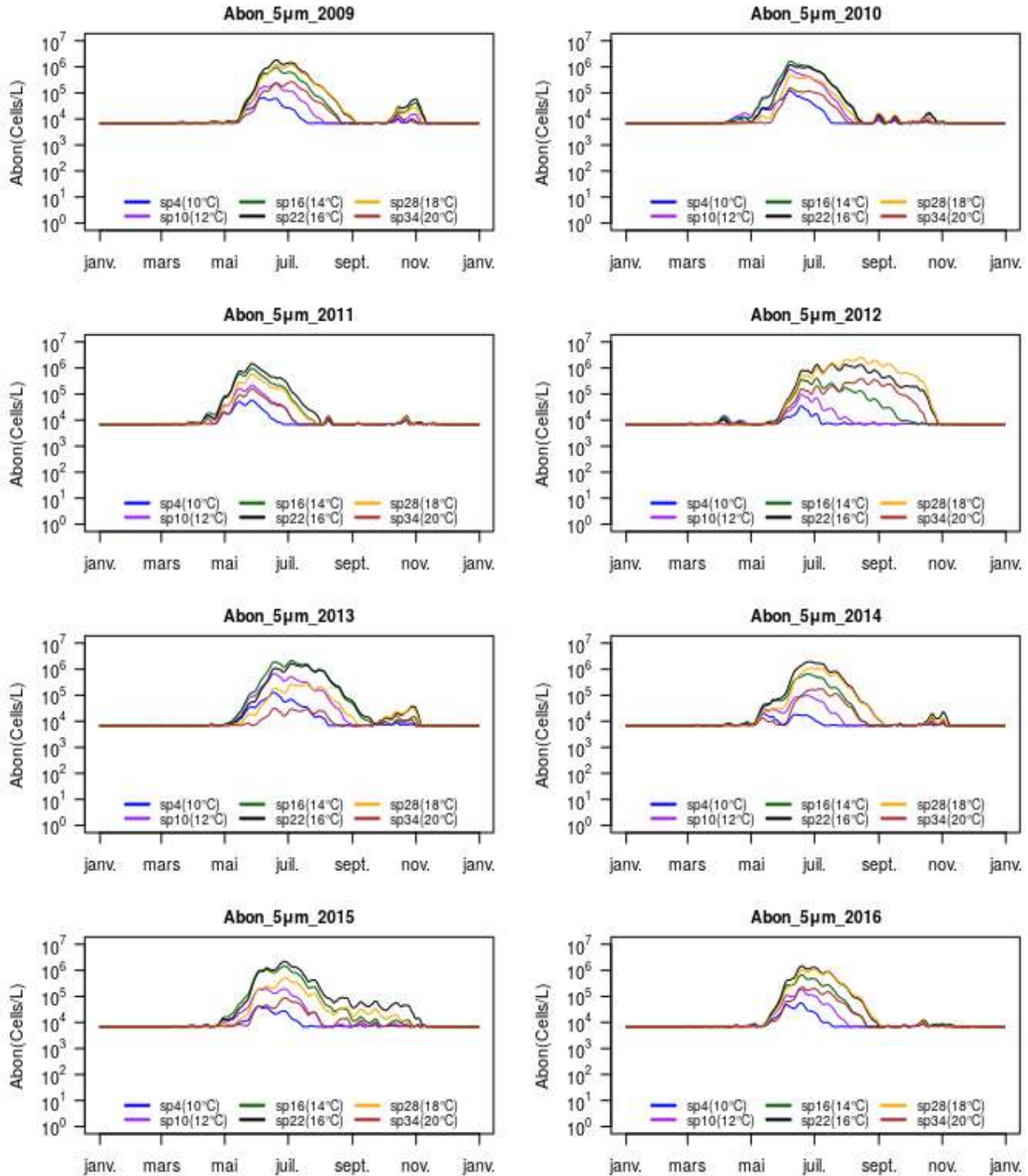


Figure A4.9: Species of 5µm

Species of 18µm: Still under the category of nanophytoplankton, this class includes *Alexandrium minutum*. The maximum concentration recorded for species of 18µm is less than $10^5 \text{ cells.L}^{-1}$ which is much lower than that of 5µm. *A. minutum* appeared to be dominant in all eight cases even outcompeting sp29 with the same T_{opt} of 18°C. This is obvious in the year 2012 where it showed a higher abundance and longer bloom duration. The reason *A. minutum* dominated the same species of same size; same T_{opt} and I_{opt} is probably linked to differences in their rates of nutrient absorption. We also observed a significant abundance in the secondary peaks for most of the species especially in years 2009 and 2014 which had abundances close to those of the summer peak.

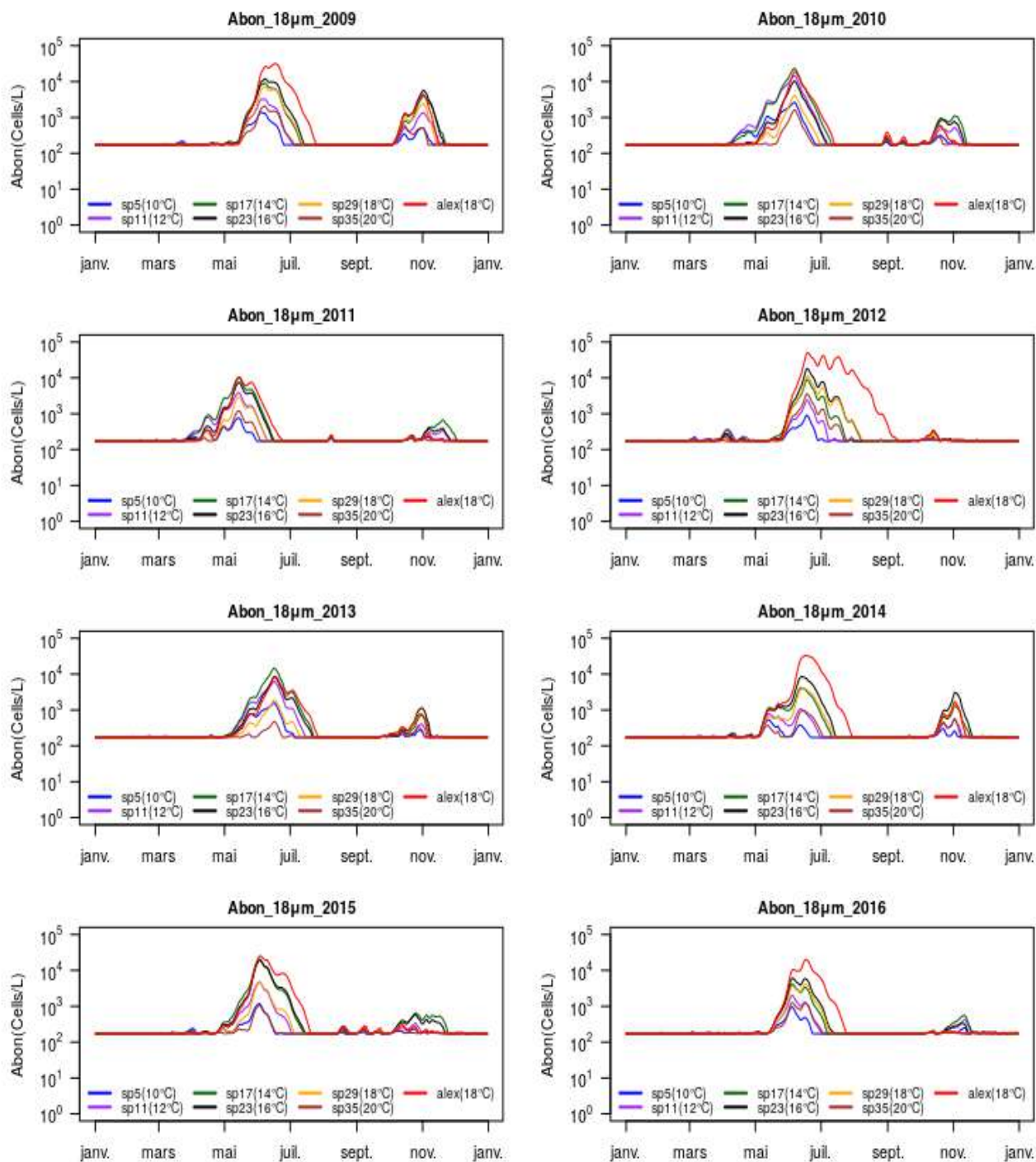
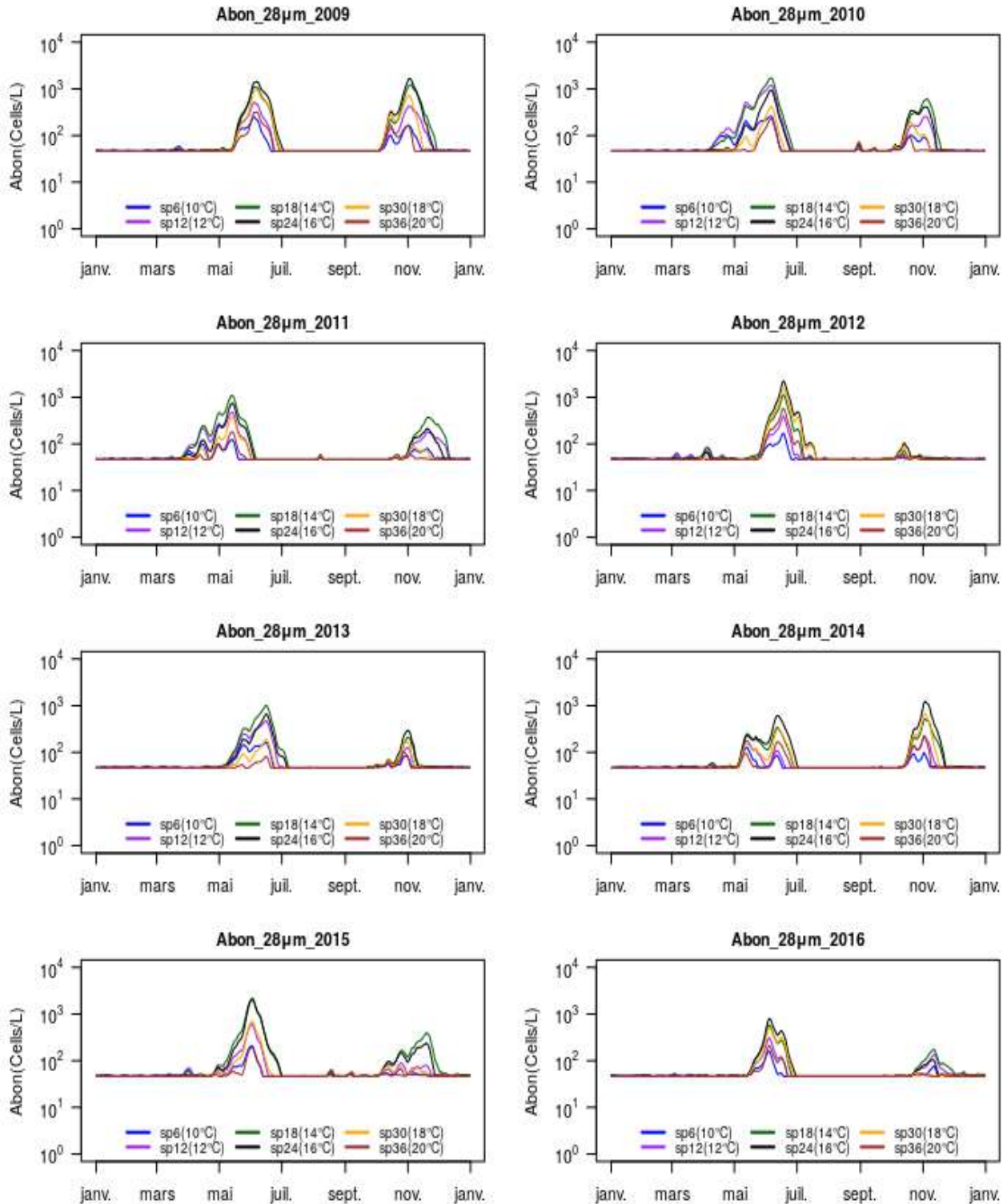


Figure A4.10: Species of 18µm

Species of 28 μ m: These species fall under the category of microphytoplankton and they are usually less abundant than the other categories of phytoplankton. In the figure below, there is similar growth in the months of June and November. The maximum autumn abundance for some species in 2009 and 2014 is equal or greater than that of summer. This result indicates that (in 2009 and 2014), large cells were more favored in November than in June. Additionally, we see the dominance of sp18 whose T_{opt} is less than 15°C. And species of 20°C was outnumbered in the autumn.

Figure A4.11: Species of 28 μ m

Species of 64 μ m: These are the largest species in our simulation and they equally fall within the category of microphytoplankton. In the results of our simulations, we observed that maximum abundance decreases with an increasing cell size. The abundance of these species is less than 100cells.L⁻¹ in all cases. There was no obvious growth in the summer but in the autumn. Species with T_{opt} less than 15°C (i.e. Sp19) once again dominated in the autumn in most of the years. It was followed very closely by sp25 with a T_{opt} of 16°C. Other species had optimal temperatures that were either too low or too high to support growth.

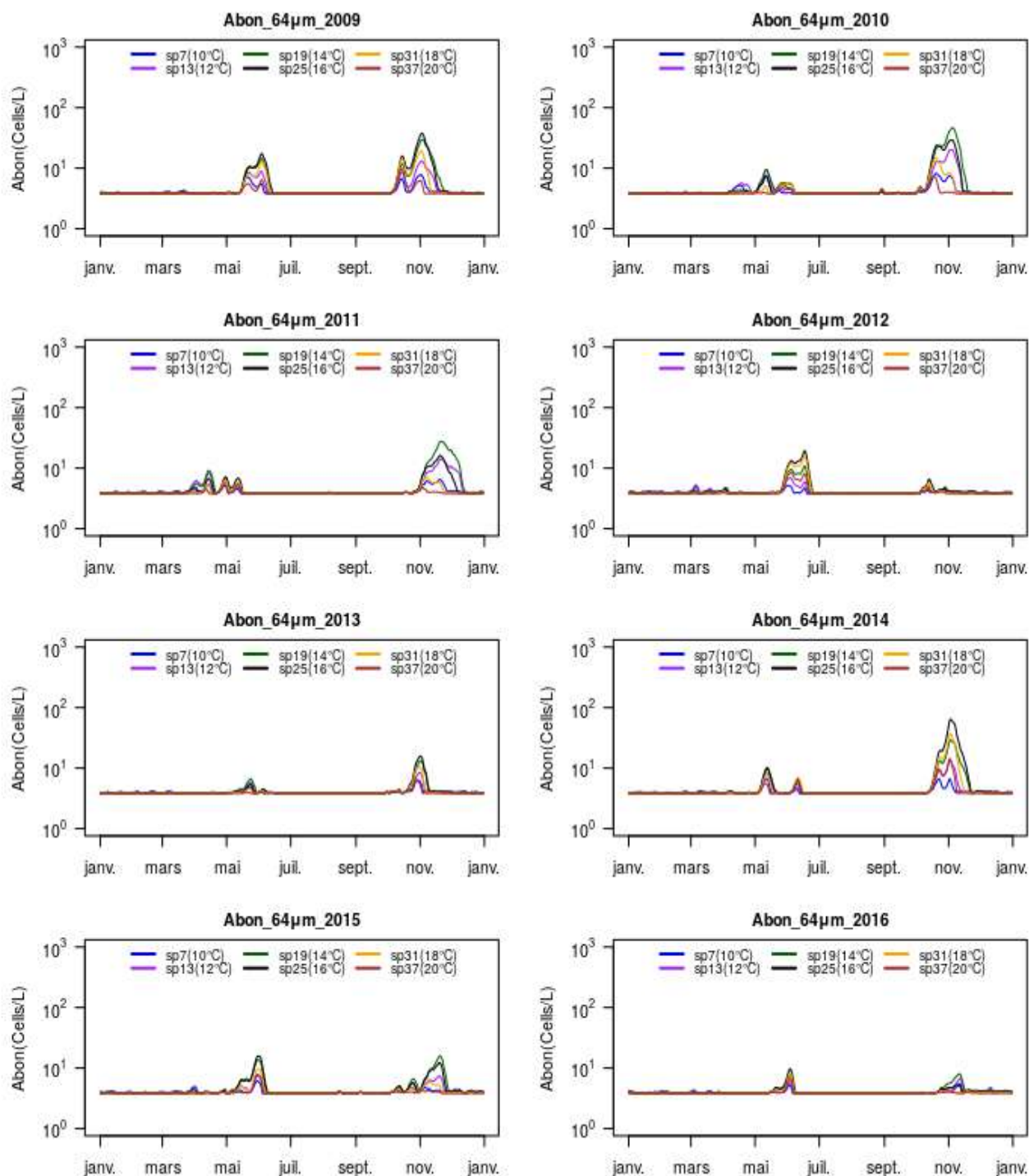


Figure A4.12: Species of 64 μ m

Alexandrium minutum and species 29

A. minutum was exclusively compared with sp29 because both species have the same size, μ_{\max} , T_{opt} and I_{opt} . Ideally, one would expect them to have the same abundance since they have similar parameters but the results in the figure below prove otherwise. The closest abundance between both species is in autumn. In summer, *A. minutum* outperformed sp29 especially in 2012. Why are there differences in the abundance of these species? In responding to this question, we need to understand that irrespective of the fact that they have similar characteristics; every species is unique in its own way and therefore; might respond differently to environmental conditions. Secondly, we found that *A. minutum* is a bit more advantaged than sp29 in terms of nutrient absorption (V_{\max}) – another contributing factor to its dominance.

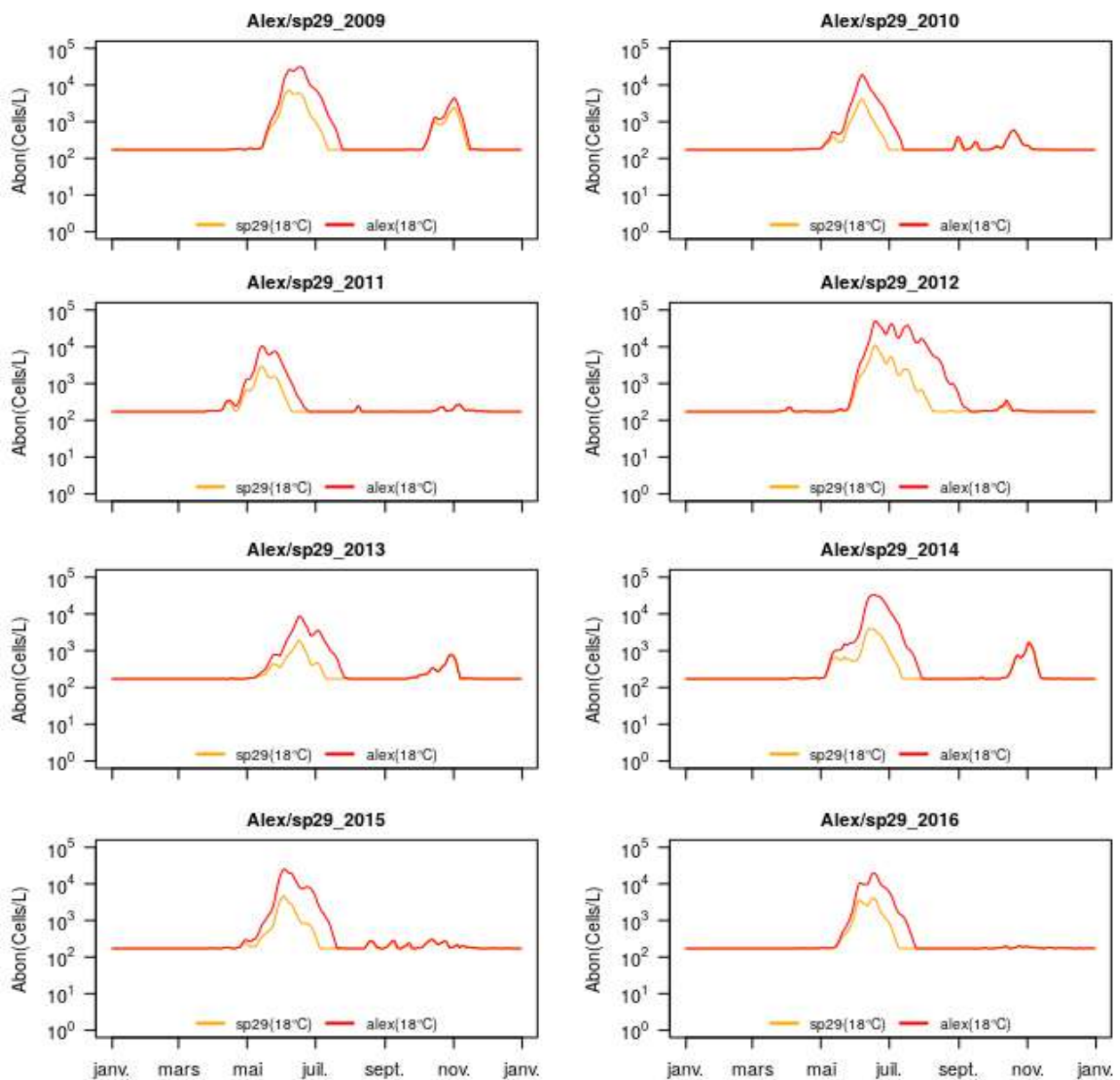


Figure A4.13: *A. minutum* and sp29

Temperature and light limitations on *A. minutum* and sp29: While trying to find out why *A. minutum* dominated sp29, we looked at their responses to light and temperature. Both species have the same T_{opt} (18°C) and μ_{max} with regards to temperature limitation and that is why they showed the exact same response in the figure below. Furthermore, there is no difference in light limitation either because they both have the same I_{opt} (24W.m⁻²) too.

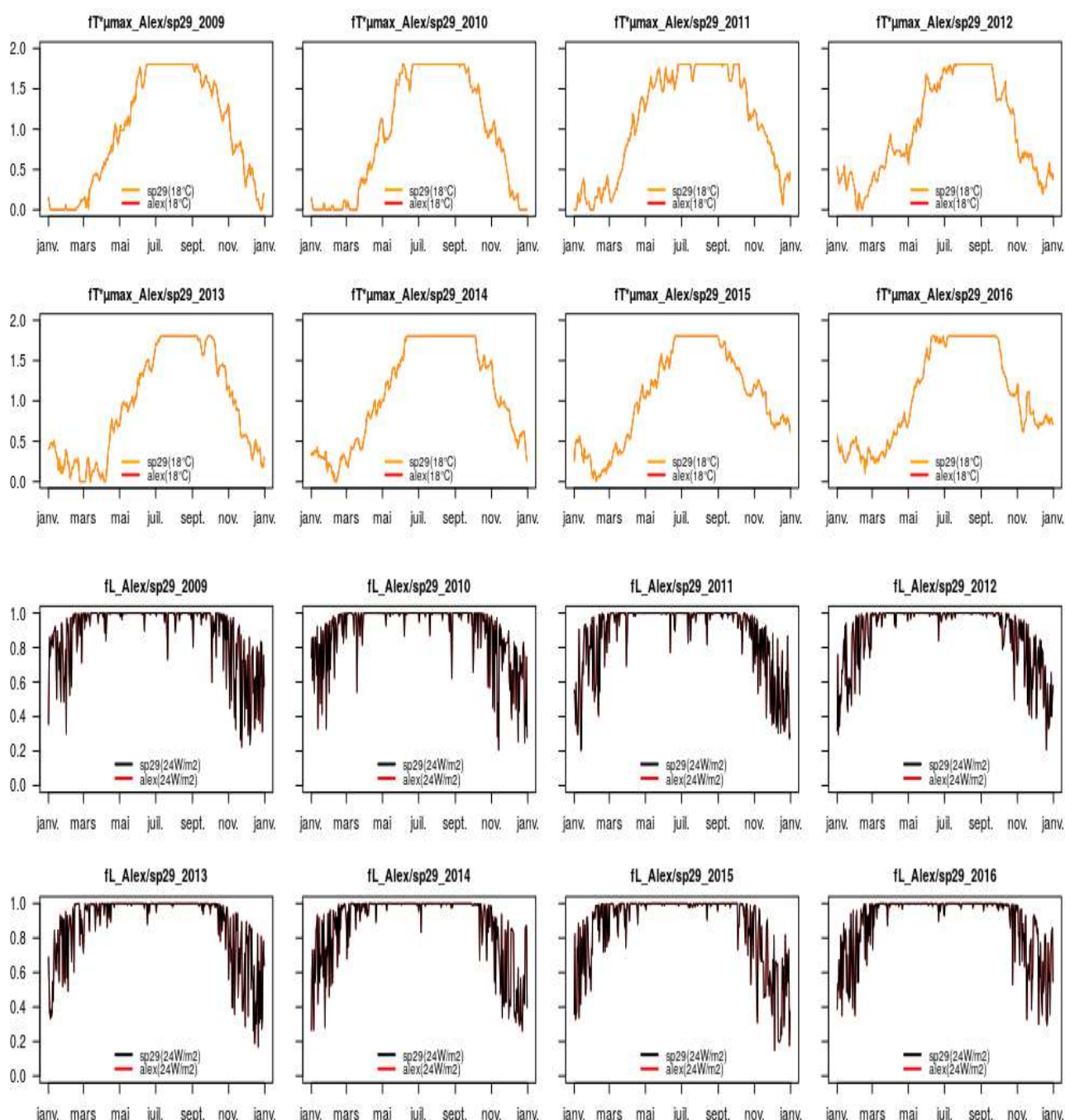


Figure A4.14: Temperature and light limitations on *A. minutum* and species 29

N and P limitations on *A. minutum* and sp29: We went further to analyze their nutrient limitations and found that *A. minutum* is slightly less limited in nitrogen than sp29 especially during the summer. This can boost nitrogen uptake and give *A. minutum* an advantage over sp29. With phosphorus however, *A. minutum* is more limited than sp29 especially in the months from November to May. This advantage of sp29 over *A. minutum* is not in any way reflected in the species abundance. Between June and October in almost all eight simulated years, both species showed the same limitation in phosphorus but *A. minutum* however remained dominant.

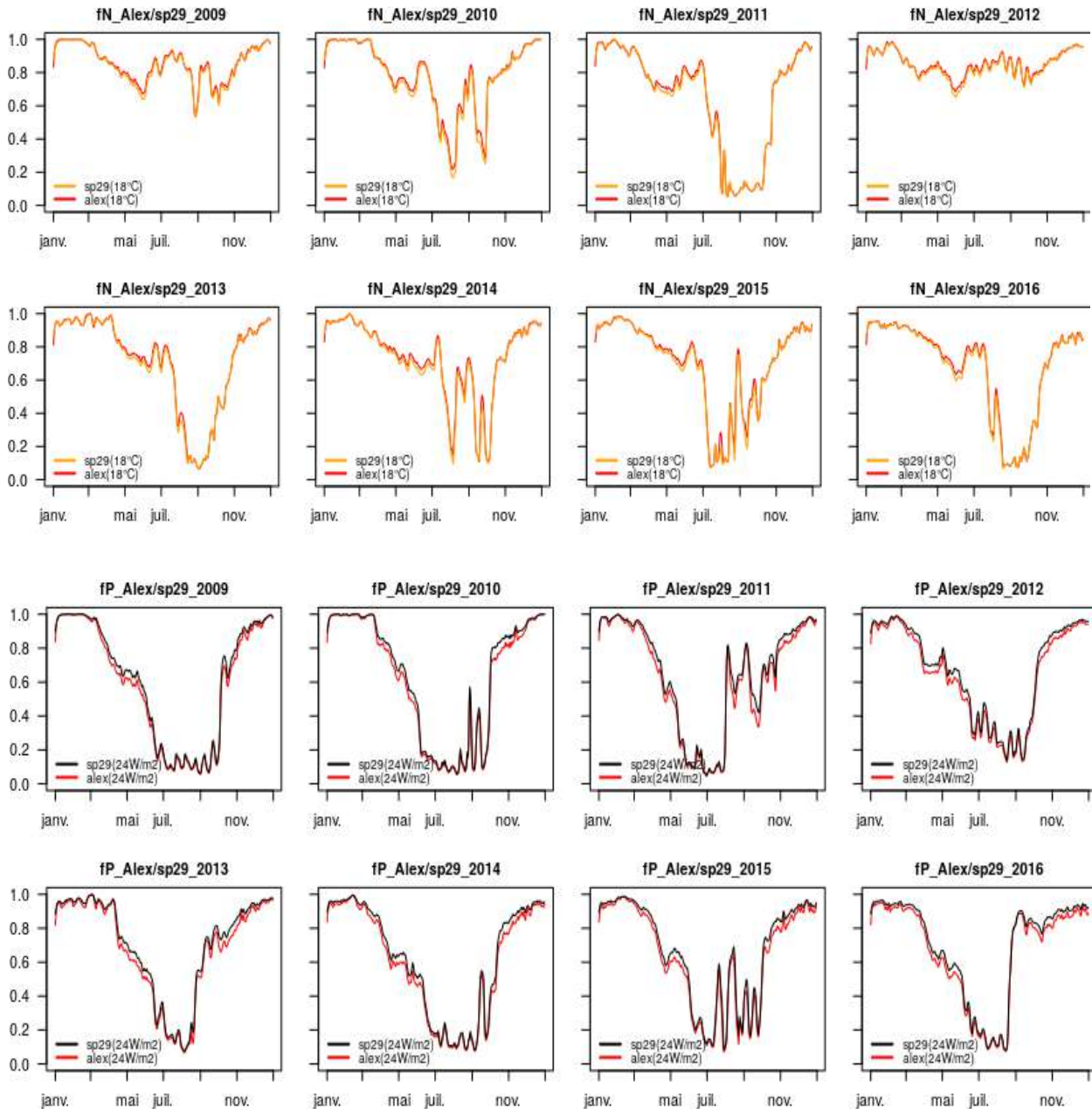


Figure A4.15: N and P limitations on *A. minutum* and species 29

Nutrient limitations by cell size

N limitation on species of 1 μ m: Ideally, nitrogen limits the growth of small cells than large cells. Here however, we looked at the limitation on the same cell size and we find that the dominant species (18°C and 20°C) were less limited by nitrogen from January to June. The least dominant species (10°C) had the highest limitation within the same period. On the other hand, all the species had almost the same limitation from July to October. This might be due to uptake rates and temperature effects on growth.

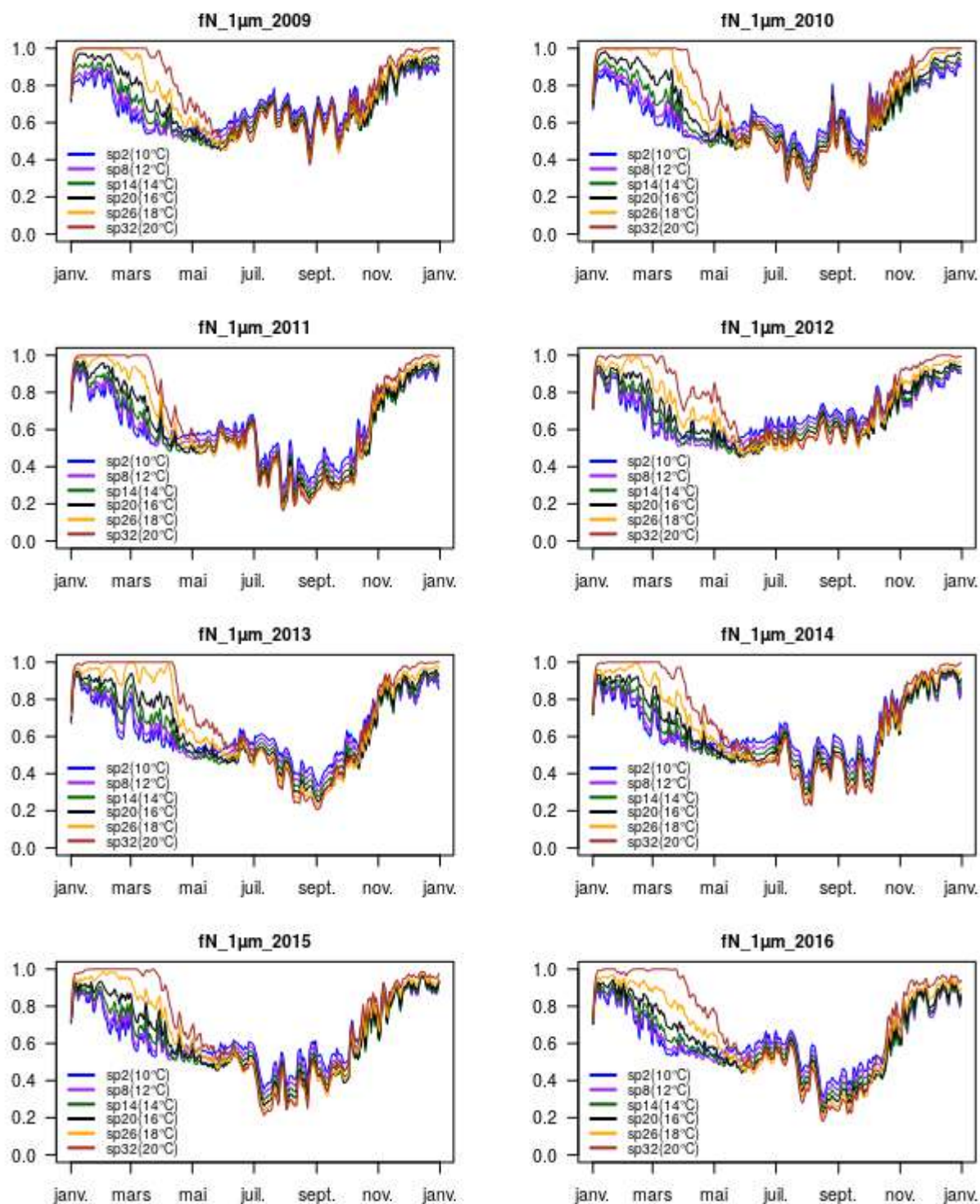


Figure A4.16: Nitrogen limitation on species of 1 μ m

P limitation on species of 1 μ m: With phosphorus limitation, we observed a similar trend seen in nitrogen limitation where sp26 and sp32 are less limited before the month of June and sp2 being more limited within the same period. Between June and August however, we see a reverse in that trend in all years. Although the growth of all species is limited by phosphorus in the summer, sp2 the least dominant appeared to be less limited than sp26 and sp32 – the most dominant.

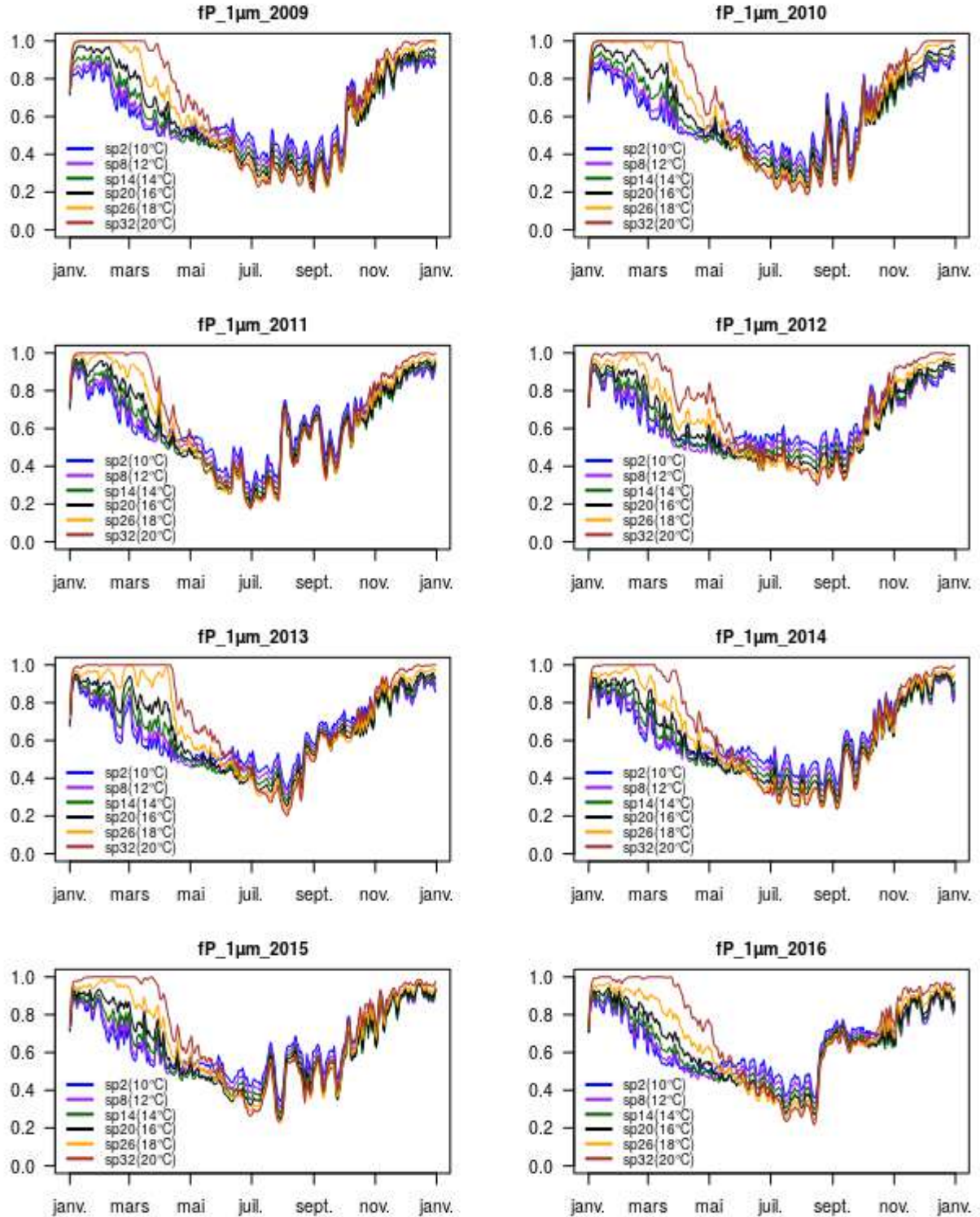


Figure A4.17: Phosphorus limitation on species of 1 μ m

N limitation on species of 2 μ m: Once again, the limitation on nitrogen on species of 2 μ m is similar to the limitation on those of 1 μ m. Species with T_{opt} greater than 15°C are less limited just before the month of June. Between June and October, all species showed the same limitation trend in each year except 2012 which is slightly different. From November to end of December, we also observed a trend similar to that seen at the beginning of each year.

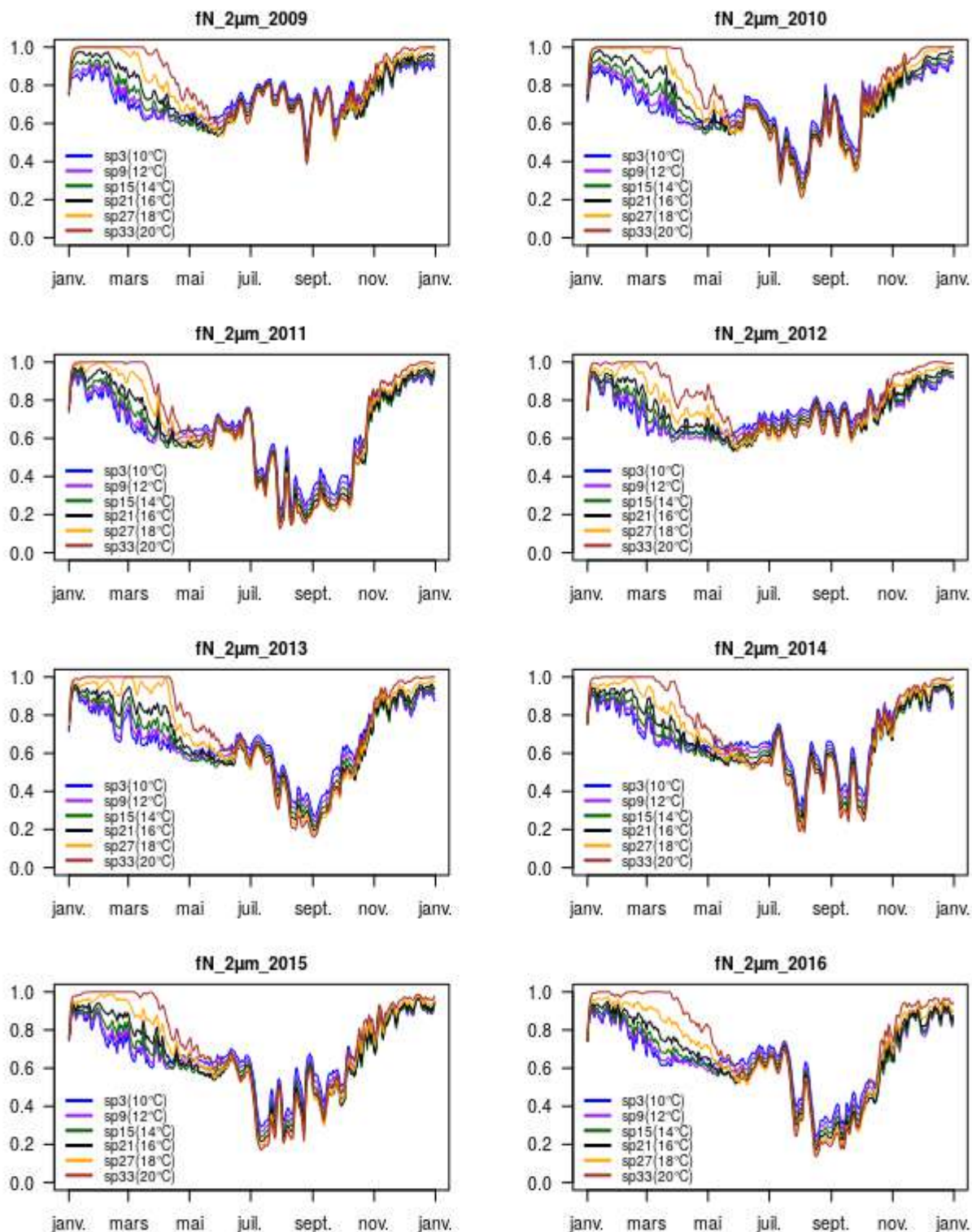


Figure A4.18: Nitrogen limitation on species of 2 μ m

P limitation on species of 2 μ m: There is not much difference on phosphorus limitation on 2 μ m when compared to species of 1 μ m. The dominating species (18°C and 20°C) were less limited before the month of May when growth was first observed among the species. The least dominant species (10°C and 12°C) showed a greater limitation. In the summer season however, all species followed the same trend.

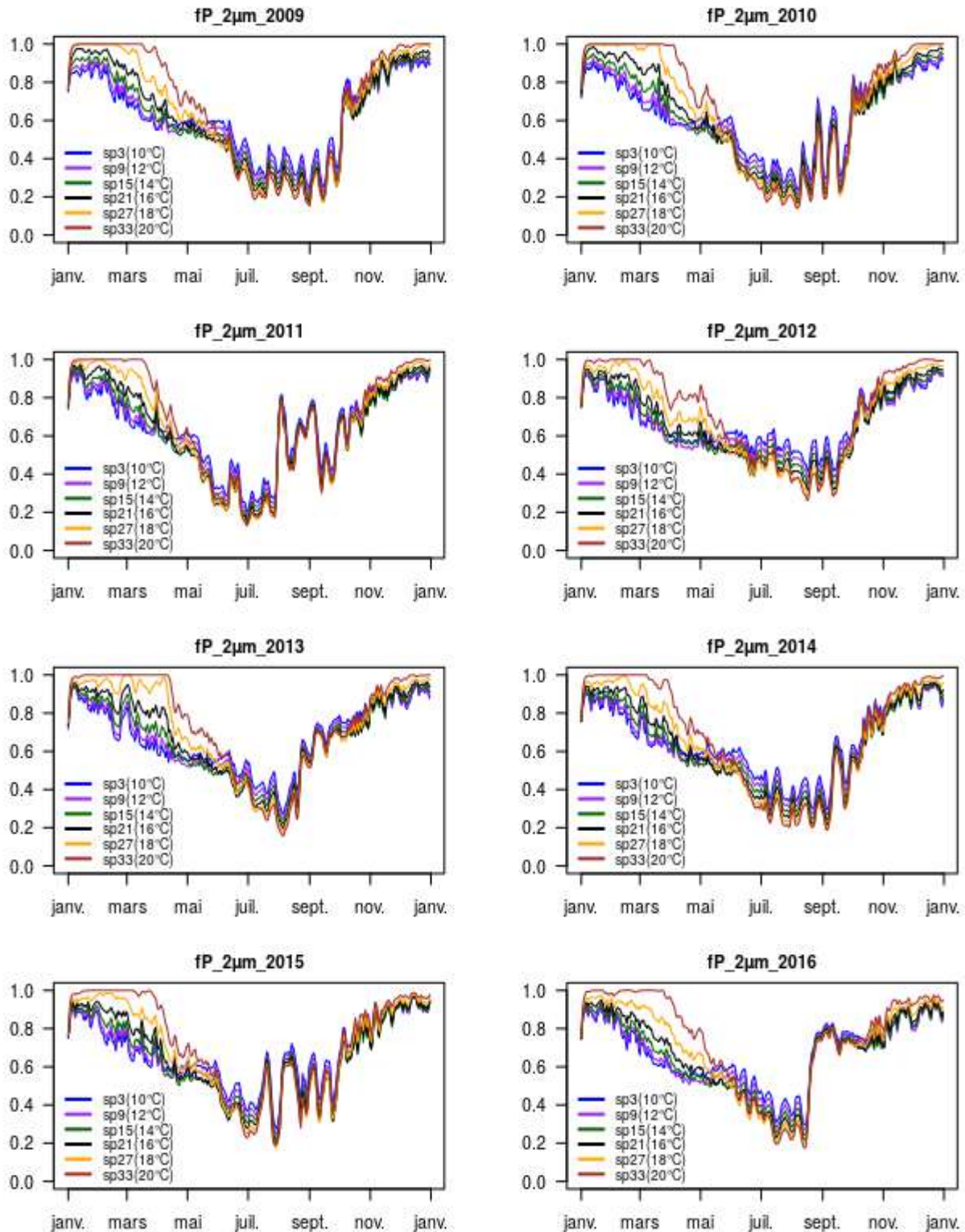


Figure A4.19: Phosphorus limitation on species of 2 μ m

N limitation on species of 5 μ m: We observed that limitation by nutrients is very confined between June and September. This is a competitive period and thus, species of the same size tend to have almost the same limitation. It is shown in the figure below for all the years except 2012 which displayed the lowest limitation during the summer. The longest N limitation during the summer period was observed in 2011 – the year with the lowest species abundance.

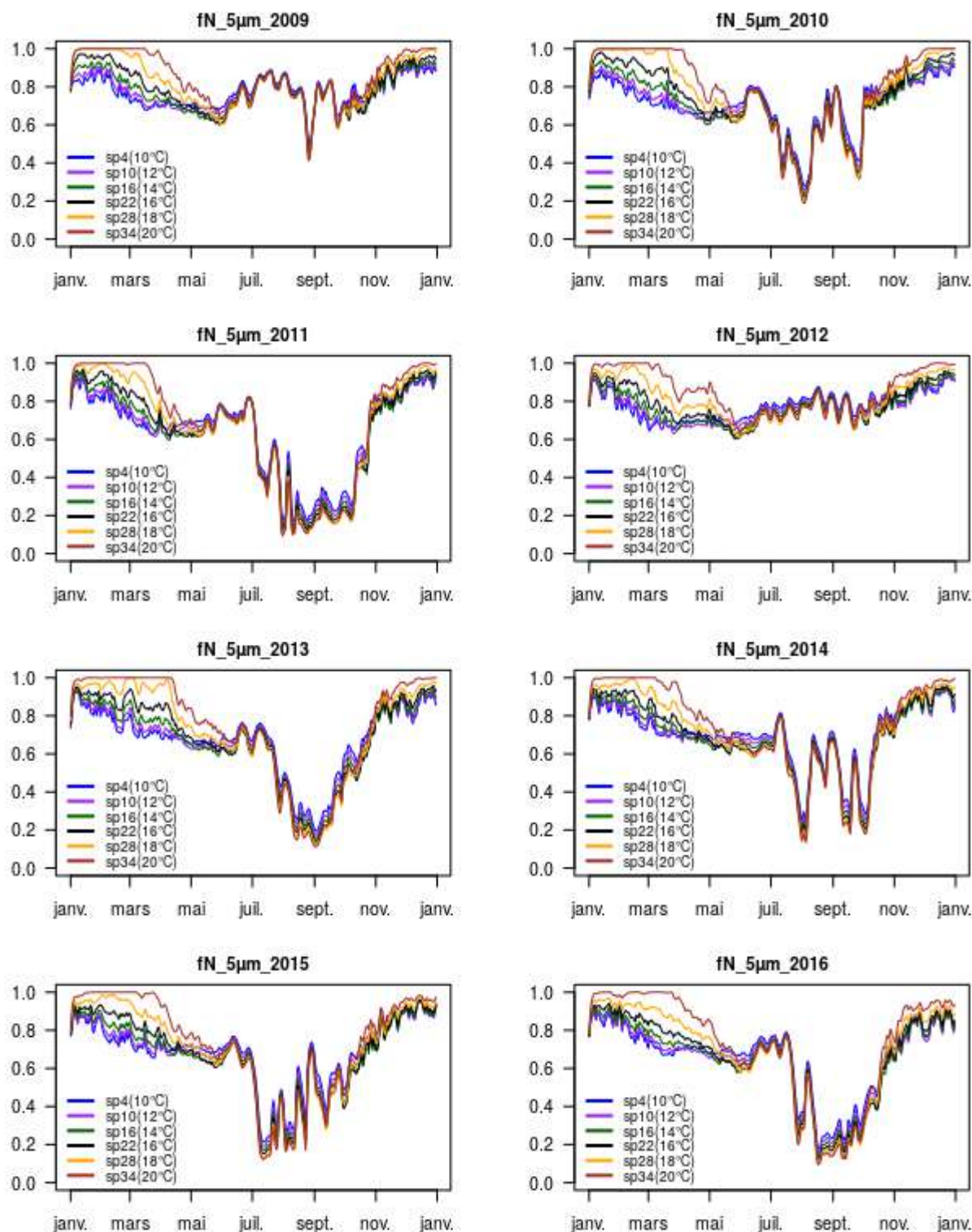


Figure A4.20: Nitrogen limitation on species of 5 μ m

P limitation on species of 5 μ m: Similarly, year 2011 also showed the highest limitation in phosphorus whereas year 2012 which had the longest bloom duration showed the lowest limitation when compared to any other year. We equally see a low level of phosphorus limitation in the month of November when the secondary peaks emerged.

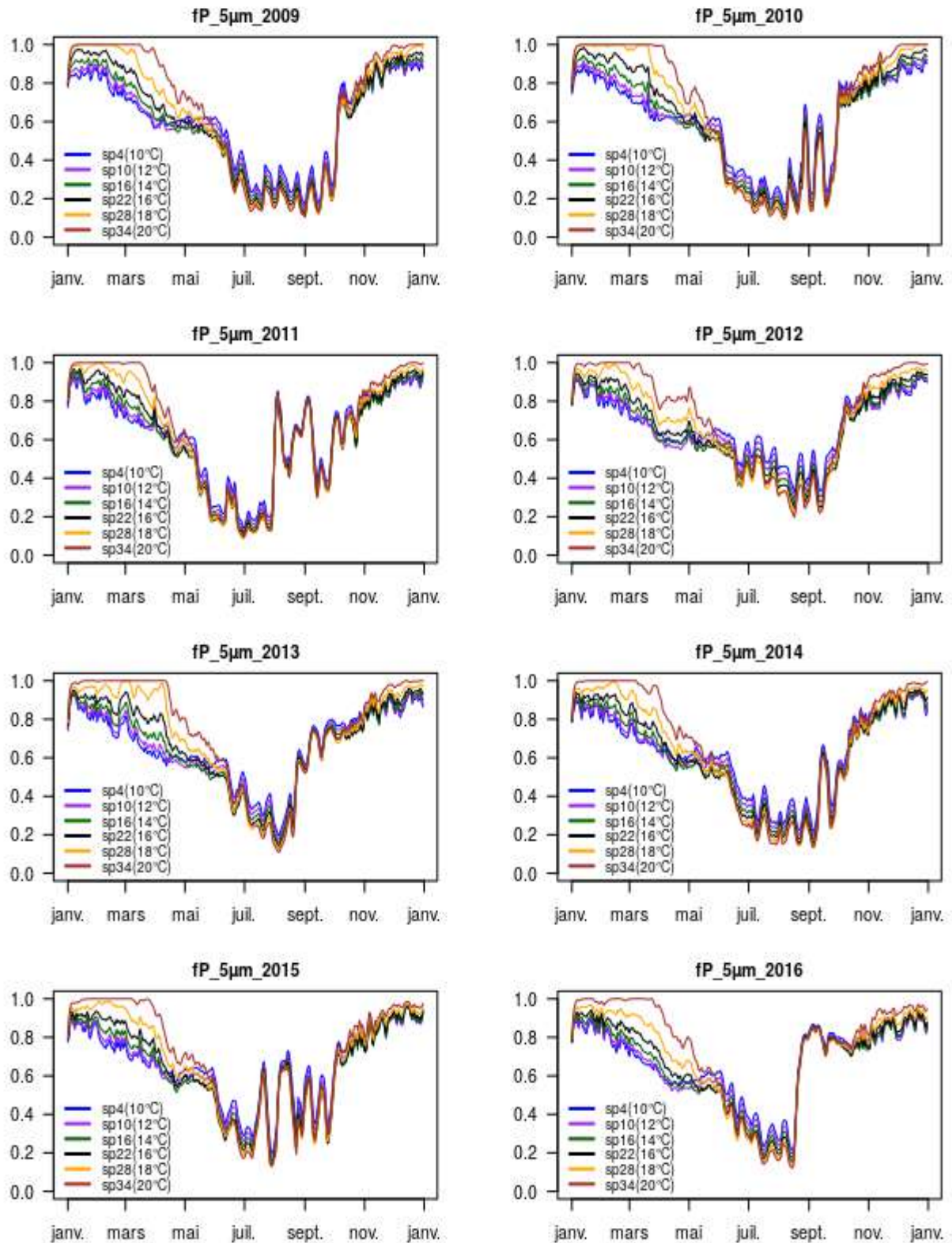


Figure A4.21: Phosphorus limitation on species of 5 μ m

N limitation on species of 18 μ m: Being the dominant species, one would expect *A. minutum* to have less nutrient limitations. On the contrary it is limited just like every other species. We remarkably observed that *A. minutum* has the same limitation trend with sp29 of same T_{opt} . These species together with sp23 and sp35 showed less nitrogen limitation in the first quarter of each year. The years which have significant autumn peaks also showed a decreased limitation in nitrogen just before the appearance of the peaks.

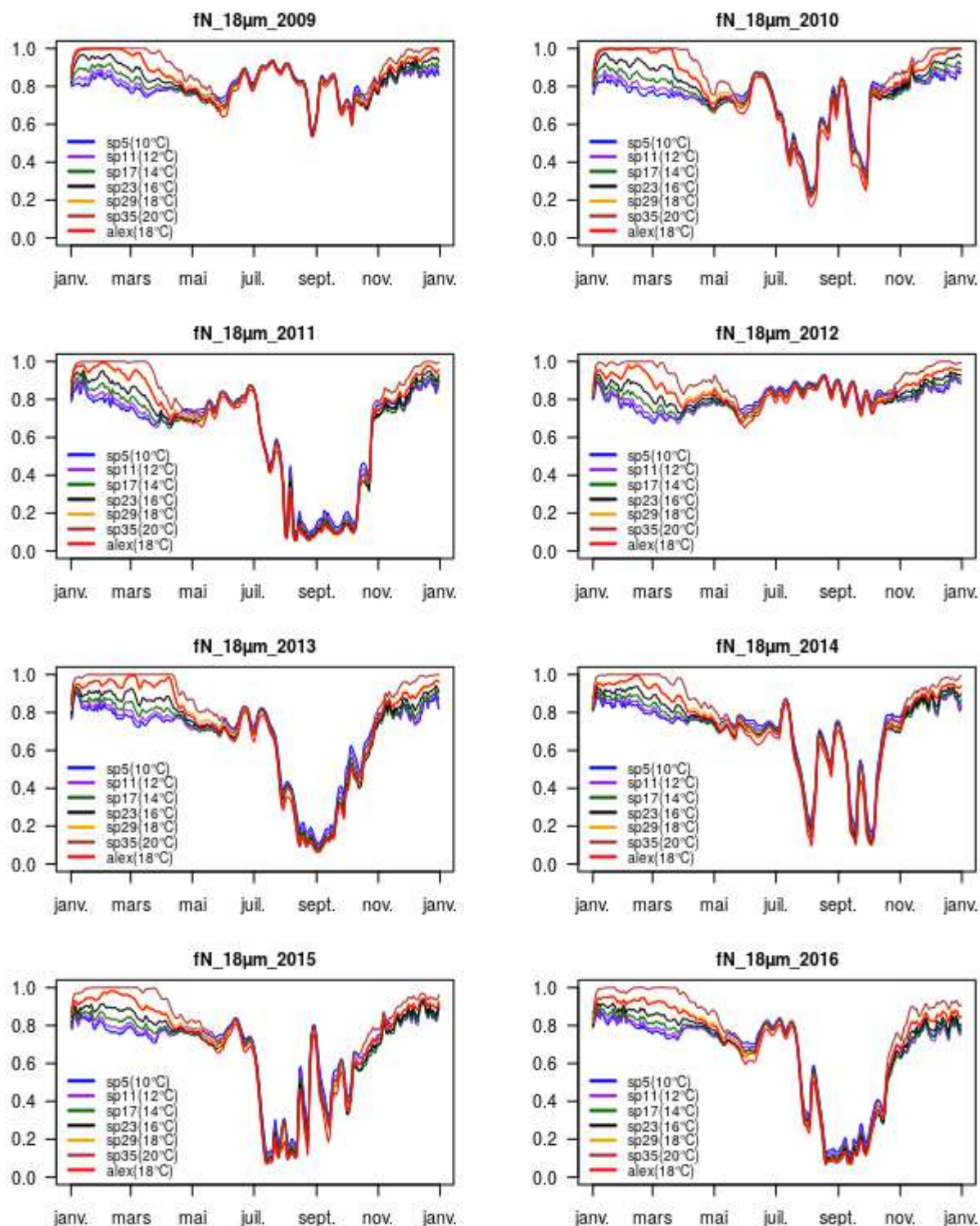


Figure A4.22: Nitrogen limitation on species of 18 μ m

P limitation on species of 18 μ m: Limitation by phosphorus is always at its highest levels between June and August. Unlike in nitrogen limitation, *A. minutum* appeared to be less limited by phosphorus when compared to sp29 of the same T_{opt} . We observed that year 2012 with the longest duration of *A. minutum* has the lowest limitation. Consequently, years 2009; 2010 and 2014 which have significant autumn peaks appeared to show less limitation during summer period.

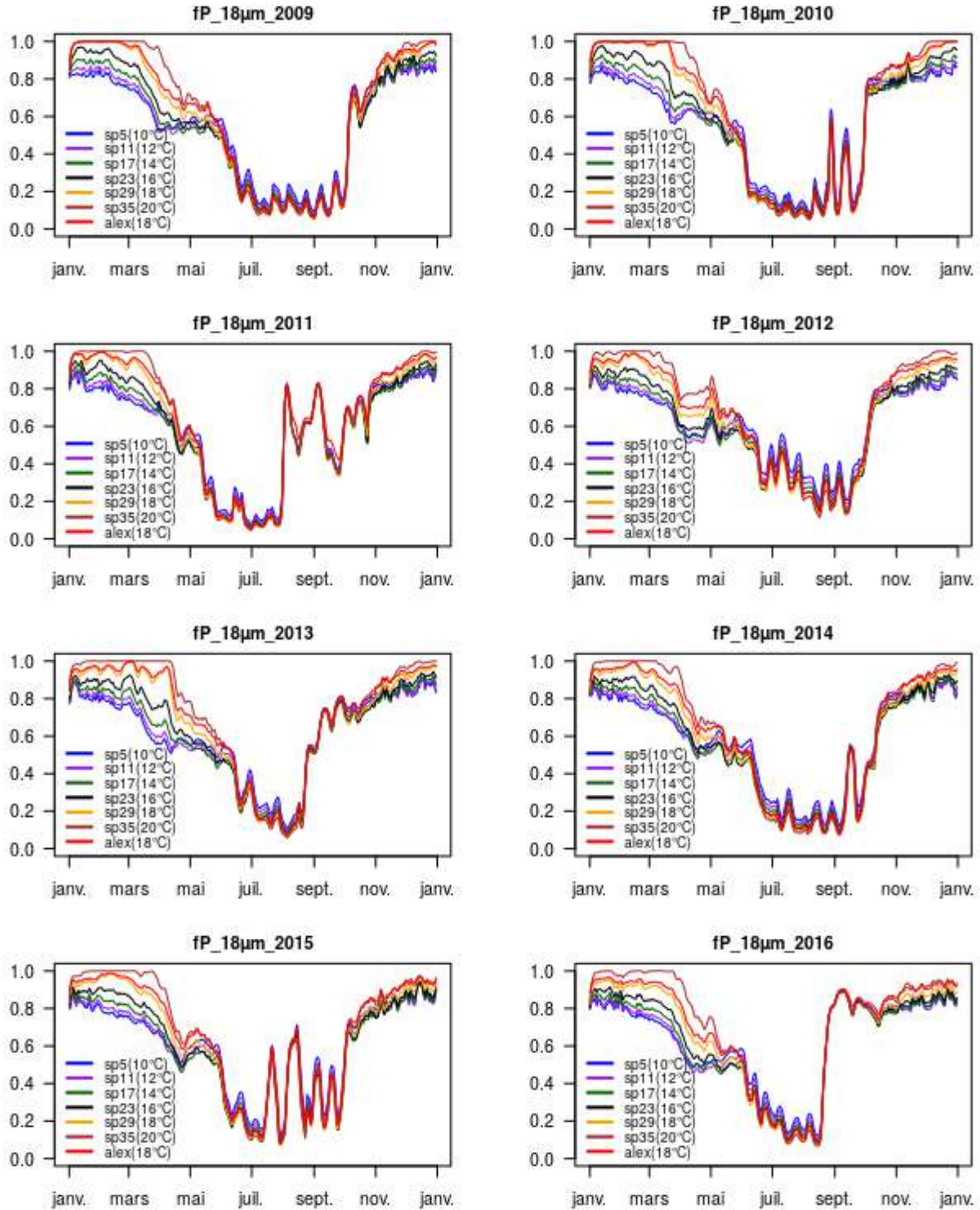


Figure A4.23: Phosphorus limitation on species of 18 μ m

N limitation on species of 28µm: The microphytoplankton are usually less limited by nitrogen than other categories. Although they might experience growth first, they are outnumbered afterwards by the small cells. The figure below shows that species of 28µm were not extremely limited by nitrogen in the summer of 2009 and 2012. Year 2012 recorded low abundance for both summer and autumn peaks because it had the maximum abundance of pico and nanophytoplankton. Maximum limitation is observed in the month of September in 2013 and 2016 – the years with the lowest abundance of autumn peak.

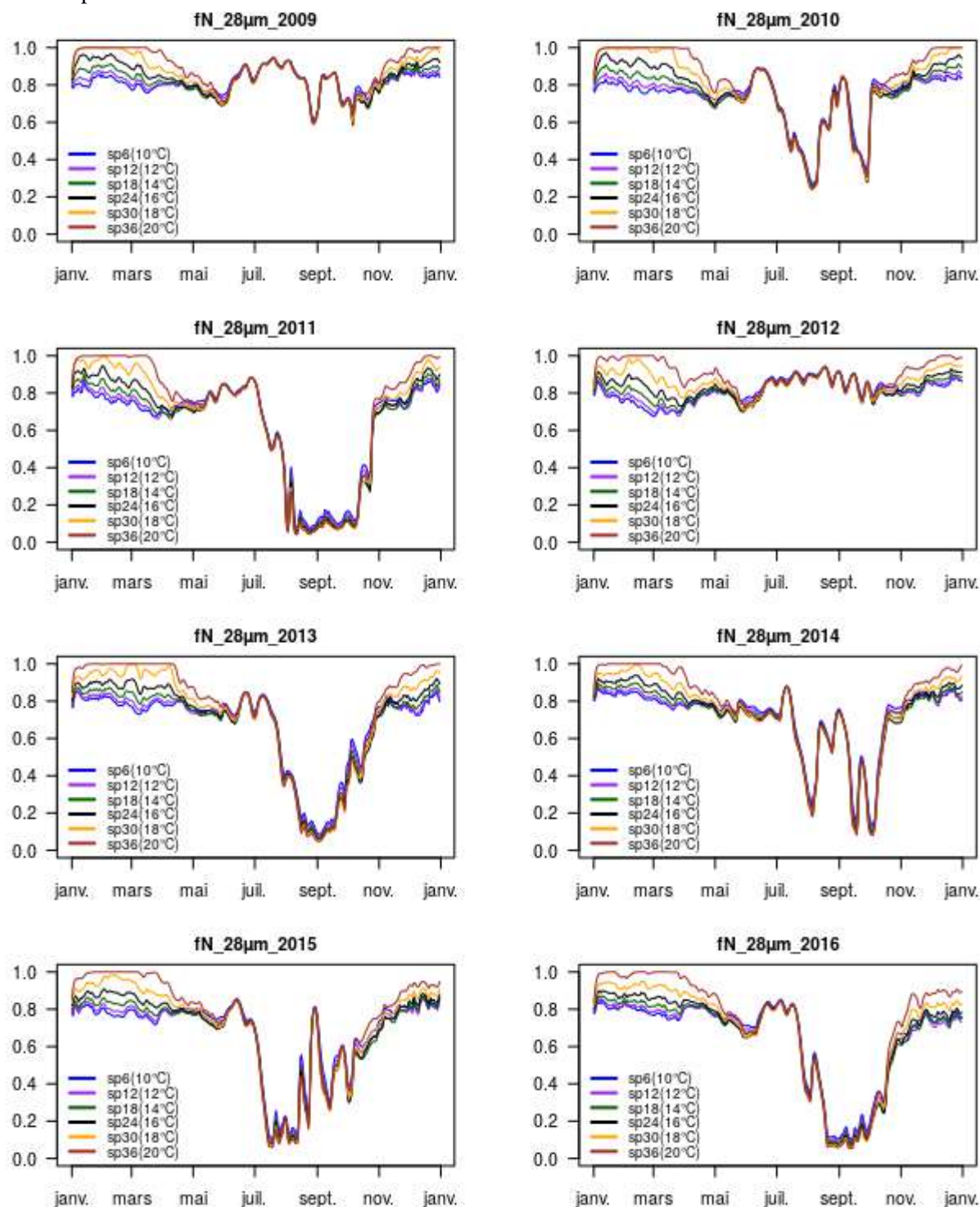


Figure A4.24: Nitrogen limitation on species of 28µm

P limitation on species of 28µm: A low concentration in this nutrient can play a role in limiting the growth of phytoplankton particularly the microphytoplankton in general. Species of 28µm experienced very little growth between July and September and this period is marked by extremely high limitations in phosphorus. Pre-summer and autumn peaks however emerged when phosphorus was less limiting.

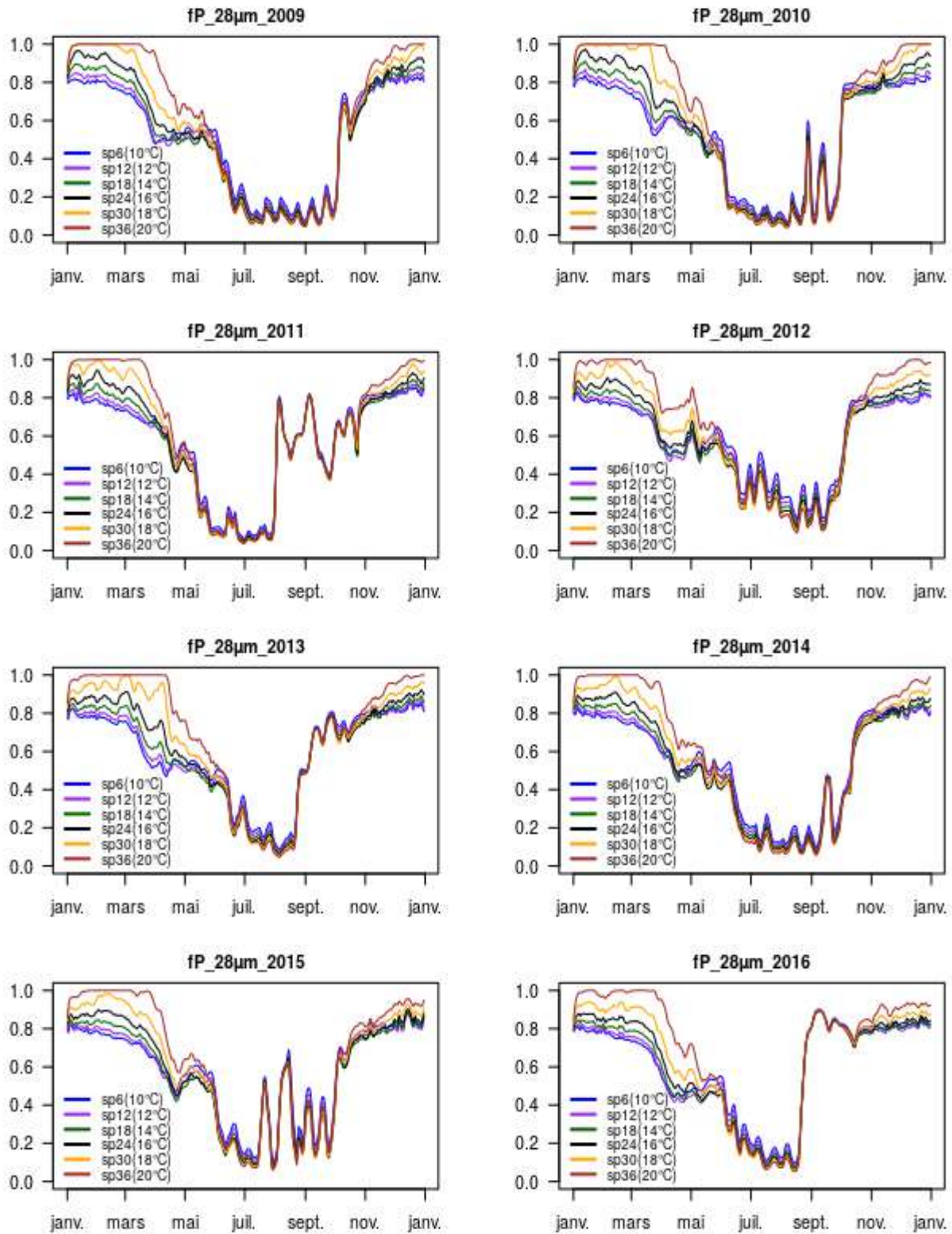


Figure A4.25: Phosphorus limitation on species of 28µm

N limitation on species of 64µm: Here, we observe a similar nitrogen limitation with species of 28µm. This implies that species of close size range could be subjected to similar limitation in nutrients. High nitrogen limitation is also noted in 2013 thereby reflecting one of the lowest species abundance in the summer. The lowest summer abundance is in 2011 which has the longest nitrogen limitation. Lastly, we see a very low autumn abundance in 2012 which evidently witnessed the maximum abundance in pico and nanophytoplankton.

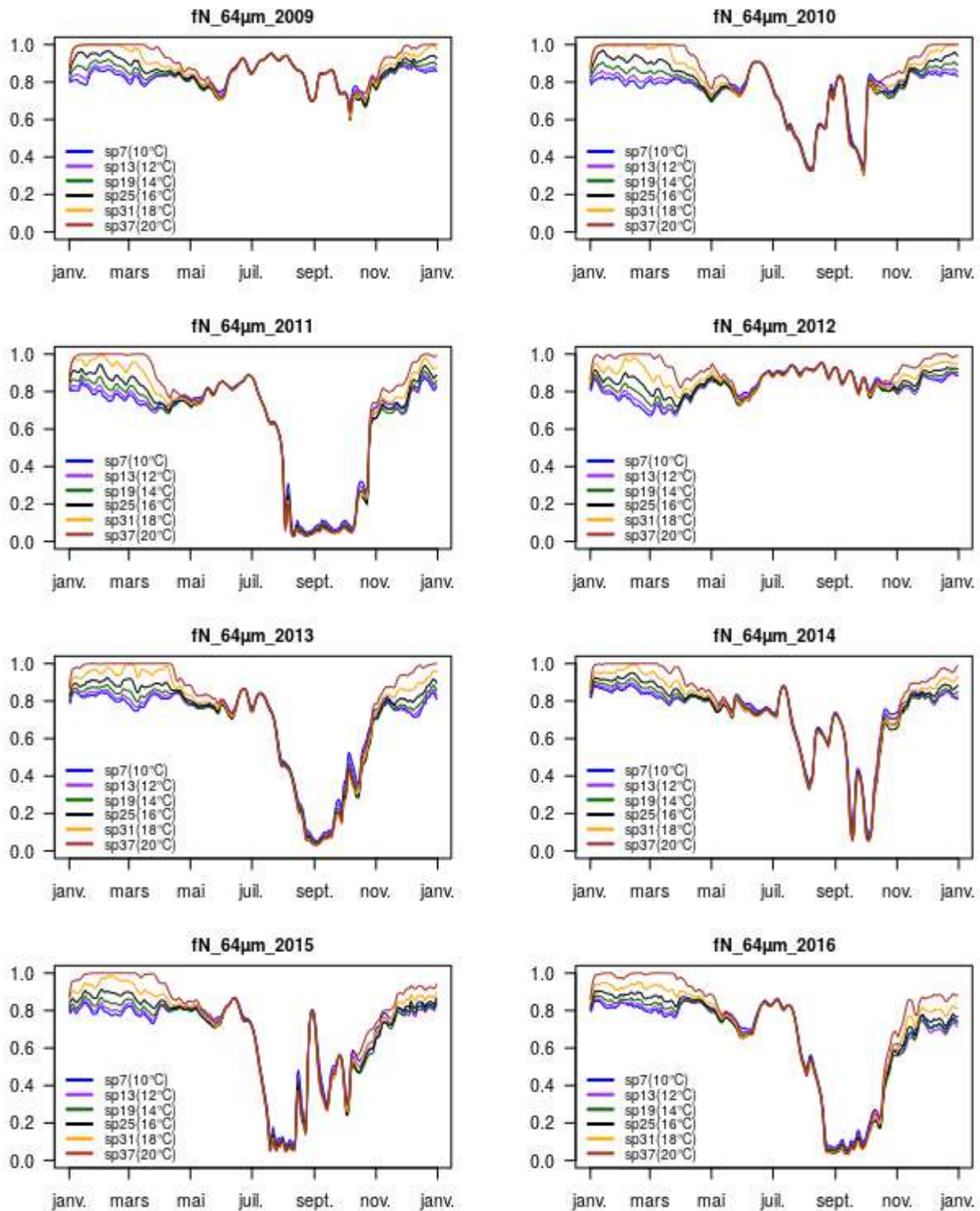


Figure A4.26: Nitrogen limitation on species of 64µm

P limitation on species of 64µm: A reduction in phosphorus no matter how small can impact heavily on the abundance of species. In as much as microphytoplankton might have similar nutrient limitations in the summer, this can increase slightly with an increase in cell size. In other words, species of 64µm could be more limited in phosphorus than species of 28µm. For example, we saw very low abundances in species of 28µm (about 1 000cells.L⁻¹ in 2012) and those of 64µm are even much lower (less than 1 000cells.L⁻¹ in 2012).

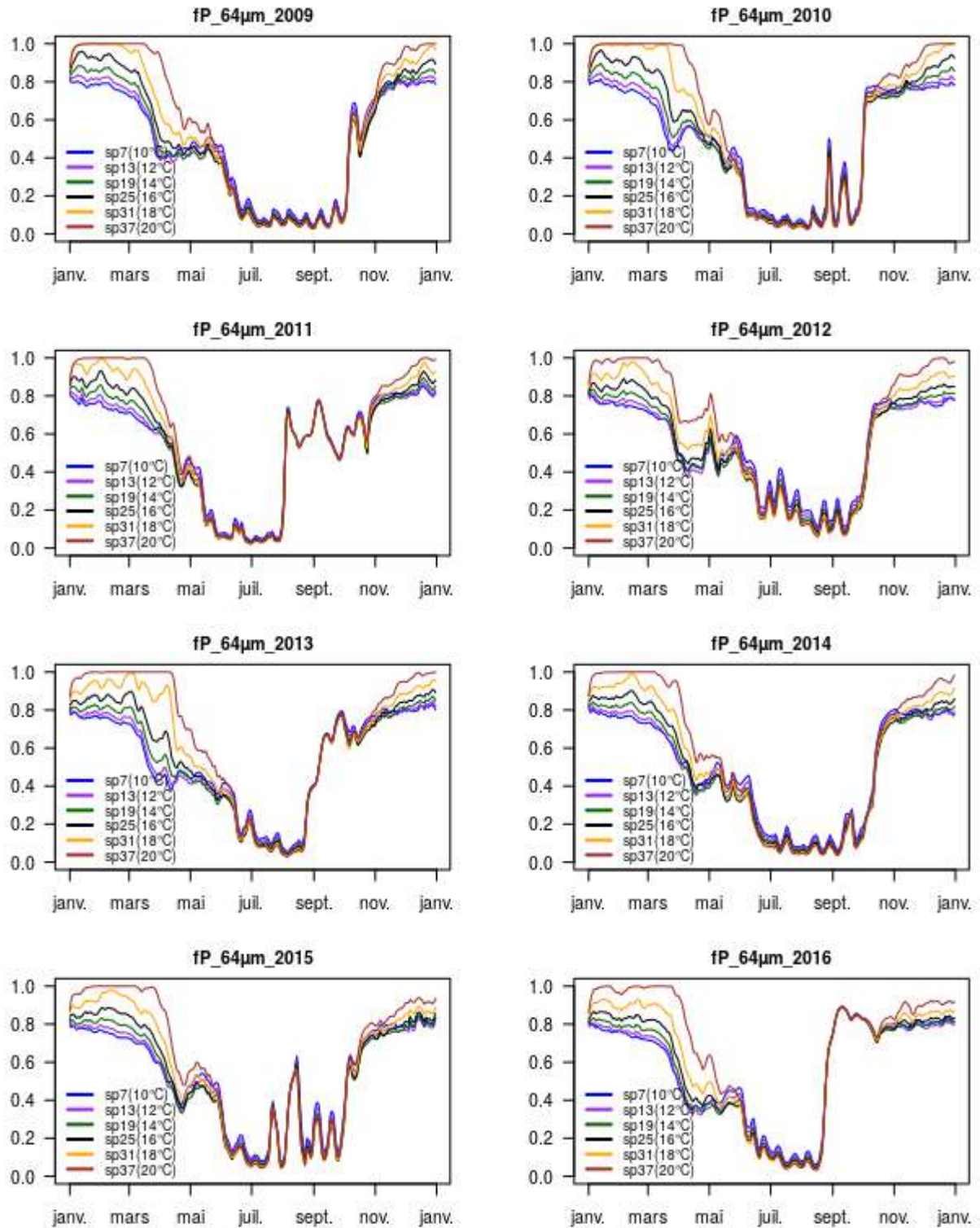


Figure A4.27: Phosphorus limitation on species of 64µm

General limitations (Light and temperature)

The term ‘general limitation’ is applicable to all species having the same parameters. For example, species with the same T_{opt} or I_{opt} have the same limitation in temperature and light respectively.

By optimal temperature, T_{opt} : There is actually no limitation by T_{opt} . The idea here is to show the level of limitation with respect to T_{opt} . In the figure below which takes maximum growth (μ_{max}) into account, we observed that in cold periods (November to April), species with high T_{opt} are highly limited by temperature whereas those with less T_{opt} are less limited. In hot periods (June to August) however, this is the opposite. Though temperature changes regularly, we found the same trend in all our simulations.

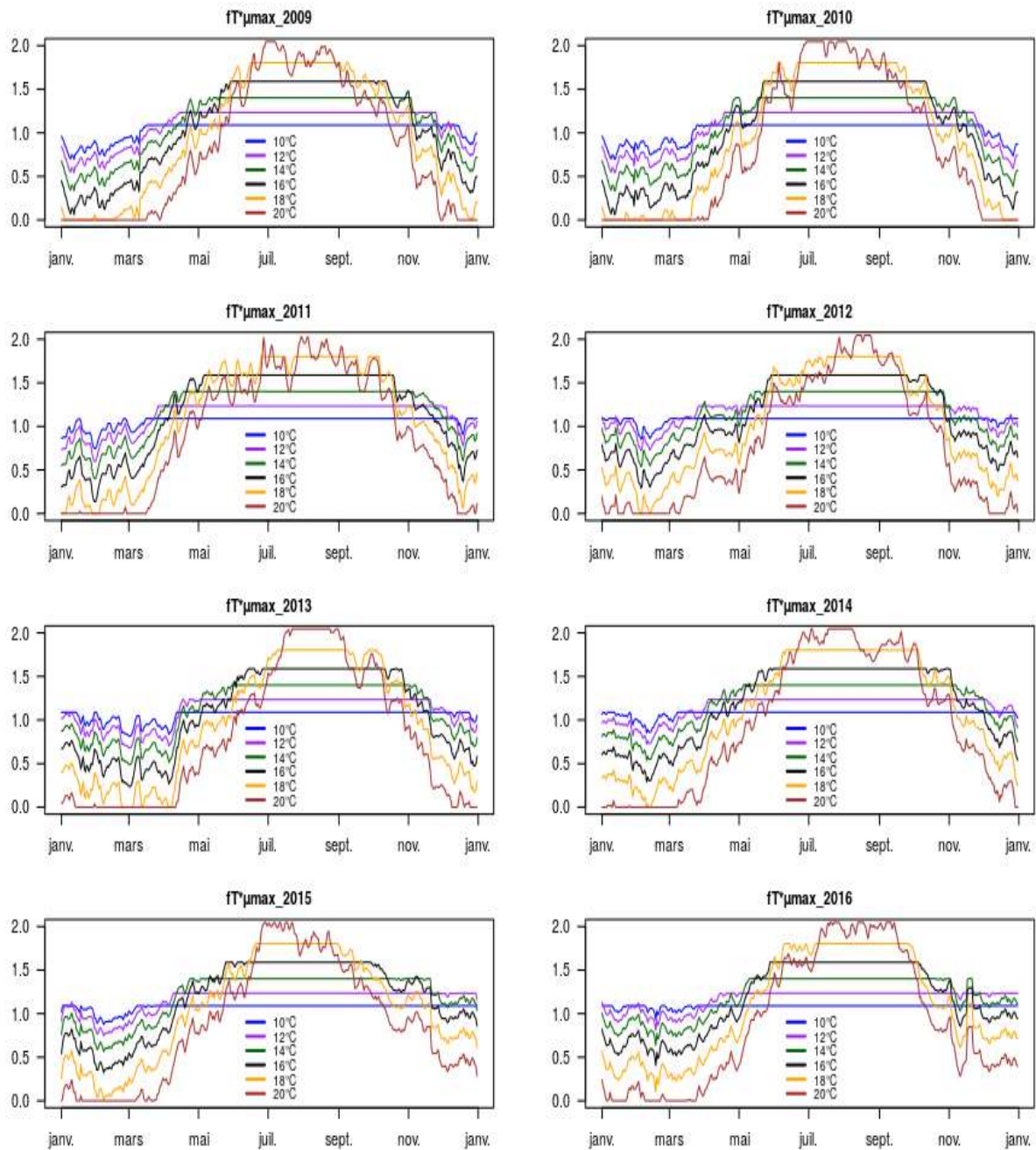
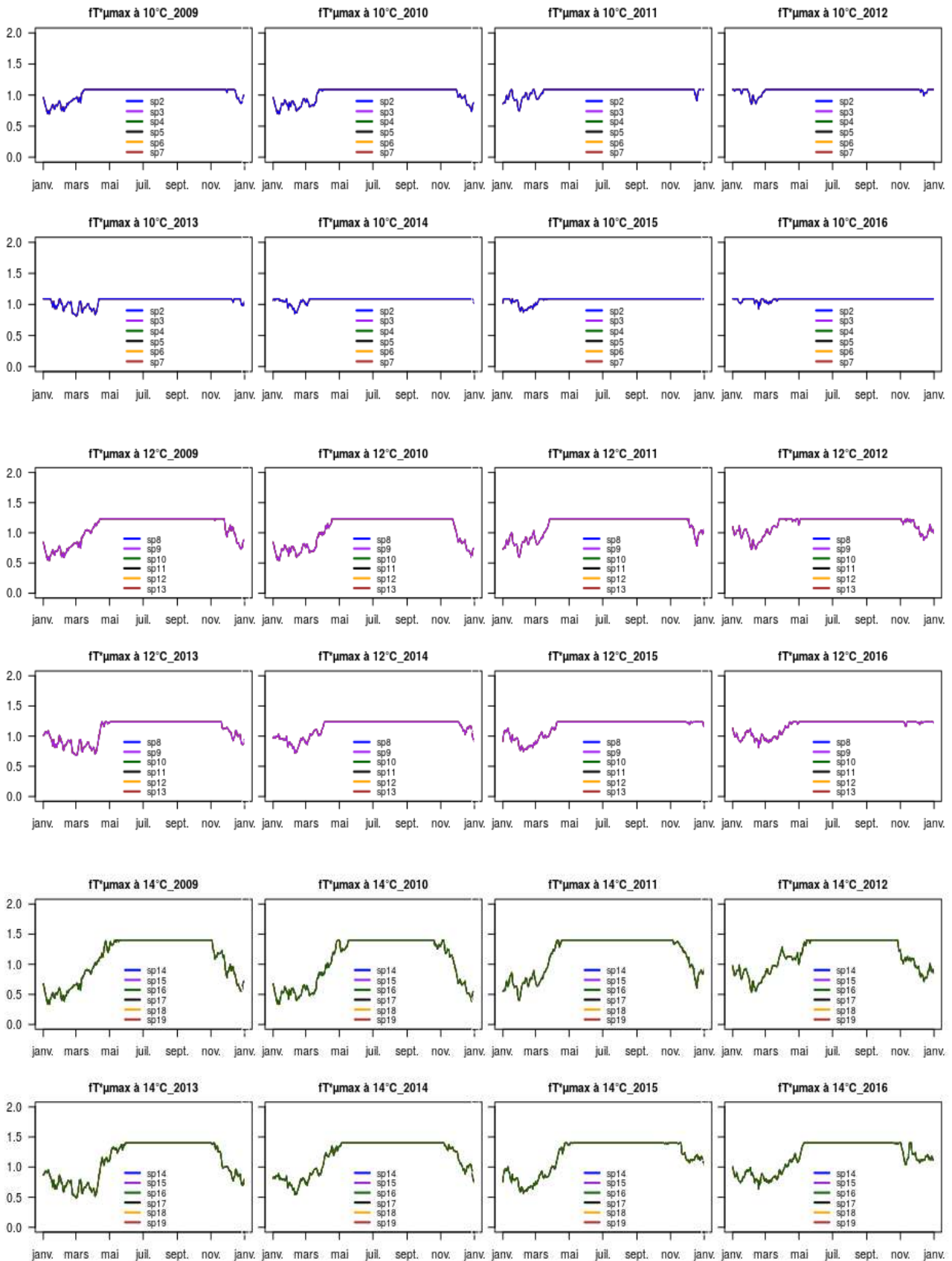


Figure A4.28: Temperature limitation by T_{opt}

Temperature limitation by species: The figure below shows the limitation in temperature in all species with the same T_{opt} . As mentioned earlier, having the same T_{opt} gives them the same level of limitation in temperature notwithstanding their size or gene.



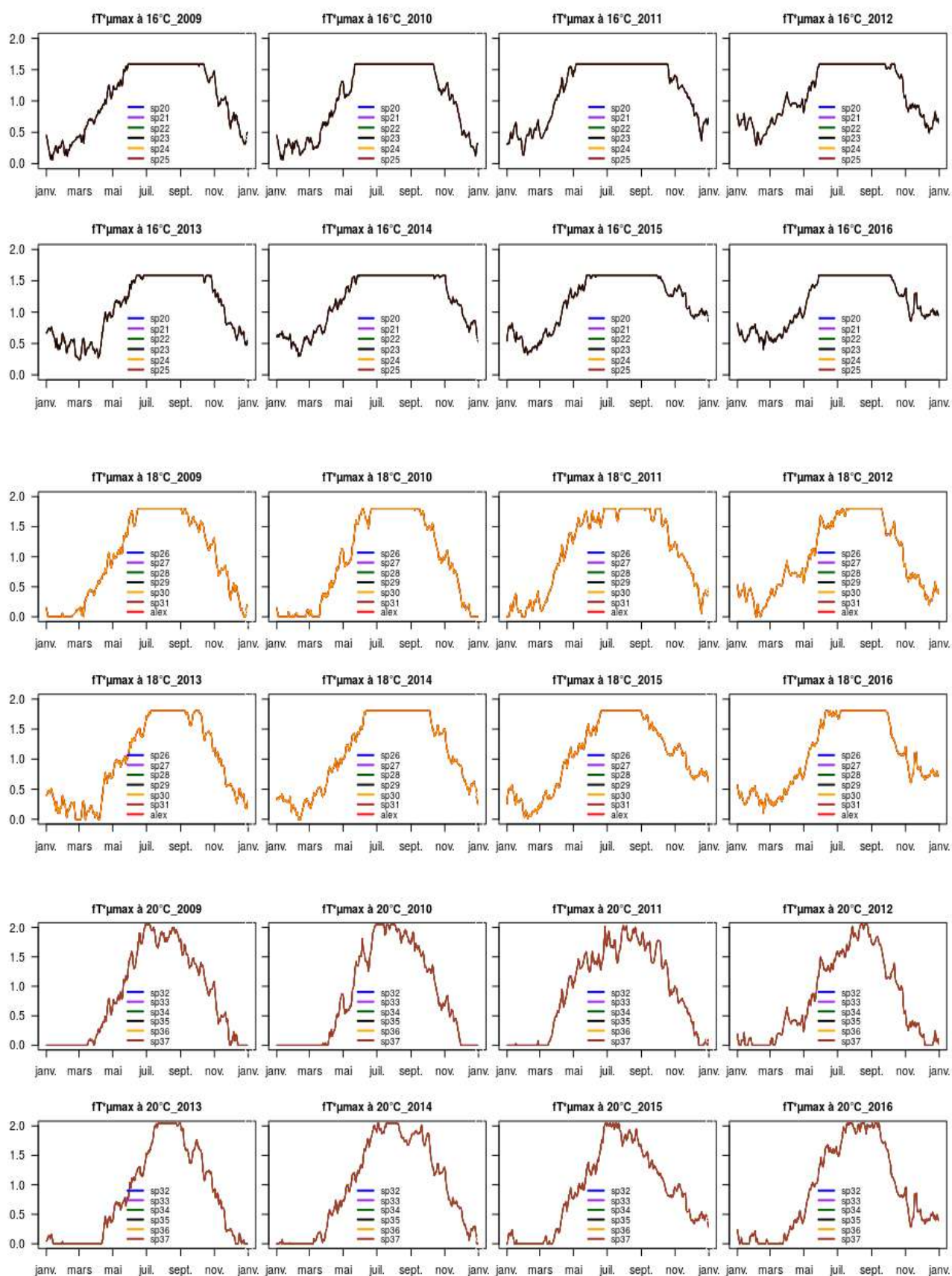


Figure A4.29: Temperature limitation by species

By optimal irradiance, I_{opt} : In a similar manner, we looked at light related limitation and found that species of low irradiance were almost not limited by light in any time of the year. The highest level of limitation found for these species was in the winter. For species of high irradiance, light limitation was quite high in the winter and also high at some points in the summer. Our simulations as shown in the figure below, illustrate the different levels of light limitation with respect to I_{opt} .

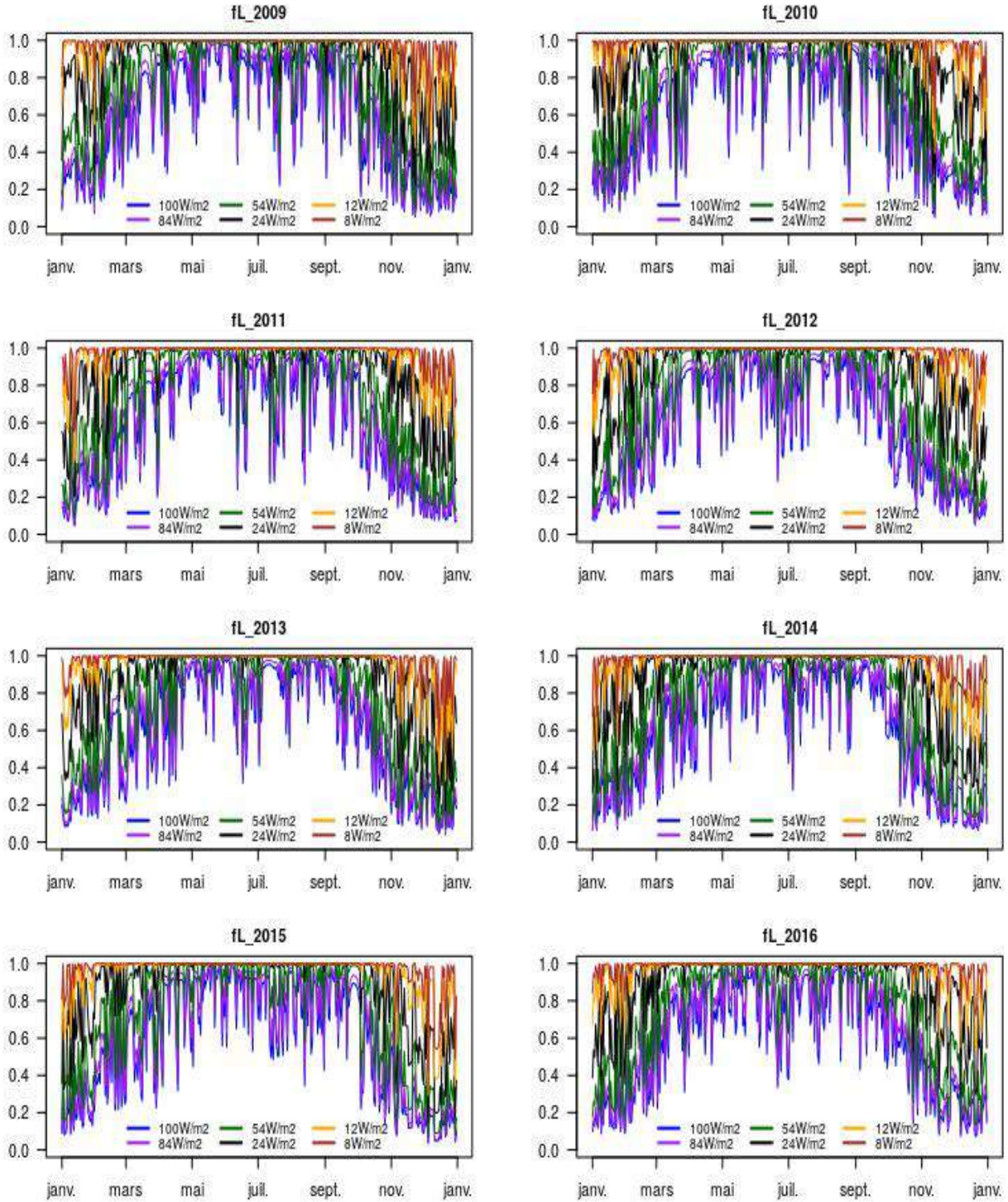
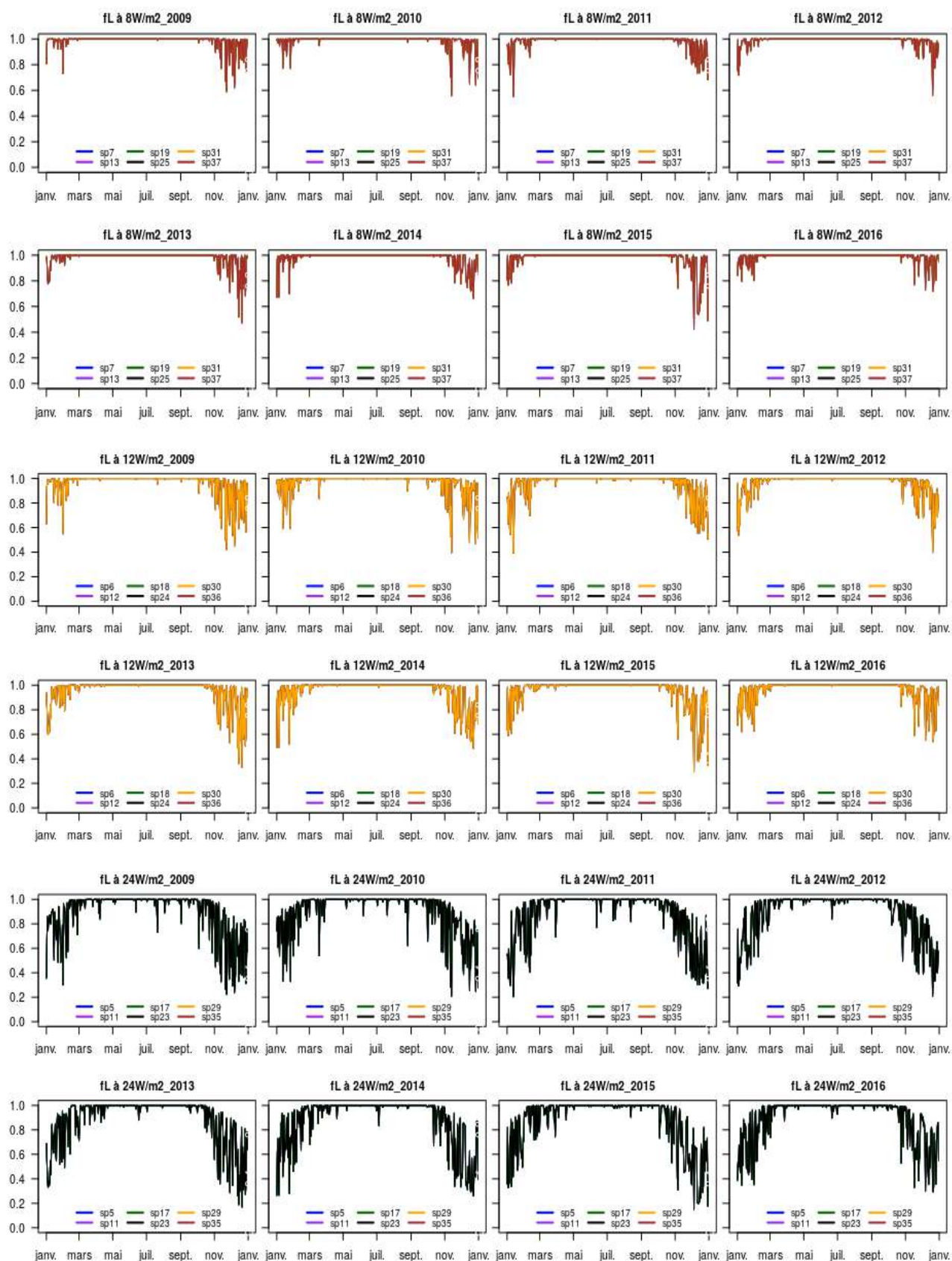


Figure A4.30: Light limitation by I_{opt}

Light limitation by species: Lastly, we equally analyzed the limitation on species of the same I_{opt} and found that they are less limited by light in the summer. Just like T_{opt} , all the species showed the same light limitation. In each given year, the species responded similarly to light – there was no observable difference.



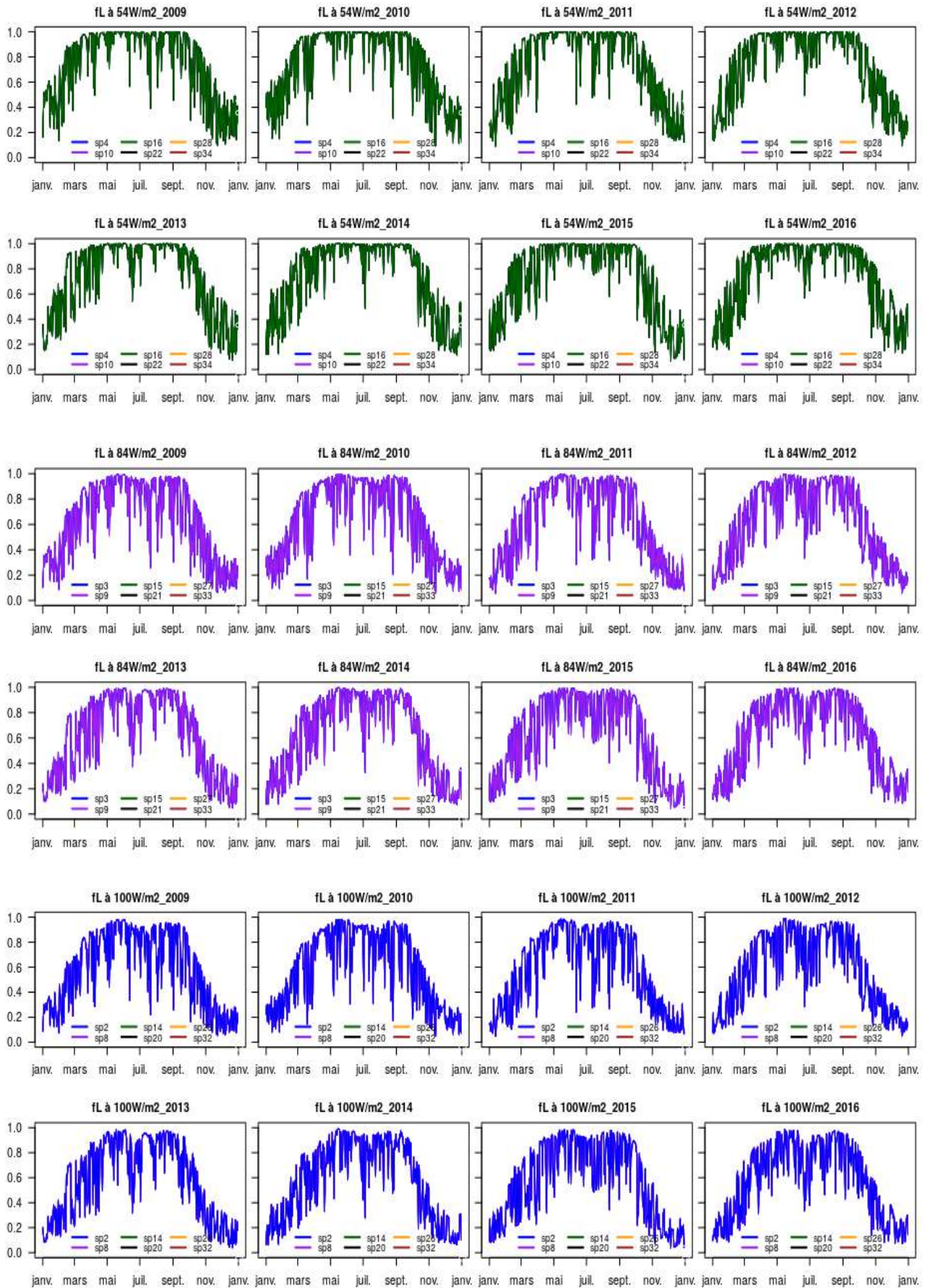


Figure A4.31: Light limitation by species

Weibull Analysis

Weibull is a very useful tool in characterizing and interpreting the different phases of harmful algal blooms.

Weibull analysis on species of 1 μ m: The dominant species among this class is sp26 whose maximum abundance was detected in September 17, 2010 both in the model and by Weibull. It started in June 12 with an abundance of 71 372 241 cells.L⁻¹ and ended in October 2 with 207 364 590 cells.L⁻¹ - an overall bloom duration of 113 days. Sp2 was the least performing species when compared to others. Its maximum abundance was in 2011 but barely present in 2016 where Weibull recorded zero abundance.

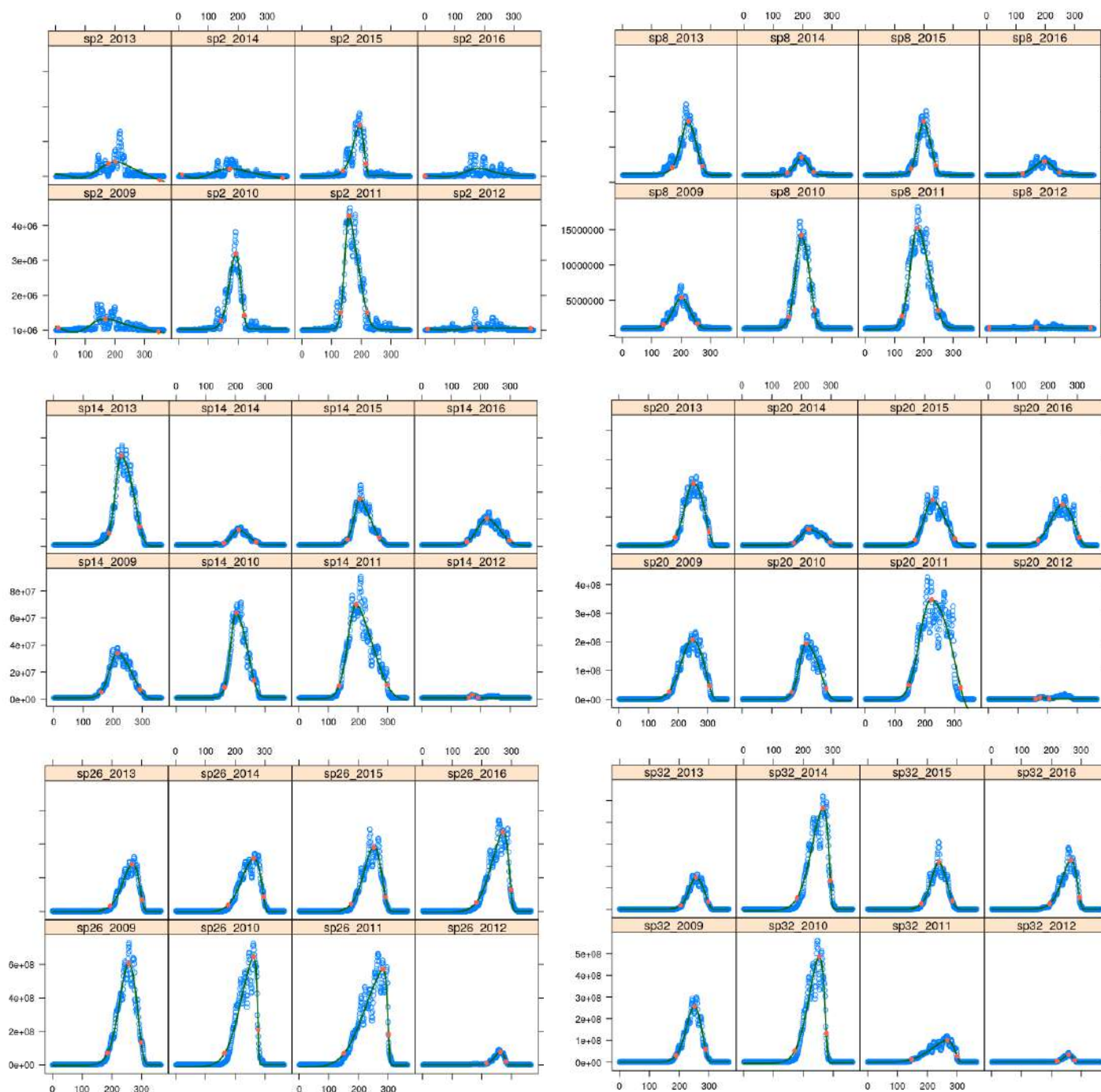


Figure A4.32: Weibull analysis on species of 1 μ m

Species	Abundance maximum	Abundance date_max	Bloom start_date	Bloom end_date	Bloom start_conc	Bloom end_conc	Bloom duration	Bloom increase	Bloom decrease
"sp2_2009"	1 321 544	168	10	346	1 072 131	949 241	337	158	178
"sp2_2010"	3 190 095	191	143	221	1 269 448	1 431 475	78	49	30
"sp2_2011"	4 284 519	159	130	219	1 506 949	1 514 792	89	28	61
"sp2_2012"	1 064 486	169	9	355	1 035 992	1 057 164	347	161	186
"sp2_2013"	1 415 166	201	178	351	1 369 847	893 605	173	23	150
"sp2_2014"	1 217 092	172	12	350	1 049 347	951 679	338	160	178
"sp2_2015"	2 456 442	194	138	216	1 160 137	1 363 601	78	56	21
"sp2_2016"	0	0	0	0	0	0	0	0	0
"sp8_2009"	5 361 228	201	141	256	1 560 362	1 735 165	115	60	54
"sp8_2010"	14 220 259	197	153	242	2 658 241	3 598 793	89	44	44
"sp8_2011"	15 280 375	179	126	249	2 795 624	3 514 234	123	52	71
"sp8_2012"	1 126 255	170	9	355	1 073 941	1 100 063	346	161	185
"sp8_2013"	8 612 868	224	169	273	2 056 361	2 320 228	103	55	48
"sp8_2014"	3 470 789	197	149	238	1 310 717	1 435 380	89	49	41
"sp8_2015"	8 587 069	199	156	241	1 920 968	2 384 004	84	43	42
"sp8_2016"	2 990 680	196	123	249	1 227 627	1 375 892	126	73	53
"sp14_2009"	33 775 155	216	160	292	5 305 634	7 095 246	133	56	77
"sp14_2010"	63 621 269	203	163	263	8 939 115	13 857 331	100	40	60
"sp14_2011"	69 898 182	194	136	298	9 966 923	10 660 950	163	58	105
"sp14_2012"	3 129 996	172	159	191	1 364 518	1 343 148	32	12	19
"sp14_2013"	67 018 454	229	186	292	9 772 463	14 497 111	106	43	63
"sp14_2014"	12 210 552	211	161	270	2 414 159	3 066 616	109	50	60
"sp14_2015"	34 899 484	206	164	272	5 157 785	6 634 804	108	42	66
"sp14_2016"	20 518 195	221	153	297	3 519 909	4 173 806	144	68	77
"sp20_2009"	207 772 970	248	169	305	26 939 856	46 424 101	136	79	57
"sp20_2010"	195 131 654	216	168	283	25 260 495	37 999 427	115	48	67
"sp20_2011"	347 452 458	223	147	321	49 557 605	42 154 948	174	76	98
"sp20_2012"	7 081 870	174	159	204	1 921 994	2 802 810	46	15	30
"sp20_2013"	217 517 560	251	190	304	27 844 569	50 279 545	114	61	53
"sp20_2014"	57 523 799	225	173	298	8 246 215	11 952 015	124	51	73
"sp20_2015"	158 531 704	227	167	301	20 004 439	24 683 268	134	60	75
"sp20_2016"	142 706 158	250	167	306	18 131 725	29 073 096	139	83	56
"sp26_2009"	605 694 754	257	186	299	71 333 511	136 242 322	113	71	42
"sp26_2010"	645 741 685	262	165	277	71 372 241	207 364 590	113	97	16
"sp26_2011"	570 399 529	282	151	301	69 662 108	182 913 689	151	131	19
"sp26_2012"	80 104 043	262	216	282	9 872 474	20 440 349	66	46	20
"sp26_2013"	281 334 102	270	194	302	31 979 771	70 337 121	108	75	32
"sp26_2014"	314 978 740	263	176	296	38 256 140	87 551 741	119	86	33
"sp26_2015"	383 620 574	252	175	291	43 179 349	85 052 121	116	77	39
"sp26_2016"	470 053 943	271	181	298	52 827 526	129 291 705	117	90	26
"sp32_2009"	256 793 871	251	189	287	30 587 102	60 541 183	98	62	37
"sp32_2010"	486 235 966	253	172	277	53 562 443	132 865 065	105	81	24
"sp32_2011"	100 310 301	266	148	300	13 107 001	27 621 509	152	118	33
"sp32_2012"	35 583 714	258	220	278	4 671 663	8 714 240	59	38	20
"sp32_2013"	146 480 638	256	205	296	17 964 385	34 500 332	92	52	40
"sp32_2014"	465 220 054	266	179	291	52 012 256	133 267 879	112	88	25
"sp32_2015"	216 777 506	239	180	284	25 273 138	39 150 049	104	58	45
"sp32_2016"	227 421 786	266	195	295	25 541 426	54 474 316	100	71	29

Table A4.1: Weibull of species 1µm

Weibull analysis on species of 2 μ m: Sp27 showed a maximum abundance in 2012 when it started with an abundance of 6 726 502cells.L⁻¹ on July 22 and ended with 14 817 794cells.L⁻¹ on October 10. In other years though, it had little abundances. Second to sp27 is sp33 with a maximum abundance of 11 643 064cells.L⁻¹ on September 10, 2012. In the same year, we found sp3 to be the least performing species with a maximum abundance of 557 878cells.L⁻¹.

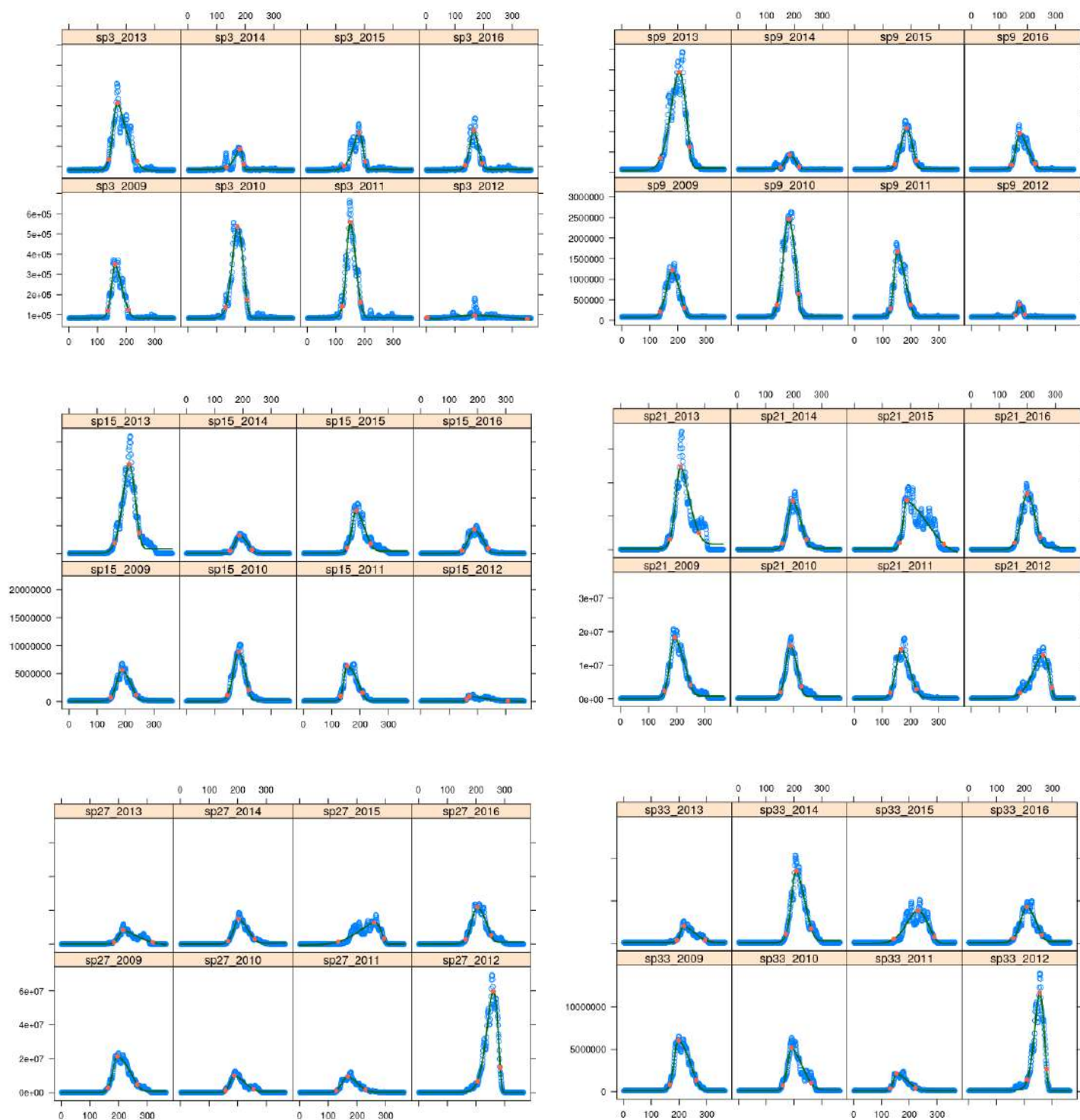


Figure A4.33: Weibull analysis on species of 2 μ m

Species	Abundance maximum	Abundance date_max	Bloom start_date	Bloom end_date	Bloom start_conc	Bloom end_conc	Bloom duration	Bloom increase	Bloom decrease
"sp3_2009"	348 688	161	135	207	119 116	124 833	73	26	46
"sp3_2010"	534 895	173	130	205	136 764	176 345	75	42	33
"sp3_2011"	557 878	150	122	186	142 335	163 544	65	29	36
"sp3_2012"	97 238	168	3	352	86 716	78 739	349	165	184
"sp3_2013"	413 440	169	139	238	135 055	126 112	99	30	69
"sp3_2014"	185 505	180	134	194	95 628	111 134	60	45	15
"sp3_2015"	265 332	181	129	202	101 901	124 537	73	52	22
"sp3_2016"	279 210	166	136	195	106 287	115 860	59	30	29
"sp9_2009"	1 216 679	180	137	223	215 344	308 475	86	43	43
"sp9_2010"	2 467 224	179	139	214	371 119	648 941	76	41	35
"sp9_2011"	1 669 058	152	126	200	284 326	381 726	73	26	47
"sp9_2012"	390 323	171	157	191	126 047	139 047	33	14	20
"sp9_2013"	2 441 100	205	138	242	350 071	627 907	104	67	37
"sp9_2014"	430 847	183	150	217	132 688	147 428	66	33	34
"sp9_2015"	1 082 482	185	143	219	201 135	287 431	76	42	34
"sp9_2016"	955 440	173	143	226	189 754	225 442	83	30	53
"sp15_2009"	5 623 228	188	147	237	742 172	1 175 292	90	41	49
"sp15_2010"	8 922 424	185	146	221	1 119 878	2 062 470	75	39	36
"sp15_2011"	6 354 888	154	130	208	901 246	1 518 443	78	24	54
"sp15_2012"	926 653	172	162	308	354 354	133 412	146	10	136
"sp15_2013"	16 021 262	213	161	250	1 951 233	3 730 603	89	52	37
"sp15_2014"	3 249 227	188	155	233	479 513	728 164	78	33	45
"sp15_2015"	7 709 935	186	154	238	1 039 253	1 786 342	84	32	51
"sp15_2016"	4 333 902	189	146	238	582 131	936 478	92	43	49
"sp21_2009"	18 314 636	192	157	249	2 313 971	4 093 837	93	36	57
"sp21_2010"	15 813 304	188	153	227	1 936 471	3 625 908	74	36	39
"sp21_2011"	14 669 562	167	127	221	1 801 277	2 840 237	94	39	54
"sp21_2012"	12 976 798	255	174	286	1 633 061	3 312 578	112	81	31
"sp21_2013"	24 760 789	214	175	278	3 116 887	5 042 039	103	39	65
"sp21_2014"	14 646 268	197	160	244	1 799 283	3 077 833	85	37	48
"sp21_2015"	14 793 840	186	162	319	2 054 022	1 616 979	157	25	132
"sp21_2016"	16 722 565	200	154	245	2 037 975	3 753 284	91	45	46
"sp27_2009"	21 392 418	196	163	265	2 769 517	4 874 543	101	33	68
"sp27_2010"	10 117 856	189	157	255	1 307 251	1 995 233	97	31	66
"sp27_2011"	9 501 959	168	128	230	1 198 637	1 795 921	103	41	62
"sp27_2012"	59 677 319	261	205	285	6 726 502	14 817 974	80	56	24
"sp27_2013"	8 279 785	216	184	319	1 154 360	1 012 806	136	32	103
"sp27_2014"	14 937 275	204	166	259	1 824 108	3 010 276	93	38	55
"sp27_2015"	12 629 562	260	135	294	1 412 338	3 359 947	159	125	34
"sp27_2016"	21 830 753	205	163	253	2 720 210	5 425 839	90	42	48
"sp33_2009"	6 034 289	197	166	263	840 926	1 347 552	96	31	65
"sp33_2010"	5 194 972	191	160	262	723 990	1 008 404	102	32	70
"sp33_2011"	2 121 061	154	132	224	348 372	456 768	92	22	69
"sp33_2012"	11 643 064	255	211	280	1 390 972	2 674 786	69	44	25
"sp33_2013"	2 043 274	218	192	294	352 019	389 438	102	26	76
"sp33_2014"	8 539 838	207	171	262	1 085 744	1 761 418	91	37	55
"sp33_2015"	3 827 034	232	145	290	495 013	768 802	145	88	58
"sp33_2016"	4 272 542	210	161	263	590 269	978 613	103	50	53

Table A4.2: Weibull of species 2µm

Weibull analysis on species of 5 μ m: Maximum abundance is gradually decreasing with an increasing cell size. The highest abundance was recorded at 1 769 433cells.L⁻¹ for sp22 on June 23, 2014. We observed that species of 5 μ m occurred before those of 1 and 2 μ m. The maximum of sp22 for example was seen in June whereas those of 1 and 2 μ m were in September and July respectively. Sp4 had the lowest maximum abundance of 98 323cells.L⁻¹ in 2013 when compared to other species and simulation years.

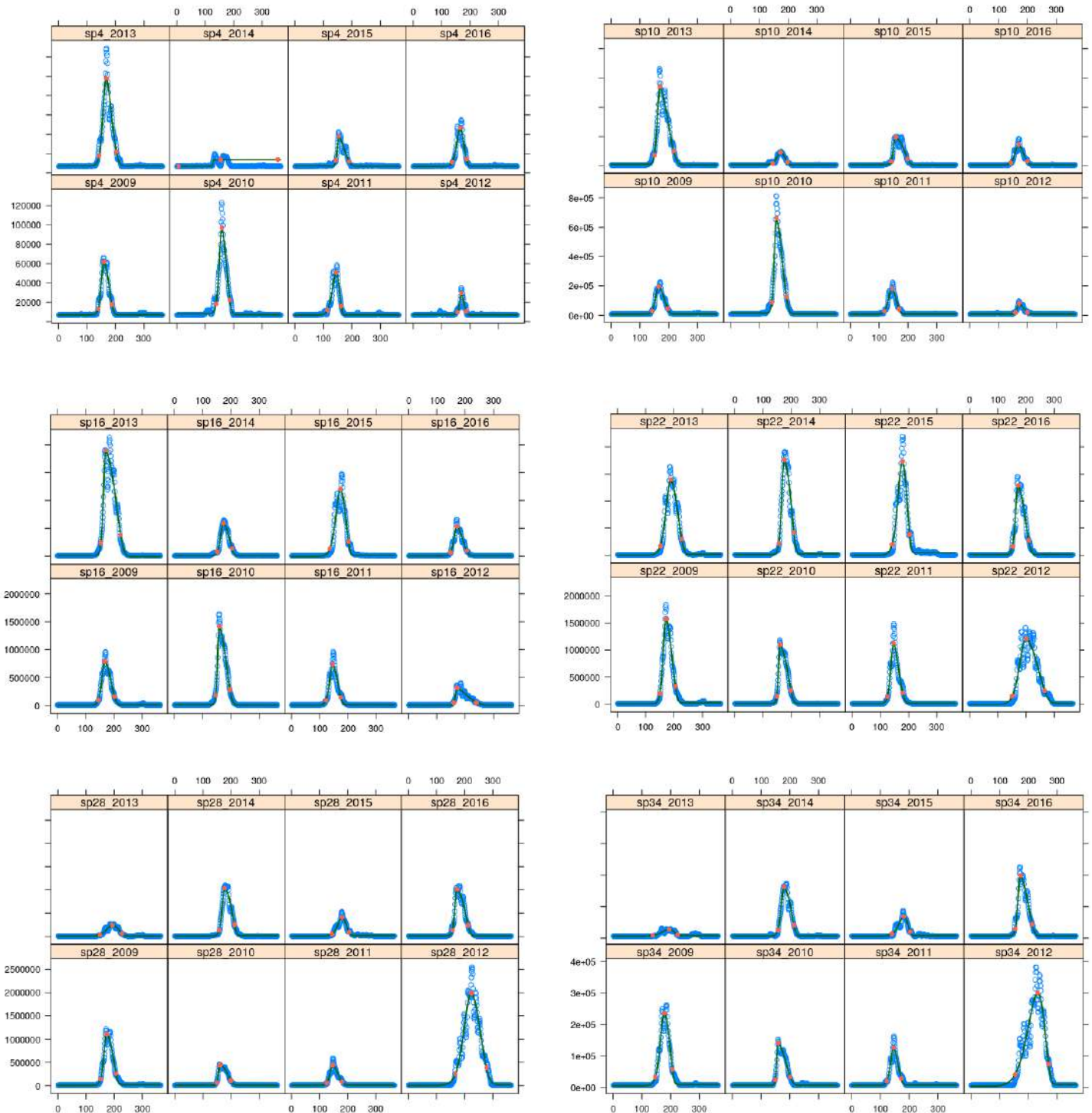


Figure A4.34: Weibull analysis on species of 5 μ m

Species	Abundance maximum	Abundance date_max	Bloom start_date	Bloom end_date	Bloom start_conc	Bloom end_conc	Bloom duration	Bloom increase	Bloom decrease
"sp4_2009"	61 877	160	139	188	13 401	17 799	49	21	28
"sp4_2010"	97 032	159	138	187	18 378	22 506	49	21	28
"sp4_2011"	50 748	144	114	163	11 753	15 915	48	30	19
"sp4_2012"	29 366	170	156	186	9 947	10 704	30	14	16
"sp4_2013"	98 323	168	142	203	17 952	22 143	61	25	35
"sp4_2014"	13 707	153	6	354	6 869	13 812	348	147	201
"sp4_2015"	38 442	154	144	190	13 234	11 983	47	10	36
"sp4_2016"	46 886	165	137	187	11 170	14 497	50	28	22
"sp10_2009"	194 875	165	142	197	28 616	43 762	55	22	32
"sp10_2010"	662 637	159	143	193	88 193	125 818	51	17	34
"sp10_2011"	180 132	145	118	169	26 679	40 507	51	26	24
"sp10_2012"	80 052	171	158	199	17 066	19 844	41	13	28
"sp10_2013"	543 330	170	150	217	73 409	101 049	67	20	47
"sp10_2014"	92 187	173	146	197	18 132	25 779	52	27	24
"sp10_2015"	194 847	157	142	199	31 169	49 001	57	15	42
"sp10_2016"	146 341	168	142	198	22 510	32 226	56	26	29
"sp16_2009"	794 462	169	146	202	96 787	160 579	57	24	33
"sp16_2010"	1 417 834	160	146	197	180 539	283 234	50	13	37
"sp16_2011"	740 558	146	122	175	90 900	140 341	53	24	29
"sp16_2012"	316 958	171	160	239	52 509	54 745	79	11	68
"sp16_2013"	1 896 558	172	155	224	241 831	382 020	70	18	52
"sp16_2014"	591 615	174	152	204	79 246	139 079	52	21	31
"sp16_2015"	1 205 891	174	135	202	136 454	263 103	67	39	28
"sp16_2016"	532 628	171	148	205	67 607	104 179	58	23	34
"sp22_2009"	1 577 360	172	150	205	188 644	328 192	55	22	34
"sp22_2010"	1 099 184	160	148	199	143 332	252 044	50	12	38
"sp22_2011"	1 126 797	147	125	179	135 450	202 265	55	22	33
"sp22_2012"	1 212 801	202	152	266	149 371	244 260	114	49	65
"sp22_2013"	1 396 649	189	151	227	166 279	295 518	76	37	38
"sp22_2014"	1 769 433	176	155	209	219 161	418 053	53	20	33
"sp22_2015"	1 736 382	178	141	203	193 870	385 964	62	37	25
"sp22_2016"	1 286 214	172	153	210	160 570	273 273	57	19	37
"sp28_2009"	1 112 889	174	151	207	137 369	258 245	55	23	33
"sp28_2010"	439 254	160	150	200	61 675	109 613	50	11	40
"sp28_2011"	443 434	147	125	179	57 276	81 869	54	21	33
"sp28_2012"	1 985 713	224	167	278	246 626	381 280	111	57	54
"sp28_2013"	241 522	193	149	228	34 138	61 716	79	44	35
"sp28_2014"	1 035 197	178	158	212	131 922	254 856	54	20	35
"sp28_2015"	411 000	180	144	205	51 401	95 139	61	36	25
"sp28_2016"	1 016 101	174	156	212	131 952	240 847	56	17	39
"sp34_2009"	235 737	178	147	207	32 597	58 128	60	31	28
"sp34_2010"	140 881	160	149	202	24 278	33 247	52	10	42
"sp34_2011"	126 468	146	123	173	20 420	28 328	50	23	26
"sp34_2012"	300 339	232	153	270	40 603	73 723	117	79	38
"sp34_2013"	27 873	194	138	225	8 922	12 074	87	57	30
"sp34_2014"	163 278	180	158	214	25 494	41 653	56	22	34
"sp34_2015"	69 068	181	140	203	13 375	20 563	63	41	22
"sp34_2016"	199 894	172	154	213	30 428	44 131	59	18	40

Table A4.3: Weibull of species 5µm

Weibull analysis on species of 18 μ m: *A. minutum* is among species of this size. In fact, it dominated every other species both in Weibull and model. We found its maximum abundance at 39 700cells.L⁻¹ on June 17, 2012 where it started with 5 177cells.L⁻¹ on June 8 and ended with 6 537cells.L⁻¹ on August 9 with total bloom duration of 63 days. We also noticed the abundance at the end of a bloom is always higher than that of the beginning. *A. minutum* equally showed abundances above 10 000cells.L⁻¹ in other years except 2011 and 2013. Among all species of this size, sp5 had the lowest maximum abundance at 2 168cells.L⁻¹.

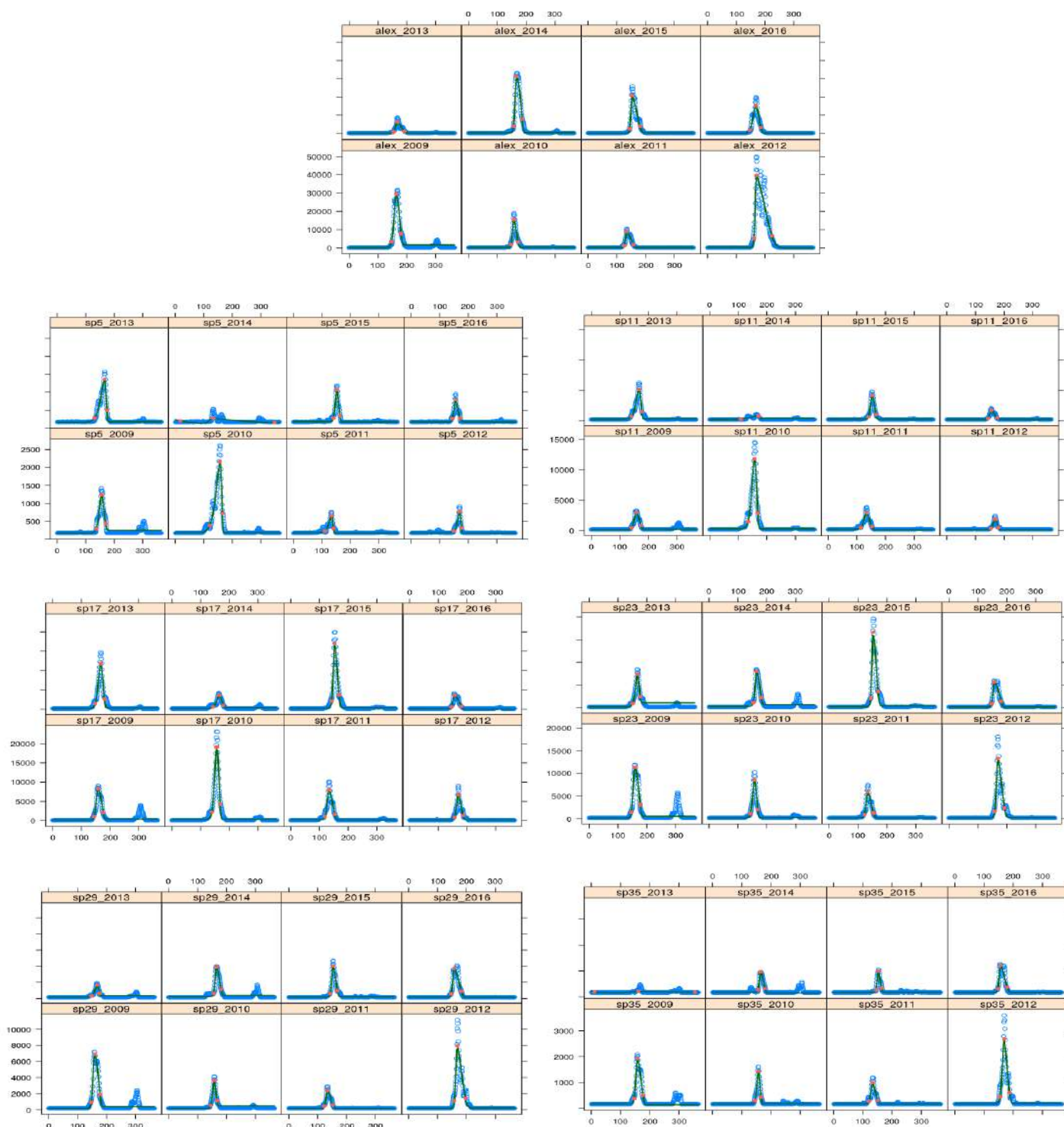


Figure A4.35: Weibull analysis on species of 18 μ m

Species	Abundance maximum	Abundance date_max	Bloom start_date	Bloom end_date	Bloom start_conc	Bloom end_conc	Bloom duration	Bloom increase	Bloom decrease
"alex_2009"	29 599	163	147	180	3 429	7 928	33	16	17
"alex_2010"	15 525	157	147	172	1 897	3 197	25	10	15
"alex_2011"	9 061	135	125	157	1 265	1 914	32	9	23
"alex_2012"	39 700	170	161	223	5 177	6 537	63	9	54
"alex_2013"	6 520	167	154	192	938	1 277	38	13	25
"alex_2014"	31 238	166	156	186	3 961	7 912	30	10	20
"alex_2015"	20 814	153	145	180	2 657	3 908	35	8	27
"alex_2016"	15 448	167	146	185	1 780	3 207	39	22	18
"sp5_2009"	1 250	156	137	170	291	437	34	20	14
"sp5_2010"	2 167	157	121	165	385	716	44	36	9
"sp5_2011"	662	134	111	141	233	300	30	23	7
"sp5_2012"	773	170	149	176	238	318	26	20	6
"sp5_2013"	1 364	166	131	175	285	499	44	35	8
"sp5_2014"	278	133	17	347	206	154	330	116	214
"sp5_2015"	1 077	153	140	163	282	350	23	12	11
"sp5_2016"	794	155	143	171	261	276	28	11	17
"sp11_2009"	2 978	157	141	174	491	799	33	16	17
"sp11_2010"	11 817	157	133	168	1 461	2 895	34	23	11
"sp11_2011"	2 957	134	113	152	532	691	38	20	18
"sp11_2012"	1 918	169	154	180	374	516	26	15	11
"sp11_2013"	5 132	167	140	177	674	1 411	36	27	10
"sp11_2014"	735	171	108	171	238	713	63	62	
"sp11_2015"	4 114	153	141	166	634	994	26	12	13
"sp11_2016"	1 683	155	144	176	365	446	32	11	21
"sp23_2009"	11 415	159	146	177	1 485	3 104	30	13	18
"sp23_2010"	8 622	157	143	169	1 108	2 005	25	14	12
"sp23_2011"	6 038	134	122	154	892	1 251	32	12	20
"sp23_2012"	13 366	169	159	192	1 721	2 442	33	10	23
"sp23_2013"	7 388	168	151	176	927	2 403	26	17	9
"sp23_2014"	8 013	165	153	180	1 159	2 228	27	12	16
"sp23_2015"	16 626	153	144	169	2 075	3 543	26	9	16
"sp23_2016"	5 707	157	147	180	845	1 442	33	9	23
"sp29_2009"	6 931	159	147	177	967	1 899	30	12	18
"sp29_2010"	3 676	157	145	166	549	1 125	21	12	9
"sp29_2011"	2 410	134	123	153	455	572	30	11	19
"sp29_2012"	7 922	169	158	196	1 119	1 432	39	11	27
"sp29_2013"	1 683	168	148	175	320	667	26	20	7
"sp29_2014"	3 916	165	155	181	653	1 164	26	10	16
"sp29_2015"	4 068	153	144	168	626	972	24	9	15
"sp29_2016"	3 748	158	147	182	598	904	35	11	24
"sp35_2009"	1 935	158	146	177	380	512	30	11	19
"sp35_2010"	1 428	157	145	166	301	437	21	12	9
"sp35_2011"	997	134	122	150	277	312	29	12	16
"sp35_2012"	2 680	169	155	187	455	611	32	14	18
"sp35_2013"	208	161	10	354	192	188	344	151	193
"sp35_2014"	963	164	157	180	280	314	23	8	16
"sp35_2015"	997	153	144	164	269	332	20	8	12
"sp35_2016"	1 215	156	148	179	315	368	31	8	23

Table A4.4: Weibull of species 18 μm

Weibull analysis on species of 28 μ m: Although the abundance of species of 28 μ m is not close to what we observed among those of pico and nano, we found a maximum abundance greater than 1 000cells.L⁻¹ in all species except sp6 and sp36. Surprisingly, these abundances were found in the month of November with average bloom duration of 24 days. The least performing species is sp6 with a maximum abundance of 233cells.L⁻¹ in 2010.

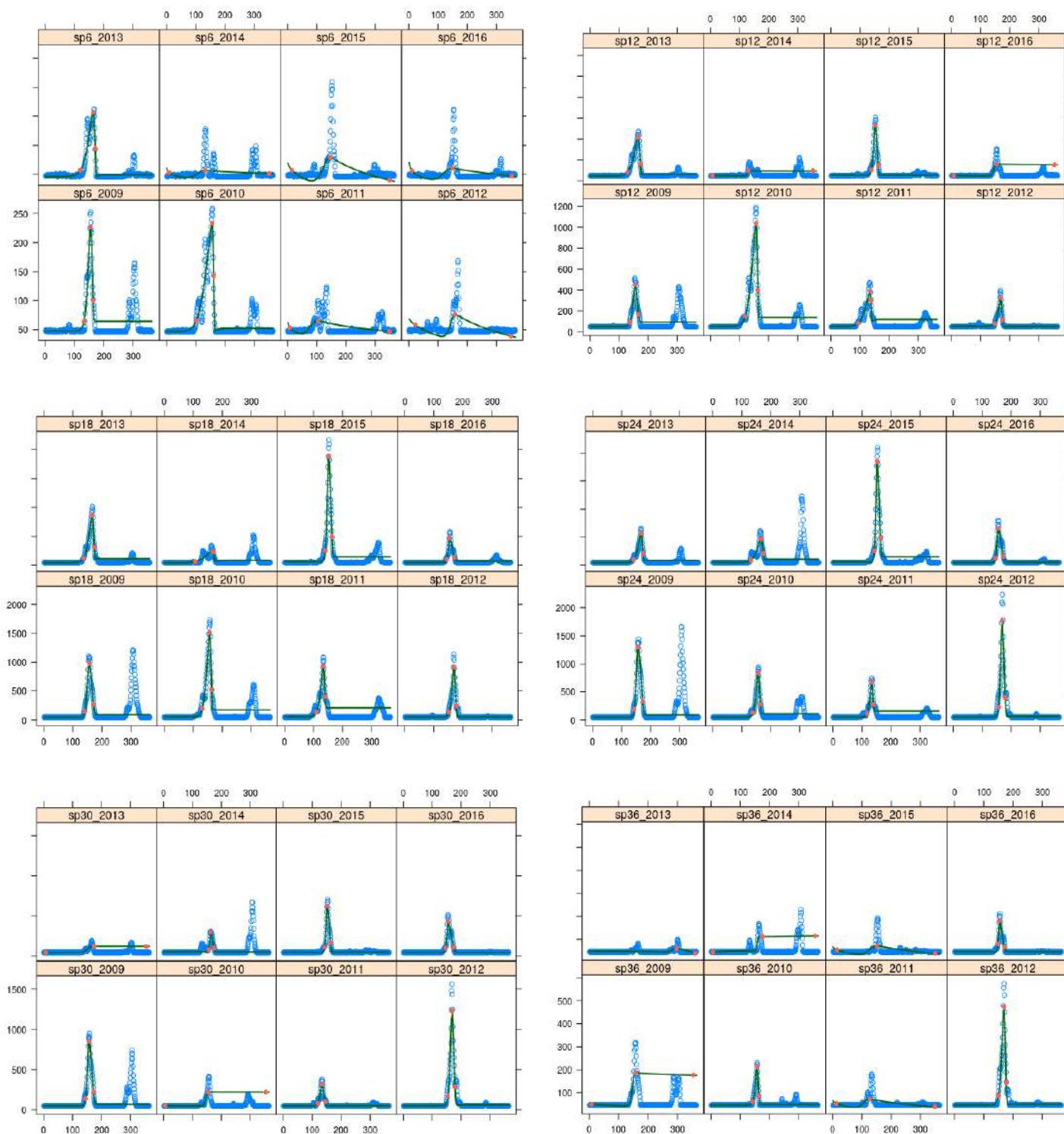


Figure A4.36: Weibull analysis on species of 28 μ m

Species	Abundance maximum	Abundance date_max	Bloom start_date	Bloom end_date	Bloom start_conc	Bloom end_conc	Bloom duration	Bloom increase	Bloom decrease
"sp6_2009"	227	155	132	164	64	101	31	23	8
"sp6_2010"	233	156	102	162	66	142	59	54	6
"sp6_2011"	65	105	8	349	53	47	342	97	244
"sp6_2012"	76	159	23	350	58	39	327	136	191
"sp6_2013"	157	164	119	171	57	95	52	45	7
"sp6_2014"	57	132	8	353	53	51	345	125	220
"sp6_2015"	79	146	15	349	57	40	334	131	203
"sp6_2016"	61	149	11	353	56	47	342	138	204
"sp12_2009"	454	156	138	167	89	162	30	18	11
"sp12_2010"	1 039	156	120	163	146	398	44	37	7
"sp12_2011"	391	134	94	138	81	296	44	40	4
"sp12_2012"	326	169	149	176	76	114	27	20	6
"sp12_2013"	419	166	129	173	81	160	44	37	8
"sp12_2014"	95	130	7	353	50	93	346	123	223
"sp12_2015"	533	152	139	162	103	151	23	13	10
"sp12_2016"	159	155	7	354	51	154	347	147	199
"sp18_2009"	1 296	157	144	172	188	336	28	13	16
"sp18_2010"	845	157	138	164	129	283	25	18	7
"sp18_2011"	673	134	117	140	112	273	22	17	6
"sp18_2012"	1 763	169	156	179	230	395	24	13	11
"sp18_2013"	566	167	142	174	96	208	32	25	7
"sp18_2014"	476	166	132	173	89	216	42	35	7
"sp18_2015"	1 850	153	143	164	249	488	21	10	11
"sp18_2016"	657	155	146	174	122	157	28	9	19
"sp24_2009"	1 296	157	144	172	188	336	28	13	16
"sp24_2010"	845	157	138	164	129	283	25	18	7
"sp24_2011"	673	134	117	140	112	273	22	17	6
"sp24_2012"	1 763	169	156	179	230	395	24	13	11
"sp24_2013"	566	167	142	174	96	208	32	25	7
"sp24_2014"	476	166	132	173	89	216	42	35	7
"sp24_2015"	1 850	153	143	164	249	488	21	10	11
"sp24_2016"	657	155	146	174	122	157	28	9	19
"sp30_2009"	851	157	145	173	138	223	28	12	16
"sp30_2010"	218	155	6	354	49	217	348	148	200
"sp30_2011"	318	133	120	144	78	100	24	13	11
"sp30_2012"	1 230	169	155	179	171	288	25	14	11
"sp30_2013"	125	175	6	355	46	125	349	168	181
"sp30_2014"	302	163	156	175	85	102	19	8	11
"sp30_2015"	630	152	143	163	112	168	20	9	11
"sp30_2016"	435	155	147	175	100	114	28	8	19
"sp36_2009"	187	157	7	354	52	177	347	150	197
"sp36_2010"	215	157	142	163	62	86	21	15	6
"sp36_2011"	73	126	12	349	54	39	337	114	223
"sp36_2012"	473	169	150	176	87	145	26	19	7
"sp36_2013"	61	298	297	361	61	40	64	1	63
"sp36_2014"	112	176	7	356	44	115	349	170	179
"sp36_2015"	72	150	16	351	55	40	335	134	200
"sp36_2016"	182	155	149	170	80	67	21	6	16

Table A4.5: Weibull of species 28 µm

Weibull analysis on species of 64 μm : These are the largest but least abundant as shown in Weibull and model. Sp25 recorded the maximum abundance at 28cells.L⁻¹ in November 1, 2010 with a start of 6cells.L⁻¹ and end of 10cells.L⁻¹ also in the month of November. Most species in this size range recorded a low abundance in 2012 – the year that was dominated mainly by pico and nanophytoplankton.

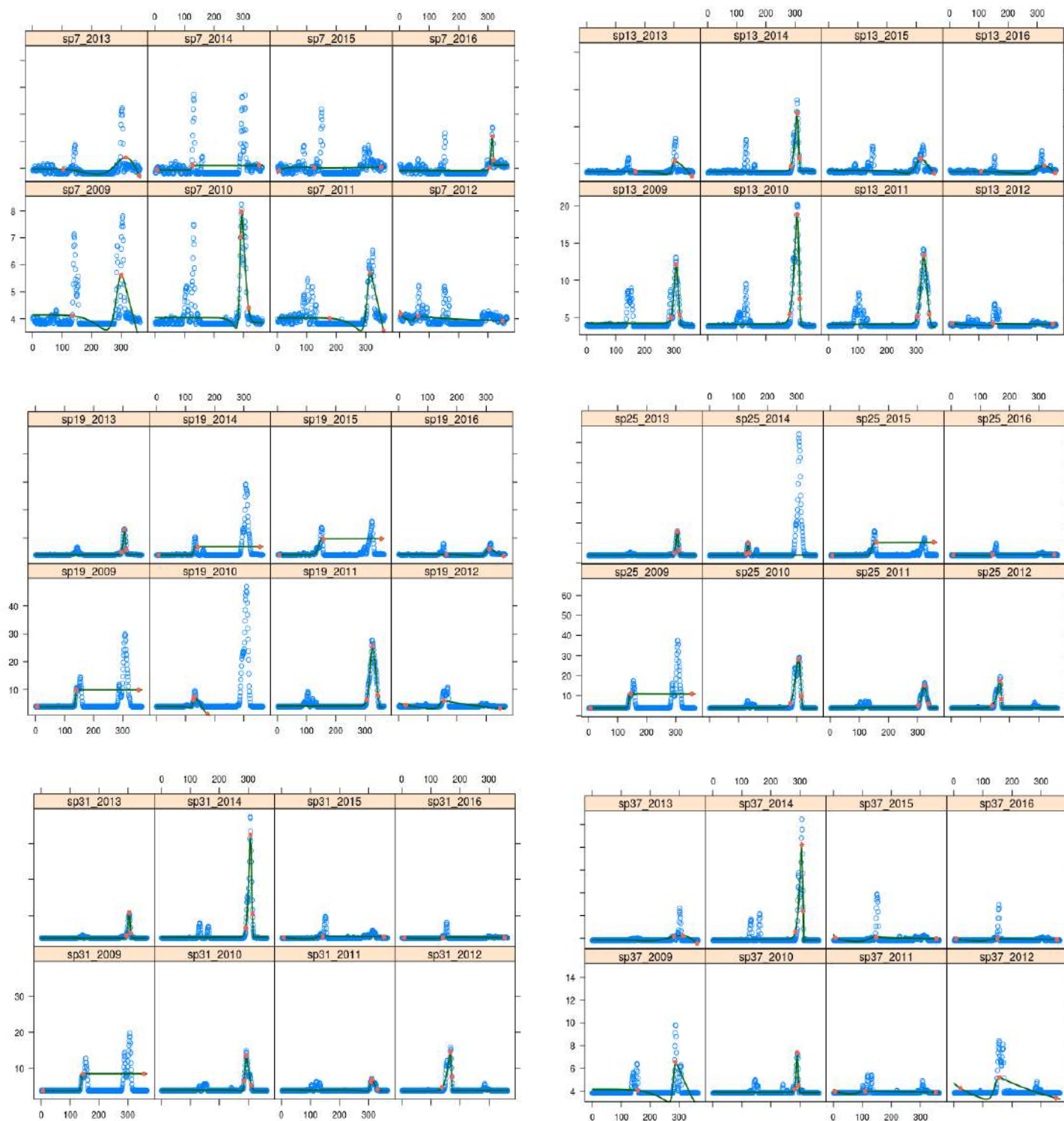


Figure A4.37: Weibull analysis on species of 64 μm

Species	Abundance maximum	Abundance date_max	Bloom start_date	Bloom end_date	Bloom start_conc	Bloom end_conc	Bloom duration	Bloom increase	Bloom decrease
"sp7_2009"	6	301	135	360	4	3	225	166	59
"sp7_2010"	8	294	290	318	7	4	27	4	24
"sp7_2011"	6	315	178	361	4	4	183	137	46
"sp7_2012"	4	62	3	349	4	4	346	59	287
"sp7_2013"	4	316	104	362	4	4	258	212	46
"sp7_2014"	4	128	6	353	4	4	347	121	225
"sp7_2015"	4	125	6	353	4	4	347	119	228
"sp7_2016"	5	316	305	319	4	4	14	11	3
"sp13_2009"	12	307	290	319	5	5	30	17	12
"sp13_2010"	19	307	281	316	5	7	35	26	9
"sp13_2011"	13	326	303	346	5	5	42	22	20
"sp13_2012"	4	148	8	354	4	4	346	140	206
"sp13_2013"	5	302	169	361	4	3	193	134	59
"sp13_2014"	12	307	286	314	5	6	28	21	7
"sp13_2015"	6	317	314	361	6	4	47	2	45
"sp13_2016"	5	324	107	362	4	4	255	216	39
"sp19_2009"	10	142	7	354	4	10	347	135	212
"sp19_2010"	7	130	127	174	6	1	47	4	44
"sp19_2011"	26	326	306	344	6	8	38	20	18
"sp19_2012"	6	155	25	349	5	3	324	131	193
"sp19_2013"	13	305	295	312	5	6	17	11	6
"sp19_2014"	7	143	6	354	4	7	347	136	211
"sp19_2015"	10	158	6	355	4	10	348	152	197
"sp19_2016"	6	311	163	361	4	3	198	148	50
"sp25_2009"	11	145	7	354	4	11	347	139	209
"sp25_2010"	28	306	278	316	6	10	38	28	10
"sp25_2011"	15	323	301	337	5	6	36	22	13
"sp25_2012"	17	168	139	173	5	8	33	29	5
"sp25_2013"	16	305	295	311	5	6	17	10	7
"sp25_2014"	10	132	125	138	5	5	13	7	6
"sp25_2015"	10	158	6	355	4	10	348	152	197
"sp25_2016"	4	142	8	354	4	4	346	134	212
"sp31_2009"	8	145	7	354	4	8	347	138	209
"sp31_2010"	13	292	286	310	7	5	25	6	18
"sp31_2011"	7	312	308	331	6	4	23	3	19
"sp31_2012"	14	167	138	172	5	8	34	30	5
"sp31_2013"	11	304	294	309	5	5	16	10	5
"sp31_2014"	32	308	291	314	7	10	23	16	7
"sp31_2015"	4	142	8	354	4	4	346	134	212
"sp31_2016"	4	143	7	354	4	4	346	135	211
"sp37_2009"	7	287	156	357	4	3	201	131	70
"sp37_2010"	7	291	281	296	4	4	15	10	5
"sp37_2011"	4	110	6	352	4	4	346	104	242
"sp37_2012"	5	156	23	352	4	3	329	133	196
"sp37_2013"	4	312	282	362	4	4	80	30	50
"sp37_2014"	12	306	284	311	5	6	27	23	5
"sp37_2015"	4	147	8	354	4	4	346	139	207
"sp37_2016"	4	149	8	354	4	4	346	142	205

Table A4.6: Weibull of species 64µm

Annex 5

Code 0D

Biotic data/Name-list**& PHY_CST**

k_minN = 0.05 ! Nitrogen mineralization rate at 0 Celsius degree (d-1) (Cugier et al, 2005 + Hoch, 1995)
 k_nitrif = 0.2 ! Nitrification rate at 0 Celsius degree (d-1) (Cugier et al, 2005 + Chapelle, 1995)
 k_minP = 0.1 ! Phosphorus mineralization rate at 0 Celsius degree (d-1) (Cugier et al, 2005)
 k_dissSi = 0.07 ! Silica dissolution rate at 0 Celsius degree (d-1) (Cugier et al, 2005)
 k_ads = 0.12 ! Adsorption rate of phosphorus by suspended particulate matter (d-1 dm3 µmol-1 (Cugier et al, 2005 + Andrieux-Loyer, 1997)
 k_des = 2.4 ! Desorption rate of phosphorus by suspended particulate matter (d-1) (Cugier et al, 2005 + Andrieux-Loyer, 1997)
 Q_maxSM = 7 ! Maximum phosphorus adsorption capacity by suspended particulate matter (µmol.g-1(Cugier et al, 2005 + Andrieux-Loyer, 1997)
 kT = 0.063 ! Rate of kinetics acceleration with temperature (degree-1) (Eppley, 1972)
 Hd = 3.75 ! Average depth of the Bay of Daoulas (m)
 Hm = 2.15 ! Average depth of the estuary of Mignonne (m)
 Vd = 4738600 ! Volume of the bay of Daoulas (m3)
 Vm = 9124543 ! Volume of the estuary of Mignonne (m3)
 nsim = 1 / ! Number of simulations

& BIO_PARAM

ns = 72 ! Total number of species in one simulation
 gmax = 0.58 ! Maximum growth rate of cells at 0 Celsius degree (d-1) (Cugier et al, 2005) (???)
 QminN = 0.0029E-6 ! Standard minimum nitrogen cell quota for 1 micron (micromol.cell-1) (???) (adapted from Edwards et al, 2012, Maranon et al, 2013 and Alexandrium data) (23)
 QminP = 0.00014E-6 ! Standard minimum phosphorus cell quota for 1 micron (micromol.cell-1) (???) (adapted from Edwards et al, 2012, Maranon et al, 2013 and Alexandrium data) (11)
 QmaxN = 2 ! Lowest maximum nitrogen cell quota, normalized by minimum quota (???) (Moore et al, 2001)
 QmaxP = 2 ! Lowest maximum phosphorus cell quota, normalized by minimum quota (???) (Moore et al, 2001)
 VmaxNH4 = 0.38 ! Standard maximum uptake of ammonium, normalized my minimum quota, at 0 degree and 0 micron3 (d-1) (Same level as Alexandrium)
 VmaxNO3 = 0.19 ! Standard maximum uptake of nitrate, at 0 degree and 0 micron (d-1) (Same level as Alexandrium)
 VmaxPO4 = 0.38 ! Standard maximum uptake of phosphate, at 0 degree and 0 micron (d-1) (Lower than Alexandrium)
 Kn = 0.23 ! Standard half-saturation concentration of nitrogen, for diatoms of 1 micron3 (micromol.L-1) (Cugier et al, 2005 + Eppley et al, 1969 + scaling) (???) (0.2)
 Kp = 0.011 ! Standa half-saturation concentration of phosphorus, for diatoms of 1 micron3 (micromol.L-1) (Cugier et al, 2005 + Aksnes et al, 1995 +scaling) (???) (0.01)
 Qsi = 0.0029E-6 ! Standard silica cell quota (micromol.micron-3) (Cugier et al, 2005 + scaling) (But there is only a Si:N ratio)
 Ksi = 0.1 ! Standard half-saturation concentration of silicium, for diatoms of 1 micrometer (micromol.L-1) (Cugier et al, 2005 + Paasche, 1973 +scaling)
 m = 0.02 ! Standard mortality rate at 0 Celsius degree for small organisms (d-1) (Cugier et al, 2005, compatible with Moore et al, 2001) (0)
 Topt = 15 ! Temperature of maximum growth (???)
 kT = 0.063 / ! Rate of kinetics acceleration with temperature (degree-1) (Eppley, 1972)

& ALEXANDRIUM

Si_alex = F ! Alexandrium is not a diatom
 gmax_alex = 1.8 ! Growth rate of Alexandrium at optimal temperature (empirical) (???)
 QminN_alex = 4.08E-6 ! Minimum nitrogen quota of Alexandrium minutum (micromol.cell-1) (Final deliverable 7)
 QminP_alex = 0.195E-6 ! Minimum phosphorus cell quota of Alexandrium minutum (micromol.cell-1) (Final deliverable 7)
 QmaxN_alex = 6.62 ! Maximum to minimum nitrogen cell quota ratio (Final deliverable 7)
 QmaxP_alex = 7.38 ! Maximum to minimum nitrogen cell quota ratio (Final deliverable 7)
 Qsi_alex = 0.0 ! Alexandrium is not a diatom
 VmaxNH4_alex = 1.16 ! Maximum ammonium uptake rate (d-1) at 0 degree (Erard-Le Denn et al 2004/06).....3.6 à 18°C
 VmaxNO3_alex = 0.58 ! Maximum nitrate uptake rate (d-1) at 0 degree (Erard-Le Denn et al 2004/06).....1.8 à 18°C
 VmaxPO4_alex = 1.86 ! Maximum phosphorus uptake rate (d-1) at 0 degree (Chapelle et al 2010).....5.4 à 18°C
 Kn_alex = 3.93 ! Nitrogen half-saturation constant (micromol.L-1) (Davidson et al, 1999)
 Kp_alex = 0.28 ! Phosphorus half-concentration constant (micromol.L-1) (Labry et al, 2004) (But varies with dilution rate! 0.28 is the lowest value)
 Ksi_alex = 0.0 ! Alexandrium is not a diatom
 m_alex = 0.016 ! Mortality (Default value, the same as in Cugier et al, 2005 for dinoflagellates) (0)
 Topt_alex = 18.0 ! Temperature of maximum growth (Final deliverable 7) (???)
 Iopt_alex = 24.0 ! Irradiance of maximum growth (Final deliverable 7) (???) (Total irradiance, or PAR?) (Unknown value)
 l_alex = 18.0 / ! Size of Alexandrium minutum (in micron)

Biotic data/Creating species

```

PROGRAM NEWDATA_BIO

!-----Declarations -----

IMPLICIT NONE

LOGICAL si_alex, si_fixe
LOGICAL, DIMENSION(:), ALLOCATABLE :: si

CHARACTER(len=2) arg
CHARACTER(len=4) year_sim
CHARACTER(len=100) a, b, c, d, e
CHARACTER(len=24) nutFileName, fltFileName, somlitFileName, dtFileName, kparFileName
CHARACTER(len=24) forcingsFileName

INTEGER kopt,kl,ks,k,koptI
REAL (KIND=4), DIMENSION(:), ALLOCATABLE :: v_ls,v_topt,v_Iopt
REAL (KIND=4) g,h

INTEGER i,j,ns,imax,eof,jmax,nsim,nb_t1,nb_t2,nb_t3
INTEGER day_nut(12), month_nut(12), year_nut(12), dn_nut(12)
INTEGER day_flt(366), month_flt(366), year_flt(366), dn_flt(366)
INTEGER day_rad(98), month_rad(98), year_rad(98), dn_rad(98)
INTEGER day_dil(366), month_dil(366), year_dil(366), dn_dil(366)
INTEGER day_kpar(366), month_kpar(366), year_kpar(366), dn_kpar(366)

REAL r,rand,odd
REAL(KIND=4) Riv_NH4(24),Riv_NO3(24),Riv_PO4(24),Riv_Pp(24),Riv_Si(24),Riv_NO2(24)
REAL(KIND=4) L(366), F(366), T(366), Tpd(366), Tpm(366), dilutd(366), dilutm(366), kpar(366)
REAL(KIND=4) Rad_NH4(98),Rad_NO3(98),Rad_NO2(98),Rad_PO4(98),Rad_Si(98)
REAL(KIND=4) gmax_alex,QminN_alex,QminP_alex,QmaxN_alex,QmaxP_alex,Qsi_alex,VmaxNH4_alex,VmaxNO3_alex,VmaxPO4_alex,&
Kn_alex,Kp_alex,Ksi_alex,m_alex,Topt_alex,Iopt_alex,l_alex
REAL(KIND=4) gmax_fixe,QminN_fixe,QminP_fixe,QmaxN_fixe,QmaxP_fixe,Qsi_fixe,VmaxNH4_fixe,VmaxNO3_fixe,VmaxPO4_fixe,&
Kn_fixe,Kp_fixe,Ksi_fixe,m_fixe,Topt_fixe,Iopt_fixe,l_fixe
REAL(KIND=4) gmax,QminN,QminP,QmaxN,QmaxP,VmaxNH4,VmaxNO3,VmaxPO4,Kn,Kp,Qsi,Ksi,m,Topt,Iopt,kT
REAL(KIND=4), DIMENSION(:), ALLOCATABLE :: gmaxs,QminNs,QminPs,QmaxNs,QmaxPs,VmaxNH4s,VmaxNO3s,VmaxPO4s, & Kns,Kps,Qsis,Ksis,ms,Topts,Iopts,ls
REAL(KIND=4) k_minN, k_nitrif, k_minP, k_dissSi,k_ads,k_des,Q_maxSM,Hd ,Hm ,Vd ,Vm

!----- Declares functions -----
INTEGER day_number
REAL interp

!----- Chooses the mode (physical inputs or species initialization) using keyboard instructions -----
100 WRITE(*,*) 'Biological (B) ? Physical (P) ? Both (BP) ? '
READ(*,*) arg
IF((arg .NE. 'B') .AND. (arg .NE. 'P') .AND. (arg .NE. 'BP')) GOTO 100

```

```

!----- Biological inputs -----
IF ((arg .EQ. 'B') .OR. (arg .EQ. 'BP')) THEN

!----- Extracts default parameters from namelist -----
OPEN(20, FILE='namelistIopt.dat', STATUS='OLD')
NAMELIST /PHY_CST/ k_minN,k_nitrif,k_minP,k_dissSi,k_ads,k_des,Q_maxSM,kT,Hd,Hm,Vd,Vm,nsim
READ(20, PHY_CST)
write(*,*)k_minN,k_nitrif,k_minP,k_dissSi,k_ads,k_des,Q_maxSM,kT,Hd,Hm,Vd,Vm,nsim

NAMELIST /BIO_PARAM/ ns,gmax,QminN,QminP,QmaxN,QmaxP,VmaxNH4,VmaxNO3,VmaxPO4,Kn,Kp,Qsi,Ksi,m,Topt,kT
READ(20, BIO_PARAM)
write(*,*)ns,gmax,QminN,QminP,QmaxN,QmaxP,VmaxNH4,VmaxNO3,VmaxPO4,Kn,Kp,Qsi,Ksi,m,Topt,Iopt,kT

!----- Extracts Alexandrium minutum parameters from namelist -----
NAMELIST /ALEXANDRIUM/ Si_alex,gmax_alex,QminN_alex,QminP_alex,QmaxN_alex,QmaxP_alex,Qsi_alex, &
VmaxNH4_alex,VmaxNO3_alex,VmaxPO4_alex,Kn_alex,Kp_alex,Ksi_alex,m_alex,Topt_alex,Iopt_alex,l_alex
READ(20, ALEXANDRIUM)

!----- Extracts fixed species parameters from namelist -----
! NAMELIST /FIXE/ gmax_fixe,QminN_fixe,QminP_fixe,QmaxN_fixe,QmaxP_fixe,VmaxNH4_fixe,VmaxNO3_fixe,&
! VmaxPO4_fixe,Kn_fixe,Kp_fixe,Qsi_fixe,Ksi_fixe,m_fixe,Topt_fixe,Iopt_fixe,l_fixe
! READ(20, FIXE)

CLOSE(20)

!----- Allocates arrays of each given parameters for all species -----
ALLOCATE(gmaxs(ns),QminNs(ns),QminPs(ns),QmaxNs(ns),QmaxPs(ns),VmaxNH4s(ns),VmaxNO3s(ns),VmaxPO4s(ns),Kns(ns),Kps(ns), &
Qsis(ns),Ksis(ns),ms(ns),Topts(ns),Iopts(ns),Si(ns),ls(ns))

OPEN(21, FILE='species6*6.dat', STATUS='UNKNOWN')
REWIND(21)
nb_t1=6 !ls !t1 and t2 are used to determine the total number of species e.g. 5*5 for 50, 7*7 for 98 etc.
nb_t2=6 !Topt
nb_t3=6 !Iopt
allocate(v_ls(nb_t1),v_topt(nb_t2),v_Iopt(nb_t3))

!.....Size.....

DO j=1, nsim
v_ls(1)=1.0
v_ls(nb_t1)=64.0
g=(v_ls(nb_t1)/v_ls(1))**(1.0/(nb_t1-1)) ! determines the size interval
do k=2,nb_t1
if (k==4) then ! k is the value of nb_t1 5/4
v_ls(k)=18.0
!v_ls(k)=v_ls(1)*g**(k-0.66) ! value of the 4th of the 5(nb_t1) .83/.66
else
v_ls(k)=v_ls(1)*g**(k-1)
endif
enddo
enddo

```



```

!.....Iopt.....

v_Iopt(1)=100.0
v_Iopt(nb_t3)=8.0
do k=2,nb_t3
  v_Iopt(k)=v_Iopt(k-1)+(v_Iopt(nb_t3)-v_Iopt(1))/(nb_t3-1)
enddo

!v_Iopt(1)=100.0
!v_Iopt(nb_t3)=8.0
!do k=2,nb_t3
!v_Iopt(k)=v_Iopt(k-1)+(v_Iopt(nb_t3)-v_Iopt(1))/(nb_t3-1)
!enddo

!.....Topt.....

v_topt(1)=10.0                                ! start of temp range
v_topt(nb_t2)=20.0                             ! determines the range of temperature or numb of temp columns
do k=2,nb_t2                                   ! Variation of Topt between 10 and 20, also numb of sp in each temp range/interval
  v_topt(k)=v_topt(k-1)+(v_topt(nb_t2)-v_topt(1))/(nb_t2-1)
enddo

!.....compiling all three parameters.....

k1=1
koptI=1
kopt=1
ks=1
do i=1,ns
  ls(i)=v_ls(k1)
  Iopts(i) = v_Iopt(koptI) Topts(i) = v_topt(kopt)
  if (ks==1) then
    Si(i) = .false.
  else
    Si(i) = .true.
  endif
  if (k1 == nb_t1) then                                ! Determines the number of sp in each temperature range
    k1=1
    kopt=kopt+1
    if (kopt==nb_t2+1) then                             ! separates nsi from si after the total numb of k1
      kopt=1
      ks=2                                             ! For Si/nSi
    endif
  else
    k1=k1+1
  endif
  if (koptI == nb_t3) then
    koptI=1
  else
    koptI=koptI+1
  endif
endif

```

```

!-----Scaling (adapted from Edwards et al, 2012) -----

Kns(i) = Kn*ls(i)                                ! Nitrogen uptake half-saturation constant (Edwards et al, 2012)
Kps(i) = Kp*ls(i)                                ! Phosphorus uptake half-saturation constant (Edwards et al, 2012)
Ksis(i) = 0
IF (Si(i)) Ksis(i) = Ksi*ls(i)                    ! The same as in Edwards et al, 2012, for silica

QminNs(i) = QminN*(ls(i)**2.5)                    ! Nitrogen minimum quota (Maranon et al, 2013)
QminPs(i) = QminP*(ls(i)**2.5)                    ! Phosphorus minimum quota (Maranon et al, 2013)
Qsis(i) = 0
IF (Si(i)) Qsis(i) = Qsi*(ls(i)**2.5)
QmaxNs(i) = QmaxN*(ls(i)**0.25)                    ! Maximum quota grows with size faster than minimum quota (Maranon et al, 2013)
QmaxPs(i) = QmaxP*(ls(i)**0.25)

VmaxNH4s(i) = VmaxNH4*(ls(i)**0.4)                ! Vmax à 0°C = Vmax à 18°C / exp(kT*T°)....exp(kT*T°) = exp(0.063*18) = 3.108
VmaxNO3s(i) = VmaxNO3*(ls(i)**0.4)                ! Maximum uptake rate (of ammonium) grows faster than cell quotas (Maranon et al, 2013)
VmaxPO4s(i) = VmaxPO4*(ls(i)**0.4)                ! Maximum uptake rate of nitrate
! Iopts(i) = Iopt                                  ! Maximum uptake rate of phosphate
! ms(i) = m                                          ! Different light requirement for each species
!                                                    ! Same mortality for each species!

gmaxs(i) = gmax*exp(kT*Topts(i))                  ! Eppley (1972) curve
! VmaxNH4s(i) = VmaxNH4s(i)*exp(kT*Topts(i))
! VmaxNO3s(i) = VmaxNO3s(i)*exp(kT*Topts(i))        ! assigns Vmax with respect to Topt. Commented cos we want the same Vmax for each Size
! VmaxPO4s(i) = VmaxPO4s(i)*exp(kT*Topts(i))

end do

WRITE(21,'(A9, A9, 16A12)') ' Species', 'Diatom', 'gmax', 'QminN', 'QminP', 'QmaxN', &
                             'QmaxP', 'Qsi', 'VmaxNH4', 'VmaxNO3', 'VmaxPO4', 'Kn', 'Kp', 'Ksi', 'Topt', 'Iopt', 'mortality', 'length'

WRITE(21,*)

!----- Chracteristics of Alexandrium minutum -----
WRITE(21,'(A6, L5, 16E13.4)') 'Alex.m', Si_alex, gmax_alex, QminN_alex, QminP_alex, QmaxN_alex, QmaxP_alex, Qsi_alex, &
                             VmaxNH4_alex, VmaxNO3_alex, VmaxPO4_alex, Kn_alex, Kp_alex, Ksi_alex, Topt_alex, Iopt_alex, m_alex, l_alex
WRITE(21,*)

!----- Chracteristics d'une espèce fixe de même taille qu'Alex -----
! WRITE(21,'(A6, L5, 16E13.4)') 'Fixe', Si_fixe, gmax_fixe, QminN_fixe, QminP_fixe, QmaxN_fixe, QmaxP_fixe, Qsi_fixe, &
! VmaxNH4_fixe, VmaxNO3_fixe, VmaxPO4_fixe, Kn_fixe, Kp_fixe, Ksi_fixe, Topt_fixe, Iopt_fixe, m_fixe, l_fixe
! WRITE(21,*)

!----- Chracteristics of species -----
do i=1,ns
  WRITE(21,'(I5, L6, 16E13.4)') i+1, Si(i), gmaxs(i), QminNs(i), QminPs(i), QmaxNs(i), QmaxPs(i), Qsis(i), &
                                VmaxNH4s(i), VmaxNO3s(i), VmaxPO4s(i), Kns(i), Kps(i), Ksis(i), Topts(i), Iopts(i), ms(i), ls(i))
  WRITE(21,*)
end do
END DO
CLOSE(21)

ENDIF

END PROGRAM

```

Biotic data/Example of species

Species	Diatom	Qmin		μ_{\max}	Qmax		Qsi	Vmax			Kn	Kp	Ksi	Topt	Iopt	mortality	length
		N	P		N	P		NH4	NO3	PO4							
Alex	F	4.08E-06	1.95E-07	1.80	6.62	7.38	0E+00	1.16	0.58	1.86	3.93	0.28	0.00	18	24	0.02	18
2	F	2.90E-09	1.40E-10	1.09	2.00	2.00	0E+00	0.38	0.19	0.38	0.23	0.01	0.00	10	100	0.02	1
3	F	2.32E-08	1.12E-09	1.09	2.46	2.46	0E+00	0.53	0.27	0.53	0.53	0.03	0.00	10	84	0.02	2
4	F	1.86E-07	8.96E-09	1.09	3.03	3.03	0E+00	0.74	0.37	0.74	1.21	0.06	0.00	10	54	0.02	5
5	F	3.99E-06	1.92E-07	1.09	4.12	4.12	0E+00	1.21	0.60	1.21	4.14	0.20	0.00	10	24	0.02	18
6	F	1.19E-05	5.73E-07	1.09	4.60	4.60	0E+00	1.44	0.72	1.44	6.41	0.31	0.00	10	12	0.02	28
7	F	9.50E-05	4.59E-06	1.09	5.66	5.66	0E+00	2.01	1.00	2.01	14.72	0.70	0.00	10	8	0.02	64
8	F	2.90E-09	1.40E-10	1.24	2.00	2.00	0E+00	0.38	0.19	0.38	0.23	0.01	0.00	12	100	0.02	1
9	F	2.32E-08	1.12E-09	1.24	2.46	2.46	0E+00	0.53	0.27	0.53	0.53	0.03	0.00	12	84	0.02	2
10	F	1.86E-07	8.96E-09	1.24	3.03	3.03	0E+00	0.74	0.37	0.74	1.21	0.06	0.00	12	54	0.02	5
11	F	3.99E-06	1.92E-07	1.24	4.12	4.12	0E+00	1.21	0.60	1.21	4.14	0.20	0.00	12	24	0.02	18
12	F	1.19E-05	5.73E-07	1.24	4.60	4.60	0E+00	1.44	0.72	1.44	6.41	0.31	0.00	12	12	0.02	28
13	F	9.50E-05	4.59E-06	1.24	5.66	5.66	0E+00	2.01	1.00	2.01	14.72	0.70	0.00	12	8	0.02	64
14	F	2.90E-09	1.40E-10	1.40	2.00	2.00	0E+00	0.38	0.19	0.38	0.23	0.01	0.00	14	100	0.02	1
15	F	2.32E-08	1.12E-09	1.40	2.46	2.46	0E+00	0.53	0.27	0.53	0.53	0.03	0.00	14	84	0.02	2
16	F	1.86E-07	8.96E-09	1.40	3.03	3.03	0E+00	0.74	0.37	0.74	1.21	0.06	0.00	14	54	0.02	5
17	F	3.99E-06	1.92E-07	1.40	4.12	4.12	0E+00	1.21	0.60	1.21	4.14	0.20	0.00	14	24	0.02	18
18	F	1.19E-05	5.73E-07	1.40	4.60	4.60	0E+00	1.44	0.72	1.44	6.41	0.31	0.00	14	12	0.02	28
19	F	9.50E-05	4.59E-06	1.40	5.66	5.66	0E+00	2.01	1.00	2.01	14.72	0.70	0.00	14	8	0.02	64
20	F	2.90E-09	1.40E-10	1.59	2.00	2.00	0E+00	0.38	0.19	0.38	0.23	0.01	0.00	16	100	0.02	1
21	F	2.32E-08	1.12E-09	1.59	2.46	2.46	0E+00	0.53	0.27	0.53	0.53	0.03	0.00	16	84	0.02	2
22	F	1.86E-07	8.96E-09	1.59	3.03	3.03	0E+00	0.74	0.37	0.74	1.21	0.06	0.00	16	54	0.02	5
23	F	3.99E-06	1.92E-07	1.59	4.12	4.12	0E+00	1.21	0.60	1.21	4.14	0.20	0.00	16	24	0.02	18
24	F	1.19E-05	5.73E-07	1.59	4.60	4.60	0E+00	1.44	0.72	1.44	6.41	0.31	0.00	16	12	0.02	28
25	F	9.50E-05	4.59E-06	1.59	5.66	5.66	0E+00	2.01	1.00	2.01	14.72	0.70	0.00	16	8	0.02	64
26	F	2.90E-09	1.40E-10	1.80	2.00	2.00	0E+00	0.38	0.19	0.38	0.23	0.01	0.00	18	100	0.02	1
27	F	2.32E-08	1.12E-09	1.80	2.46	2.46	0E+00	0.53	0.27	0.53	0.53	0.03	0.00	18	84	0.02	2
28	F	1.86E-07	8.96E-09	1.80	3.03	3.03	0E+00	0.74	0.37	0.74	1.21	0.06	0.00	18	54	0.02	5
29	F	3.99E-06	1.92E-07	1.80	4.12	4.12	0E+00	1.21	0.60	1.21	4.14	0.20	0.00	18	24	0.02	18
30	F	1.19E-05	5.73E-07	1.80	4.60	4.60	0E+00	1.44	0.72	1.44	6.41	0.31	0.00	18	12	0.02	28
31	F	9.50E-05	4.59E-06	1.80	5.66	5.66	0E+00	2.01	1.00	2.01	14.72	0.70	0.00	18	8	0.02	64
32	F	2.90E-09	1.40E-10	2.05	2.00	2.00	0E+00	0.38	0.19	0.38	0.23	0.01	0.00	20	100	0.02	1
33	F	2.32E-08	1.12E-09	2.05	2.46	2.46	0E+00	0.53	0.27	0.53	0.53	0.03	0.00	20	84	0.02	2
34	F	1.86E-07	8.96E-09	2.05	3.03	3.03	0E+00	0.74	0.37	0.74	1.21	0.06	0.00	20	54	0.02	5
35	F	3.99E-06	1.92E-07	2.05	4.12	4.12	0E+00	1.21	0.60	1.21	4.14	0.20	0.00	20	24	0.02	18
36	F	1.19E-05	5.73E-07	2.05	4.60	4.60	0E+00	1.44	0.72	1.44	6.41	0.31	0.00	20	12	0.02	28
37	F	9.50E-05	4.59E-06	2.05	5.66	5.66	0E+00	2.01	1.00	2.01	14.72	0.70	0.00	20	8	0.02	64

39	T	2.32E-08	1.12E-09	1.09	2.46	2.46	2.32E-08	0.53	0.27	0.53	0.53	0.03	0.23	10	84	0.02	2
40	T	1.86E-07	8.96E-09	1.09	3.03	3.03	1.86E-07	0.74	0.37	0.74	1.21	0.06	0.53	10	54	0.02	5
41	T	3.99E-06	1.92E-07	1.09	4.12	4.12	3.99E-06	1.21	0.60	1.21	4.14	0.20	1.80	10	24	0.02	18
42	T	1.19E-05	5.73E-07	1.09	4.60	4.60	1.19E-05	1.44	0.72	1.44	6.41	0.31	2.79	10	12	0.02	28
43	T	9.50E-05	4.59E-06	1.09	5.66	5.66	9.50E-05	2.01	1.00	2.01	14.72	0.70	6.40	10	8	0.02	64
44	T	2.90E-09	1.40E-10	1.24	2.00	2.00	2.90E-09	0.38	0.19	0.38	0.23	0.01	0.10	12	100	0.02	1
45	T	2.32E-08	1.12E-09	1.24	2.46	2.46	2.32E-08	0.53	0.27	0.53	0.53	0.03	0.23	12	84	0.02	2
46	T	1.86E-07	8.96E-09	1.24	3.03	3.03	1.86E-07	0.74	0.37	0.74	1.21	0.06	0.53	12	54	0.02	5
47	T	3.99E-06	1.92E-07	1.24	4.12	4.12	3.99E-06	1.21	0.60	1.21	4.14	0.20	1.80	12	24	0.02	18
48	T	1.19E-05	5.73E-07	1.24	4.60	4.60	1.19E-05	1.44	0.72	1.44	6.41	0.31	2.79	12	12	0.02	28
49	T	9.50E-05	4.59E-06	1.24	5.66	5.66	9.50E-05	2.01	1.00	2.01	14.72	0.70	6.40	12	8	0.02	64
50	T	2.90E-09	1.40E-10	1.40	2.00	2.00	2.90E-09	0.38	0.19	0.38	0.23	0.01	0.10	14	100	0.02	1
51	T	2.32E-08	1.12E-09	1.40	2.46	2.46	2.32E-08	0.53	0.27	0.53	0.53	0.03	0.23	14	84	0.02	2
52	T	1.86E-07	8.96E-09	1.40	3.03	3.03	1.86E-07	0.74	0.37	0.74	1.21	0.06	0.53	14	54	0.02	5
53	T	3.99E-06	1.92E-07	1.40	4.12	4.12	3.99E-06	1.21	0.60	1.21	4.14	0.20	1.80	14	24	0.02	18
54	T	1.19E-05	5.73E-07	1.40	4.60	4.60	1.19E-05	1.44	0.72	1.44	6.41	0.31	2.79	14	12	0.02	28
55	T	9.50E-05	4.59E-06	1.40	5.66	5.66	9.50E-05	2.01	1.00	2.01	14.72	0.70	6.40	14	8	0.02	64
56	T	2.90E-09	1.40E-10	1.59	2.00	2.00	2.90E-09	0.38	0.19	0.38	0.23	0.01	0.10	16	100	0.02	1
57	T	2.32E-08	1.12E-09	1.59	2.46	2.46	2.32E-08	0.53	0.27	0.53	0.53	0.03	0.23	16	84	0.02	2
58	T	1.86E-07	8.96E-09	1.59	3.03	3.03	1.86E-07	0.74	0.37	0.74	1.21	0.06	0.53	16	54	0.02	5
59	T	3.99E-06	1.92E-07	1.59	4.12	4.12	3.99E-06	1.21	0.60	1.21	4.14	0.20	1.80	16	24	0.02	18
60	T	1.19E-05	5.73E-07	1.59	4.60	4.60	1.19E-05	1.44	0.72	1.44	6.41	0.31	2.79	16	12	0.02	28
61	T	9.50E-05	4.59E-06	1.59	5.66	5.66	9.50E-05	2.01	1.00	2.01	14.72	0.70	6.40	16	8	0.02	64
62	T	2.90E-09	1.40E-10	1.80	2.00	2.00	2.90E-09	0.38	0.19	0.38	0.23	0.01	0.10	18	100	0.02	1
63	T	2.32E-08	1.12E-09	1.80	2.46	2.46	2.32E-08	0.53	0.27	0.53	0.53	0.03	0.23	18	84	0.02	2
64	T	1.86E-07	8.96E-09	1.80	3.03	3.03	1.86E-07	0.74	0.37	0.74	1.21	0.06	0.53	18	54	0.02	5
65	T	3.99E-06	1.92E-07	1.80	4.12	4.12	3.99E-06	1.21	0.60	1.21	4.14	0.20	1.80	18	24	0.02	18
66	T	1.19E-05	5.73E-07	1.80	4.60	4.60	1.19E-05	1.44	0.72	1.44	6.41	0.31	2.79	18	12	0.02	28
67	T	9.50E-05	4.59E-06	1.80	5.66	5.66	9.50E-05	2.01	1.00	2.01	14.72	0.70	6.40	18	8	0.02	64
68	T	2.90E-09	1.40E-10	2.05	2.00	2.00	2.90E-09	0.38	0.19	0.38	0.23	0.01	0.10	20	100	0.02	1
69	T	2.32E-08	1.12E-09	2.05	2.46	2.46	2.32E-08	0.53	0.27	0.53	0.53	0.03	0.23	20	84	0.02	2
70	T	1.86E-07	8.96E-09	2.05	3.03	3.03	1.86E-07	0.74	0.37	0.74	1.21	0.06	0.53	20	54	0.02	5
71	T	3.99E-06	1.92E-07	2.05	4.12	4.12	3.99E-06	1.21	0.60	1.21	4.14	0.20	1.80	20	24	0.02	18
72	T	1.19E-05	5.73E-07	2.05	4.60	4.60	1.19E-05	1.44	0.72	1.44	6.41	0.31	2.79	20	12	0.02	28
73	T	9.50E-05	4.59E-06	2.05	5.66	5.66	9.50E-05	2.01	1.00	2.01	14.72	0.70	6.40	20	8	0.02	64

Abiotic data/Creating forcings

```
PROGRAM NEWDATA_PHY
```

```
!-----Declarations -----
```

```
IMPLICIT NONE
```

```
LOGICAL si_alex
```

```
LOGICAL, DIMENSION(:), ALLOCATABLE :: si
```

```
CHARACTER(len=2) arg
```

```
CHARACTER(len=4) year_sim
```

```
CHARACTER(len=100) a, b, c, d, e
```

```
CHARACTER(len=24) orgFileName, nutFileName, fltFileName, somlitFileName, dtFileName, kparFileName
```

```
CHARACTER(len=24) forcingsFileName
```

```
INTEGER i,j,ns,imax,eof,jmax,ymax,nsim
```

```
INTEGER day_nut(12), month_nut(12), year_nut(12), dn_nut(12)
```

```
INTEGER day_org(12), month_org(12), year_org(12), dn_org(12)
```

```
INTEGER dayflt(366), monthflt(366), yearflt(366), dnflt(366)
```

```
INTEGER dayrad(98), monthrad(98), yearrad(98), dnrad(98)
```

```
INTEGER daydil(366), monthdil(366), yeardil(366), dndil(366)
```

```
INTEGER daykpar(366), monthkpar(366), yearkpar(366), dnkpar(366)
```

```
REAL r,rand,odd
```

```
REAL(KIND=4) Riv_NH4(24),Riv_NO3(24),Riv_PO4(24),Riv_Pp(24),Riv_Si(24),Riv_NO2(24),N_orgRiv(24),P_orgRiv(24),N_orgRad(24),P_orgRad(24)
```

```
REAL(KIND=4) L(366), F(366), T(366), Tpd(366), Tpm(366), dilutd(366), dilutm(366), kpar(366)
```

```
REAL(KIND=4) Rad_NH4(98),Rad_NO3(98),Rad_NO2(98),Rad_PO4(98),Rad_Si(98)
```

```
REAL(KIND=4) gmax_alex,qminN_alex,qminP_alex,qmaxN_alex,qmaxP_alex,qsi_alex,vmaxNH4_alex,vmaxNO3_alex,vmaxPO4_alex,&  
Kn_alex,kp_alex,ksi_alex,m_alex,topt_alex,iopt_alex,l_alex
```

```
REAL(KIND=4) gmax,qminN,qminP,qmaxN,qmaxP,vmaxNH4,vmaxNO3,vmaxPO4,Kn,Kp,Qsi,Ksi,m,topt,I0,kT
```

```
REAL(KIND=4), DIMENSION(:), ALLOCATABLE :: gmaxs,qminNs,qminPs,qmaxNs,qmaxPs,vmaxNH4s,vmaxNO3s,vmaxPO4s, & Kns,Kps,Qsis,Ksis,ms,Topts,I0s,ls
```

```
REAL(KIND=4) k_minN, k_nitrif, k_minP, k_disssi,k_ads,k_des,Q_maxSM,Hd ,Hm ,Vd ,Vm
```

```
!----- Declares functions -----
```

```
INTEGER day_number
```

```
REAL interp
```

```
!----- Chooses the mode (physical inputs or species initialization) using keyboard instructions -----
```

```
!100 WRITE(*,*) 'Biological (B) ? Physical (P) ? Both (BP) ?'
```

```
!READ(*,*) arg
```

```
!IF((arg .NE. 'B') .AND. (arg .NE. 'P') .AND. (arg .NE. 'BP')) GOTO 100
```

```
arg = 'P'
```

```
IF((arg .EQ. 'P') .OR. (arg .EQ. 'BP')) then
```

```
200 WRITE(*,*) '2009 ? 2010 ? 2011 ? 2012 ? 2013 ? 2014 ? 2015 ? 2016 ? 2017 ? 2018 ? 2019 ?'
```

```
READ(*,*) year_sim
```

```
IF((year_sim .NE. '2009') .AND. (year_sim .NE. '2010') .AND. (year_sim .NE. '2011') .AND. (year_sim .NE. '2012') .AND. (year_sim .NE. '2013') .AND. (year_sim .NE. '2014') .AND. (year_sim .NE. '2015') .AND. (year_sim .NE. '2016') .AND. (year_sim .NE. '2017') .AND. (year_sim .NE. '2018') .AND. (year_sim .NE. '2019')) GOTO 200
```

```
END IF
```

```
orgFileName = "input_orga_"//year_sim//".dat"
```

```
write(*,*) orgFileName
```

```
nutFileName = "input_nutrients_"//year_sim//".dat"
```

```
write(*,*) nutFileName
```

```
fltFileName = "input_flt_"//year_sim//".dat"
```

```
write(*,*) fltFileName
```

```

dtFileName = "input_dt_"//year_sim//".dat"
write(*,*) dtFileName

kparFileName = "input_kpar_"//year_sim//".dat"
write(*,*) kparFileName

somlitFileName = "input_somlit_"//year_sim//".dat"
write(*,*) somlitFileName

forcingsFileName = "forcings_"//year_sim//".dat"
write(*,*) forcingsFileName

!----- Physical inputs -----

IF ((arg .EQ. 'P') .OR. (arg .EQ. 'BP')) THEN

  WRITE(*,*)
  WRITE(*,*) '----- Reads the organic nutrient data file ----- '
  OPEN(10, FILE=orgFileName, FORM='formatted') ! Opens monthly data on nutrients concentration in the Mignonne river from 2009 to 2016
  REWIND(10)
  READ(10,*)
  READ(10,*)

  IF ((year_sim .EQ. '2009' .AND. year_sim .EQ. '2010' .AND. year_sim .EQ. '2011' .AND. year_sim .EQ. '2012')) THEN
    ymax = 12
  ELSE
    ymax = 6
  END IF

  DO i=1,ymax
    READ(10,'(a)') a ! Reads all the lines
    READ(a(1:2),'(I2)') day_org(i) ! Extracts day from 2 first characters (date : dd/mm/yyyy)
    READ(a(4:5),'(I2)') month_org(i) ! Extracts month from characters 4 and 5 (date : dd/mm/yyyy)
    READ(a(7:10),'(I4)') year_org(i) ! Extracts year from character 7 to 10 (date : dd/mm/yyyy)
    dn_org(i) = day_number(day_org(i),month_org(i),year_org(i)) ! Computes the day number of current day for further use (interpolation)

    READ(a(11:),*) N_orgRiv(i), P_orgRiv(i), N_orgRad(i), P_orgRad(i) ! Already in micromol/l, N:P <- 16:1
  END DO
  CLOSE(10)

  do i=1,ymax
    WRITE(*,*) dn_org(i), N_orgRiv(i), P_orgRiv(i), N_orgRad(i), P_orgRad(i)
  end do

  WRITE(*,*) ' ----- '
  WRITE(*,*)

  WRITE(*,*) '----- Reads the inorganic nutrient data file ----- '
  OPEN(11, FILE=nutFileName, FORM='formatted') ! Opens monthly data on nutrients concentration in the Mignonne river from 2009 to 2016
  REWIND(11)
  READ(11,*)
  READ(11,*)

```



```

DO i=1,12
  READ(11,'(a)') a
  READ(a(1:2),'(I2)') day_nut(i)
  READ(a(4:5),'(I2)') month_nut(i)
  READ(a(7:10),'(I4)') year_nut(i)
  dn_nut(i) = day_number(day_nut(i),month_nut(i),year_nut(i))
  ! Reads all the line
  ! Extracts day from 2 first characters (date : dd/mm/yyyy)
  ! Extracts month from characters 4 and 5 (date : dd/mm/yyyy)
  ! Extracts year from charcater 7 to 10 (date : dd/mm/yyyy)
  ! Computes the day number of current day for further use (interpolation)

  READ(a(11:),*) Riv_NH4(i), Riv_NO3(i), Riv_PO4(i), Riv_Si(i), Riv_NO2(i)
  Riv_NH4(i) = Riv_NH4(i) * (1000d0/18d0)
  Riv_NO3(i) = Riv_NO3(i) * (1000d0/62d0)
  Riv_PO4(i) = Riv_PO4(i) * (1000d0/95d0)
  !Riv_Pp(i) = Riv_Pp(i) * (1000d0/31d0)
  Riv_Si(i) = Riv_Si(i) * (1000d0/28d0)
  Riv_NO2(i) = Riv_NO2(i) * (1000d0/46d0)
  ! Converts mg/l into micromol/l. .... ((mg/l)/(g/mol))*1000
  ! Converts mg/l into micromol/l
  ! Converts mg/l into micromol/l
  ! Converts mg/l into micromol/l
  ! Converts mg/l into micromol/l
  ! Converts mg/l into micromol/l
END DO
CLOSE(11)

do i=1,12
  WRITE(*,*) dn_nut(i),Riv_NH4(i),Riv_NO3(i),Riv_PO4(i),Riv_Si(i),Riv_NO2(i)
end do

WRITE(*,*) ' ----- '
WRITE(*,*)
WRITE(*,*)
WRITE(*,*) '--- Reads the light, temperature and flow data file -- '
WRITE(*,*)
OPEN(12, FILE=fltFileName, FORM='formatted')
REWIND(12)
READ(12,*)
READ(12,*)
IF (year_sim .EQ. '2012' .OR. year_sim .EQ. '2016') THEN
  imax = 366
ELSE
  imax = 365
END IF

do i=1,imax
  READ(12,'(a)') b
  READ(b(1:2),'(I2)') day_flt(i)
  READ(b(4:5),'(I2)') month_flt(i)
  READ(b(7:10),'(I4)') year_flt(i)
  dn_flt(i) = day_number(day_flt(i),month_flt(i),year_flt(i))
  READ(b(11:),*) L(i), T(i), F(i)
  F(i) = F(i)*86400d0
  ! Reads all the line
  ! Extracts day from 2 first characters (date : dd/mm/yyyy)
  ! Extracts month from characters 4 and 5 (date : dd/mm/yyyy)
  ! Extracts year from charcater 7 to 10 (date : dd/mm/yyyy)
  ! Computes the day number of current day for further use (interpolation)
  ! Converts m3/s into m3/d
end do
CLOSE(12)

do i=1,imax
  WRITE(*,*) dn_flt(i),L(i),T(i),F(i)
end do
WRITE(*,*) ' ----- '
WRITE(*,*)
WRITE(*,*)

```

```

WRITE(*,*) '----- Reads the dilution data file ----- '
WRITE(*,*)
! dilutd(:) = 0.331 ! Default initialization of dilution in the bay of Daoulas
! dilutm(:) = 0.355 ! Default initialization of dilution in the estuary of Mignonne

OPEN(13, FILE=dtFileName, FORM='formatted')
REWIND(13)
READ(13,*)
IF (year_sim .EQ. '2012' .OR. year_sim .EQ. '2016') THEN
    imax = 366
ELSE
    imax = 365
END IF

do i=1,imax
    READ(13,'(a)') c ! Puts the whole line into a character string
    READ(c(1:2),'(I2)') day_dil(i) ! Reads the beginning date of the simulation
    READ(c(4:5),'(I2)') month_dil(i)
    READ(c(7:10),'(I4)') year_dil(i)
    dn_dil(i) = day_number(day_dil(i),month_dil(i),year_dil(i)) ! Computes the day number of current day for further use (interpolation)
    READ(c(11:),*) dilutm(i) ! Dilution (Mignonne) for current date
end do
CLOSE(13)

do i=1,imax
    WRITE(*,*) dn_dil(i),dilutm(i)
end do
WRITE(*,*)
WRITE(*,*) '----- '
WRITE(*,*)

kpar(:) = 0.3
WRITE(*,*)
WRITE(*,*) '----- Reads the Kpar data file ----- '
WRITE(*,*)

OPEN(14, FILE=kparFileName, FORM='formatted') ! Opens daily Kpar data file
REWIND(14)
READ(14,*)
IF (year_sim .EQ. '2012' .OR. year_sim .EQ. '2016') THEN
    imax = 366
ELSE
    imax = 365
END IF

do i=1,imax
    READ(14,'(a)') d ! Puts the whole line into a character string
    READ(d(1:2),'(I2)') day_kpar(i) ! Reads the date of the value
    READ(d(4:5),'(I2)') month_kpar(i)
    READ(d(7:10),'(I4)') year_kpar(i)
    dn_kpar(i) = day_number(day_kpar(i),month_kpar(i),year_kpar(i)) ! Computes the day number of current day for further use (interpolation)
    READ(d(11:),*) kpar(i) ! Kpar (Daoulas) for current date. Diff between Daoulas and Mignonne is neglected
end do
CLOSE(14)

```

```

do i=1,imax
  WRITE(*,*) dn_kpar(i),kpar(i)
end do
WRITE(*,*)
WRITE(*,*) '-----'

WRITE(*,*)
WRITE(*,*) '----- SOMLIT data file open -----'
WRITE(*,*)

OPEN(15, FILE=somlitFileName, STATUS='OLD')
WRITE(*,*)
REWIND(15)
READ(15,*)
READ(15,*)

jmax=0
DO WHILE(eof==0)
  READ(15,*,iostat=eof)
  IF(eof==0) jmax=jmax+1
END DO

WRITE(*,*)jmax, ' records in ',somlitFileName
WRITE(*,*)
REWIND(15)
READ(15,*)
READ(15,*) ! Line 1 is name of variables

do i=1,jmax
  READ(15,'(a)') e ! Read nutrient data is the rade de Brest
  READ(e(1:4),'(I4)') year_rad(i) ! Reads all the line
  READ(e(6:7),'(I2)') month_rad(i) ! Extracts day from 2 first characters (date : dd/mm/yyyy)
  READ(e(9:10),'(I2)') day_rad(i) ! Extracts month from characters 4 and 5 (date : dd/mm/yyyy)
  ! Extracts year from charcater 7 to 10 (date : dd/mm/yyyy)
  dn_rad(i) = day_number(day_rad(i),month_rad(i),year_rad(i)) ! Computes the day number of current day for further use (interpolation)
  READ(e(11:),*) Rad_NH4(i),Rad_NO3(i),Rad_PO4(i),Rad_Si(i),Rad_NO2(i)
end do
CLOSE(15)

WRITE(*,*) '-----Reads Rad_NH4, Rad_NO3, Rad_PO4, Rad_Si and Rad_NO2-----'
WRITE(*,*)

do i=1,jmax
  WRITE(*,*) dn_rad(i),Rad_NH4(i),Rad_NO3(i),Rad_PO4(i),Rad_Si(i),Rad_NO2(i)
end do WRITE(*,*)

WRITE(*,*) 'All input files read'
WRITE(*,*)
WRITE(*,*) '-----'

WRITE(*,*) '----- Creating physical parameters -----'
OPEN(16, FILE=forcingsFileName, FORM='formatted')
WRITE(*,*) 'Output file open'
REWIND(16)

IF (year_sim.EQ. '2012' .OR. year_sim.EQ. '2016') THEN
  imax = 366
ELSE
  imax = 365
END IF

```

```

WRITE(16,'(A19)') 'Temp in (degC)', 'Light in (w/m2)', 'Flow in (m3/d)', 'Riv_XXX in (muMol)', 'Kpar in (m-1)', 'Rad_XXX in (muMol)'
WRITE(16,*)
WRITE(16,'(A3, 19A13)') 'Day', 'Temperature', 'Light', 'Dilution', 'Flow', 'Riv_NH4', 'Riv_NO3+NO2', 'Riv_PO4+Pp', &
                        'Riv_Si', 'Kpar', 'Rad_NH4', 'Rad_NO3+NO2', 'Rad_PO4', 'Rad_Si', 'N_orgRiv', 'P_orgRiv', 'N_orgRad', 'P_orgRad'

do i=1,imax
  WRITE(16,'(I3, 19F13.4)') i, T(i), L(i), dilutm(i), F(i), interp(Riv_NH4,dn_nut(1:12),12,i), interp(Riv_NO3+Riv_NO2,dn_nut(1:12),12,i), &
    interp(Riv_PO4,dn_nut(1:12),12,i), interp(Riv_Si,dn_nut(1:12),12,i), Kpar(i), interp(Rad_NH4,dn_rad(1:jmax),jmax,i), &
    interp(Rad_NO3+Rad_NO2,dn_rad(1:jmax),jmax,i), interp(Rad_PO4,dn_rad(1:jmax),jmax,i), interp(Rad_Si,dn_rad(1:jmax),jmax,i), &
    interp(N_orgRiv,dn_org(1:ymax),ymax,i), interp(P_orgRiv,dn_org(1:ymax),ymax,i), interp(N_orgRad,dn_org(1:ymax),ymax,i), &
    interp(P_orgRad,dn_org(1:ymax),ymax,i)

end do
CLOSE(16)

WRITE(*,*) 'File written'
WRITE(*,*) '-----'
WRITE(*,*)

ENDIF

END PROGRAM

!-----
INTEGER FUNCTION day_number(day, month)
! This function transforms a date into a day_number of the year (from 1 to 365)
!-----

INTEGER, intent(in) :: day, month

day_number = day + floor((month-1)*30.5 -1.5)
IF ((month .EQ. 9) .OR. (month .EQ. 11)) day_number = day_number + 1
IF ((month .EQ. 1) .OR. (month .EQ. 2)) day_number = day_number + 2

return

END FUNCTION

!-----
REAL FUNCTION interp(arr,dn,l,i)
! This function interpolates a value in a linear way using monthly values in array arr taken at times in array dn
!-----

REAL, intent(in) :: arr(l)
INTEGER, intent(in) :: dn(l)
INTEGER, intent(in) :: l,i
INTEGER j
! l is the length of the arrays, i is the current day
! i is in the (j-1)th interval (j from 0 to l)

IF (i .LT. dn(1)) interp = arr(1)
do j=1,l-1
  IF ((i .GE. dn(j)) .AND. (i .LT. dn(j+1))) then
    interp = arr(j) + ((REAL(i-dn(j)))/(REAL(dn(j+1)-dn(j))))*(arr(j+1)-arr(j))
    exit
  ENDIF
end do
IF (i .GE. dn(l)) interp = arr(l)

return

END FUNCTION

```

Abiotic data/Example of forcings

Day	Temper.	Light	Dilution	Flow	Riv_NH4	Riv_NO3	Riv_PO4	Riv_Si	Kpar	Rad_NH4	Rad_NO3	Rad_PO4	Rad_Si	N_org	P_org
1	10.9	17	0.45	1,130,112	5.56	404.1	0.74	204	0.43	0.87	15.43	0.41	6.32	35.71	0.32
2	10.4	50	0.42	802,656	5.56	404.1	0.74	204	0.42	0.87	15.43	0.41	6.32	35.71	0.32
3	10.4	15	0.33	523,584	5.56	404.1	0.74	204	0.42	0.87	15.43	0.41	6.32	35.71	0.32
4	9.8	29	0.35	412,992	5.56	404.1	0.74	204	0.43	0.87	15.43	0.41	6.32	35.71	0.32
5	9.9	19	0.32	358,560	5.56	404.1	0.74	204	0.43	0.87	15.43	0.41	6.32	35.71	0.32
6	9.9	29	0.44	307,584	5.56	404.1	0.74	204	0.42	0.87	15.43	0.41	6.32	35.71	0.31
7	10.0	25	0.43	286,848	5.56	404.1	0.74	204	0.40	0.87	15.43	0.41	6.32	35.71	0.31
8	10.3	28	0.48	257,472	5.56	404.1	0.74	204	0.38	0.86	15.94	0.41	6.48	35.71	0.31
9	10.4	36	0.5	235,008	5.56	404.1	0.74	204	0.37	0.85	16.44	0.41	6.63	35.71	0.31
10	10.4	34	0.51	209,088	5.56	404.1	0.74	204	0.36	0.85	16.95	0.41	6.79	35.71	0.30
11	10.4	36	0.52	190,080	5.51	403.6	0.73	292	0.34	0.84	17.46	0.41	6.95	35.71	0.30
12	10.4	53	0.49	174,528	5.46	403.1	0.72	381	0.36	0.83	17.96	0.41	7.10	35.71	0.30
13	11.1	42	0.47	164,160	5.41	402.7	0.72	469	0.37	0.82	18.47	0.41	7.26	35.71	0.30
14	10.5	75	0.42	153,792	5.36	402.2	0.71	558	0.39	0.82	18.98	0.41	7.42	35.71	0.29
15	9.8	32	0.4	145,152	5.31	401.7	0.71	646	0.41	0.81	19.48	0.41	7.57	35.71	0.29
16	9.5	78	0.42	135,648	5.26	401.2	0.70	735	0.38	0.80	19.99	0.41	7.73	35.71	0.29
17	9.4	41	0.39	126,144	5.21	400.8	0.69	823	0.39	0.79	19.62	0.43	7.62	35.71	0.29
18	9.6	25	0.36	138,240	5.16	400.3	0.69	912	0.41	0.79	19.24	0.44	7.52	35.71	0.28
19	9.9	21	0.32	140,832	5.11	399.8	0.68	1,001	0.40	0.78	18.87	0.46	7.41	35.71	0.28
20	10.0	34	0.34	130,464	5.07	399.4	0.67	1,089	0.40	0.77	18.49	0.47	7.30	35.71	0.28
21	10.3	27	0.35	139,104	5.02	398.9	0.67	1,178	0.39	0.76	18.17	0.46	7.20	35.71	0.28
22	10.5	33	0.41	129,600	4.97	398.4	0.66	1,266	0.40	0.74	17.85	0.46	7.09	35.71	0.27
23	10.6	32	0.44	114,912	4.92	397.9	0.66	1,355	0.40	0.73	17.52	0.45	6.99	35.71	0.27
24	10.6	30	0.42	120,960	4.87	397.5	0.65	1,443	0.40	0.71	17.20	0.45	6.89	35.71	0.27
25	10.6	23	0.41	113,184	4.82	397.0	0.64	1,532	0.40	0.70	16.88	0.44	6.78	35.71	0.27
26	10.4	63	0.42	129,600	4.77	396.5	0.64	1,620	0.40	0.68	16.56	0.44	6.68	35.71	0.26
27	10.1	76	0.43	112,320	4.72	396.0	0.63	1,709	0.41	0.67	16.23	0.43	6.58	35.71	0.26
28	10.0	82	0.41	129,600	4.67	395.6	0.63	1,797	0.40	0.65	15.91	0.43	6.47	35.71	0.26
29	9.7	60	0.42	108,000	4.62	395.1	0.62	1,886	0.41	0.64	15.59	0.42	6.37	35.71	0.26
30	9.6	45	0.4	177,984	4.58	394.6	0.61	1,975	0.41	0.63	15.73	0.42	6.41	35.71	0.25
31	9.4	27	0.36	191,808	4.53	394.1	0.61	2,063	0.39	0.62	15.86	0.42	6.45	35.71	0.25

Day	Temper.	Light	Dilution	Flow	Riv_NH4	Riv_NO3	Riv_PO4	Riv_Si	Kpar	Rad_NH4	Rad_NO3	Rad_PO4	Rad_Si	N_org	P_org
32	8.8	75	0.32	135,648	4.48	393.7	0.60	2,152	0.38	0.61	16.00	0.42	6.49	35.71	0.25
33	8.3	105	0.32	124,416	4.43	393.2	0.59	2,240	0.38	0.61	16.13	0.42	6.53	35.71	0.24
34	8.2	98	0.37	117,504	4.38	392.7	0.59	2,329	0.39	0.60	16.27	0.42	6.56	35.71	0.24
35	7.9	37	0.37	119,232	4.33	392.2	0.58	2,417	0.38	0.59	16.40	0.42	6.60	35.71	0.24
36	8.0	87	0.41	274,752	4.28	391.8	0.58	2,506	0.37	0.58	16.54	0.42	6.64	35.71	0.24
37	9.1	36	0.47	151,200	4.23	391.3	0.57	2,594	0.39	0.57	16.67	0.42	6.68	35.71	0.23
38	9.2	113	0.46	143,424	4.18	390.8	0.56	2,683	0.39	0.54	16.19	0.42	6.48	35.71	0.23
39	8.7	26	0.45	130,464	4.13	390.3	0.56	2,772	0.39	0.50	15.71	0.42	6.27	35.71	0.23
40	8.5	47	0.49	124,416	4.09	389.9	0.55	2,860	0.39	0.47	15.22	0.42	6.07	35.71	0.23
41	8.4	51	0.49	122,688	4.04	389.4	0.54	2,949	0.40	0.43	14.74	0.42	5.86	35.71	0.22
42	8.1	125	0.47	115,776	3.99	388.9	0.54	3,037	0.39	0.40	14.26	0.42	5.66	35.71	0.22
43	7.9	69	0.46	109,728	3.94	388.4	0.53	3,126	0.39	0.36	13.78	0.42	5.45	35.71	0.22
44	8.1	62	0.4	113,184	3.89	388.0	0.53	3,214	0.37	0.33	13.29	0.42	5.25	35.71	0.22
45	8.4	92	0.36	110,592	3.95	387.0	0.55	3,125	0.36	0.29	12.81	0.42	5.04	35.71	0.21
46	8.5	37	0.32	101,952	4.02	386.1	0.58	3,037	0.36	0.31	12.81	0.42	5.06	35.71	0.21
47	8.7	43	0.35	97,632	4.09	385.1	0.60	2,948	0.36	0.32	12.80	0.42	5.08	35.71	0.21
48	8.8	45	0.37	95,040	4.15	384.2	0.63	2,859	0.35	0.34	12.80	0.42	5.09	35.71	0.21
49	8.9	71	0.33	97,632	4.22	383.3	0.65	2,770	0.36	0.35	12.79	0.42	5.11	35.71	0.20
50	8.9	131	0.4	102,816	4.28	382.3	0.67	2,681	0.37	0.37	12.79	0.42	5.13	35.71	0.20
51	8.9	99	0.43	88,128	4.35	381.4	0.70	2,592	0.38	0.37	12.62	0.42	5.04	35.71	0.20
52	9.0	140	0.41	82,944	4.41	380.4	0.72	2,503	0.38	0.38	12.44	0.41	4.96	35.71	0.20
53	9.0	55	0.39	81,216	4.48	379.5	0.75	2,414	0.39	0.38	12.27	0.41	4.87	35.71	0.19
54	9.3	46	0.43	96,768	4.54	378.5	0.77	2,326	0.37	0.39	12.09	0.40	4.79	35.71	0.19
55	9.5	46	0.46	86,400	4.61	377.6	0.80	2,237	0.39	0.39	11.92	0.40	4.70	35.71	0.19
56	9.6	39	0.42	82,944	4.67	376.7	0.82	2,148	0.39	0.39	11.74	0.39	4.61	37.14	0.20
57	9.7	121	0.42	78,624	4.74	375.7	0.85	2,059	0.39	0.40	11.57	0.39	4.53	38.57	0.20
58	9.6	44	0.41	74,304	4.80	374.8	0.87	1,970	0.40	0.40	11.39	0.38	4.44	40.00	0.21
59	9.8	93	0.38	73,440	4.87	373.8	0.90	1,881	0.40	0.40	11.39	0.37	4.43	41.43	0.21
60	9.9	164	0.34	68,256	4.93	372.9	0.92	1,792	0.40	0.40	11.39	0.37	4.42	42.86	0.22
61	10.3	163	0.31	65,664	5.00	371.9	0.95	1,704	0.41	0.41	11.39	0.36	4.41	44.28	0.23
62	10.3	100	0.29	64,800	5.07	371.0	0.97	1,615	0.41	0.41	11.38	0.35	4.40	45.71	0.23

Day	Temper.	Light	Dilution	Flow	Riv_NH4	Riv_NO3	Riv_PO4	Riv_Si	Kpar	Rad_NH4	Rad_NO3	Rad_PO4	Rad_Si	N_org	P_org
63	10.6	122	0.26	68,256	5.13	370.1	1.00	1,526	0.42	0.41	11.38	0.35	4.39	47.14	0.24
64	10.6	130	0.32	218,592	5.20	369.1	1.02	1,437	0.42	0.41	11.38	0.34	4.38	48.57	0.25
65	10.1	136	0.35	110,592	5.26	368.2	1.05	1,348	0.42	0.41	11.01	0.34	4.21	50.00	0.25
66	10.1	158	0.41	89,856	5.33	367.2	1.07	1,259	0.42	0.41	10.64	0.34	4.04	50.00	0.26
67	10.1	78	0.36	105,408	5.39	366.3	1.10	1,170	0.42	0.41	10.28	0.34	3.87	50.00	0.26
68	9.9	68	0.46	98,496	5.46	365.3	1.12	1,082	0.42	0.41	9.91	0.34	3.70	50.00	0.26
69	10.0	115	0.48	85,536	5.52	364.4	1.15	993	0.42	0.42	9.54	0.33	3.54	50.00	0.27
70	10.3	79	0.48	81,216	5.59	363.5	1.17	904	0.42	0.42	9.17	0.33	3.37	50.00	0.27
71	10.5	98	0.44	79,488	5.65	362.5	1.20	815	0.43	0.42	8.81	0.33	3.20	50.00	0.27
72	10.7	193	0.42	77,760	5.72	361.6	1.22	726	0.44	0.42	8.44	0.33	3.03	50.00	0.28
73	10.9	198	0.4	75,168	5.78	360.6	1.24	637	0.44	0.42	8.07	0.33	2.86	50.00	0.28
74	10.9	201	0.37	72,576	5.85	359.7	1.27	548	0.44	0.44	7.95	0.32	2.80	50.00	0.28
75	11.0	113	0.35	70,848	5.92	358.8	1.29	459	0.43	0.45	7.82	0.31	2.73	50.00	0.29
76	11.0	66	0.32	69,120	5.98	357.8	1.32	371	0.42	0.47	7.70	0.30	2.67	50.00	0.29
77	10.9	75	0.33	80,352	6.05	356.9	1.34	282	0.44	0.48	7.57	0.29	2.60	50.00	0.29
78	11.0	150	0.34	77,760	6.11	355.9	1.37	193	0.43	0.50	7.45	0.28	2.54	50.00	0.30
79	10.9	216	0.37	66,528	6.06	355.9	1.36	193	0.44	0.48	6.78	0.25	2.31	50.00	0.30
80	10.9	173	0.4	63,072	6.01	355.9	1.34	193	0.46	0.47	6.11	0.23	2.09	50.00	0.30
81	10.9	122	0.4	62,208	5.95	355.9	1.33	192	0.47	0.45	5.43	0.20	1.86	50.00	0.31
82	11.0	96	0.41	63,072	5.90	355.9	1.32	192	0.47	0.44	4.76	0.17	1.63	50.00	0.31
83	11.2	206	0.39	60,480	5.85	355.9	1.30	192	0.48	0.42	4.09	0.14	1.40	50.00	0.31
84	11.5	228	0.38	59,616	5.79	355.8	1.29	192	0.48	0.40	3.42	0.12	1.18	50.00	0.32
85	11.9	230	0.38	57,024	5.74	355.8	1.27	192	0.47	0.39	2.74	0.09	0.95	50.00	0.32
86	12.1	221	0.36	55,296	5.69	355.8	1.26	191	0.46	0.37	2.07	0.06	0.72	50.00	0.32
87	12.2	237	0.34	53,568	5.63	355.8	1.25	191	0.45	0.39	1.91	0.06	0.66	50.00	0.33
88	12.5	241	0.33	51,840	5.58	355.8	1.23	191	0.45	0.40	1.76	0.05	0.59	50.00	0.33
89	12.7	243	0.31	51,840	5.53	355.8	1.22	191	0.46	0.42	1.60	0.05	0.53	50.00	0.33
90	13.0	242	0.29	50,976	5.48	355.8	1.21	191	0.44	0.44	1.44	0.04	0.47	50.00	0.34
91	13.2	246	0.25	50,112	5.42	355.7	1.19	191	0.46	0.46	1.28	0.04	0.41	50.00	0.34
92	12.6	251	0.26	49,248	5.37	355.7	1.18	190	0.45	0.47	1.13	0.03	0.34	50.00	0.34
93	12.5	251	0.3	47,520	5.32	355.7	1.17	190	0.46	0.49	0.97	0.03	0.28	50.00	0.35

Day	Temper.	Light	Dilution	Flow	Riv_NH4	Riv_NO3	Riv_PO4	Riv_Si	Kpar	Rad_NH4	Rad_NO3	Rad_PO4	Rad_Si	N_org	P_org
94	12.3	158	0.31	47,520	5.26	355.7	1.15	190	0.48	0.46	0.92	0.03	0.31	50.00	0.35
95	12.1	234	0.33	49,248	5.21	355.7	1.14	190	0.48	0.43	0.88	0.04	0.35	50.00	0.35
96	11.9	250	0.37	46,656	5.16	355.7	1.13	190	0.47	0.40	0.83	0.04	0.38	50.00	0.36
97	11.9	264	0.35	44,064	5.11	355.7	1.11	190	0.48	0.37	0.79	0.04	0.41	50.00	0.36
98	11.8	74	0.4	43,200	5.05	355.6	1.10	189	0.50	0.35	0.74	0.05	0.45	50.00	0.36
99	12.0	144	0.4	42,336	5.00	355.6	1.09	189	0.50	0.32	0.70	0.05	0.48	50.00	0.37
100	12.0	70	0.38	96,768	4.95	355.6	1.07	189	0.50	0.29	0.65	0.05	0.51	50.00	0.37
101	12.0	234	0.46	195,264	4.89	355.6	1.06	189	0.50	0.26	0.61	0.06	0.55	50.00	0.37
102	12.1	264	0.36	68,256	4.84	355.6	1.05	189	0.49	0.23	0.56	0.06	0.58	50.00	0.38
103	12.1	199	0.38	70,848	4.79	355.6	1.03	189	0.48	0.21	0.48	0.05	0.60	50.00	0.38
104	12.0	214	0.41	164,160	4.74	355.6	1.02	188	0.46	0.18	0.40	0.05	0.61	50.00	0.38
105	12.1	237	0.37	114,912	4.68	355.6	1.01	188	0.49	0.16	0.33	0.04	0.63	50.00	0.39
106	12.1	247	0.3	68,256	4.63	355.5	0.99	188	0.49	0.13	0.25	0.04	0.64	50.00	0.39
107	12.0	203	0.31	57,888	4.58	355.5	0.98	188	0.51	0.11	0.17	0.03	0.66	50.00	0.39
108	12.0	237	0.3	101,088	4.52	355.5	0.97	188	0.53	0.12	0.19	0.03	0.71	50.00	0.40
109	11.7	158	0.3	94,176	4.47	355.5	0.95	188	0.52	0.12	0.21	0.04	0.77	50.00	0.40
110	11.7	225	0.36	108,000	4.42	355.5	0.94	187	0.52	0.13	0.22	0.04	0.82	49.45	0.39
111	11.8	228	0.37	88,128	4.37	355.5	0.93	187	0.52	0.13	0.24	0.04	0.88	48.90	0.39
112	11.9	234	0.35	88,128	4.31	355.5	0.91	187	0.52	0.14	0.26	0.05	0.93	48.35	0.38
113	11.9	257	0.35	82,944	4.26	355.4	0.90	187	0.53	0.14	0.28	0.05	0.99	47.80	0.37
114	11.7	128	0.39	312,768	4.21	355.4	0.89	187	0.51	0.15	0.29	0.05	1.04	47.25	0.36
115	11.7	240	0.4	229,824	4.15	355.4	0.87	187	0.51	0.15	0.31	0.06	1.10	46.70	0.36
116	11.9	152	0.44	1,099,008	4.10	355.4	0.86	186	0.48	0.16	0.33	0.06	1.15	46.15	0.35
117	12.0	262	0.4	419,904	4.05	355.4	0.85	186	0.48	0.18	0.79	0.06	1.41	45.60	0.34
118	12.5	270	0.42	293,760	3.99	355.4	0.83	186	0.46	0.19	1.24	0.06	1.66	45.05	0.33
119	12.4	127	0.41	265,248	3.94	355.4	0.82	186	0.45	0.21	1.70	0.06	1.92	44.50	0.33
120	11.5	70	0.39	840,672	3.89	355.3	0.81	186	0.45	0.22	2.16	0.05	2.18	43.95	0.32
121	11.1	150	0.42	1,824,768	3.84	355.3	0.79	186	0.44	0.24	2.62	0.05	2.44	43.40	0.31
122	11.5	223	0.46	566,784	3.78	355.3	0.78	185	0.45	0.25	3.07	0.05	2.69	42.86	0.31
123	11.9	245	0.47	394,848	3.73	355.3	0.77	185	0.44	0.27	3.53	0.05	2.95	42.31	0.30
124	12.4	246	0.49	322,272	3.68	355.3	0.75	185	0.44	0.26	3.21	0.05	2.80	41.76	0.29

Day	Temper.	Light	Dilution	Flow	Riv_NH4	Riv_NO3	Riv_PO4	Riv_Si	Kpar	Rad_NH4	Rad_NO3	Rad_PO4	Rad_Si	N_org	P_org
125	12.4	75	0.58	590,112	3.62	355.3	0.74	185	0.45	0.25	2.89	0.05	2.66	41.21	0.28
126	12.3	114	0.54	393,984	3.57	355.3	0.73	185	0.46	0.24	2.56	0.05	2.51	40.66	0.28
127	12.5	315	0.55	302,400	3.52	355.2	0.71	185	0.48	0.24	2.24	0.05	2.37	40.11	0.27
128	13.0	186	0.5	273,024	3.47	355.2	0.70	184	0.47	0.23	1.92	0.04	2.22	39.56	0.26
129	13.2	188	0.52	240,192	3.41	355.2	0.69	184	0.43	0.22	1.60	0.04	2.07	39.01	0.25
130	13.6	94	0.46	343,008	3.36	355.2	0.67	184	0.41	0.21	1.27	0.04	1.93	38.46	0.25
131	13.8	75	0.55	1,368,576	3.31	355.2	0.66	184	0.40	0.20	0.95	0.04	1.78	37.91	0.24
132	13.6	207	0.49	483,840	3.25	355.2	0.65	184	0.39	0.31	2.26	0.05	2.30	37.36	0.23
133	13.5	334	0.43	347,328	3.20	355.2	0.63	184	0.39	0.41	3.57	0.05	2.81	36.81	0.23
134	13.3	336	0.44	298,944	3.15	355.2	0.62	183	0.38	0.52	4.88	0.06	3.33	36.26	0.22
135	14.2	286	0.41	265,248	3.10	355.1	0.61	183	0.37	0.63	6.19	0.07	3.85	35.71	0.21
136	14.0	298	0.37	236,736	3.04	355.1	0.59	183	0.37	0.73	7.50	0.07	4.36	36.32	0.21
137	14.3	335	0.43	203,904	2.99	355.1	0.58	183	0.37	0.84	8.81	0.08	4.88	36.93	0.22
138	14.3	181	0.39	186,624	2.94	355.1	0.57	183	0.39	0.87	8.58	0.09	4.75	37.55	0.22
139	14.3	117	0.39	181,440	2.88	355.1	0.55	182	0.39	0.90	8.34	0.11	4.61	38.16	0.23
140	13.9	132	0.45	164,160	2.83	355.1	0.54	182	0.40	0.92	8.11	0.12	4.48	38.77	0.23
141	13.7	170	0.42	158,976	2.78	355.1	0.53	182	0.40	0.95	7.87	0.13	4.34	39.38	0.23
142	13.8	277	0.4	148,608	2.78	352.2	0.54	183	0.41	0.98	7.64	0.14	4.21	40.00	0.24
143	14.2	191	0.43	133,056	2.78	349.3	0.55	185	0.43	1.01	7.40	0.16	4.07	40.61	0.24
144	14.7	287	0.43	123,552	2.78	346.4	0.56	186	0.46	1.03	7.17	0.17	3.94	41.22	0.25
145	15.1	343	0.42	113,184	2.78	343.5	0.56	187	0.48	1.06	6.93	0.18	3.80	41.83	0.25
146	15.6	322	0.39	105,408	2.78	340.6	0.57	189	0.48	0.95	6.27	0.16	3.47	42.45	0.25
147	15.7	156	0.37	100,224	2.78	337.7	0.58	190	0.48	0.84	5.61	0.13	3.14	43.06	0.26
148	15.7	211	0.36	96,768	2.78	334.8	0.59	191	0.48	0.73	4.95	0.11	2.81	43.67	0.26
149	16.2	218	0.34	91,584	2.78	331.9	0.60	193	0.49	0.62	4.28	0.09	2.49	44.28	0.27
150	16.5	329	0.36	87,264	2.78	329.0	0.61	194	0.49	0.51	3.62	0.07	2.16	44.89	0.27
151	17.3	234	0.36	81,216	2.78	326.1	0.62	195	0.48	0.40	2.96	0.04	1.83	45.51	0.27
152	17.3	257	0.37	74,304	2.78	323.2	0.63	196	0.48	0.29	2.30	0.02	1.50	46.12	0.28
153	17.0	346	0.38	69,120	2.78	320.3	0.64	198	0.48	0.31	2.25	0.03	1.50	46.73	0.28
154	17.1	159	0.36	66,528	2.78	317.4	0.65	199	0.47	0.33	2.20	0.03	1.50	47.34	0.28
155	16.9	252	0.35	65,664	2.78	314.6	0.66	200	0.49	0.36	2.15	0.04	1.50	47.96	0.29

Day	Temper.	Light	Dilution	Flow	Riv_NH4	Riv_NO3	Riv_PO4	Riv_Si	Kpar	Rad_NH4	Rad_NO3	Rad_PO4	Rad_Si	N_org	P_org
156	16.7	207	0.4	63,936	2.78	311.7	0.67	202	0.48	0.38	2.10	0.04	1.50	48.57	0.29
157	16.5	87	0.4	69,120	2.78	308.8	0.68	203	0.49	0.41	2.05	0.05	1.50	49.18	0.30
158	16.3	166	0.38	81,216	2.78	305.9	0.69	204	0.49	0.43	2.00	0.05	1.50	49.79	0.30
159	16.4	190	0.37	161,568	2.78	303.0	0.70	206	0.50	0.45	1.95	0.06	1.50	50.40	0.30
160	16.2	321	0.34	93,312	2.78	300.1	0.71	207	0.51	0.48	1.90	0.06	1.50	51.02	0.31
161	16.2	137	0.36	66,528	2.78	297.2	0.72	208	0.51	0.47	1.81	0.06	1.50	51.63	0.31
162	16.2	105	0.34	90,720	2.78	294.3	0.73	209	0.52	0.47	1.72	0.06	1.50	52.24	0.32
163	16.3	221	0.39	120,096	2.78	291.4	0.74	211	0.54	0.46	1.63	0.06	1.50	52.85	0.32
164	16.5	308	0.32	88,128	2.78	293.1	0.73	210	0.54	0.46	1.54	0.06	1.50	53.47	0.32
165	16.6	321	0.31	70,848	2.78	294.9	0.73	210	0.54	0.45	1.46	0.05	1.50	54.08	0.33
166	16.5	127	0.26	67,392	2.78	296.6	0.73	210	0.55	0.45	1.37	0.05	1.50	54.69	0.33
167	16.3	141	0.25	68,256	2.78	298.3	0.72	210	0.56	0.44	1.28	0.05	1.50	55.30	0.34
168	16.1	264	0.25	60,480	2.78	300.0	0.72	209	0.64	0.44	1.19	0.05	1.50	55.92	0.34
169	16.1	143	0.34	63,936	2.78	301.7	0.71	209	0.65	0.43	1.10	0.05	1.50	56.53	0.34
170	16.3	301	0.36	70,848	2.78	303.5	0.71	209	0.67	0.41	1.03	0.05	1.45	57.14	0.35
171	16.8	349	0.37	55,296	2.78	305.2	0.71	209	0.65	0.38	0.96	0.04	1.40	57.14	0.35
172	16.6	63	0.38	58,752	2.78	306.9	0.70	208	0.65	0.36	0.89	0.04	1.35	57.14	0.35
173	16.3	153	0.36	101,952	2.78	308.6	0.70	208	0.64	0.34	0.82	0.03	1.30	57.14	0.35
174	16.3	291	0.35	86,400	2.78	310.3	0.70	208	0.63	0.32	0.75	0.03	1.25	57.14	0.35
175	16.8	338	0.33	57,888	2.78	312.1	0.69	208	0.63	0.29	0.68	0.02	1.20	57.14	0.35
176	17.1	96	0.4	171,072	2.78	313.8	0.69	207	0.64	0.27	0.61	0.02	1.15	57.14	0.35
177	16.9	93	0.44	191,808	2.78	315.5	0.68	207	0.64	0.37	0.65	0.03	1.20	57.14	0.35
178	17.1	120	0.43	158,976	2.78	317.2	0.68	207	0.63	0.47	0.69	0.05	1.25	57.14	0.35
179	17.4	132	0.4	109,728	2.78	318.9	0.68	207	0.64	0.56	0.72	0.06	1.29	57.14	0.35
180	17.7	224	0.32	93,312	2.78	320.7	0.67	206	0.62	0.66	0.76	0.07	1.34	57.14	0.35
181	17.6	153	0.3	94,176	2.78	322.4	0.67	206	0.61	0.65	0.76	0.07	1.35	57.14	0.35
182	17.8	274	0.34	101,952	2.78	324.1	0.67	206	0.62	0.64	0.75	0.07	1.36	57.14	0.35
183	17.7	317	0.34	75,168	2.78	325.8	0.66	206	0.62	0.63	0.75	0.06	1.37	57.14	0.35
184	17.5	96	0.35	77,760	2.78	327.5	0.66	205	0.60	0.62	0.75	0.06	1.38	57.14	0.35
185	17.4	96	0.4	101,088	2.78	329.3	0.65	205	0.61	0.61	0.75	0.06	1.39	57.14	0.35
186	17.5	220	0.47	191,808	2.78	331.0	0.65	205	0.63	0.59	0.74	0.06	1.39	57.14	0.35

Day	Temper.	Light	Dilution	Flow	Riv_NH4	Riv_NO3	Riv_PO4	Riv_Si	Kpar	Rad_NH4	Rad_NO3	Rad_PO4	Rad_Si	N_org	P_org
187	17.7	226	0.5	218,592	2.78	332.7	0.65	205	0.61	0.58	0.74	0.06	1.40	57.14	0.35
188	17.8	306	0.52	346,464	2.78	334.4	0.64	204	0.61	0.57	0.74	0.05	1.41	57.14	0.35
189	17.7	116	0.5	486,432	2.78	336.1	0.64	204	0.60	0.56	0.73	0.05	1.42	57.14	0.35
190	17.6	298	0.47	311,904	2.78	337.9	0.64	204	0.60	0.55	0.73	0.05	1.43	57.14	0.35
191	18.0	183	0.44	216,000	2.78	339.6	0.63	204	0.59	0.53	0.69	0.05	1.35	57.14	0.35
192	17.9	198	0.39	182,304	2.78	340.7	0.64	204	0.58	0.51	0.65	0.05	1.27	57.14	0.35
193	17.9	234	0.35	171,936	2.78	341.9	0.65	204	0.58	0.49	0.61	0.04	1.19	57.14	0.35
194	17.7	90	0.33	190,944	2.78	343.0	0.65	205	0.57	0.47	0.57	0.04	1.11	57.14	0.35
195	17.3	93	0.38	232,416	2.78	344.1	0.66	205	0.58	0.45	0.53	0.04	1.03	57.14	0.35
196	17.3	273	0.37	250,560	2.78	345.3	0.67	205	0.59	0.43	0.49	0.04	0.95	57.14	0.35
197	17.6	338	0.35	156,384	2.78	346.4	0.68	206	0.60	0.41	0.45	0.03	0.87	57.14	0.35
198	17.9	280	0.34	139,104	2.78	347.5	0.68	206	0.59	0.39	0.41	0.03	0.79	57.14	0.35
199	18.4	245	0.4	134,784	2.78	348.7	0.69	207	0.58	0.38	0.41	0.03	0.76	57.14	0.35
200	18.2	102	0.39	130,464	2.78	349.8	0.70	207	0.59	0.37	0.42	0.03	0.73	57.14	0.35
201	17.9	202	0.41	126,144	2.78	350.9	0.71	207	0.56	0.37	0.42	0.03	0.70	57.14	0.35
202	18.0	323	0.44	115,776	2.78	352.1	0.71	208	0.56	0.36	0.43	0.03	0.67	57.14	0.35
203	18.1	322	0.44	104,544	2.78	353.2	0.72	208	0.56	0.35	0.43	0.03	0.63	57.14	0.35
204	18.3	334	0.44	95,904	2.78	354.4	0.73	209	0.57	0.34	0.44	0.03	0.60	57.14	0.35
205	18.8	332	0.43	88,128	2.78	355.5	0.74	209	0.56	0.34	0.44	0.03	0.57	57.14	0.35
206	19.0	332	0.4	81,216	2.78	356.6	0.74	209	0.57	0.33	0.45	0.03	0.54	57.14	0.35
207	19.3	331	0.38	74,304	2.78	357.8	0.75	210	0.56	0.32	0.45	0.03	0.51	57.14	0.35
208	19.7	296	0.36	69,984	2.78	358.9	0.76	210	0.53	0.31	0.57	0.03	0.53	57.14	0.35
209	19.9	275	0.3	67,392	2.78	360.0	0.77	210	0.51	0.30	0.69	0.04	0.54	57.14	0.35
210	19.3	284	0.31	63,936	2.78	361.2	0.77	211	0.50	0.28	0.80	0.04	0.56	57.14	0.35
211	19.0	263	0.34	74,304	2.78	362.3	0.78	211	0.49	0.27	0.92	0.04	0.57	57.14	0.35
212	19.1	308	0.35	63,072	2.78	363.4	0.79	212	0.50	0.27	0.91	0.04	0.61	57.14	0.35
213	19.3	243	0.35	62,208	2.78	364.6	0.80	212	0.49	0.27	0.91	0.05	0.66	57.14	0.35
214	19.3	136	0.36	63,936	2.78	365.7	0.80	212	0.48	0.27	0.90	0.05	0.70	57.14	0.35
215	19.1	209	0.36	63,072	2.78	366.9	0.81	213	0.47	0.27	0.90	0.05	0.74	57.14	0.35
216	19.0	221	0.35	59,616	2.78	368.0	0.82	213	0.47	0.26	0.89	0.05	0.78	57.14	0.35
217	18.9	191	0.36	61,344	2.78	369.1	0.83	214	0.47	0.26	0.88	0.06	0.83	57.14	0.35

Day	Temper.	Light	Dilution	Flow	Riv_NH4	Riv_NO3	Riv_PO4	Riv_Si	Kpar	Rad_NH4	Rad_NO3	Rad_PO4	Rad_Si	N_org	P_org
218	18.9	198	0.35	59,616	2.78	370.3	0.83	214	0.45	0.26	0.88	0.06	0.87	57.14	0.35
219	18.7	190	0.36	57,024	2.78	371.4	0.84	214	0.44	0.26	0.87	0.06	0.91	57.14	0.35
220	18.9	281	0.35	52,704	2.78	370.9	0.91	215	0.44	0.26	0.80	0.06	0.88	57.14	0.35
221	19.5	305	0.33	49,248	2.78	370.5	0.97	215	0.44	0.25	0.73	0.06	0.84	57.14	0.35
222	19.7	301	0.3	46,656	2.78	370.0	1.03	216	0.45	0.25	0.66	0.05	0.81	57.14	0.35
223	19.9	300	0.27	44,064	2.78	369.6	1.09	216	0.43	0.25	0.59	0.05	0.77	57.14	0.35
224	20.4	239	0.26	41,472	2.78	369.1	1.16	216	0.43	0.24	0.51	0.05	0.74	57.14	0.35
225	20.8	199	0.25	43,200	2.78	368.7	1.22	217	0.42	0.24	0.44	0.05	0.70	57.14	0.35
226	20.8	164	0.26	52,704	2.78	368.2	1.28	217	0.41	0.24	0.37	0.04	0.67	57.14	0.35
227	20.6	93	0.29	50,976	2.78	367.8	1.35	218	0.38	0.23	0.30	0.04	0.63	57.14	0.35
228	20.2	243	0.24	59,616	2.78	367.3	1.41	218	0.36	0.23	0.23	0.04	0.60	57.14	0.35
229	19.6	96	0.3	52,704	2.78	366.9	1.47	218	0.36	0.27	0.37	0.05	0.81	57.14	0.35
230	19.8	265	0.38	93,312	2.78	366.4	1.54	219	0.37	0.32	0.51	0.06	1.02	57.14	0.35
231	20.1	198	0.39	50,976	2.78	365.9	1.60	219	0.37	0.36	0.65	0.07	1.23	57.14	0.35
232	20.4	184	0.4	46,656	2.78	365.5	1.66	220	0.37	0.40	0.79	0.08	1.44	57.14	0.35
233	20.6	244	0.39	44,064	2.78	365.0	1.73	220	0.36	0.44	0.93	0.09	1.65	57.14	0.35
234	20.5	191	0.38	41,472	2.78	364.6	1.79	220	0.34	0.49	1.07	0.10	1.86	57.14	0.35
235	20.3	259	0.36	39,744	2.78	364.1	1.85	221	0.35	0.53	1.21	0.11	2.07	57.14	0.35
236	20.1	183	0.36	38,016	2.78	363.7	1.92	221	0.34	0.57	1.35	0.12	2.28	57.14	0.35
237	19.8	105	0.27	50,112	2.78	363.2	1.98	222	0.34	0.69	1.29	0.13	2.50	57.14	0.35
238	19.3	210	0.21	50,976	2.78	362.8	2.04	222	0.33	0.81	1.23	0.14	2.72	57.14	0.35
239	19.0	201	0.28	44,064	2.78	362.3	2.11	222	0.31	0.93	1.17	0.14	2.93	57.14	0.35
240	19.1	126	0.26	46,656	2.78	361.9	2.17	223	0.31	1.05	1.11	0.15	3.15	57.14	0.35
241	19.2	240	0.33	74,304	2.78	361.4	2.23	223	0.32	1.05	1.19	0.15	3.23	57.14	0.35
242	19.0	96	0.29	48,384	2.78	360.9	2.29	224	0.34	1.05	1.28	0.16	3.30	57.14	0.35
243	18.6	183	0.32	45,792	2.78	360.5	2.36	224	0.36	1.05	1.36	0.16	3.38	57.14	0.35
244	18.5	242	0.36	39,744	2.78	360.0	2.42	224	0.37	1.05	1.45	0.16	3.46	57.14	0.35
245	18.4	104	0.39	38,016	2.78	359.6	2.48	225	0.37	1.04	1.53	0.17	3.53	57.14	0.35
246	18.3	130	0.38	38,880	2.78	359.1	2.55	225	0.40	1.04	1.62	0.17	3.61	57.14	0.35
247	18.3	88	0.39	38,880	2.78	358.7	2.61	226	0.38	1.04	1.70	0.17	3.69	57.14	0.35
248	18.4	142	0.36	38,880	2.78	358.2	2.67	226	0.36	1.04	1.79	0.18	3.76	57.14	0.35

Day	Temper.	Light	Dilution	Flow	Riv_NH4	Riv_NO3	Riv_PO4	Riv_Si	Kpar	Rad_NH4	Rad_NO3	Rad_PO4	Rad_Si	N_org	P_org
249	18.5	140	0.31	37,152	2.78	357.8	2.74	227	0.34	1.04	1.87	0.18	3.84	57.14	0.35
250	18.6	249	0.31	34,560	2.78	357.3	2.80	227	0.33	1.06	1.95	0.18	3.87	57.14	0.35
251	18.8	242	0.28	31,968	2.78	356.9	2.86	227	0.32	1.07	2.02	0.18	3.90	57.14	0.35
252	18.9	241	0.27	31,104	2.78	356.4	2.93	228	0.31	1.09	2.10	0.18	3.93	57.14	0.35
253	19.0	67	0.21	31,104	2.78	355.9	2.99	228	0.32	1.10	2.17	0.19	3.96	57.14	0.35
254	19.0	171	0.23	33,696	2.78	355.5	3.05	229	0.31	1.12	2.25	0.19	3.99	57.14	0.35
255	19.0	161	0.27	44,064	2.78	351.9	2.99	228	0.29	1.13	2.32	0.19	4.02	57.14	0.35
256	18.7	115	0.26	36,288	2.78	348.3	2.92	227	0.29	1.15	2.40	0.19	4.05	57.14	0.35
257	18.6	228	0.3	34,560	2.78	344.7	2.86	227	0.31	1.08	2.45	0.19	4.02	57.14	0.35
258	18.4	105	0.3	32,832	2.78	341.2	2.80	226	0.31	1.01	2.51	0.19	3.99	57.14	0.35
259	18.3	168	0.37	32,832	2.78	337.6	2.73	226	0.32	0.94	2.56	0.19	3.96	57.14	0.35
260	18.3	134	0.39	31,104	2.78	334.0	2.67	225	0.29	0.87	2.61	0.20	3.93	57.14	0.35
261	18.1	91	0.38	31,104	2.78	330.4	2.60	224	0.29	0.79	2.66	0.20	3.89	57.14	0.35
262	18.0	190	0.35	31,968	2.78	326.8	2.54	224	0.28	0.72	2.72	0.20	3.86	57.14	0.35
263	17.7	209	0.38	28,512	2.78	323.2	2.47	223	0.26	0.65	2.77	0.20	3.83	57.14	0.35
264	17.4	188	0.35	27,648	2.78	319.6	2.41	223	0.26	0.58	2.82	0.20	3.80	57.14	0.35
265	17.1	70	0.33	26,784	2.78	316.1	2.35	222	0.28	0.64	2.83	0.21	3.91	57.14	0.35
266	16.8	84	0.29	27,648	2.78	312.5	2.28	221	0.28	0.70	2.83	0.21	4.01	57.14	0.35
267	16.7	74	0.32	83,808	2.78	308.9	2.22	221	0.30	0.76	2.84	0.22	4.12	57.14	0.35
268	16.4	93	0.27	86,400	2.78	305.3	2.15	220	0.31	0.82	2.85	0.22	4.23	57.14	0.35
269	15.8	141	0.31	81,216	2.78	301.7	2.09	220	0.30	0.88	2.85	0.23	4.33	57.14	0.35
270	15.5	151	0.31	60,480	2.78	298.1	2.02	219	0.32	0.94	2.86	0.23	4.44	57.14	0.35
271	15.5	154	0.32	45,792	2.78	294.6	1.96	218	0.31	0.92	3.00	0.24	4.48	57.14	0.35
272	15.6	99	0.34	38,880	2.78	291.0	1.89	218	0.32	0.90	3.14	0.24	4.53	57.14	0.35
273	15.6	179	0.36	36,288	2.78	287.4	1.83	217	0.31	0.88	3.28	0.25	4.57	57.14	0.35
274	15.6	157	0.35	32,832	2.78	283.8	1.77	217	0.32	0.86	3.43	0.26	4.62	57.14	0.35
275	15.6	58	0.32	35,424	2.78	280.2	1.70	216	0.33	0.84	3.57	0.26	4.66	57.14	0.35
276	15.6	89	0.31	40,608	2.78	276.6	1.64	215	0.38	0.82	3.71	0.27	4.70	57.14	0.35
277	15.5	60	0.38	118,368	2.78	273.1	1.57	215	0.38	0.80	3.85	0.27	4.75	57.14	0.35
278	15.6	141	0.43	185,760	2.78	269.5	1.51	214	0.40	0.78	3.99	0.28	4.79	57.14	0.35
279	16.0	95	0.29	63,936	2.78	265.9	1.44	214	0.41	0.87	4.14	0.29	4.96	57.14	0.35

Day	Temper.	Light	Dilution	Flow	Riv_NH4	Riv_NO3	Riv_PO4	Riv_Si	Kpar	Rad_NH4	Rad_NO3	Rad_PO4	Rad_Si	N_org	P_org
280	16.1	44	0.36	151,200	2.78	262.3	1.38	213	0.41	0.97	4.29	0.29	5.12	57.14	0.35
281	16.1	46	0.35	120,960	2.78	258.7	1.32	213	0.39	1.06	4.44	0.30	5.29	57.14	0.35
282	16.3	42	0.41	503,712	2.78	255.1	1.25	212	0.36	1.16	4.59	0.31	5.45	57.14	0.35
283	16.4	51	0.41	244,512	2.78	251.5	1.19	211	0.36	1.25	4.74	0.32	5.62	57.14	0.35
284	16.7	63	0.39	170,208	2.78	248.0	1.12	211	0.37	1.35	4.89	0.32	5.78	57.14	0.35
285	16.8	63	0.35	221,184	2.78	244.4	1.06	210	0.39	1.44	5.04	0.33	5.95	57.14	0.35
286	15.8	139	0.38	181,440	2.78	240.8	0.99	210	0.41	1.41	5.45	0.33	6.07	57.14	0.35
287	15.4	86	0.49	306,720	2.78	237.2	0.93	209	0.42	1.38	5.86	0.34	6.20	57.14	0.35
288	15.3	122	0.48	179,712	2.78	233.6	0.87	208	0.41	1.34	6.27	0.34	6.32	57.14	0.35
289	15.1	104	0.45	161,568	2.78	230.0	0.80	208	0.41	1.31	6.68	0.35	6.44	57.14	0.35
290	15.0	132	0.48	213,408	2.78	226.5	0.74	207	0.41	1.28	7.09	0.35	6.57	57.14	0.35
291	15.0	79	0.47	259,200	2.80	230.5	0.73	208	0.40	1.25	7.50	0.36	6.69	57.14	0.35
292	14.8	81	0.52	301,536	2.82	234.6	0.73	208	0.40	1.21	7.91	0.36	6.81	57.14	0.35
293	14.8	50	0.51	191,808	2.84	238.6	0.73	208	0.40	1.18	8.32	0.37	6.94	57.14	0.35
294	14.6	86	0.47	169,344	2.86	242.7	0.72	209	0.40	1.15	8.73	0.37	7.06	57.14	0.35
295	14.6	83	0.43	151,200	2.88	246.7	0.72	209	0.40	1.19	9.19	0.37	7.22	57.14	0.35
296	14.8	45	0.41	143,424	2.90	250.8	0.71	209	0.40	1.23	9.65	0.37	7.38	57.14	0.35
297	14.9	80	0.4	133,920	2.92	254.8	0.71	210	0.40	1.28	10.11	0.38	7.53	57.14	0.35
298	14.9	46	0.39	125,280	2.94	258.9	0.71	210	0.40	1.32	10.57	0.38	7.69	57.14	0.35
299	14.6	37	0.39	117,504	2.96	263.0	0.70	211	0.40	1.36	11.03	0.38	7.85	57.14	0.35
300	14.5	24	0.36	110,592	2.98	267.0	0.70	211	0.41	1.32	10.47	0.38	7.60	57.14	0.35
301	13.5	109	0.34	101,952	3.00	271.1	0.70	211	0.41	1.29	9.90	0.38	7.35	57.14	0.35
302	12.9	95	0.4	91,584	3.02	275.1	0.69	212	0.41	1.25	9.34	0.38	7.10	57.14	0.35
303	12.6	71	0.4	88,992	3.04	279.2	0.69	212	0.40	1.21	8.77	0.37	6.84	57.14	0.35
304	12.7	43	0.44	85,536	3.06	283.2	0.68	213	0.40	1.18	8.21	0.37	6.59	57.14	0.35
305	12.9	38	0.36	100,224	3.08	287.3	0.68	213	0.41	1.14	7.64	0.37	6.34	57.14	0.35
306	12.2	41	0.4	209,088	3.10	291.3	0.68	213	0.40	1.12	8.15	0.37	6.51	57.14	0.35
307	11.7	68	0.39	139,104	3.12	295.4	0.67	214	0.39	1.09	8.67	0.37	6.68	57.14	0.35
308	11.6	87	0.39	130,464	3.13	299.5	0.67	214	0.40	1.07	9.18	0.38	6.85	57.14	0.35
309	11.5	66	0.37	238,464	3.15	303.5	0.67	214	0.40	1.04	9.70	0.38	7.02	57.14	0.35
310	11.2	57	0.36	217,728	3.17	307.6	0.66	215	0.40	1.02	10.21	0.38	7.18	57.14	0.35

Day	Temper.	Light	Dilution	Flow	Riv_NH4	Riv_NO3	Riv_PO4	Riv_Si	Kpar	Rad_NH4	Rad_NO3	Rad_PO4	Rad_Si	N_org	P_org
311	11.5	86	0.39	179,712	3.19	311.6	0.66	215	0.40	0.99	10.73	0.38	7.35	57.14	0.35
312	11.6	55	0.39	146,880	3.21	315.7	0.65	216	0.40	0.97	11.24	0.39	7.52	57.14	0.35
313	11.8	79	0.41	138,240	3.23	319.7	0.65	216	0.40	0.94	11.76	0.39	7.69	57.14	0.35
314	11.9	54	0.38	131,328	3.25	323.8	0.65	216	0.39	0.92	12.27	0.39	7.86	57.14	0.35
315	11.5	70	0.42	191,808	3.27	327.8	0.64	217	0.39	0.91	12.04	0.39	7.73	57.14	0.35
316	11.7	87	0.44	139,104	3.29	331.9	0.64	217	0.40	0.90	11.82	0.39	7.61	57.14	0.35
317	11.8	31	0.44	123,552	3.31	336.0	0.64	217	0.41	0.89	11.59	0.38	7.48	57.14	0.35
318	12.0	41	0.46	122,688	3.33	340.0	0.63	218	0.43	0.88	11.36	0.38	7.36	57.14	0.35
319	11.9	45	0.48	114,912	3.35	341.8	0.63	218	0.43	0.88	11.14	0.38	7.23	57.14	0.35
320	11.6	86	0.49	108,000	3.37	343.6	0.62	218	0.44	0.87	10.91	0.38	7.11	57.14	0.35
321	11.7	62	0.45	107,136	3.40	345.3	0.62	219	0.44	0.86	10.68	0.37	6.98	57.14	0.35
322	11.9	25	0.46	135,648	3.42	347.1	0.62	219	0.43	0.85	10.46	0.37	6.86	57.14	0.35
323	11.7	83	0.45	119,232	3.44	348.9	0.61	219	0.43	0.84	10.23	0.37	6.73	57.14	0.35
324	11.5	27	0.35	114,912	3.46	350.6	0.61	219	0.41	0.90	10.59	0.37	6.89	57.14	0.35
325	11.8	20	0.38	285,120	3.48	352.4	0.60	220	0.40	0.96	10.95	0.38	7.05	57.14	0.35
326	11.9	57	0.39	309,312	3.50	354.2	0.60	220	0.38	1.02	11.31	0.38	7.21	57.14	0.35
327	11.7	41	0.32	285,984	3.52	355.9	0.60	220	0.39	1.07	11.66	0.38	7.37	57.14	0.35
328	11.7	29	0.38	1,907,712	3.54	357.7	0.59	221	0.41	1.13	12.02	0.38	7.53	57.14	0.35
329	11.8	20	0.43	613,440	3.56	359.5	0.59	221	0.40	1.19	12.38	0.39	7.69	57.14	0.35
330	11.5	40	0.41	476,928	3.58	361.2	0.58	221	0.41	1.25	12.74	0.39	7.85	57.14	0.35
331	11.0	29	0.44	743,040	3.60	363.0	0.58	221	0.39	1.21	13.15	0.39	7.93	57.14	0.35
332	10.8	37	0.53	1,088,640	3.62	364.8	0.58	222	0.39	1.17	13.55	0.39	8.00	57.14	0.35
333	11.0	59	0.51	659,232	3.64	366.5	0.57	222	0.39	1.13	13.96	0.39	8.08	57.14	0.35
334	10.7	39	0.54	488,160	3.66	368.3	0.57	222	0.38	1.08	14.37	0.40	8.15	57.14	0.35
335	10.7	57	0.54	399,168	3.68	370.1	0.57	222	0.39	1.04	14.78	0.40	8.23	57.14	0.35
336	10.7	62	0.51	342,144	3.70	371.8	0.56	223	0.39	1.00	15.18	0.40	8.30	57.14	0.35
337	10.9	20	0.46	337,824	3.72	373.6	0.56	223	0.41	0.96	15.59	0.40	8.38	57.14	0.35
338	10.9	22	0.43	397,440	3.74	375.4	0.55	223	0.41	0.94	17.51	0.39	8.31	57.14	0.35
339	10.4	43	0.39	364,608	3.77	377.1	0.55	223	0.40	0.91	19.44	0.39	8.25	57.14	0.35
340	9.9	52	0.43	384,480	3.79	378.9	0.55	224	0.40	0.89	21.36	0.38	8.18	57.14	0.35
341	9.8	44	0.43	304,992	3.81	380.7	0.54	224	0.41	0.86	23.29	0.37	8.11	57.14	0.35

Day	Temper.	Light	Dilution	Flow	Riv_NH4	Riv_NO3	Riv_PO4	Riv_Si	Kpar	Rad_NH4	Rad_NO3	Rad_PO4	Rad_Si	N_org	P_org
342	9.6	39	0.38	413,856	3.83	382.4	0.54	224	0.42	0.84	25.21	0.36	8.04	57.14	0.35
343	10.0	64	0.44	292,032	3.85	384.2	0.53	224	0.44	0.81	27.14	0.36	7.98	57.14	0.35
344	9.8	33	0.46	266,112	3.87	386.0	0.53	225	0.44	0.79	29.06	0.35	7.91	57.14	0.35
345	9.9	62	0.48	264,384	3.89	387.7	0.53	225	0.43	0.79	27.78	0.35	7.89	57.14	0.35
346	9.8	45	0.48	235,008	3.89	387.7	0.53	225	0.45	0.78	26.50	0.35	7.87	57.14	0.35
347	9.2	58	0.46	222,048	3.89	387.7	0.53	225	0.45	0.78	25.21	0.35	7.84	57.14	0.35
348	9.1	56	0.5	224,640	3.89	387.7	0.53	225	0.46	0.78	23.93	0.36	7.82	57.14	0.35
349	9.5	27	0.52	716,256	3.89	387.7	0.53	225	0.46	0.77	22.65	0.36	7.80	57.14	0.35
350	9.6	26	0.5	513,216	3.89	387.7	0.53	225	0.43	0.77	21.37	0.36	7.78	57.14	0.35
351	9.5	39	0.49	558,144	3.89	387.7	0.53	225	0.42	0.76	20.08	0.36	7.75	57.14	0.35
352	9.5	44	0.48	542,592	3.89	387.7	0.53	225	0.43	0.76	18.80	0.36	7.73	57.14	0.35
353	9.5	31	0.5	405,216	3.89	387.7	0.53	225	0.43	0.78	19.76	0.37	8.03	57.14	0.35
354	9.8	11	0.51	1,171,584	3.89	387.7	0.53	225	0.43	0.80	20.72	0.37	8.33	57.14	0.35
355	10.3	18	0.5	1,710,720	3.89	387.7	0.53	225	0.41	0.82	21.68	0.38	8.64	57.14	0.35
356	10.3	33	0.49	701,568	3.89	387.7	0.53	225	0.40	0.84	22.64	0.39	8.94	57.14	0.35
357	10.5	21	0.42	1,410,048	3.89	387.7	0.53	225	0.39	0.86	23.61	0.39	9.24	57.14	0.35
358	11.0	16	0.41	846,720	3.89	387.7	0.53	225	0.39	0.88	24.57	0.40	9.54	57.14	0.35
359	11.2	18	0.43	679,968	3.89	387.7	0.53	225	0.40	0.90	25.53	0.41	9.85	57.14	0.35
360	10.8	32	0.43	940,032	3.89	387.7	0.53	225	0.40	0.92	26.49	0.41	10.15	57.14	0.35
361	10.4	21	0.43	653,184	3.89	387.7	0.53	225	0.40	0.94	27.45	0.42	10.45	57.14	0.35
362	10.3	37	0.43	705,888	3.89	387.7	0.53	225	0.39	0.94	27.45	0.42	10.45	57.14	0.35
363	10.5	21	0.43	517,536	3.89	387.7	0.53	225	0.41	0.94	27.45	0.42	10.45	57.14	0.35
364	10.5	28	0.42	503,712	3.89	387.7	0.53	225	0.41	0.94	27.45	0.42	10.45	57.14	0.35
365	10.1	32	0.46	494,208	3.89	387.7	0.53	225	0.41	0.94	27.45	0.42	10.45	57.14	0.35

Simulation (Biotic + Abiotic)**PROGRAM MAIN**

```
! This program simulates the growths of a given number of phytoplankton species in the bay of Daoulas during a year,
! including toxic dinoflagellate Alexandrium minutum, in order to identify their ecological niche.
```

```
!-----
!----- Declarations -----
```

IMPLICIT NONE

```
CHARACTER(len=4) a,arg1,arg2,arg3,arg4
CHARACTER(len=25) Outputfile,forcingsFileName
LOGICAL, DIMENSION(:,:), ALLOCATABLE :: diat
INTEGER*4 sim,nsim,i,imax,j,k,ns,nt,op,nd,cd,nb_t1,nb_t2,nb_t3,nb_t4
INTEGER*4, DIMENSION(:), ALLOCATABLE :: nsmall,nsavgm,nsavgp,nslarge,nsmallsi,nsavgmsi,nsavgpsi,nslargesi,nsmallnsi,nsavgmnsi,nsavgpnsi,&
nslargensi,nsfico,nsnano,nsmicro,nsnanominus,nsnanomicro,nsflore
REAL n,dt
REAL k_minN,k_nitrif,k_minP,k_dissSi,k_ads,k_des,Q_maxSM,kT,Hd,Hm,H,Vd,Vm,V,Ksi
REAL Td(366),Tm(366),T(366),Ir(366),dilutd(366),dilutm(366),dilut(366),flow(366),NH4_f(366),NO3_f(366),PO4_f(366),Si_f(366),Kpar(366)
REAL NH4_r(366),NO3_r(366),PO4_r(366),Si_r(366),Dn_f(366),Dp_f(366),Dn_r(366),Dp_r(366)
REAL fTm,lim_DLT,salt,DL,limL,fluxbenth_NH4,fluxbenth_NO3,fluxbenth_PO4,fluxbenth_Si
REAL, DIMENSION(:), ALLOCATABLE :: NH4,NO3,PO4,Si,Pp,Dn,Dp,Dsi,SM
REAL, DIMENSION(:), ALLOCATABLE :: VNH4_tot,VNO3_tot,VPO4_tot,VSi_tot,mort_N,mort_P,mort_Si,ads_P,des_P
REAL, DIMENSION(:), ALLOCATABLE :: PAR
REAL, DIMENSION(:,:), ALLOCATABLE :: gmax,VmaxNH4,VmaxNO3,VmaxPO4,QminN,QminP,QmaxN,QmaxP,Qsi,Kn,Kp,Ks,Topt,m,l
REAL, DIMENSION(:,:), ALLOCATABLE :: fT,fN,fP,fS,VNH4,VNO3,VPO4,g,VNd,VPd,VSid,gd,fL
REAL, DIMENSION(:,:), ALLOCATABLE :: Nc,Qn,Qp,Ncmin
REAL N_alex(366),N_phyto(366)
```

```
!----- Choose mode -----
```

```
100 WRITE(*,*) 'All Species (S) ? Alexandrium only (A) ? Without Alexandrium (W) ?'
```

```
!READ(*,*) arg1
```

```
arg1 = 'S'
```

```
!IF ((arg1.NE. 'S') .AND. (arg1.NE. 'A') .AND. (arg1.NE. 'W')) GOTO 100
```

```
200 WRITE(*,*) 'Estuary of Mignonne (M)'
```

```
!READ(*,*) arg2
```

```
arg2='M'
```

```
!IF((arg2.NE. 'D') .AND. (arg2.NE. 'M')) GOTO 200
```

```
300 WRITE(*,*) 'Year?'
```

```
!READ(*,*) arg3
```

```
!IF((arg3.NE. '2012') .AND. (arg3.NE. '2013')) GOTO 300
```

```
arg3 = '2009'
```

```
400 WRITE(*,*) 'Mass conservation test (Y/N) ?'
```

```
!READ(*,*) arg4
```

```
arg4='N'
```

```
!IF((arg4.NE. 'Y') .AND. (arg4.NE. 'N')) GOTO 300
```

```
!-----
```

```

!----- Loading constants -----
WRITE(*,*)
WRITE(*,*) '----- Main.f90 ----- '
WRITE(*,*)

OPEN(10, FILE = 'IN/namelistIopt72.dat', STATUS='OLD')
REWIND(10)

IF (arg3 .EQ. '2012' .OR. arg3 .EQ. '2016') THEN
imax = 365
ELSE
imax = 365
END IF

dt = 1d0/1440d0 ! Time step (1min)
nt = int(real(imax)/dt) ! Number of time steps (in 1 year)
nd = 20 ! Number of depth levels considered for integration (only light attenuation differs)
nsim = 1 ! Number of simulations
ns = 72 ! Number of species
nb_t1 = 5 ! Number of size classes
nb_t2 = 5 ! Number of temperature classes
nb_t3 = 5 ! Number of Iopt classes
nb_t4 = 2 ! Si/nonSi

WRITE(*,*) 'Time step is', dt, '(in days)'
WRITE(*,*)

!-----Physical constants (+ number of species) -----
! Nitrogen mineralization, nitrification, phosphorus mineralization, silica dissolution, phosphorus
! adsorption and desorption by suspended particulate matter, maximum adsorbed phosphorus by quantity
! of suspended particulate matter, rate of biological kinetics increase with temperature, depth
! and volume of the bay (Hd and Vd) and the estuary (Hm and Vm). ns is the number of species

NAMELIST /PHY_CST/ k_minN,k_nitrif,k_minP,k_dissSi,k_ads,k_des,Q_maxSM,KT,Hd,Hm,Vd,Vm,nsim
READ(10, PHY_CST)

ns = ns + 1 ! First species is Alexandrium minutum
IF (arg1 .EQ. 'A') ns = 1

V = Vm
H = Hm

CLOSE(10)

!----- Allocating variable arrays -----

ALLOCATE (NH4(nsim),NO3(nsim),PO4(nsim),Si(nsim),Pp(nsim),Dn(nsim),Dp(nsim),Dsi(nsim),SM(nsim),nssmall(nsim),nsavgm(nsim),nsavgp(nsim),&
nslarge(nsim),nssmallsi(nsim),nsavgmsi(nsim),nsavgpsi(nsim),nslargesi(nsim),nssmallnsi(nsim),nsavgmnsi(nsim),nsavgpnssi(nsim),&
nslargensi(nsim),nspico(nsim),nnsano(nsim),nsmicro(nsim),nsnanominus(nsim),nsnanomicro(nsim),nsflore(nsim))
ALLOCATE (VNH4_tot(nsim),VNO3_tot(nsim),VPO4_tot(nsim),VSi_tot(nsim),mort_N(nsim),mort_P(nsim),mort_Si(nsim),ads_P(nsim),des_P(nsim))
ALLOCATE (diat(ns,nsim),gmax(ns,nsim),QminN(ns,nsim),QminP(ns,nsim),QmaxN(ns,nsim),QmaxP(ns,nsim),Qsi(ns,nsim),VmaxNH4(ns,nsim), &
VmaxNO3(ns,nsim),VmaxPO4(ns,nsim),Kn(ns,nsim),Kp(ns,nsim),Ks(ns,nsim),Topt(ns,nsim),Iopt(ns,nsim),m(ns,nsim),l(ns,nsim))
ALLOCATE (PAR(nd))
ALLOCATE (fT(ns,nsim),fN(ns,nsim),fP(ns,nsim),fS(ns,nsim),VNH4(ns,nsim),VNO3(ns,nsim),VPO4(ns,nsim),g(ns,nsim),VNd(ns,nsim),VPd(ns,nsim),Vsid(ns,nsim),gd(ns,nsim),fL (ns,nsim))
ALLOCATE (Nc(ns,nsim),Qn(ns,nsim),Qp(ns,nsim),Ncmin(ns,nsim)) ! Number of cells and cell quotas of nutrients at a given time
WRITE(*,*) 'Loop arrays allocated'
WRITE(*,*)

```



```

!-----Forcings -----
forcingsFileName = "IN/forcings_"//arg3//".dat"
OPEN(11, FILE=forcingsFileName, STATUS='OLD')
REWIND(11)
WRITE(*,*) 'Physical forcing file open',forcingsFileName
WRITE(*,*)
READ(11,*)
do i=1,imax
! Reading physical constants : temperature, irradiance, dilution (Daoulas bay and Mignonne), river flow,
! river nutrient concentrations, light attenuation coefficient, rade nutrient concentration.
READ(11,*) a, Tm(i), Ir(i),dilutm(i),flow(i),NH4_f(i),NO3_f(i),PO4_f(i),Si_f(i),Kpar(i),&
NH4_r(i), NO3_r(i), PO4_r(i), Si_r(i), Dn_f(i), Dp_f(i), Dn_r(i), Dp_r(i)

dilutm(i) = -log(1-dilutm(i)) ! Turns day dilution into exponential dilution
IF (arg2 .EQ. 'M') dilut(i) = dilutm(i)
IF (arg2 .EQ. 'M') T(i) = Tm(i)
IF (arg4 .EQ. 'Y') then
dilut(i) = 0d0
flow(i) = 0d0
END IF
end do
CLOSE(11)

WRITE(*,*) 'Physical forcings read'
WRITE(*,*)
!----- Characteristics of species -----
! Reading biological parameters of each species : diatom or not, max growth, min and max cell
! nutrient quota (silica quota is constant), maximum nutrient uptake rates(V),
! half-saturation constants(K), optimal irradiance(I0), mortality and size

OPEN(12, FILE = 'IN/species6*6.dat', STATUS='OLD')
REWIND(12)
WRITE(*,*) 'Species file open'
WRITE(*,*)
DO sim=1,nsim
READ(12,*)
READ(12,*)
READ(12,*) a,diat(1,sim),gmax(1,sim),QminN(1,sim),QminP(1,sim),QmaxN(1,sim),QmaxP(1,sim),Qsi(1,sim), &
VmaxNH4(1,sim),VmaxNO3(1,sim),VmaxPO4(1,sim),Kn(1,sim),Kp(1,sim),Ks(1,sim),Topt(1,sim),Iopt(1,sim),m(1,sim),l(1,sim)

READ(12,*)
gmax(1,sim) = 0.58d0*exp(0.063d0*Topt(1,sim))
m(1,sim) = 0.00d0
do i=2,ns
READ(12,*) a,diat(i,sim),gmax(i,sim),QminN(i,sim),QminP(i,sim),QmaxN(i,sim),QmaxP(i,sim),Qsi(i,sim), &
VmaxNH4(i,sim),VmaxNO3(i,sim),VmaxPO4(i,sim),Kn(i,sim),Kp(i,sim),Ks(i,sim),Topt(i,sim),Iopt(i,sim),m(i,sim),l(i,sim)

READ(12,*)
gmax(i,sim) = 0.58d0*exp(0.063d0*Topt(i,sim))
m(i,sim) = 0.00d0
end do
IF (arg1 .EQ. 'w') gmax(1,sim) = 0.0d0
END DO
CLOSE(12)

```

```

WRITE(*,*) 'Species file read for all simulations'

!----- Outputs -----
WRITE(*,*) WRITE(*,*)
WRITE(*,*) '-----Creating outputfile----- '

op = int(1/dt)
Outputfile = 'OUT/Uniform/6*6_'//TRIM(arg3)//'.csv'
OPEN(20, FILE=Outputfile, FORM='formatted')
WRITE(*,*) 'Output file open'
REWIND(20)

WRITE
(20, '(A)') 'Day;NH4;NO3;PO4;Si;Alex;pico;nano;micro;fL_alex;fL_pico;fL_nano;fL_micro;fT_alex;fT_pico;fT_nano;fT_micro;fN_alex;fN_pico;fN_nano;fN_micro;fP_alex;
fP_pico;fP_nano;fP_micro'

WRITE(*,*)
!----- Initialization -----
nssmall(:) = 0
nsavgm(:) = 0
nsavgp(:) = 0
nslarge(:) = 0

nssmallsi(:) = 0
nsavgmsi(:) = 0
nsavgpsi(:) = 0
nslargesi(:) = 0

nssmallnsi(:) = 0
nsavgmnsi(:) = 0
nsavgpnsi(:) = 0
nslargensi(:) = 0

nspico(:) = 0
nsnano(:) = 0
nsmicro(:) = 0
nsnanominus(:) = 0
nsnanomicro(:) = 0
nsflore(:) = 0

do sim=1,nsim
do i=1,ns
Ncmin(i,sim) = (100.0/l(i,sim))**3.0
Nc(i,sim) = Ncmin(i,sim)
Qn(i,sim) = QminN(i,sim)*(1+QmaxN(i,sim))/2.0
Qp(i,sim) = QminP(i,sim)*(1+QmaxP(i,sim))/2.0

if(l(i,sim) .lt. 5.0) nssmall(sim)=nssmall(sim)+1
if((l(i,sim) .ge. 5.0) .AND. (l(i,sim) .lt. 10.0)) nsavgm(sim)=nsavgm(sim)+1
if((l(i,sim) .ge. 10.0) .AND. (l(i,sim) .lt. 20.0)) nsavgp(sim)=nsavgp(sim)+1
if(l(i,sim) .gt. 20.0) nslarge(sim)=nslarge(sim)+1

if((l(i,sim) .lt. 5.0) .AND. (diat(i,sim) .EQV. .TRUE.)) nssmallsi(sim)=nssmallsi(sim)+1
if((l(i,sim) .ge. 5.0) .AND. (l(i,sim) .lt. 10.0) .AND. (diat(i,sim) .EQV. .TRUE.)) nsavgmsi(sim)=nsavgmsi(sim)+1
if((l(i,sim) .ge. 10.0) .AND. (l(i,sim) .lt. 20.0) .AND. (diat(i,sim) .EQV. .TRUE.)) nsavgpsi(sim)=nsavgpsi(sim)+1
if((l(i,sim) .gt. 20.0) .AND. (diat(i,sim) .EQV. .TRUE.)) nslargesi(sim)=nslargesi(sim)+1

```

```

if((l(i,sim) .lt. 5.0) .AND. (diat(i,sim) .EQV. .FALSE.)) nssmallnsi(sim)=nssmallnsi(sim)+1
if((l(i,sim) .ge. 5.0) .AND. (l(i,sim) .lt. 10.0) .AND. (diat(i,sim) .EQV. .FALSE.)) nsavgmnsi(sim)=nsavgmnsi(sim)+1
if((l(i,sim) .ge. 10.0) .AND. (l(i,sim) .lt. 20.0) .AND. (diat(i,sim) .EQV. .FALSE.)) nsavgpnsi(sim)=nsavgpnsi(sim)+1
if((l(i,sim) .gt. 20.0) .AND. (diat(i,sim) .EQV. .FALSE.)) nslargensi(sim)=nslargensi(sim)+1

if(l(i,sim) .lt. 3.0) nspico(sim)=nspico(sim)+1
if((l(i,sim) .ge. 3.0) .AND. (l(i,sim) .lt. 20.0)) nsnano(sim)=nsnano(sim)+1
if(l(i,sim) .gt. 20.0) nsmicro(sim)=nsmicro(sim)+1

if((l(i,sim) .ge. 2.0) .AND. (l(i,sim) .le. 10.0)) nsnanominus(sim)=nsnanominus(sim)+1
if(l(i,sim) .gt. 10.0) nsnanomicro(sim)=nsnanomicro(sim)+1
if(l(i,sim) .ge. 18.0) nsflore(sim)=nsflore(sim)+1

end do
end do
!-----
salt = 34.0          ! Salinity is initialized
                    ! All nutrient concentrations (in micromoles.l-1) are initialized
NO3(:) = 78.0
NH4(:) = 1.5
Si(:) = 21.4
PO4(:) = 0.7
Pp(:) = 0.0
Dn(:) = 36.0
Dp(:) = 0.1
Dsi(:) = 0.0

WRITE(*,*) 'Concentrations initialized'
WRITE(*,*)
!-----
lim_DLT = 0.0
gd(:, :) = 0.0
VNd(:, :) = 0.0
VPd(:, :) = 0.0
VSid(:, :) = 0.0
!----- Loop -----

DO i=1,nt
!----- Physical parameters, independent from biology -----
cd = int(i*dt)+1
fTm = exp(kT*T(int(i*dt)))
! Current day
! Coefficient of mineralization and mortality processes acceleration by temperature (Q10)
IF(mod(i,op) .EQ. 1) then
call daylength(cd,48.3,12.0,DL)
! Length of the current day, including nautical twilight
lim_DLT = 0
! Initializes lim_DLT to 0
END IF
call irradiance(Ir(cd),DL,24*(i*dt-int((i)*dt)),PAR(1))
! Computes Photosynthetically Available Radiation (PAR)
PAR(1) = 0.95*0.425*PAR(1)
! 5% of light is reflected, and only 42.5% is photosynthetically available
do k=1,nd
PAR(k) = PAR(1)*exp((1-k)*(H/(nd-1))*Kpar(cd))
! PAR(k) = PAR(1)*exp(-(H/(nd-1))*Kpar(cd))
! Photosynthetically Available Radiation (PAR) at each level (Bay of Daoulas)
IF (mod(i,op) .LE. op/2) lim_DLT = lim_DLT + (1.0/nd)*(1.0/(op/2))*0.58*exp(kT*T(cd))*tanh(PAR(k)/20.0)
end do

salt = salt*(1-dt*dilut(cd)) + dt*(34.6*(dilut(cd)-flow(cd)/V))
! The average salinity of the box is computed
!-----

```

```

do sim=1,nsim
do j=1,ns
!----- Temperature-induced kinetic multiplier -----
! Empirical law, inspired by the modelization of Alexandrium minutum in the bay of Cork (Final deliverable 7)
fT(j,sim) = 0.0
IF (T(cd) .GT. Topt(j,sim)) fT(j,sim) = 1
IF ((T(cd) .LE. Topt(j,sim)) .AND. (T(cd) .GT. (Topt(j,sim) - 10.0))) fT(j,sim) = (10-Topt(j,sim)+T(cd))/10.0

!----- Limitation functions (the lowest is that of the limiting factor) -----
!fL(j) = 1.184*(1-exp(-3.258*light/Iopt(j)))*exp(-0.13*light/Iopt(j)) ! Limitation by light (Platt formula), only surface irradiance is considered

fN(j,sim) = (QmaxN(j,sim)/(QmaxN(j,sim)-1))*(1-(QminN(j,sim)/Qn(j,sim))) ! Limitation by nitrogen
IF (Qn(j,sim) .LE. QminN(j,sim)) fN(j,sim) = 0.0 ! Negative limitation prohibited
IF (Qn(j,sim) .GE. QmaxN(j,sim)*QminN(j,sim)) fN(j,sim) = 1.0 ! Limitation function is always lower or equal to 1

fP(j,sim) = (QmaxP(j,sim)/(QmaxP(j,sim)-1))*(1-(QminP(j,sim)/Qp(j,sim))) ! Limitation by phosphorus
IF (Qp(j,sim) .LE. QminP(j,sim)) fP(j,sim) = 0.0 ! Negative limitation prohibited
IF (Qp(j,sim) .GE. QmaxP(j,sim)*QminP(j,sim)) fP(j,sim) = 1.0 ! Limitation function is always lower or equal to 1

fS(j,sim) = 1.0
IF (diat(j,sim)) fS(j,sim) = Si(sim)/(Ks(j,sim)+Si(sim)) ! Limitation by silica
IF (diat(j,sim) .AND. (Si(sim) .LE. 0)) fS(j,sim) = 0.0 ! Negative limitation prohibited

!----- Real uptake rates -----
! Phosphorus uptake rate (linear decrease with quota, Chapelle et al, 2010)
VPO4(j,sim) = fTm*vmaxPO4(j,sim)*(PO4(sim)/(Kp(j,sim)+PO4(sim)))*((QmaxP(j,sim)-(Qp(j,sim)/QminP(j,sim)))/(QmaxP(j,sim)-1))
! Negative phosphorus uptake prohibited
IF ((PO4(sim) .LE. 0.0) .OR. (Qp(j,sim) .GE. QminP(j,sim)*QmaxP(j,sim))) VPO4(j,sim) = 0.0
! No excess phosphorus uptake when cell quota under theoretical minimum
IF (Qp(j,sim) .LE. QminP(j,sim)) VPO4(j,sim) = VmaxPO4(j,sim)*(PO4(sim)/(Kp(j,sim)+PO4(sim)))
! Ammonium uptake rate
VNH4(j,sim) = fTm*vmaxNH4(j,sim)*(NH4(sim)/(Kn(j,sim)+NH4(sim)))*((QmaxN(j,sim)-(Qn(j,sim)/QminN(j,sim)))/(QmaxN(j,sim)-1))
! Negative ammonium uptake prohibited
IF ((NH4(sim) .LE. 0.0) .OR. (Qn(j,sim) .GE. QminN(j,sim)*QmaxN(j,sim))) VNH4(j,sim) = 0.0
! No excess ammonium uptake when cell quota lower than theoretical minimum
IF (Qn(j,sim) .LE. QminN(j,sim)) VNH4(j,sim) = VmaxNH4(j,sim)*(NH4(sim)/(Kn(j,sim)+NH4(sim)))
! Nitrate uptake rate, with inhibition by ammonium (Parker, 1993)
VNO3(j,sim) = fTm*vmaxNO3(j,sim)*(NO3(sim)/(Kn(j,sim)+NO3(sim)))*((1.0-NH4(sim)/(Kn(j,sim)+NH4(sim)))*((QmaxN(j,sim)-(Qn(j,sim)/QminN(j,sim)))/(QmaxN(j,sim)-1)))
! Negative nitrate uptake prohibited
IF ((NO3(sim) .LE. 0.0) .OR. (Qn(j,sim) .GE. QminN(j,sim)*QmaxN(j,sim))) VNO3(j,sim) = 0.0
! No excess nitrate uptake when cell quota lower than theoretical minimum
IF (Qn(j,sim) .LE. QminN(j,sim)) VNO3(j,sim) = VmaxNO3(j,sim)*(NO3(sim)/(Kn(j,sim)+NO3(sim)))*((1.0-NH4(sim)/(Kn(j,sim)+NH4(sim))))
! No negative inhibition by ammonium
IF (NH4(sim) .LE. 0.0) VNO3(j,sim) = VmaxNO3(j,sim)*(NO3(sim)/(Kn(j,sim)+NO3(sim)))*((QmaxN(j,sim)-(Qn(j,sim)/QminN(j,sim)))/(QmaxN(j,sim)-1))
Vnd(j,sim) = Vnd(j,sim) + (1.0/op)*(VNO3(j,sim)+VNH4(j,sim))*QminN(j,sim)*Nc(j,sim) ! Progressively builds the day total uptake of nitrogen
Vpd(j,sim) = Vpd(j,sim) + (1.0/op)*VPO4(j,sim)*QminP(j,sim)*Nc(j,sim) ! Progressively builds the day total uptake of phosphorus

!----- Growth of each species -----
g(j,sim) = 0.0
fL(j,sim) = 0.0
do k=1,nd
!fL(j,sim) = fL(j,sim)+limL*(1.0/nd) ! Integration of growth rate over nd depths
fL(j,sim) = tanh(PAR(k)/Iopt(j,sim)) ! Photoinhibition for each species
! Light limitation by Jassby and Platt
g(j,sim) = g(j,sim) + fT(j,sim)*(1.0/nd)*gmax(j,sim)*min(fL(j,sim),fN(j,sim),fP(j,sim),fS(j,sim)) ! Growth of species
end do
Vsid(j,sim) = Vsid(j,sim) + (1.0/op)*fT(j,sim)*g(j,sim)*Qsi(j,sim)*Nc(j,sim) ! Progressively builds the day total uptake of silica
gd(j,sim) = gd(j,sim) + (1.0/op)*g(j,sim) ! gd(j,sim) is going to be the ave. growth rate of species j during one day
Nc(j,sim) = Nc(j,sim)*exp((g(j,sim)-m(j,sim)*fTm-dilut(cd))*dt) ! Number of cells of species number j
Qn(j,sim) = Qn(j,sim)*(1-g(j,sim)*dt) + QminN(j,sim)*(VNH4(j,sim)+VNO3(j,sim))*dt ! Nitrogen cell quota of species number j
Qp(j,sim) = Qp(j,sim)*(1-g(j,sim)*dt) + QminP(j,sim)*VPO4(j,sim)*dt ! Phosphorus cell quota of species number j
IF (Nc(j,sim) .LT. Ncmin(j,sim)) Nc(j,sim) = Ncmin(j,sim) ! No species extinction is allowed (???)
end do

```

```

VPO4_tot(sim) = SUM(VPO4(:,sim)*QminP(:,sim)*Nc(:,sim))      ! Total phosphorus uptake rate by phytoplankton
VNH4_tot(sim) = SUM(VNH4(:,sim)*QminN(:,sim)*Nc(:,sim))      ! Total ammonium uptake rate by phytoplankton
VNO3_tot(sim) = SUM(VNO3(:,sim)*QminN(:,sim)*Nc(:,sim))      ! Total nitrate uptake rate by phytoplankton
VSi_tot(sim) = SUM(FT(:,sim)*g(:,sim)*Qsi(:,sim)*Nc(:,sim))   ! Total silica uptake rate by diatoms

mort_N(sim) = SUM(m(:,sim)*Qn(:,sim)*Nc(:,sim))*fTm          ! Total detrital nitrogen created by mortality
mort_P(sim) = SUM(m(:,sim)*Qp(:,sim)*Nc(:,sim))*fTm          ! Total detrital phosphorus created by mortality
mort_Si(sim) = SUM(m(:,sim)*Qsi(:,sim)*Nc(:,sim))*fTm         ! Total detrital silica created by mortality

! -----Fluxes from sediment (in µmol/L/day)-----
fluxbenth_PO4 = 5.9*exp(0.15*T(cd))*(1/H)*1/1000             ! 5.9*exp(0.104*temperature) is the regression (in µmol/m-2/day) used by Françoise.
                                                           (1/H)*1/1000 is for unit conversion
! fluxbenth_NH4 = 72.7*exp(0.132*T(cd))*(1/H)*1/1000
! fluxbenth_Si = 221.65*exp(0.136*T(cd))*(1/H)*1/1000

!----- Changes in nutrient concentrations -----
! (Dissolved nutrients, phosphorus adsorbed by particulate matter, detrital nutrients)
NO3(sim) = NO3(sim)*(1-dilut(cd)*dt) + (dilut(cd) - flow(cd)/V)*NO3_r(cd)*dt + flow(cd)*NO3_f(cd)*dt/V + fTm*(k_nitriF*NH4(sim))*dt - VNO3_tot(sim)*dt
NH4(sim) = NH4(sim)*(1-dilut(cd)*dt) + (dilut(cd) - flow(cd)/V)*NH4_r(cd)*dt + flow(cd)*NH4_f(cd)*dt/V + fTm*(k_minN*Dn(sim)-k_nitriF*NH4(sim))*dt-VNH4_tot(sim)*dt
Si(sim) = Si(sim)*(1-dilut(cd)*dt) + (dilut(cd) - flow(cd)/V)*Si_r(cd)*dt + flow(cd)*Si_f(cd)*dt/V + fTm*(k_dissSi*Dsi(sim))*dt - VSi_tot(sim)*dt
PO4(sim) = PO4(sim)*(1-dilut(cd)*dt) + (dilut(cd) - flow(cd)/V)*PO4_r(cd)*dt + flow(cd)*PO4_f(cd)*dt/V + fTm*(k_minP*Dp(sim))*dt - VPO4_tot(sim)*dt + fluxbenth_PO4*dt
!Pp = 0.0 ! Particulate phosphorus is not considered separately from phosphate
Dn(sim) = Dn(sim)*(1-dilut(cd)*dt) + flow(cd)*Dn_r(cd)*Dn_f(cd)*dt/V + (mort_N(sim) - fTm*k_minN*Dn(sim))*dt
Dsi(sim) = Dsi(sim)*(1-dilut(cd)*dt) + (mort_Si(sim) - fTm*k_dissSi*Dsi(sim))*dt
Dp(sim) = Dp(sim)*(1-dilut(cd)*dt) + flow(cd)*Dp_r(cd)*Dp_f(cd)*dt/V + (mort_P(sim) - fTm*k_minP*Dp(sim))*dt
IF(mod(i,op) .EQ. op/2) THEN ! One output per day, at noon (???)

WRITE(*,*) 'Entering output phase'
!Outputs, including total nitrogen, phosphorus and silica, computed in order to check mass conservation, number of Alexandrium cells, of
!total cells and number of cells by size class, nitrogen and phosphorus quantities for the same groups, uptakes, growth rates,
!average and modal sizes, maximum possible growth at a given light and temperature.

WRITE(20,('I3,36(A1,E11.4)')) cd, ';', NH4(sim), ';', NO3(sim), ';', PO4(sim), ';', Si(sim), ';', &
Nc(1,sim), ';', &
SUM(Nc(:,sim), MASK = 1(:,sim) .LT. 3.0), ';', &
SUM(Nc(:,sim), MASK = ((1(:,sim) .GE. 3.0) .AND. (1(:,sim) .LE. 20.0))), ';', &
SUM(Nc(:,sim), MASK = 1(:,sim) .GT. 20.0), ';', &
fL(1,sim), ';', &
SUM(fL(:,sim), MASK = 1(:,sim) .LT. 3.0), ';', &
SUM(fL(:,sim), MASK = ((1(:,sim) .GE. 3.0) .AND. (1(:,sim) .LE. 20.0))), ';', &
SUM(fL(:,sim), MASK = 1(:,sim) .GT. 20.0), ';', &
fT(1,sim), ';', &
SUM(fT(:,sim), MASK = 1(:,sim) .LT. 3.0), ';', &
SUM(fT(:,sim), MASK = ((1(:,sim) .GE. 3.0) .AND. (1(:,sim) .LE. 20.0))), ';', &
SUM(fT(:,sim), MASK = 1(:,sim) .GT. 20.0), ';', &
fN(1,sim), ';', &
SUM(fN(:,sim), MASK = 1(:,sim) .LT. 3.0), ';', &
SUM(fN(:,sim), MASK = ((1(:,sim) .GE. 3.0) .AND. (1(:,sim) .LE. 20.0))), ';', &
SUM(fN(:,sim), MASK = 1(:,sim) .GT. 20.0), ';', &
fP(1,sim), ';', &
SUM(fP(:,sim), MASK = 1(:,sim) .LT. 3.0), ';', &
SUM(fP(:,sim), MASK = ((1(:,sim) .GE. 3.0) .AND. (1(:,sim) .LE. 20.0))), ';', &
SUM(fP(:,sim), MASK = 1(:,sim) .GT. 20.0)

WRITE(*,*) 'Data written'
WRITE(*,*) 'Day number', cd, 'processed'
WRITE(*,*)
END IF

```

```

end do
  lim_DLT = 0.0          ! Reinitializes the limitation
  gd(:, :) = 0.0         ! Reinitializes the day-averaged growth rate
  VNd(:, :) = 0.0        ! Reinitializes the total nitrogen uptake of the current day
  VPd(:, :) = 0.0        ! Reinitializes the total phosphorus uptake of the current day
  VSid(:, :) = 0.0       ! Reinitializes the total silicium uptake of the current day

END DO

DEALLOCATE(NH4, NO3, PO4, Si, Pp, Dn, Dp, Dsi, SM, VNH4_tot, VNO3_tot, VPO4_tot, VSi_tot, mort_N, mort_P, mort_Si, ads_P, des_P)
DEALLOCATE(diat)
DEALLOCATE(gmax, VmaxNH4, VmaxNO3, VmaxPO4, QminN, QminP, QmaxN, QmaxP, Qsi, Kn, Kp, Ks, Topt, Iopt, m, l)
DEALLOCATE(fT, fN, fP, fS, VNH4, VNO3, VPO4, g, NC, Ncmin, Qn, Qp, VNd, VPd, VSid, gd, fL)
DEALLOCATE(PAR)
WRITE(*,*)
WRITE(*,*) 'Arrays deallocated'
WRITE(*,*)
CLOSE(20)
WRITE(*,*) 'Simulation finished'
WRITE(*,*) '-----'

END PROGRAM

SUBROUTINE daylength(J, L, p, D)

!----- 23rd April 2014 -----
! This subroutine, inspired by Forsythe et al (1995) computes the length of one day
! with the day of the year (J), the latitude (L) and daylength correction (p) as
! inputs (CBM method). p is the angle between the center of the Sun and the horizon
! where the day is considered to end, thus enabling to consider twilights.
! The magnitude of error is less than or equal to 2 minutes.
!-----
INTEGER, intent(in) :: J          ! Day of the year
REAL, intent(in) :: L, p         ! Latitude and daylength correction
REAL, intent(out) :: D           ! Length of the day (h)
REAL pi                          ! number pi
REAL theta, phi                  ! Revolution angle and Sun's declination angle
pi = 2*acos(0.0)
theta = 0.2163108 + 2*atan(0.9671396*tan(0.00860*(J-186))) ! Constants are from Forsythe et al (1995)
phi = asin(0.39795*cos(theta))
D = 24.0 - (24.0/pi) * acos((sin(p*pi/180.0) + sin(L*pi/180.0)*sin(phi))/(cos(L*pi/180.0)*cos(phi)))

END SUBROUTINE

SUBROUTINE irradiance(I, D, h, light)

!-----
REAL, intent(in) :: I, D, h      ! Average irradiance, day length and hour of the day
REAL, intent(out) :: light       ! Current irradiance
REAL pi                          ! number pi
pi = 2*acos(0.0)
light = 0.0                      ! Default value, during night
IF (abs(12.0-h) .LE. D/2.0) light = I * (cos(pi*(12.0-h)/12.0)-cos(pi*(D/2.0)/12.0))
light = light / ((1.0/pi)*(sin(pi*(D/2.0)/12.0) - (D/24.0)*cos(pi*(D/2.0)/12.0)))

END SUBROUTINE

```

Annex 6

Formation Doctorale

Intitulé	Nombre d'heure
Aide à la publication scientifique en anglais	15
Philosophie des sciences	15
Français sur Objectifs Scientifiques (FOS)	14
Techniques de communication : l'écrit professionnel	15
Je construis mes bibliographies avec ZOTERO	3
Utiliser l'activité test dans Moodle	2.3
La facilitation graphique (mutualisée)	6
Improviser à l'Université, ça ne s'improvise pas (mutualisée)	6
La dynamique de groupe (mutualisée)	6
Modélisation et Analyse pour la Recherche Scientifique (MARS)	24
Quels outils pour mieux animer ses réunions? (mutualisée)	3
Initiation au langage R	17.5
Je mène mes recherches documentaires : UBODOC, méthodologie, bases de données	2
Transférer des technologies et expertises innovantes à des entreprises	6
éthique et intégrité scientifique	3



MODELING HARMFUL ALGAL BLOOMS IN INTERSPECIFIC COMPETITION

A case study of *Alexandrium minutum* in the Bay of Brest, France

Samuelson Nzeneri, Annie Chapelle, Marc Sourisseau and Martin Plus

Department of Oceanography and Dynamics of the Ecosystem, IFREMER Brest-Iroise, France

Abstract

The proliferation of Harmful Algal Blooms (HABs) is today, a subject of study with strong societal demands and research has been intense because the frequency of observed events has rapidly increased in global coastal waters. *Alexandrium minutum* is one of the toxic species that have the ability to threaten public health, aquaculture and tourism. In France, it was observed in 1988 in the region Bretagne and has continued to proliferate ever since. High levels of PSP toxicity have been detected in the estuaries of Morlaix, Penze, Rance, Abers and more recently, in the Bay of Brest. Its presence in the Bay led to a ban on aquacultural activities and restrictions on the sale and consumption of sea food. Following this incident, the project '*Alex-Breizh*' was launched with the objectives to understand - why *Alexandrium minutum* dominates the microphytoplankton community during a short period, what parameters control its dynamics and how to place them in order of hierarchy. Two approaches were adopted in this study. The first was analyzing field data (abundance of species, temperature and concentration of nutrients) obtained from the study site since 2009 to 2016. The second approach was the use of a 0D numerical model to integrate the existing interactions between the physical and biological processes in the ecosystem. It evaluates the ability of a species to grow with respect to environmental factors such as light, temperature and nutrients (PO_4 , NH_4 , NO_3 and Si), while competing with other species. This modeling technique is based on physiological traits that take phosphorus and nitrogen cell quotas into account. Simulation was performed with 50 species which were uniformly selected with a defined cell size ranging from 1 to $100\mu\text{m}$, an optimal temperature of 10 to 20°C and an irradiance of 8 to $100\text{W}/\text{m}^2$ and consisted of diatoms and dinoflagellate phenotypes. Results of the model show similar resolution in all simulated years where the bloom succession is marked by micro followed by nano and then pico phytoplankton. We noticed an increase in diversity during the spring and autumn but less during the summer due to an increase in competition. We studied the inter-annual variability by comparing a year with *Alexandrium minutum* bloom (2012) and a year without the bloom (2016). Year 2012 shows a higher abundance, specific richness and Shannon indice than 2016. We equally tested scenarios of nutrient reduction and observed that a reduction in nitrogen by 50% has no effect on any of the phenotypes whereas such a reduction in phosphorus slightly reduced the abundance of species. Growth limitation by PO_4 in 2016 is also higher than in 2012. In general, maximum growth and abundance of species were observed between June and August with high inter-annual variability. Our model equally showed that growth is limited by temperature and light during cold periods but limited by phosphate in warm periods. Finally, the model was validated using the field data.

Key words: Bay of Brest, *Alexandrium minutum*, competition, diversity

Modeling Seasonal and Interannual Variability of *Alexandrium minutum* in the Bay of Brest, France

Samuelson Nzeneri, Annie Chapelle, Marc Sourisseau and Martin Plus
Laboratory of Pelagic Ecology
Department of Oceanography and Dynamics of the Ecosystem
IFREMER Brest-Iroise, France
zenerisam@gmail.com

Alexandrium minutum is one of the toxic species that have the ability to produce Harmful Algal Blooms (HABs), threaten public health, aquaculture and tourism. In France, it was observed in 1988 in the region Bretagne and has continued to proliferate ever since. High levels of paralytic shellfish poisoning (PSP) toxicity have been detected in the estuaries of Morlaix, Penzé, Rance, Abers and more recently, in the Bay of Brest. This work tries to define and place in order of hierarchy, the parameters driving *A. minutum* success in the phytoplankton community. A temporal survey (abundance of species, temperature and concentration of nutrients) was done at the site (Daoulas estuary) between 2009 and 2016 and a numerical model was used to simulate the potential impact of known and parameterized interactions between the physical and biological processes in the ecosystem. This model is based on physiological traits (optimal temperature, optimal irradiance, cell size, siliceous/non siliceous) which can be used to evaluate the ability of a species to grow with respect to environmental factors such as light, temperature and nutrients (PO_4 , NH_4 , NO_3 and Si), while competing with other species. *A. minutum* was placed in competition with 72 species which were uniformly selected. Results showed both seasonal and interannual variability of bloom phenology. It was marked by micro, followed by nano and then pico phytoplankton from April to October. Phytoplankton bloom in the area is limited by temperature and light during the winter and by nutrients in the summer – first by Phosphorus and then Nitrogen. *A. minutum* bloom occurred between June and August, at the beginning of the period marked by low nutrient concentrations and high resource competition. The delayed bloom start of *A. minutum* in a cold spring (2013) and the early bloom start in a warm spring (2014) are well simulated. In addition, the year 2012 with the highest rainfall in summer which implies increased nutrient inputs; showed higher abundances than the year 2011 with the lowest summer rainfall. In 2012, *A. minutum* is also the dominant species over the microphytoplankton diversity, both *in situ* and in the model. However, environmental factors and competition explain only a part of the interannual variability in *A. minutum* bloom duration and intensity within the phytoplankton community. Though the model was able to reproduce parts of the seasonal and interannual variability of *A. minutum*, it was not consistent over the study period. Model highlights the increasing relevance of other biological processes (the intraspecific diversity, the predators and sexual reproduction) in bloom regulation at decade scale.

Key words: *A. minutum*, HABs, Bay of Brest, Resource Competition, Physiological Traits, Modeling, Variability

Introduction

Research on Harmful Algal Blooms (HABs) has been intense in recent years because the frequency of observed events has rapidly increased in global coastal waters (Hallegraeff, 2010, 1993). HABs are related to a number of events especially the production of toxins (by microalgae) that are poisonous to man and the environment. Human health is usually affected through the consumption of contaminated sea food, skin

contact and possible inhalation. Some of these toxins are powerful and deadly (Anderson et al., 2002) and thus, cause a problem across several coastal and sea waters. In addition, one of the characteristics of HABs is their ability to colonize and dominate multiple habitats within a short period. For these reasons, the proliferation of HABs has become a subject of study with strong societal demands. They pose numerous scientific questions such as - why/when some toxic species become dominant in the

phytoplankton community; is the occurrence/frequency of toxic events related to human activity etc. Harmful algae are therefore, ideal models to study ecological niches and to contribute to more global research challenges (Sourisseau et al., 2017).

HAB events in France date back to the late 1980s (Probert, 1999; Erard-Le Denn, 1997; Belin, 1993) and one of the causative species is *Alexandrium minutum*. Halim (1960) formally established the description of *Alexandrium*, a small-sized dinoflagellate that produced a 'red tide' in the harbor of Alexandria in Egypt. This genus is believed to include more than 30 species, many of which have been described under a different genus name (Anderson et al., 2012). *A. minutum* produces the Paralytic Shellfish Poison (PSP) toxin. In France, it is found in rich-nutrient confined ecosystems, mostly estuaries, from mid-May to August when nutrients, water temperature and irradiance support sufficient growth to compensate mortality rates mostly due to tidal dilution (Chapelle et al., 2015). High abundances of the species have been detected in northern Brittany in the estuaries of Morlaix, Penzé, Rance, Abers and recently, in the Bay of Brest (Chapelle, 2016; Chambouvet et al. 2008; Maguer et al. 2004) given PSP toxicity events. The bloom events in the region present similar temporal and geographical patterns and in most cases, bloom toxicity (in shellfish) corresponds with the period of maximum cell concentration in the water column and maximum concentration or production of toxins which is enhanced by high temperatures (Guallar et al., 2017; Lim et al., 2006).

The study of *A. minutum* was focused on the Daoulas estuary which has so far experienced the maximum level of toxicity in the Bay of Brest as recorded in the French National Phytoplankton and Phycotoxins Survey – REPHY (Réseau d'Observation et de Surveillance du Phytoplancton et des Phycotoxines). By doing this, we attempted to address the following questions -

- What environmental factors are responsible for seasonal and interannual variations at a decade scale?

- How does *A. minutum* compete with other species under different environmental conditions?

To answer these questions, we surveyed and analyzed field data (abundance of species, temperature and concentration of nutrients) obtained from the study site (Daoulas estuary) since 2009-2016 and integrate them with a numerical model. Previous models have been developed to simulate *Alexandrium* population dynamics in order to explore the interactions between cyst germination, cellular growth and water circulation and to identify the effect of physical processes on bloom development and transport across the estuary (Fauchot et al., 2008). They can demonstrate high fidelity at reproducing observations (He et al., 2008; Stock et al., 2005) and thus be used for hindcasts (looking at past events to understand underlying mechanisms; Li et al., 2009), issue weekly nowcasts and forecasts (looking forward 3 or 4 days) and even seasonal or annual forecasts (McGillicuddy et al., 2011). It is a useful tool or technique to unravel the growth rate and spread of *Alexandrium* blooms and takes into account the biotic and abiotic parameters which sustain and promote the development of species.

The originality of the model used in the current study was inspired by Sourisseau et al. (2017) who studied the main driver of species selection using a trait-based model that keeps phenotypic variability through physiological trait parameterization. This model allows the simulation of *A. minutum* in order to evaluate its ability to grow under different environmental conditions while competing interspecifically with other species.

2. MATERIALS AND METHODS

2.1. Study site

Situated in North/West of France, France, the Bay of Brest is a macrotidal semi-enclosed embayment which has an oceanic temperate climate, characterized by a vast basin of 180km² (Le Pape and Menesguen, 1997). Its largest dimensions are 27km in the East/West direction and 11km in the North/South (Monbet and Bas-

soullet, 1989). This ecosystem has two principal continental river flows (the Elorn and Aulne rivers), a central zone and narrow estuaries such as Daoulas (Fig. 1).

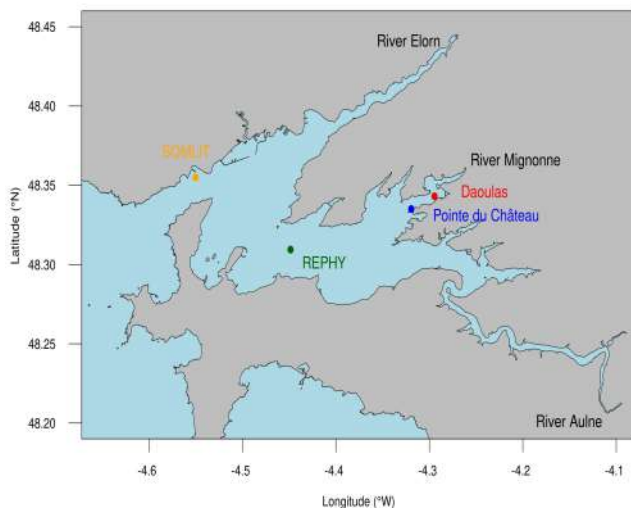


Figure 1. The Bay of Brest showing study site (Pointe du Château), rivers and measurement stations

The site - ‘Pointe du Château’ which is located in the Daoulas estuary, observed the maximum abundance of *A. minutum* than anywhere else in the Bay (Chapelle et al. 2015). The Bay of Brest undergoes water changes linked to river inputs (Del Amo et al., 1997) and some of the physical parameters (tide, residence time, nutrient exchanges and water temperature) have been previously studied with a hydrodynamic model (Le Pape and Menesguen, 1997).

2.2. Numerical model

To evaluate the ability of *A. minutum* to grow with respect to environmental factors (light, temperature dilution and nutrients) while competing with other species, a numerical model was used. Models of various types have been developed to describe and investigate the physiology and bloom dynamics of phytoplankton (Flynn, 2005). Droop and Monod are two of such common macroscopic models. Although both models share the same interest, the Monod (1942) model linking growth directly to ‘extracellular’ nutrient concentrations is one of the simplest models, but it is not adapted to simulate transient growth dynamics related to a non steady-state environment, despite its wide use in 3D ecosystem models (Haney and Jackson, 1996). Alternatively, a more physiologically

defensible, yet still highly idealized and accurate in many comparative studies (Grover, 1992, 1991), is the Droop/Caperone ‘internal-stores’ approach (Droop 1968, Caperone 1968) which links growth to the internal nutrient pool (or quota). It provides a hyperbolic form of the growth curve using only two parameters - the minimum quota to sustain growth and a maximum theoretical growth rate at infinite quota.

Using the Droop approach, we thus performed simulations with a trait-based model (Litchman et al. 2012) that includes a phenotypic variability of different parameter sets (Barton et al., 2010; Dutkiewicz et al., 2009). The main part of the model is described in Sourisseau et al. (2017). This modeling technique is associated with the selection of three relevant and independent physiological traits: cell size (a continuous trait in ESD, Equivalent Spherical Diameter), cell cover (a categorical trait: siliceous or not) and optimal temperature (a continuous trait in degree Celsius). Other parameters are described as trade-off of cell size, assuming that nutrient acquisition scale with cell volume or mass (Litchman et al., 2007; Finkel, 2001; Kooijman 2001; Tang, 1995; Banse, 1982; Laws, 1975), so the maximum rate of nutrient absorption (V_{max}), cell quota and half saturation constants for nutrient assimilation were determined using allometric relationships. Irradiance is also described as a trade-off of cell size which differs from Sourisseau et al. (2017). To decrease the computing time required for inter-annual simulations and better environmental representations, the initial model in Sourisseau et al. (2017) was improved with three modifications - uniform distribution of phenotypes in the trait space, a variation of optimal irradiance based on cell size and the introduction of sedimentary nutrient fluxes.

2.3. Phenotypic variability

Phenotypic variability was determined based on a combination of the above-mentioned traits (the cell size, the optimal temperature and the ability/inability of the phenotype to assimilate silicate). The parameterization of each trait was accompanied by relevant trade-offs that are well defined for phytoplankton groups (Litchman and Klausmeier, 2008). For exam-

ple, a small cell will have a high affinity for nutrients but a weak capability in stocking them (quotas). Different numbers of phenotypes (e.g. 25, 50, 72, 100 and 200) in competition with *A. minutum* were tested and the best representation of field data with a reasonable computing time was obtained with 72. The selected configuration includes 36 siliceous and 36 non-siliceous phenotypes with size distribution on log scale from 1 to 64 μ m of ESD (Fig. 2). In characterizing them, the picophytoplankton (pico) was represented by phenotypes of 1 and 2 μ m, nanophytoplankton (nano) by 5 and 18 μ m and microphytoplankton (micro) by 28 and 64 μ m (Table 1). For *A. minutum*, 18 μ m (Maranon et al., 2013) is attributed to its mean length since its shape is considered sub-spherical (Balech, 1989), spherical (Probert, 1999) or ellipsoidal (Hillebrand et al., 1999).

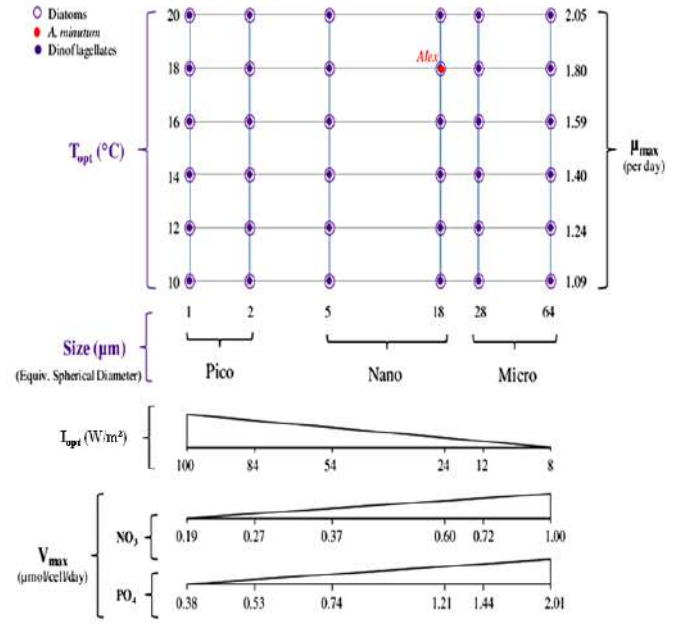


Figure 2: Distribution of 73 phenotypes (*A. minutum*, 36 diatoms and 36 dinoflagellates)

Category	Size (μm)	Phenotype		T_{opt}	μ_{max}	I_{opt}	Q_{min}^N	Q_{min}^P	Q_{max}^N	Q_{max}^P	Qsi	Kn	Kp	Ksi	Mort	V_{max}		
		Dino	Diat													NH ₄	NO ₃	PO ₄
Pico	1	2	38	10	1.09	100	2.9E-09	1.4E-10	2.00	2.00	0	0.23	0.01	0	0.02	0.38	0.19	0.38
		8	44	12	1.24													
		14	50	14	1.40													
		20	56	16	1.59													
		26	62	18	1.80													
	2	32	68	20	2.05	84	2.3E-08	1.1E-09	2.46	2.46	0	0.53	0.03	0	0.02	0.53	0.265	0.53
		3	39	10	1.09													
		9	45	12	1.24													
		15	51	14	1.40													
		21	57	16	1.59													
Nano	5	27	63	18	1.80	54	1.9E-07	9.0E-09	3.03	3.03	0	1.21	0.06	0	0.02	0.73	0.36	0.73
		33	69	20	2.05													
		4	40	10	1.09													
		10	46	12	1.24													
		16	52	14	1.40													
	18	22	58	16	1.59	24	4.0E-06	1.9E-07	4.12	4.12	0	4.14	0.20	0	0.02	1.20	0.60	1.20
		28	64	18	1.80													
		34	70	20	2.05													
		Alex	-	18	1.80													
		5	41	10	1.09													
Micro	28	11	47	12	1.24	12	1.2E-05	5.7E-07	4.60	4.60	0	6.41	0.31	0	0.02	1.43	0.71	1.43
		17	53	14	1.40													
		23	59	16	1.59													
		29	65	18	1.80													
		35	71	20	2.05													
	64	6	42	10	1.09	8	9.5E-05	4.6E-06	5.66	5.66	0	14.72	0.70	0	0.02	2.00	1.00	2.00
		12	48	12	1.24													
		18	54	14	1.40													
		24	60	16	1.59													
		30	66	18	1.80													
Micro	64	36	72	20	2.05													
		7	43	10	1.09													
		13	49	12	1.24													
		19	55	14	1.40													
		25	61	16	1.59													
Micro	64	31	67	18	1.80													
		37	73	20	2.05													

Table 1: Characteristics of phenotypes

Temperature being a major environmental parameter that regulates metabolic rates such as photosynthesis, respiration, growth, resource acquisition and motility (Sourisseau et al., 2017; Litchman and Klausmeier, 2008; Eppley, 1985), this dependence may be simulated with an optimal temperature (T_{opt}). T_{opt} in our configuration was linearly distributed from 10 to 20°C to cover only the temperature range of seawater in the Bay. *A. minutum* was assigned a T_{opt} of 18°C because its optimum growth occurs between 17 and 20°C (Bill et al., 2016) and also because its maximum bloom densities in Bretagne (Penze and Rance) have been observed when water temperatures were between 16 and 20°C (Chapelle et al., 2007).

In our model, the maximum growth rate for species i ($\mu_{max,i}$) depends on temperature and can be simulated with a global exponential law according to Eppley, 1972.

$$\mu_{max,i} = \mu_{max,ref} * e^{(K_T * T_{opt,i})}$$

Where $\mu_{max,ref}$ (0.58 d⁻¹) is the growth rate at 0°C without limitation and K_T (0.063 °C⁻¹) is the temperature coefficient for growth rate (Sourisseau et al. 2017)

The nutrient absorption rate (V_{max}) is dependent on cell size through an allometric relationship (see Sourisseau et al., 2017, and Fig. 2). The cell size equally determines the nutrient storage capacity (cell quota). Nutrient uptake rate increases with an increasing external nutrient pool following Michaelis-Menten kinetics (with K the half-saturation constant), but decreases when cell quota approaches maximum. Species of similar size were therefore, assigned similar K , V_{max} and intracellular storage capacity for P and N.

Lastly, irradiance is a trade-off that is modulated by the quantity and quality of pigment content in a cell. It was distributed from 8 to 100W.m⁻² in our configuration to cover the Photosynthetically Available Radiation (PAR) observed in the Bay of Brest. According to Edwards et al. (2015), optimal irradiance is linked to cell size i.e. it decreases with increasing cell size (Finkel, 2001). Size of the cell itself is very

important in classifying and modeling photosynthetic rates in phytoplankton (Tang, 1995; Agusti, 1991; Joint and Pomroy, 1988). Cullen et al. (1993) also suggested that cell size should be included in the description of phytoplankton growth intended for biogeochemical models. Using an I_{opt} of 100μmol.m⁻².s⁻¹ or 24W.m⁻² (FiNAL, 2008; Chang and McClean, 1997) for *A. minutum* and a cell size of 18μm as points of reference, I_{opt} was assigned to other phenotypes based on their cell size.

2.4. Model equations

Most of the equations are described in Sourisseau et al., 2017. Described here are two of the main equations. The first determines the total abundance of each phytoplankton species (φ_i) simulated with respect to growth (μ_i), dilution (D) and mortality (m).

$$\frac{\partial \varphi_i}{\partial t} = \mu_i \varphi_i - D \varphi_i - m \varphi_i$$

Where i represents each of the 73 species

A minimal abundance was considered in order to avoid the extinction of species due to dilution and mortality. It was determined as Sourisseau et al. (2017) in a way that the minimal volume occupied by each species is 10⁶μm³.L⁻¹. This implies a minimal abundance of 3.8cells.L⁻¹ for the largest cells (64μm), 10⁶cells.L⁻¹ for the smallest cells (1μm) and 171cells.L⁻¹ for *A. minutum* (18μm) similar to the detection threshold for microphytoplankton (100cells.L⁻¹) used in the protocol of REPHY monitoring program.

The second equation is used to describe the limiting factors on the growth rate of species. This equation can be expressed with Liebig's law (Legovic and Cruzado, 1997) as –

$$\mu_i = \mu_{max,i} \cdot f_{T,i} \cdot f_{min}(L_{L,i} L_{N,i} L_{P,i} L_{Si,i})$$

Where $\mu_{max,i}$ is the maximum growth, $f_{T,i}$ is the limitation by temperature and $f_{min}(L_{L,i} L_{N,i} L_{P,i} L_{Si,i})$ is the minimum limitation by light, nitrogen, phosphorus and silicon for each species i

Species thus, compete for N, P and Si. The principle nutrient source is the river (or productive areas like estuaries) but the sediment also contains high concentrations of organic matter and therefore, implies a secondary nutrient source based on the remineralization that releases irregular phosphate and nitrogen (Andrieux-Loyer et al., 2008). This additional nutrients input from sediment can stimulate the growth of species like *A. minutum* which is able to store phosphate in high quantities (Yamamoto and Tarutani, 1999) thereby, making it appear more like a ‘storage specialist’ that uptakes PO_4 pulses for luxury consumption (storage) and then, utilizes the stored PO_4 for cell growth (Labry et al. 2008). Phosphates fluxes from the sediment were obtained with the slope:

$$f(x) = 5.9 * e^{(0.1 * T)}$$

Where $f(x)$ is the PO_4 flux (in $\mu\text{mol.L}^{-1}.\text{d}^{-1}$) and T is temperature (in $^{\circ}\text{C}$). This relationship was determined by Andrieux-Loyer et al. (2008) for marine coastal sediments.

Nitrogen fluxes were not included because Trommer et al. (2013) found that the phytoplankton community in the Bay of Brest generally experience longer P limitation than N limitation. They equally found a significantly increased growth rate in all samples containing P additions.

2.5. Simulated area

The Daoulas estuary (Fig. 3) was considered homogeneous in our 0D model, with a river inflow (Riv) and a dilution rate due to wind, river flow and the tidal inflow/outflow (Rad). Both flows are accompanied by the macronutrients (PO_4 , NH_4 , NO_3 and Si) which are commonly known to drive phytoplankton dynamics in coastal waters. Nutrient concentrations in river Daoulas were interpolated from monthly data measured by Brest Metropole Océane while those of ‘Rad’ were interpolated from weekly data provided by the Service d’Observation en Milieu Littoral (SOMLIT) situated at the Portzic station. Data on light and temperature were provided by METEOSAT Second generation satellites and Meteo-France respectively.

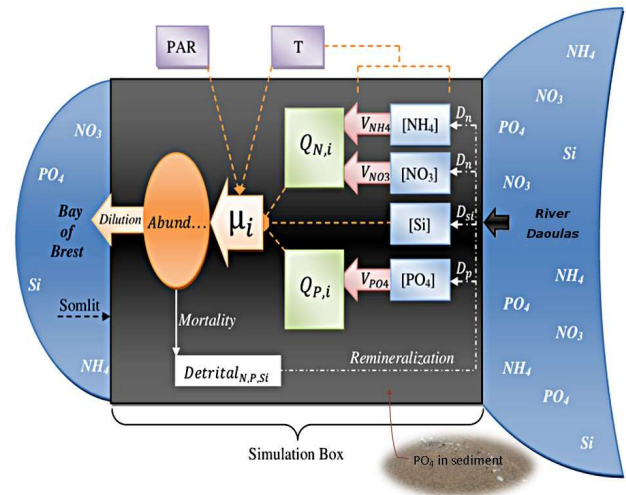


Figure 3: Concept of the model describing the simulated area and Daoulas estuary

The rate of dilution was calculated using a hydrodynamic model (Lazure and Dumas, 2008) applied to a realistic configuration of the Bay of Brest from 2009 to 2016. The daily Daoulas river flow data were provided by HYDRO – a government environmental database.

2.6. Data set

Nutrients and the composition of phytoplankton community were obtained from a weekly sampling project (*Alex-Breizh*) which was launched in 2016 with focus on the Daoulas estuary which has a sampling point at Pointe du Château (following the bloom outbreak of 2012). Water samples were collected at high tides with Niskin bottles and further analyzed in the laboratory with optical microscopy and cytometry together with fluorimetry/colorimetry for the concentration of inorganic nutrients (NH_4 , PO_4 , NO_3 and Si). This project was complimented by VELYGER monitoring program dedicated to studying the factors that control oyster growth in the Bay of Brest. It provided us with the abundances of *A. minutum* and microphytoplankton species in Pointe du Château since 2009. Among the years studied, 2016 has the highest number of *in situ* data. We shall use this year to evaluate the seasonal variability of phytoplankton.

2.7. Simulation analysis

In comparing the simulated dynamics of *A. minutum* and phytoplankton with the field data,

the method developed by Rolinski et al. (2007), commonly referred to as Weibull, was considered. It provided values of cumulative abundance, maximum abundance (MA), date of the maximum (DMA), the beginning, end and duration of bloom by using the input of either model or field data. For the seasonal variability of phytoplankton and environmental variables, the approach of Del Amo et al. (1997) was used to divide the annual cycle of the Bay of Brest into four seasons: Season I, Spring (March 1 to May 31); Season II, Summer (June 1 to August 31); Season III, autumn (September 1 to November 30); and Season IV, Winter (December 1 to February 28). To summarize the relationship (correlation and deviation) between model and field data, Taylor diagrams were plotted (Taylor, 2001). To study the observed and simulated interannual variability, Heatmap correlation distance per year was estimated to identify the cluster of rows of variables with similar patterns. Lastly, to determine which years had the highest and lowest river flows, we used the approach of Van-Rooy (1965) to analyze rainfall anomaly index (RAI). The same approach was equally used to determine temperature and light anomalies.

3. RESULTS

3.1. Seasonal variability

All environmental variables change with respect

to season and the three categories of phytoplankton showed the same global seasonal phenological trend over the study period. We therefore, used the data of year 2016 to illustrate the seasonal variations because this year has more observations than the other years.

3.1.1. Environmental variables

Temperature and light follow strong and similar seasonal patterns with low values of 8.6°C and 15W.m⁻² in the winter respectively in January and December but high values in the summer with a maximum of 20.5°C in August and 349W.m⁻² in July (Fig. 4). River flow is highest (10⁶ m³.d⁻¹) in the winter but lowest (10⁴ m³.d⁻¹) in the summer. Dilution rate results from both the daily/seasonal patterns of river flow and the moon tidal variations (two-week cycle of neap and spring tides). Out of the productive periods (from January to March), rainfall influences the concentration of nutrients which increases with increasing river flow. From April to October, nutrients remain low due to less river flow and high productivity of phytoplankton. The model closely followed the trends of field data especially those of NO₃ and Si. PO₄ was however underestimated by the model in the summer and beginning of autumn. Reversely, between January and June, the model overestimated NH₄ field data but slightly followed the trend from November to December.

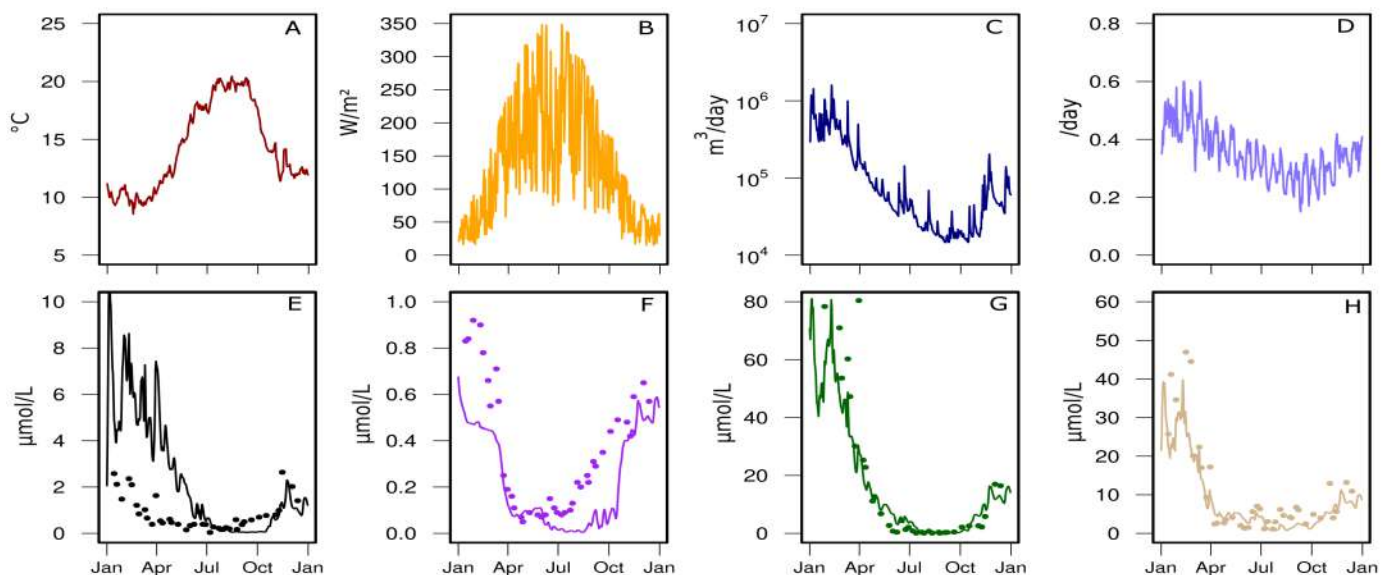


Figure 4: Seasonal variability of environmental variables. A: Temperature, B: Light, C: River flow, D: Dilution, E: NH₄, F: PO₄, G: NO₃, H: Si. Observed nutrients are points while simulated are lines.

3.1.2. Phytoplankton community

December to the end of April showed a stable abundance of simulated phytoplankton which corresponds to the minimal values fixed in the model (Fig. 5A). In May, there is first – a gradual increase of micro and nano and slight increase of pico. The micro reached its maximum abundances first ($5 \times 10^4 \text{ cells.L}^{-1}$) followed by the nano ($10^6 \text{ cells.L}^{-1}$) in June and pico (over $10^9 \text{ cells.L}^{-1}$) in October. At the end of June, the microphytoplankton size fraction had decreased to its lowest abundance whereas, nano is about its maximum but pico is still on the increase. By September, pico continued to increase in abundance but no further net growth is simulated in nano and micro size fractions. The abundance of pico remained relatively stable until late October and early November when it experienced a sharp decrease. The same period is marked by

a slight increase in the abundance of micro before the last decrease. There are also seasonal variations in the abundance of each phenotype of the same size with regards to their optimal temperature. Among those of $1\mu\text{m}$ (Fig. 5B), species of 10°C have the lowest abundance while species of 16°C to 20°C have the highest abundance. Those of 16°C were the first to bloom, 18°C being the most abundant and 20°C having MA below those of 18°C but above those of 16°C . With species of $5\mu\text{m}$ (Fig. 5C), there is a similar timing of bloom increase and all the species have a good summer peak. Their peaks started to decrease at the same period but species of lower T_{opt} were the first to completely decrease. For the $28\mu\text{m}$ (Fig. 5D), species of 16°C are the most abundant in the spring bloom but those of 14°C dominated in autumn bloom.

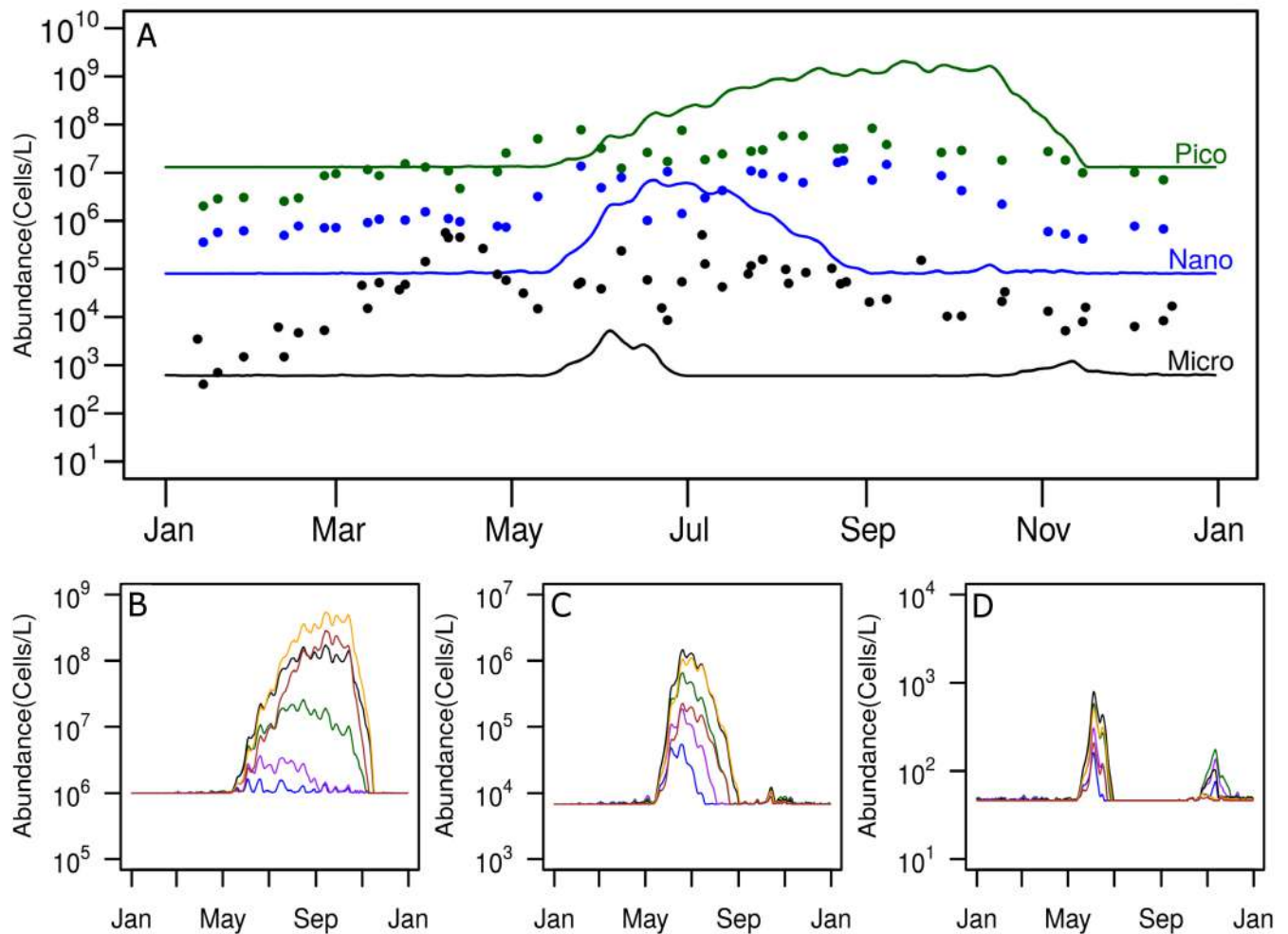


Figure 5: A: Field (points) and model (line) seasonal variability of phytoplankton abundance in 2016. B: Species of $1\mu\text{m}$, C: Species of $5\mu\text{m}$, D: Species of $28\mu\text{m}$. B, C and D show the variability in the simulated abundance of species of same size as a function of optimal temperature in 2016: blue (10°C), purple (12°C), green (14°C), black (16°C), orange (18°C), brown (20°C).

With *in situ* data, field abundances of pico, nano and micro appeared steady in the winter but increased earlier in spring with a slightly faster increase for the micro size fraction from March. Pico and nano experienced high abundances in June whereas micro decreased in the same month. Micro however, showed two maxima – one in April and another from June to August and then, decreased in October. Nano remained stable all summer but decreased in September to reach winter abundances. Pico decreased in late October and early November. At this period, there is a slight increase in micro which might represent the autumn peak. Final densities of the micro size fraction in December 2016 are different from the initial conditions in January 2016 thereby, indicating some interannual variability of this seasonal cycle. There is a difference in the timing of abundance increase and decrease between field and model in several cases. For example, the comparison of model and observation shows underestimation of micro, nano and pico in winter/spring but good timing in summer micro bloom. Nano showed similar increasing time in May, pico and micro showed similar decreasing time in November. The model closely followed *in situ* pico between March and mid-June after which, it overestimated observation until mid-November to December when both showed similar abundances.

3.1.3. *Alexandrium minutum*

Observed *A. minutum* blooms occurred during summer between May and August with MA between June and the end of August (Figs. 6A-H). By the end of September, abundances dropped to the lowest levels and consequently disappearing during the winter. Simulated *A. minutum* also has similar dynamics. Despite sometimes, a slight delay of the abundance increase compared to observations (e.g. Figs. 6E, 6F), the model showed a similar timing in the beginning of the bloom but its MA occurred much earlier in some of the years (2010, 2012 2013, 2014 and 2015). Between August and mid October, no significant net growth was noted in the model. In November however, another bloom (autumn peak) was detected in the model but none was observed in the field. From December until the end of April, growth was absent in both field and model. To evaluate what environmental factors control *A. minutum* growth, the maximum limiting factors (T, L, P, and N) are shown in figures 6I-P. *A. minutum* is first limited by temperature at the beginning of the year then it becomes limited by nutrients – first by P and then N from May to October. The end of the year is marked by temperature and light limitations.

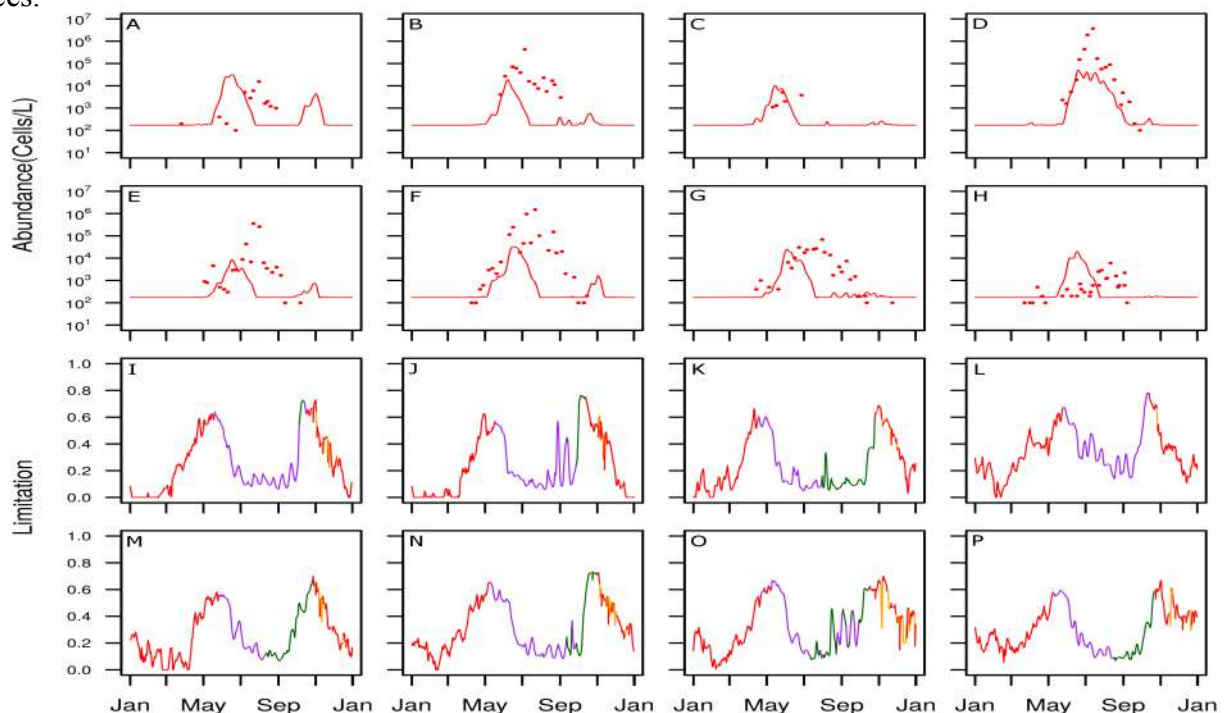


Figure 6: Field (points) and model (line) seasonal and interannual variability in the abundances of *A. minutum* and its maximum limitations. 2009: A and I, 2010: B and J, 2011: C and K, 2012: D and L, 2013: E and M, 2014: F and N, 2015: G and O, 2016: H and P. Temperature in red, Light in orange, Nitrogen in green and Phosphorus in purple.

3.2. Interannual variability

3.2.1. *Alexandrium minutum*

Highest MA in the field (3 675 330 cells.L⁻¹) and model (49 810 cells.L⁻¹) occurred in 2012 which has not just the highest MA but also the longest bloom duration (Table 2). In 2010, 2012, 2013, 2014 and 2015 (Figs. 6B, D-G), both model and field increase simultaneously but model declined before field data – leading to lower and early date of maximum abundance. DMA is quite close in 2011. Years 2009 and 2016 are not properly represented by the model as MA and highest concentrations occurred much earlier in the model. Regarding environmental limitations, year 2012 showed exceptional less nutrient limitation in summer with P limitation over 0.2 and no N limitation.

The interannual variability in the abundance of *A. minutum* is described with scaled value patterns (Fig. 7A). There appears to be an obvious similarity in the temporal patterns on the MA of *A. minutum* (in both field and model) with higher scores in 2012 and 2014 in contrast to 2011 and 2013, having lower scores. In the same manner, some similarities were observed in the cumulative abundance, DMA, bloom start and end of *A. minutum*.

The overall quantitative performance of the model in relation to the abundance of *A. minutum* is summarized in Taylor diagram (Fig. 7B) where the simulations of 2010, 2012, 2014 and 2015 are much closer to the observations with positive correlation coefficient and similar variability than other years especially 2011 which

	Year	Field					Model				
		MA	DMA	Bloom (Weibull)			MA	DMA	Bloom (Weibull)		
				Start	End	Duration			Start	End	Duration
<i>A. minutum</i>	2009	15 400	Jul 31	Jun 30	Aug 08	37	31 600	Jun 11	May 27	Jun 29	33
	2010	432 600	Jul 04	Jun 27	Jul 10	12	19 030	Jun 05	May 27	Jun 21	25
	2011	5 100	May 22	Apr 17	Dec 06	339	10 450	May 14	May 05	Jun 06	32
	2012	3 675 330	Jul 11	Jun 27	Jul 18	23	49 810	Jun 18	Jun 10	Aug 11	62
	2013	358 400	Jul 09	Jul 02	Jul 16	15	8 728	Jun 15	Jun 03	Jul 11	38
	2014	1 496 480	Jun 16	May 29	Jun 24	26	33 130	Jun 14	Jun 05	Jul 05	30
	2015	68 800	Aug 02	May 30	Sep 08	101	25 770	Jun 01	May 25	Jun 29	35
	2016	6 000	May 29	Mar 02	Dec 25	346	19 760	Jun 15	May 26	Jul 04	39
Pico	2009	-	-	-	-	-	2 596 800 000	Sep 15	Jun 25	Oct 25	122
	2010	-	-	-	-	-	2 407 200 000	Sep 04	Jun 06	Oct 05	121
	2011	-	-	-	-	-	2 398 560 000	Sep 22	May 11	Oct 30	172
	2012	-	-	-	-	-	513 600 000	Sep 14	Jul 27	Oct 10	75
	2013	-	-	-	-	-	1 563 120 000	Sep 17	Jul 06	Oct 29	115
	2014	-	-	-	-	-	1 843 920 000	Sep 23	Jun 21	Oct 21	121
	2015	-	-	-	-	-	2 139 840 000	Aug 26	Jun 15	Oct 19	126
	2016	84 036 364	Sep 03	Feb 14	Apr 14	59	2 069 520 000	Sep 14	Jun 20	Oct 25	127
Nano	2009	-	-	-	-	-	8 786 400	Jun 20	May 28	Jul 24	57
	2010	-	-	-	-	-	8 488 800	Jun 08	May 27	Jul 14	49
	2011	-	-	-	-	-	6 712 800	May 27	May 03	Jun 26	54
	2012	-	-	-	-	-	8 440 800	Aug 14	May 30	Oct 01	124
	2013	-	-	-	-	-	8 937 600	Jul 04	May 28	Aug 04	78
	2014	-	-	-	-	-	7 524 000	Jun 27	Jun 04	Jul 29	54
	2015	-	-	-	-	-	8 652 000	Jun 27	May 17	Jul 22	66
	2016	17 760 181	Aug 24	May 06	Jun 13	38	6 991 200	Jun 19	Jun 01	Jul 29	58
Micro	2009	4 909 700	Jun 18	Jun 08	Jun 25	17	8 981	Jun 07	May 22	Jun 20	29
	2010	3 436 498	Aug 05	Apr 08	May 10	32	8 813	Jun 06	May 09	Jun 12	34
	2011	1 841 408	May 31	Apr 14	May 16	32	5 930	May 13	Apr 21	May 19	29
	2012	2 921 035	Jul 13	Apr 19	May 20	31	12 257	Jun 18	Jun 03	Jun 27	24
	2013	4 490 923	Jun 18	Apr 17	May 07	20	5 213	Jun 16	May 15	Jun 22	38
	2014	1 082 600	Jul 22	Feb 16	Mar 24	35	5 830	Nov 03	-	-	-
	2015	1 579 687	Jun 11	Mar 05	Apr 07	32	12 053	Jun 02	May 22	Jun 12	21
	2016	561 500	Apr 08	Feb 25	Mar 11	13	5 222	Jun 04	May 26	Jun 21	27

Table 2. Field and model interannual variability in the MA, DMA and bloom characteristics of phytoplankton

is the most poorly simulated year. Over the eight year period, having the lowest mean square difference, the DMA appears to be better represented (Fig. 7C) than other variables of *A. minutum*. Despite a good representation of the DMA, the bloom start, end and duration are not consistently simulated over the period.

3.2.2. Phytoplankton community

Over all simulated years, an average MA of approximately $10^8 \text{ cells.L}^{-1}$ was noted for the pico-phytoplankton which appeared to be the most abundant phytoplankton group. It showed a long duration in 2011 (the year with little

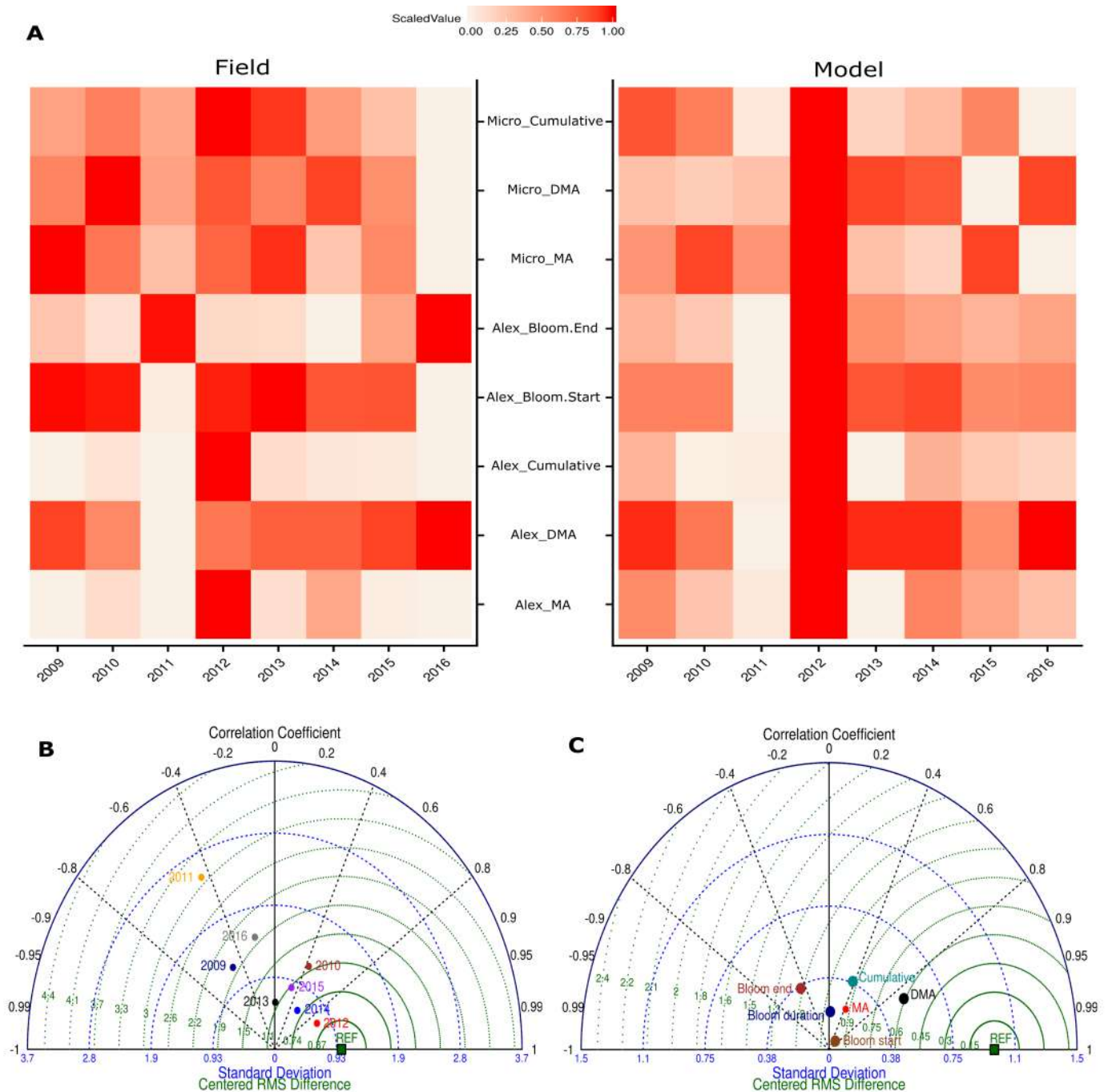


Figure 7. A: Heatmap comparing interannual field and model variables of phytoplankton in the years studied. Each year is represented in a column and each variable is represented in a row. Comparison can be made per variable per year in both field and model or collectively for interannual variations in either field or model. Scaled value (color assigned to a variable) is a correlation distance or a normalization which is obtained by dividing the mean of each row by its standard deviation. All variables are directly extracted from actual data except Alex_Bloom.Start, Alex_Bloom.End and Alex_Cumulative which were obtained with the fitting of a Weibull function. B: Taylor diagram of log *A. minutum* abundance of each simulated year. C: Sum of each variable over the eight year period - MA, DMA and Cumulative are actual values whereas Bloom start, end and duration were determined with Weibull. REF is the field data equivalence of each simulated variable.

growth in large cells) and a very short duration in 2012 (the year with high growth in large cells) – Table 2. The nanophytoplankton on the other hand, had an average MA of $10^5 \text{ cells.L}^{-1}$, with the longest duration in 2012 and short durations in 2010 and 2011. Comparing field and model, there is a similarity in the MA of Micro in 2014 and 2016 and in its cumulative abundances in 2010, 2012 and 2016 (Fig. 7A). Their DMAs correspond only in 2011 and 2014. As a global evaluation, highest values were recorded in 2012 for most of the variables. Micro had very short duration with low average MA of $10^2 \text{ cells.L}^{-1}$ over the eight simulated years. It also showed significant secondary peaks over the years except in 2012 and equally underestimated field data in all cases (Fig. 8).

Interannually variability exists not only among pico, nano and micro but also among phenotypes of similar size (Table 3). Among those of $18\mu\text{m}$, *A. minutum* appeared to be dominant in most of the years simulated. This is obvious in the year 2012 where it showed a higher abundance and longer bloom duration (Fig. 9). The MAs of these phenotypes varied from one year to the other but phenotype of 10°C appeared to be the least dominant. We equally observed autumn peaks for most of the species especially in 2009 and 2014 which had abundances close to those of the summer peak. The peak is however, insignificant in 2012 compared to other years. There was a very close competition between *A. minutum* and phenotype of 14°C in 2010 and 2011. Phenotype of 14°C however,

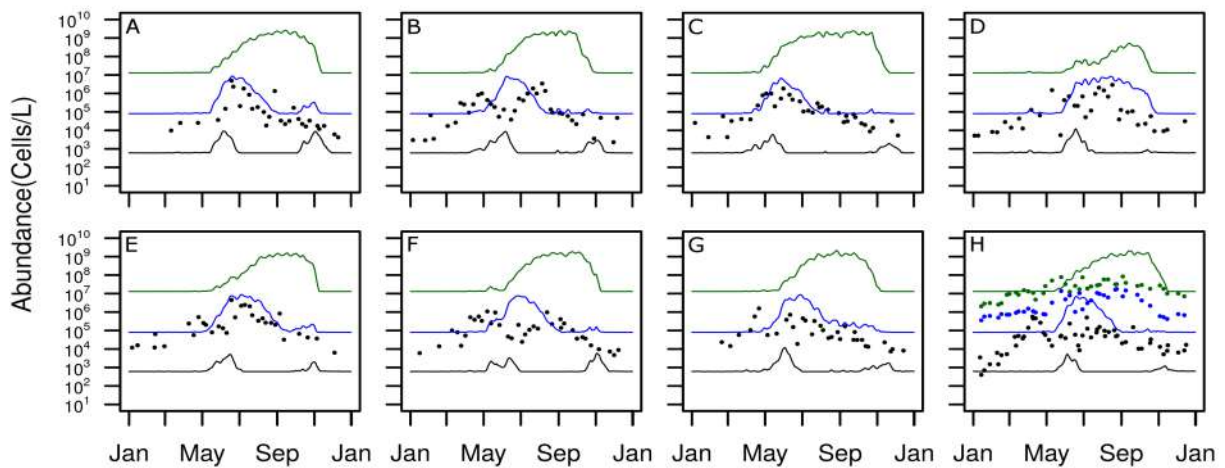


Figure 8. Field (points) and model (line) interannual variability of phytoplankton abundances. Pico in green, nano in blue and micro in black. Observed abundances are points while simulated are lines. 2009: A, 2010: B, 2011: C, 2012: D, 2013: E, 2014: F, 2015: G, 2016: H.

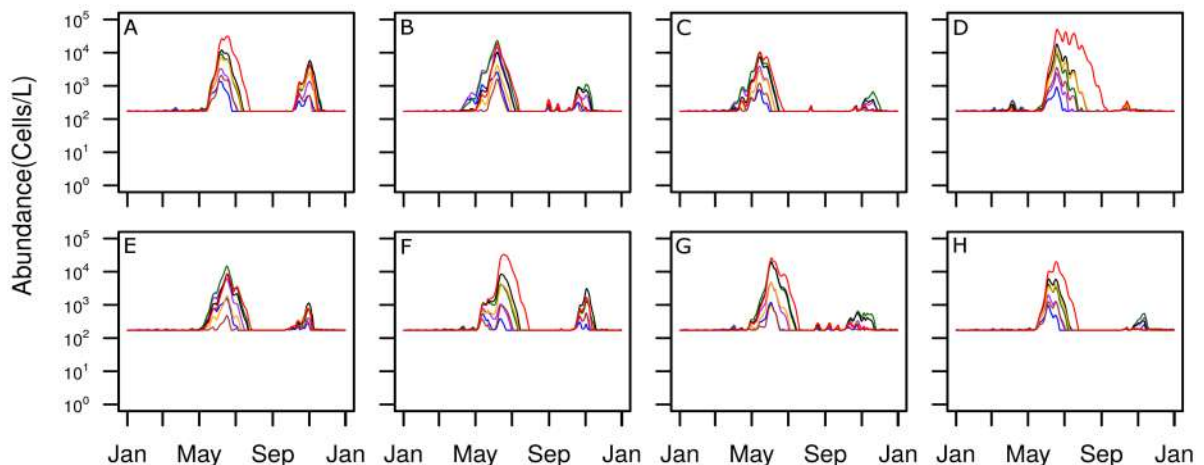


Figure 9. Simulated abundances of phytoplankton phenotypes of $18\mu\text{m}$ in relation to optimal temperature: Blue (10°C), purple (12°C), green (14°C), black (16°C), orange (18°C), red (18°C) and brown (20°C). 2009: A, 2010: B, 2011: C, 2012: D, 2013: E, 2014: F, 2015: G, 2016: H.

Category	Size (µm)	Phenotype	Topt	Maximum Abundance (Model)							
				2009	2010	2011	2012	2013	2014	2015	2016
Pico	1	2	10	1 745 000	3 816 000	4 496 000	1 590 000	2 292 000	1 495 000	2 807 000	1 632 000
		8	12	7 060 000	16 220 000	18 220 000	1 883 000	11 050 000	3 876 000	10 120 000	3 644 000
		14	14	38 180 000	71 430 000	90 340 000	3 389 000	74 510 000	14 130 000	45 160 000	25 520 000
		20	16	234 700 000	222 800 000	425 600 000	18 270 000	239 500 000	64 260 000	201 100 000	171 500 000
		26	18	727 200 000	723 600 000	662 700 000	92 750 000	324 000 000	342 800 000	487 700 000	545 500 000
		32	20	299 700 000	558 500 000	120 700 000	42 730 000	162 700 000	520 000 000	311 200 000	284 300 000
	2	3	10	371 500	556 200	663 900	181 100	510 200	195 000	309 800	339 000
		9	12	1 374 000	2 633 000	1 879 000	431 900	2 928 000	459 500	1 265 000	1 154 000
		15	14	6 789 000	10 220 000	6 705 000	1 259 000	21 050 000	3 686 000	8 965 000	5 045 000
		21	16	20 880 000	18 410 000	18 130 000	15 310 000	35 330 000	17 380 000	18 710 000	19 650 000
		27	18	23 270 000	12 690 000	12 100 000	69 440 000	11 840 000	18 680 000	17 280 000	23 900 000
		33	20	6 559 000	6 347 000	2 362 000	13 960 000	2 607 000	10 350 000	5 144 000	5 015 000
Nano	5	4	10	65 790	123 200	58 510	34 890	128 500	19 800	42 560	54 670
		10	12	225 600	813 600	223 800	95 500	661 100	98 530	203 400	185 300
		16	14	955 500	1 635 000	962 700	402 900	2 128 000	647 800	1 472 000	657 300
		22	16	1 832 000	1 184 000	1 484 000	1 415 000	1 637 000	1 916 000	2 193 000	1 452 000
		28	18	1 221 000	459 500	587 400	2 550 000	263 200	1 101 000	524 000	1 088 000
		34	20	261 900	152 800	163 700	382 400	30 840	173 200	86 730	226 300
	18	Alex	18	31 600	19 030	10 450	49 810	8 728	33 130	25 770	19 760
		5	10	1 417	2 624	759	919	1 579	540	1 189	957
		11	12	3 290	14 510	3 851	2 409	6 232	1 065	4 761	1 989
		17	14	9 069	23 080	10 180	9 071	14 770	4 196	19 990	4 159
		23	16	11 900	10 250	7 430	18 110	8 489	8 494	19 620	6 036
		29	18	7 199	4 117	2 899	11 130	1 906	3 983	4 659	4 100
		35	20	2 088	1 603	1 193	3 590	478	951	1 053	1 255
Micro	28	6	10	252	259	123	169	162	128	209	162
		12	12	513	1 193	472	393	474	218	607	306
		18	14	1 211	1 725	1 084	1 137	1 012	517	2 169	583
		24	16	1 660	936	742	2 233	661	1 229	2 094	797
		30	18	948	416	373	1 561	192	670	705	515
		36	20	317	230	180	575	100	229	193	211
	64	7	10	8	8	7	5	6	7	6	6
		13	12	13	20	14	7	8	14	8	7
		19	14	30	47	28	11	13	29	16	8
		25	16	37	29	16	19	16	64	16	10
		31	18	20	15	7	16	11	37	10	8
		37	20	10	7	5	8	7	14	8	7

Table 3. Interannual variability in the maximum abundance of each dinoflagellate phenotype

Year	2009	2010	2011	2012	2013	2014	2015	2016
Date @15°C	May 22	May 21	Apr 22	May 25	Jun 01	May 16	May 11	May 17
Ave. Temperature	12.1	11.6	13.6	12.4	10.8	12.7	12.6	12.1
Spring	-	-	Warm	-	Cold	Warm	-	-
Ave. River Flow	108 253	127 834	62 712	194 247	125 920	165 054	122 693	144 888
Spring	-	-	Dry	Wet	-	Wet	-	-

Table 4. Interannual variability in temperature dates at 15°C and spring (March 1 to May31) conditions - average temperature in Celsius degree and river flow in m³d⁻¹. Cold/Warm and Dry/Wet are determined by the interannual differences.

dominated other phenotypes in terms of MA in 2013. The same phenotype was also dominant in autumn in most of the years except in 2012.

3.2.3. Environmental variables

Cumulative anomalies of the measured variables (from May to August) show interannual variations (Fig. 10). Year 2011 was the first to reach a temperature of 15°C while 2013 was the last, in a difference of 39 days (Table 4). Positive temperature values in 2014 from May to July and negative values in 2013 during the same period, were also observed on the anomalies thereby, giving an indication of warm spring/summer in 2014 and cold spring/summer in 2013. Irradiance equally varied interannually with lowest values in 2014 and high values in 2012 and 2013. Being the source of nutrients, the river flow in 2012 (from May to August) was exceptionally high thereby, giving an indication that 2012 was wet during these months. 2014 and 2015 were slightly wet in May and August respectively. On the contrary, 2011 showed negative river flow anomalies during the same period - indicating a dry spring and

summer. The flow in other years varied with mainly negative anomalies except in 2014.

4. DISCUSSION

Bloom definition in the present study follows the criteria established by Smayda (1997) regarding HABs, i.e. when species experience growth in the ecosystem and exceed certain cell concentrations which result in harmful consequences. Unlike Valbi et al. (2019), the originality of this study (model) is not to accurately predict bloom or reproduce past bloom events but to act as a tool which can evaluate the impact of potential drivers on seasonal and interannual variability together with bloom occurrences. The current study went beyond Sourisseau et al. (2017) by incorporating light trait, selecting phenotypes uniformly and studying the competition for resources not just among the different size fractions but also between phenotypes of the same size. Since the study was conducted locally, results of the model can only be validated locally using *in situ* observations.

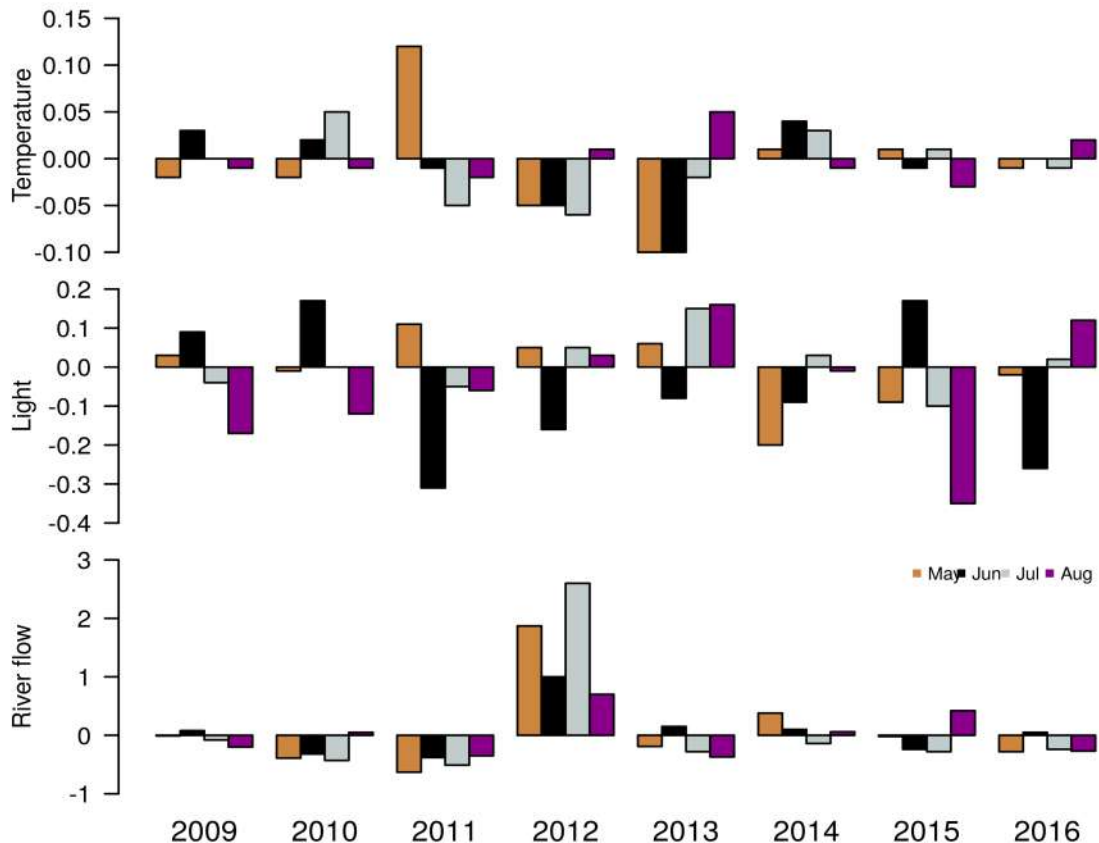


Figure 10. Interannual variability of environmental variables. Cumulative anomalies in river flow (1972 to 2018), temperature (2006 to 2018) and irradiance (2000 and 2018).

4.1. Methodological challenges

The first assumption of using 0D model is that it only tackles how local growth can modulate observed bloom events. All migration processes were neglected whereas numerous studies have shown that such physical-biological interactions could create strong cell accumulations in local areas and from several origins (Crespo et al. 2011). In our case, there have been observations of *A. minutum* blooms outside the Bay of Brest over the last decade e.g. in the Iroise Sea - a strongly mixed tidal area with very low vertical stratification. The possibility of other *A. minutum* sources in another part of the Bay such as the Aulne estuary cannot therefore be excluded from observations. This source is probably limited and the biomass observed in this part of the Bay cannot be explained by aggregation processes only. In addition, the migration of other fractions of the phytoplankton community is obvious and this area seems to account for a small part of the phytoplankton growth during the spring. We already know that a strong phytoplankton production occurs over the Bay of Brest (Del Amo et al., 1997) in summer for all the other phenotypes. A great bias was probably introduced by considering the same dilution rates for the phenotypes describing the community.

The second assumption is the model's capacity to reproduce a consistent competition for resources with the integrated phytoplankton diversity. The initial model (Sourisseau et al. 2017) was based on random selection and consisted of 200 phenotypes with 100 simulations, assuming that each phenotype represented one species through one mean traits composition. By using this approach, the initial model was able to produce some consistent simulations for a period of 3 years (from 2012 to 2014). Here, a uniform distribution over the traits space was used to reduce the duration of simulation for a longer time series. Several simulations with different numbers of phenotypes (e.g. 25, 50, 72, 100 and 200) were obviously conducted but with the same minimal density per phenotype. Those with less number of phenotypes had lower minimal cumulated-abundance but some maximal abundance per phenotype greater than those with more phenotypes. Despite the selec-

tion of the configuration with 72 phenotypes due to a closer fit with *in situ* data, the simulated densities were considered semi-quantitative because the behavior of the model is more relevant than a direct comparison with *in situ* data (Figs. 7A and 7B). For the same periods (2012-2014), this new configuration produced similar dynamics but with lower densities. However, out of these periods, some limitations emerged.

A third assumption is the absence of intraspecific variability of *A. minutum*, which is more and more described for a lot of species (Menden-Deuer and Rowlett, 2014; Ryneerson and Menden-Deuer, 2016; Pigliucci, 2001; Whitlock et al., 2007; Vellend, 2006). Using a fixed phenotype evaluated from a single strain to define species fitness also limits the capacity of species to adapt to the environment and, despite a successful first attempt by Sourisseau et al. (2017) in a three year period, is probably an increasing limitation with increased simulation period (2009-2016).

There was equally a challenge in analyzing the bloom phenology of *A. minutum* using the method of Rolinski et al. (2007) because of the smoothing property of the curve fitting procedures (Ji et al., 2010) and the irregular shape of the abundances. Bloom durations of field data were sometimes exaggerated e.g. in 2011, 2015 and 2016 (Table 2).

Most data were obtained on weekly or monthly instead of daily basis and in some cases, less than 10 data points were sometimes available out of a possible 365 points for several years. Linear interpolation is the procedure to avoid these gaps but it might be inaccurate if high variabilities occurred. The real natural variability is probably underestimated.

4.2. *Alexandrium minutum* and environmental variables

Previous studies (Labry et al., 2008; Chapelle et al., 2007) on the analysis of *A. minutum* blooms in closed areas such as the Penzé estuary located on the coast of the French Brittany, as well as in other coastal areas have shown that light, temperature and nutrients are the first

abiotic factors controlling the blooms, with light being less important. Our own study shows similar abiotic conditions where irradiance was found to have little effect on *A. minutum* growth despite the implicit seasonal link between light, heat fluxes and water temperature. During the winter until late spring, the local growth in the Daoulas bay is thus reduced by temperature as also noted in Sourisseau et al. (2017). In the same period, dilution is high and exceeds growth. A lot of statistic analyses based on *in-situ* observations at local or larger scale also found sea surface temperature to be an important predictive variable for the occurrence, bloom initiation and possibly, the magnitude of *A. minutum* blooms (Valbi et al., 2019; Figueroa et al., 2007; Lim et al., 2006; Guallar et al., 2017; Chapelle et al., 2015; Raine, 2014; Bravo et al., 2008; Giacobbe et al., 1996; Delgado et al., 1990). More precisely, Guallar et al. (2017) noted that *A. minutum* bloom starts when water temperature is up to 15°C and this value remains stable at regional scale because Cosgrove et al. (2014) also observed that bloom initiation occurs after the first large spring tide in June when water column temperatures are above this threshold. This means that above 15°C, *in situ* growth may be sufficient to exceed dilution losses. The simulated dynamic also respects this pattern with 2011 being the first year to exceed 15°C in April and year 2013 the last to cross it in June thus, confirming the late and early bloom start respectively in 2013 and 2011 (Table 2). Furthermore, temperature limitation just before the end of spring in 2013 was quite high and longer compared to 2011 (Figs. 6M and 6K respectively).

When temperature no longer reduces *A. minutum*, its growth becomes quickly limited by nutrients usually in late spring and throughout summer. Nutrients are in low concentrations during this period due to reduced inputs by the river (Fig. 4), which is the main source of nutrients in coastal ecosystems (Tréguer et al., 2014, Del Amo et al., 1997), and also assimilation by phytoplankton leading a competition for resources. In line with Labry et al. (2008), our model shows that phosphorus is the first limiting nutrient. Later in the summer is nitrogen which might be potentially limiting when concentrations fall below 2 $\mu\text{mol.L}^{-1}$. N:P river in-

put ratio greater than 16:1 (Krom et al., 1991), gives an indication that nitrogen is never limiting during periods with a significant river flow. Reversely, when river flow decreases, N concentrations decrease as well. A significant fraction of the interannual variability of the MA appeared related to this enrichment. When river flow was quite high in summer 2012 (Fig. 8), P limitation was less severe and N limitation was almost absent (Fig. 6), causing the most intense bloom – both simulated and observed over this period. The opposite is recorded in 2011 which had a dry summer, low river flow anomaly, low nutrient concentration and least intense bloom. The dominance of *A. minutum* in the phytoplankton community during low P conditions (after the growth of larger cells) can be explained by higher PO_4 uptake capacity and its ability to store P for a delayed or progressive growth. These abilities are thus specific advantages to face competition at local scale and probably contribute significantly to its capacity to dominate the community in this environment.

A good representation of *A. minutum* blooms by the model (in 2012 and 2014) and the high degree of agreement between REF and simulations of MA, DMA, cumulative abundance and bloom start of *A. minutum* in the eight year period (Taylor diagram, Fig. 7C) indicates that the considered factors explained a great part of the interannual variability. However, some significant differences between simulated and observed *A. minutum* remain (Fig. 6). For example, early declines, leading to early DMAs, were simulated. A reason could be the underestimation of Phosphorus concentrations by the model (Fig. 4.F) which is permanent over the years, giving an interrogation on other possible source of P not described here. Moreover, the inconsistency of these differences over the years could indicate some different origins. In addition to the limitations previously described in the methodological challenges, only few factors controlling the bloom termination are simulated. With the exception of the competition effect, light and temperature effects do not appear to be strong drivers of bloom termination. Our results thus show that other biological processes like sexual reproduction (Brosnahan et al., 2013) or other key players such as para-

sitism by eukaryotes and grazing by microzooplankton (Montagnes et al., 2008) may have occurred in the observed bay and therefore, explain some interannual variability of bloom occurrence.

4.3. Phytoplankton community and environmental variables

The phytoplankton dynamic in the bay of Brest (out of the considered box) was well described by previous work (Beucher et al., 2004; Del Amo et al., 1997) with a first bloom dominated by diatoms, occurring in April. This first bloom is next often followed along the summer by secondary blooms developed under low nutrient concentrations. The first bloom, leading to a strong decrease in Si, is not simulated by our model (neither in microphytoplankton biomass or Si reduction). This bloom observed in the center of the Bay of Brest is thus not driven by a local growth in the Daoulas bay but probably occurs downstream to the Bay of Brest. It explains also the inability of the model to simulate correctly the timing of the micro-phytoplankton bloom. The model is however in agreement with the observed nutrient limitation firstly driven by P and next switching to N from March to August. According to this observation, our model probably slightly overestimated the competition by the siliceous phenotypes and limited the growth capacities of *A. minutum* and non-siliceous phenotypes. The model also overestimated the competition for resources which results in a strong selection towards the smallest cell size fraction. If the pico- size fraction is well represented in the phytoplankton community at the end of the summer (Fig 5), there is still a significant fraction of the nano- size fraction (50% of the total phytoplankton densities in September). It is thus difficult to assume that this observation was only due to a migration process. This bulk of species, simulated only by several phenotypes, develop complex interactions (commensalism, mutualism etc) that are not integrated in the model and are probably of great relevance for resource access.

Very low growth was noted among species with an optimal temperature of 10°C and 12°C both seasonally and interannually (Figs. 5B-5D). The difference between these species and those of higher T_{opt} is their maximum growth (Table 1) which is lower. In winter and early spring when water temperature is 10°C or 12°C, dilution is high due to high river flow and species of low T_{opt} have insufficient growth to compensate dilution losses even though temperature is more adapted. This may also explain part of the non simulation of early spring blooms.

5. CONCLUSION

The present study provides information on the seasonal and interannual variability of *A. minutum* and phytoplankton in the Daoulas estuary from 2009 to 2016. This ecosystem is exposed to high rainfalls and river flows during the winter, giving rise to high dilution and high nutrient concentrations but also low temperatures which, associated with dilution processes, prevent bloom initiation. The opposite is also observed in the summer – leading to bloom outbreaks. The interannual variability is linked to changes in environmental conditions with some hot/cold or dry/wet summers having an influence on the degree of limitation and on the species competition. Although some results of our model did not correspond with field data in certain cases, the model is able to point out the best conditions that are necessary, although not sufficient, to trigger HAB events. As a perspective, advanced version of the model in 2D or 3D would reduce some of the challenges associated with the current 0D model.

Acknowledgement

The authors gratefully acknowledge IFREMER and the region Bretagne together with the VELYGER network for their support in the Daoulas (*Alex-Breizh*) project.

Titre: Modélisation des efflorescences de l'algue toxique (*Alexandrium minutum*) en compétition interspécifique en Rade de Brest, France

Mots clés : *A. minutum*; Efflorescences toxiques (HABs); Rade de Brest; Compétition pour les ressources; Traits physiologiques; Variabilité saisonnière et interannuelle.

Résumé *Alexandrium minutum* est un dinoflagellé toxique responsable de crises sanitaires et économiques. En France, cette espèce est observée depuis 1988. Cette étude tente de hiérarchiser les paramètres contrôlant le succès d'*A. minutum* au sein de la communauté phytoplanctonique par un suivi dans l'estuaire de Daoulas (Rade de Brest) et le développement d'un modèle 0D. Ce modèle basé sur des traits physiologiques met en compétition. *A. minutum* avec 72 autres espèces réparties de manière uniforme dans l'espace des traits. Les résultats montrent une variabilité saisonnière et inter-annuelle des efflorescences. D'avril à octobre se succèdent le micro puis le nano et enfin le picophytoplancton, contrôlés par la température et la lumière en hiver puis par le phosphore puis l'azote, durant l'été. Les blooms d'*A. minutum* apparaissent entre juin et août.

Les résultats de la modélisation, corroborés par les données, ont montré une efflorescence tardive d'*A. minutum* lors d'un printemps froid (2013) et précoce lors d'un printemps chaud (2014). Le maximum d'abondance d'*A. minutum* est observé et simulé en 2012 où les forts débits durant l'été ont entraîné des apports en nutriments très élevés et la plus faible abondance en 2011, été le plus sec sur la période considérée. Le modèle a permis de tester l'impact de scénarios de réduction de 50% d'azote et de phosphore dans les apports. Seule une réduction de phosphore entraîne une diminution de l'abondance d'*A. minutum*, les apports de la rivière restant très riches en azote. Le modèle n'est toutefois pas consistant sur toute la période d'étude ce qui met en lumière l'importance probable d'autres facteurs dans la régulation des efflorescences.

Title: Modeling the bloom of toxic algae (*Alexandrium minutum*) in interspecific competition in the Bay of Brest, France

Keywords: *A. minutum*, HABs, Bay of Brest, Resource Competition, Physiological Traits, Seasonal and interannual variability.

Abstract: *Alexandrium minutum* is one of the toxic species that produce Harmful Algal Blooms (HABs), threaten public health, aquaculture and tourism. In France, it was observed in 1988 in the region Bretagne. High levels of Paralytic Shellfish Poisoning (PSP) toxicity have been detected in the estuaries of Morlaix, Penzé, Rance, Abers and more recently, in the Bay of Brest. This work tries to define and place in order of hierarchy, the parameters driving *A. minutum* success in the phytoplankton community. Two approaches were adopted. The first was a temporal survey at the study site since 2009-2018. The second was the use of a 0D numerical model (based on physiological traits) to simulate the potential impact between physical and biological processes. *A. minutum* was placed in competition with 72 species which were uniformly selected.

Results showed both seasonal and interannual variability of bloom phenology. It was marked by micro, followed by nano and then pico phytoplankton from April to October. *A. minutum* bloom occurred between June and August, a period of high temperature, low nutrient concentrations and high resource competition. However, environmental factors and competition explain only a part of its phenology. Though the model was able to reproduce the seasonal and interannual variability of *A. minutum*, simulation was inconsistent over the study period. The model highlights the increasing relevance of other biological processes in bloom regulation at decade scale. It might improve some models which are able to correctly predict instances of *A. minutum* presence or absence. The perspective is to have a model which can be applied and validated for the entire Bay of Brest.